ADOPTIVE NK CELL THERAPY FOR SOLID TUMOURS

HARNESSING NATURAL KILLER CELLS FOR IMMUNOTHERAPY AGAINST SOLID TUMOURS

By SOPHIE M. POZNANSKI, B.H.Sc.

A Thesis Submitted to the School of Graduate Studies in Partial Fulfillment of the Requirements for the Degree Doctor of Philosophy

– DESCRIPTIVE NOTE –

DOCTOR OF PHILOSOPHY (2023) McMaster University,

(Medical Sciences) Hamilton, Ontario

TITLE: Harnessing Natural Killer cells for immunotherapy against solid tumours

AUTHOR: Sophie M. Poznanski, B.H.Sc. (McMaster University)

SUPERVISOR: Dr. Ali A. Ashkar

NUMBER OF PAGES: xx, 244

– LAY ABSTRACT –

Harnessing the body's natural immune defenses against cancer in the form of immunotherapy has emerged as a powerful treatment modality. Over the past decade, immune cell therapies have revolutionized the treatment of blood cancers like leukemia and lymphoma. Yet despite the potential, immune cell therapies have failed to be broadly effective against solid tumours because the anti-cancer activity of immune cells, such as Natural Killer (NK) cells, becomes severely impaired by the tumour environment. In this work, we identify that NK cells expanded from cancer patients and healthy donors overcome suppression by tumours and eliminate detectable tumour in pre-clinical models of advanced ovarian and lung cancer. These expanded NK cells also enhanced the functions of other immunotherapies. Further, we shed new light on how NK cells become dysfunctional in tumours. We uncover that NK cells undergo a metabolic energy crisis in tumours that causes their dysfunction, but that expanded NK cells have increased metabolic fitness which allows them to overcome this energy crisis and remain highly functional. Finally, we also characterize the metabolism of a subset of NK cells that are tumour-promoting and find that they harbour metabolic advantages to thrive in tumours. Overall, our work provides new insight as to how to overcome immunosuppression by tumours. This work identifies that expanded NK cells are a promising therapeutic candidate that exploit the hostility of tumours and synergize with other immunotherapies.

– ABSTRACT –

Suppression of anti-tumour immunity by the tumour microenvironment remains a major barrier to the development of broadly effective immunotherapies to treat solid tumours. Cytotoxic natural killer (NK) cells are vital to anti-cancer immunity and have shown clinical efficacy for treating hematologic malignancies. However, NK cell therapies have failed to be effective against solid tumours as cytotoxic NK cells become dysfunctional in the tumour microenvironment. While tumours hinder cytotoxic NK cells, they stimulate the tumour-promoting functions of regulatory NK cells. The mechanisms that dictate NK cell polarization and their fate in the tumour microenvironment remain poorly defined but harbour key therapeutic potential. Glucose-driven cellular metabolism has emerged as a central regulator of NK cell anti-tumour activity. Notably, tumour cells have deregulated metabolism, causing a metabolically hostile environment that is low in glucose and oxygen and high in metabolic waste. In the work presented, we demonstrate that NK cells expanded from cancer patients or healthy donors exert strong anti-tumour activity and dismantle the immunosuppressive tumour microenvironments of advanced ovarian and lung cancer. As a result, expanded NK cells were capable of sensitising initially non-responsive patient tumours to PD1 checkpoint-blockade therapy. Further, we uncover that the activity of cellular metabolic pathways plays a key role in NK cell functional fate in tumour microenvironment. We show that the tumour microenvironment induces paralysis of cytotoxic NK cell glucose metabolism to cause their dysfunction. However, reprogramming of NK cell metabolism through expansion arms expanded NK cells with enhanced metabolic flexibility which enabled their anti-tumour activity to be paradoxically strengthened by the tumour microenvironment. We further identify that regulatory NK cells have a distinct metabolic program compared to cytotoxic NK cells, including lower glucose-driven metabolism, that is amenable with the tumour

microenvironment. Our work provides new mechanistic insight into how NK cell fate is regulated and how the pathological environment of a tumour capitalizes on this. This knowledge provides new therapeutic targets to intervene with the suppression of cytotoxic immunity in tumours. Further, this work identifies that expanded NK cells are a promising therapeutic candidate that exploit the metabolic hostility of the tumour microenvironment and synergize with other immunotherapies.

– ACKNOWLEDGMENTS –

My PhD journey has been a hugely formative experience both from a professional and personal standpoint. Perhaps the biggest lesson I've taken from the process has been the value of good teamsmanship. I am so grateful to all who contributed to and supported my journey – I have become not only a better scientist, but a better person thanks to you.

First and foremost, I would like to thank my supervisor, Dr. Ali Ashkar. Thank you for taking a chance on me as a 4th year undergraduate thesis student with absolutely no research experience. From the get-go, you fostered such a supportive and encouraging environment without which I would not have developed the kind of scientific creativity I have today. The hours of scientific debate we had in your office synergizing ideas will remain some of my most treasured memories and learning moments. Your optimism and enthusiasm for science and research that is unwavering even in the face of failed experiments permeates through the entire lab and forms an inspired work environment. I am so grateful for your profound investment in helping me to shape and achieve my goals – I could not have asked for a better mentor. If I can inspire those around me half as much as you've inspired me, I will consider my career a great success.

To my supervisory committee, Dr. Hal Hirte and Dr. Jonathan Schertzer, thank you for dedicating your time to support my graduate work. Your guidance and expertise were invaluable throughout my project. Dr. Parameswaran Nair and Dr. Manali Mukherjee, I am very grateful for the opportunities you provided for me to branch into the field of clinical research during my PhD. I learned so much from the experience and both of you and am fortunate to have worked with you. Dr. Dawn Bowdish, your 4th year undergraduate immunology class instigated my passion for immunology and set the course for my career. Thank you for helping me get started with research and your continued support throughout my PhD.

I would also like to thank everyone at the McMaster Immunology Research Centre. I am so fortunate to have done my graduate studies in such a supportive and collaborative environment. The feeling of being “all in this together” was invaluable to completing this marathon.

Thank you to all past and current members of the Ashkar Lab, I am so thankful for your guidance, support, teamsmanship, and friendship. In particular, Amanda, Marianne, and Leila, you have been amazing role models for the kind of researcher and person I strive to be. Thank you for your mentorship, patience in answering my many questions, and willingness to always provide guidance and help when I needed it. To Tyrah, Ana, Eddy, and Isabella, thank you for all of your help with my project. I will fondly remember our marathon hours in tissue culture and late nights processing samples where we required dance parties to stay awake. Thank you for not only bearing, but embracing, the chaos of my big experiments and your willingness to help at the drop of a hat when samples were arriving.

I cannot express enough gratitude to my family for supporting and encouraging me during my many years of education. To my parents, Bernard and Julie, thank you for being my life mentors and for opening so many doors for me and encouraging me to always step beyond the threshold. To my sisters, Nathalie and Olivia, thank you for your rock-solid sisterhood, unconditional friendship, and your great care in looking out for me. To my husband Rory, your love and support were my anchor during all the highs and lows. Thank you for always believing in me and being my cheer squad when I needed it. Thank you also for understanding that sometimes you had to come second to my cells or mice! To my daughter Maxine, thank you for bringing a beautiful perspective to my life. You inspire me to strive to be the best that I can.

– TABLE OF CONTENTS –

– LIST OF FIGURES –

Chapter 1

Chapter 2

Chapter 3

Chapter 4

Chapter 5

– LIST OF TABLES –

- LIST OF ABBREVIATIONS AND SYMBOLS -

$C0_2$	Carbon dioxide
cm^2	centimeters squared
°C	Degree(s) Celsius
g	Gram
h	Hour
kDa	Kilodalton
μm	Micrometer
mL	Milliliter
mm	Millimeter
ng	Nanogram
nM	Nanomolar
N_2	Nitrogen
O_2	Oxygen
%	Percent
U	Units
αMEM	Alpha minimum essential media
2DG	2-deoxy-D-glucose
ACT	Adoptive cell therapy
ADCC	Antibody-dependent cell cytotoxicity
ALK	Anaplastic lymphoma kinase
AML	Acute myeloid leukemia
ANOVA	Analysis of variance
ATP	Adenosine triphosphate
ascTME	Ascites tumour microenvironment
BRAF	V-raf murine sarcoma viral oncogene homolog B1
CAR	Chimeric antigen receptor
CA-125	Cancer antigen 125
CD	Cluster of differentiation
CFSE	Carboxyfluorescein succinimidyl ester

CTLA4	Cytotoxic T lymphocyte antigen 4
CXCR3	Chemokine receptor 3
DNA	Deoxyribonucleic acid
DNAM-1	DNAX accessory molecule 1
EBV	Epstein-Barr virus
ECAR	Extracellular acidification rate
EF-1 alpha	Human elongation factor-1 alpha
EGFR	Epidermal growth factor receptor
ELISA	Enzyme-linked immunosorbent assay
EOC	Epithelial ovarian cancer
exNK	Expanded NK cell
FABP4	Fatty acid-binding protein 4
$FADH_2$	Reduced flavin adenine dinucleotide
FAO	Fatty acid oxidation
FDA	Food and drug administration
FSC-A	Forward scatter
GLUT	Glucose transporter
H&E	Hematoxylin and eosin stain
HD	Healthy donor
HD PB-NK	Healthy donor peripheral blood NK cells
HEPES	4-(2-hydroxyethyl)-1-piperazineethanesulfonic acid
HGSOC	High grade serous ovarian cancer
HIF1α	Hypoxia inducible factor 1 subunit alpha
HLA	Human leukocyte antigen
ICI	Immune checkpoint inhibitor
IFNγ	Interferon-gamma
IL	Interleukin
i.p.	Intraperitoneal
IP	Interferon-inducible protein
ITAM	Immunoreceptor tyrosine-based activation motif
ITIM	Immune tyrosine-based inhibitory motif

Keap1	Kelch-like ECH-associated protein 1
KIR	Killer immunoglobin receptor
KRAS	Kirsten rat sarcoma
LAK	Lymphokine activated killer
LCP	Lung cancer patients
LDH	Lactate dehydrogenase
mAbs	Monoclonal antibodies
MAPK	Mitogen-activated protein kinase
MDA-MB 231	M.D. Anderson – metastatic breast 231
MET	c-MET encoding gene
MFI	Mean fluorescence intensity
MIBI	Multiplexed ion-beam imaging
Min	Minutes
MCT1	Monocarboxylate transporter 1
MFI	Mean fluorescence intensity
MHC	Major histocompatibility complex
mTOR	Mechanistic target of rapamycin
NADH	Nicotinamide adenine dinucleotide
NADPH	Nicotinamide adenine dinucleotide phosphate
NCR	Natural cytotoxicity receptor
NK	Natural killer
NKreg	Natural killer regulatory
NKctx	Natural killer cytotoxic
Nrf2	Nuclear factor erythroid 2-related factor 2
NRG	NOD-*Rag1*^{null} *IL2rg*^{null}
NSCLC	Non-small cell lung cancer
NTRK	Neurotrophic receptor tyrosine kinase
OCP ascites-NK	Ovarian cancer patient ascites-NK cells
OCP PB-NK	Ovarian cancer patient peripheral blood-NK cells
OCR	Oxygen consumption rate
OVCAR-Luc	Luciferase-expressing OVCAR8 cells

PARP	Poly-ADP ribose polymerase
PBMC	Peripheral blood mononuclear cell
pbNK	Peripheral blood NK cell
PBS	Phosphate buffered saline
PD1	Programmed death-1
PDGF	Platelet-derived growth factor
PDX	Patient-derived xenograft
PDL1/2	Programmed death ligand-1 and -2
PE	Pleural effusion
peNK	Pleural effusion NK cells
PFS	Progression-free survival
PI3K	Phosphatidylinositol-3-kinase
PLGF	Placental growth factor
PSAT1	Phosphoserine aminotransferase 1
PUFA	Polyunsaturated fatty acids
OKT3	CD3 monoclonal antibody
OXCT1	3-oxoacid CoA-transferase 1
OxPhos	Oxidative phosphorylation
RANTES	Regulated on activation, normal T cell expressed and secreted
rh	Recombinant human
RNA	Ribonucleic acid
RNA-seq	RNA sequencing
ROS	Reactive oxygen species
ROS1	c-ROS oncogene 1
RPMI	Roswell Park Memorial institute medium
RTA-408	Omaveloxolone
SCLC	Small cell lung cancer
SEM	Standard error of the mean
SSC-A	Side scatter
STAT	Signal transducer and activator of transcription
taNK	Tumour-associated NK

TARC	Thymus and activation regulated chemokine
TCA	Tricarboxylic acid
TCR	T cell receptor
TGFβ	Transforming growth factor beta
Th1	Type 1 T helper
TILs	Tumour-infiltrating lymphocytes
TME	Tumour microenvironment
TPS	Tumour proportion score
TRAIL	Tumour necrosis factor-related apoptosis-inducing ligand
Treg	Regulatory T cell
UCP2	Uncoupling protein 2
uNK	Uterine NK
VEGF	Vascular endothelial growth factor
WT	Wild-type

– DECLARATION OF ACADEMIC ACHIEVEMENT –

Experiments were conceived and designed by Sophie M. Poznanski and Ali A. Ashkar. Sophie M. Poznanski wrote this dissertation with contributions from Ali A. Ashkar. Sophie M. Poznanski performed experiments with the assistance of others. For specific contributions to the experiments and papers in **Chapters 2-5**, please refer to the **Preface** at the beginning of each chapter.

– CHAPTER 1 –

INTRODUCTION

1.1 Challenges of cancer treatment

Cancer is among the most prevalent and deadly diseases across the globe, accounting for 10 million deaths worldwide in 2020 (Ferlay, Colombet et al. 2021). In Canada, cancer remains the leading cause of death. Approximately 43% of Canadians will be diagnosed with cancer in their lifetime and one quarter of Canadians will die from the disease (CCSAC 2021). With Canada's aging demographic, the physical and financial burden of cancer on the population are ever-increasing (CCSAC 2021). Substantial improvements in cancer treatment and prognosis have been achieved in the past few decades, with many effective first-line therapies including debulking surgery and/or chemotherapy that now extend patient survival. Despite these advances, many cancers, including ovarian and lung cancer, remain with a poor 5-year survival rate of less than 50% (Heuvers, Hegmans et al. 2012, Lowe, Chia et al. 2013). Developing novel therapeutic platforms to tackle the disease are urgently needed to reduce the burden that cancer poses on society.

1.1.1 Ovarian cancer

Ovarian cancer is the most lethal gynecological cancer: well over 20,000 women in North America are diagnosed with ovarian cancer each year and over half of these women will not survive 5 years (Howlader, Noone et al. 2019). In one year alone, there is an estimated loss of 29,600 potential years of life for women in Canada due to ovarian cancer (CCSAC 2021). Known as a "silent killer," symptoms often do not present until the cancer has disseminated. As such, over 75% of ovarian cancer cases are diagnosed at advanced stage (stages III-IV) (Ahmed and Stenvers 2013).

Approximately 90% of ovarian cancer cases are of epithelial origin, whereby ovarian cancer cells originate in the epithelial surface of the ovary or fallopian tube (Yeung, Leung et al.

2015). The majority (70%) of epithelial ovarian cancer (EOC) cases are high grade serous ovarian cancer (HGSOC), making it the most common subtype. Other EOC histological subtypes include clear cell carcinoma, endometroid carcinoma, mucinous carcinoma, and low grade serous carcinoma (Kuroki and Guntupalli 2020).

The standard treatment for patients with advanced-stage EOC consists of cytoreductive surgery followed by platinum-based chemotherapy. However, for patients with high tumour burden that is unlikely to be completely cytoreduced, neoadjuvant chemotherapy is also considered (Kuroki and Guntupalli 2020). Maintenance therapies of poly-ADP ribose polymerase (PARP) inhibitors and/or bevacizumab, a monoclonal antibody that targets vascular endothelial growth factor (VEGF) to inhibit angiogenesis, are also utilized in certain cases. However, these produce only modest improvements in progression-free survival (PFS) (Kuroki and Guntupalli 2020). While first-line treatments including chemotherapy and cytoreductive surgery are initially effective, nearly 80% of EOC patients experience disease recurrence and platinum resistance, at which point there remain a paucity of effective treatment options (Hansen, Coleman et al. 2016). Thus, there is a critical need for novel, effective second-line therapies for ovarian cancer.

At the time of diagnosis, over one third of ovarian cancer patients present with ascites: an accumulation of peritoneal fluid which facilitates peritoneal dissemination of the cancer and is associated with poor prognosis (Ahmed and Stenvers 2013). As the tumour develops, some EOC cells shed into the peritoneal fluid, where they can subsequently secrete factors to increase fluid transport across endothelial cells and block lymphatic duct drainage. This combination of increased fluid leakage and blocked drainage leads to the accumulation of ascites (Ahmed and Stenvers 2013, Yeung, Leung et al. 2015). Ascites harbours the tumour microenvironment of EOC and facilitates dissemination and progression of EOC via numerous mechanisms. Ascites acts as a

large reservoir for shedding EOC cells; these cells are carried by the flow of ascites fluid to distant peritoneal organs, where they may anchor and metastasize (Ahmed and Stenvers 2013). In fact, there is a high rate of metastasis to organs in contact with ascites fluid (Yeung, Leung et al. 2015). In addition, ascites contains an abundance of immunosuppressive factors that impair immune cells and thus promote escape of EOC cells from immune detection (Ahmed and Stenvers 2013, Tanizaki, Kobayashi et al. 2014, Hansen, Coleman et al. 2016). Therefore, targeting the ascites tumour microenvironment may be a promising approach to improving therapeutic outcomes for ovarian cancer treatments.

1.1.2 Lung cancer

Lung cancer is the leading cause of cancer-related deaths worldwide and accounted for 1.8 million deaths in 2020 (Ferlay, Colombet et al. 2021). Lung cancer has a poor 5-year relative survival rate of 22.9%. Similar to ovarian cancer, the majority of lung cancer cases (55%) present as stage IV disease, in which the cancer has already metastasized to distant sites (Howlader, Noone et al. 2019). Non-small cell lung cancer (NSCLC) is the most common histological subset, accounting for 85% of lung cancer cases. Lung adenocarcinoma and lung squamous cell carcinoma are the most common subsets of NSCLC (Herbst, Morgensztern et al. 2018). The most common genetic alterations in adeno- and squamous cell- carcinoma are Kirsten rat sarcoma (KRAS) and epidermal growth factor receptor (EGFR) mutations. These tend to occur in founder clones and are thus involved in tumour initiation. Other driver mutations include ALK, ROS1, BRAF, MET, and NTRK (Herbst, Morgensztern et al. 2018). As with ascites in ovarian cancer, 50% of lung cancer patients develop malignant pleural effusions (PE). PE usually develop as a result of metastasis of malignant cells to the pleura, which increase fluid transport across endothelial cells

and disrupt lymphatic drainage. PE are associated with poor survival, with a median survival time ranging from 3-12 months following PE presentation (Aydin, Turkyilmaz et al. 2009).

The management of NSCLC varies greatly depending on the stage of disease. Standard care for patients with NSCLC stage I, II, and some IIIA is surgical resection followed by adjuvant systemic chemotherapy. However, approximately half of patients with stage I and over 75% of patients with stage IIIA experience disease recurrence following treatment and consequent progression to more advanced disease stages (III-IV) (Mithoowani and Febbraro 2022). The majority of patients with stage III and IV NSCLC have tumours that are considered unresectable. For years, the best outcomes for stage III patients were achieved with the combination of chemotherapy and radiation, which only produced a 5-year survival rate of around 10%. However, more recent incorporation of immunotherapies following chemotherapy and radiation has further reduced the risk of death. The management goals for stage IV NSCLC patients, i.e., those with metastatic disease, consist of improving quality of life and extending overall survival. Chemotherapy, targeted therapy, and immunotherapy are all possible treatment options. The course of treatment depends on the histological subset, the presence of a driver mutation (i.e., EGFR) for which targeted therapies are available, or the presence of immune markers for which immunotherapies (namely immune checkpoint inhibitors) are available (Mithoowani and Febbraro 2022). Despite such advancements, the 5-year survival for metastatic lung cancer remains a dismal 7% (Howlader, Noone et al. 2019).

While first-line therapies are often initially effective, major hurdles that underpin the poor prognosis of these cancers include the high rate of disease recurrence following first-line therapies and lack of effective second-line therapies for recurrent disease (Markman, Markman et al. 2004,

Markman, Webster et al. 2004, Maringe, Walters et al. 2012, Genestreti, Grossi et al. 2014). Therefore, significant attention is now being directed to the development of new effective second-line therapies to treat poor prognosis tumours.

1.2 Cancer immunotherapy: potential and current limitations

1.2.1 Cancer immunosurveillance and immunoediting

Harnessing the body's natural immune defenses against cancer in the form of immunotherapy has emerged as a promising treatment modality for cancer. The concept that the immune system has a role in suppressing cancer stems back to the early 1900's, when Paul Ehrlich was among the first to propose such an idea (Ehrlich 1908). However, it was not until the 1960s that an accumulation of findings determined mice could be immunized to reject syngeneic tumours transplants (Old and Boyse 1964). These results led to Burnet's proposal of the cancer immunosurveillance hypothesis, whereby immune cells constantly survey the body and eliminate malignant cells, regularly hindering the development of cancer (Burnet 1964, Burnet 1970). However, the cancer immunosurveillance hypothesis failed to address why cancer does develop in some cases in immunocompetent people. Along these lines, studies began to shed light on the fact that the immune system shapes the tumour during development. For instance, the repassage of tumours in immunocompetent hosts produced tumour variants with weaker immunogenicity compared to the original tumour (Uyttenhove, Van Snick et al. 1980). In addition, tumours raised in immunodeficient hosts were more immunogenic than tumours raised in immunocompetent hosts (Shankaran, Ikeda et al. 2001). Such findings suggested that the immune system selects for tumour variants that can better survive in an immunocompetent environment. The fact that the immune system can therefore exert both host-protective and tumour-shaping effects led Dunn and

colleagues to propose the concept of cancer immunoediting (Dunn, Bruce et al. 2002). They defined three stages (or E's) of cancer immunoediting: 1) elimination of the tumour via immunosurveillance, 2) equilibrium whereby the immune system selects for tumour variants or favourable conditions in the tumour microenvironment that aid the tumour in surviving immune attack, and 3) escape of the surviving tumour variants from immune attack and resulting uncontrolled tumour growth.

Evidence of cancer immunoediting in humans emerged from reports that showed that patients with primary immunodeficiencies or who were immunosuppressed following organ transplant had a higher risk of developing cancer (Gatti and Good 1971, Birkeland, Storm et al. 1995, Penn 1995, Penn 1996). Further, it became apparent that the amount, type, and location of tumour-infiltrating lymphocytes (TILs) correlated with patient prognosis and survival. Tumours with high levels of type 1 T helper (Th1)-polarized cluster of differentiation (CD)4+ T cells, CD8+ effector T cells, and their associated anti-tumour cytokine interferon-gamma (IFNγ) and cytotoxic granzyme B molecule were positively associated with improved patient survival in a multitude of cancers, including ovarian, colorectal, and lung cancer (Sato, Olson et al. 2005, Galon, Costes et al. 2006, Al-Shibli, Donnem et al. 2008). In addition, a higher ratio of anti-tumour CD8 T cells to immunosuppressive regulatory T cells (Treg) was indicative of favourable prognosis (Sato, Olson et al. 2005). Notably, these immune parameters were found to better predict patient survival than conventional histopathological methods (Galon, Costes et al. 2006). Such knowledge that the immune system can prevent, shape, or even promote cancer progression propelled the field of cancer immunotherapy.

1.2.2 Types of cancer immunotherapy

Proof-of-concept that immunotherapy can exert potent anti-tumour therapeutic potential is evidenced by clinical immunotherapeutic successes to date, most notably immune checkpoint inhibitors (ICIs) and CD19-(chimeric antigen receptor) CAR T cells (Ott, Hodi et al. 2013, Vici, Pizzuti et al. 2014, Gong, Chehrazi-Raffle et al. 2018, Park, Riviere et al. 2018).

1.2.2.1 Immune checkpoint inhibitors

ICIs have revolutionized the treatment of several cancers, including subsets of melanoma and lung cancer. Immune checkpoints are cell-surface receptors that limit the activation and duration of an immune response. Such checkpoints are essential to preventing the development of autoimmunity by maintaining self-tolerance to normal tissue (Nishimura, Okazaki et al. 2001, Carlino, Larkin et al. 2021). However, they were also found to be used by neoplastic cells to evade immune attack. The first checkpoint receptor to be discovered was cytotoxic T lymphocyte antigen 4 (CTLA4) on T cells. CTLA4 binds to the family of B7 receptors, with greater affinity than the costimulatory molecule CD28, to negatively regulate T cell activation (Brunet, Denizot et al. 1987, Linsley, Brady et al. 1991, Linsley, Greene et al. 1994). A landmark study by the Allison group demonstrated that administration of antibodies against CTLA4 to mice with preestablished tumours caused tumour rejection and immunity against a secondary exposure to the tumour cells (Leach, Krummel et al. 1996). In two separate phase 3 trials, the first CTLA4 blocking antibody ipilumimab improved overall survival in metastatic melanoma patients (Hodi, O'Day et al. 2010, Robert, Thomas et al. 2011). However, survival was only improved by a median of 2 and 4 months, respectively, and severe and at times lethal toxicities were associated with ipilumimab treatment. Given these drawbacks, focus turned to identifying additional checkpoint blockade receptors.

The programmed death-1 (PD1) receptor has emerged as a central negative regulator of T cell anti-tumour functions, including IFNγ production and tumour cytotoxicity (Freeman, Long et al. 2000). The inhibitory functions of PD1 are mediated by tyrosine phosphatases that inhibit signaling molecules downstream of the T cell receptor (TCR) and CD28 co-stimulatory receptor (Hui, Cheung et al. 2017, Kamphorst, Wieland et al. 2017, Mizuno, Sugiura et al. 2019). PD1 recognizes two ligands, programmed death ligand-1 and -2 (PDL1/2) (Freeman, Long et al. 2000). Expression of PDL1 is highly inducible on cancer cells in response to inflammatory stimuli, namely IFNγ, whereas expression of PDL2, while induced to a lesser degree on tumours, is more highly induced on antigen presenting cells (Latchman, Wood et al. 2001, Dong, Strome et al. 2002). The fact that PDL1 is induced by inflammation restricts the inhibitory effects of PD1 to a preexistent immune response which reduced its toxicity profile compared to CTLA4 (Robert, Schachter et al. 2015).

Antibody blockade of the PD1/PDL1 interaction, via either anti-PD1 or anti-PDL1 antibodies, has induced unprecedented durable responses against multiple cancers. An initial phase 1 trial with nivolumab, a PD1-blocking antibody, achieved a 37.5% response rate with limited toxicity in patients with various cancers including melanoma, renal cell carcinoma, and NSCLC (Sznol, Powderly et al. 2010). Since, multiple other trials of different PD1/L1 blocking agents have demonstrated significant antitumour activity in subsets of patients across a broad range of cancers including Hodgkin's lymphoma, melanoma, NSCLC, head and neck, renal cell, hepatocellular, and bladder cancers (Ansell, Lesokhin et al. 2015, Borghaei, Paz-Ares et al. 2015, Motzer, Escudier et al. 2015, Robert, Schachter et al. 2015, Ferris, Blumenschein et al. 2016, Bellmunt, de Wit et al. 2017, El-Khoueiry, Sangro et al. 2017). The most remarkable result of PD1 blockade therapy has been in Hodgkin's lymphoma, where it achieved durable tumour regression in a

staggering 87% of patients with heavily treated relapsed or refractory disease (Ansell, Lesokhin et al. 2015). For melanoma, tumour responses occur in approximately 35% of patients (Robert, Schachter et al. 2015). However, success with most other cancers has been limited to a smaller proportion (10-20%) of patients (Borghaei, Paz-Ares et al. 2015, Garon, Rizvi et al. 2015, Ferris, Blumenschein et al. 2016, Bellmunt, de Wit et al. 2017). For instance, a phase 3 trial in patients with NSCLC showed that while nivolumab improved overall survival compared to treatment with docetaxel, it only achieved tumour responses in 19% of patients (Borghaei, Paz-Ares et al. 2015). Thus, there is intense focus on discovering new strategies that can increase the proportion of cancer patients who respond to PD1/L1 blockade therapy.

Response to PD1/L1 blockade is largely dictated by the tumour proportion score (TPS) of PDL1 (i.e., the percent of tumour cells that express PDL1) and the immunogenicity of the tumour microenvironment (TME). The high response rate to PD1-blockade therapy in Hodgkin's lymphoma is largely due to the fact that PDL1 is constitutively expressed by these tumour cells (Ansell, Lesokhin et al. 2015). In the context of NSCLC, it was shown that patients with high tumour PDL1 expression (PDL1 TPS of ≥50%) had the greatest response rate to PD1-blockade compared to patients with low- (TPS ≥1 – ≤49%) or no- (TPS <1%) tumour PDL1 expression (Garon, Rizvi et al. 2015). As a result, PDL1 TPS guides clinical management: PD1/L1-blockade therapy is administered as a first-line treatment for patients with $PDL1^{hi}$ NSCLC and as second line therapy for patients with $PDL1^{low}$ NSCLC (Kazandjian, Suzman et al. 2016, Pai-Scherf, Blumenthal et al. 2017). However, only 20% of lung cancer patients have $PDL1^{hi}$ tumours and only 50% of patients have tumours that express PDL1 to any degree (Dietel, Savelov et al. 2019). Thus, strategies to increase PDL1 TPS may prove beneficial.

1.2.2.3 Adoptive cell therapy

Adoptive cell therapy (ACT), in which lymphocytes with anti-tumour activity are extracted, activated, and then adoptively transferred to cancer patients, has evolved as another major arm of cancer immunotherapy. A significant advantage of ACT is that, as a living therapy, cells can expand over 1000-fold following administration and survive long term in the patient (Rosenberg, Yang et al. 2011). Initial studies demonstrated that the adoptive transfer of T cells to rodents immunized against the tumour induced some inhibition of tumour growth, which was further enhanced by neoadjuvant lymphodepleting regimens (Delorme and Alexander 1964, Fefer 1969, Berendt and North 1980, Fernandez-Cruz, Woda et al. 1980). Other reports by the Rosenberg group found that the activation of human peripheral blood lymphocytes or murine splenocytes with interleukin (IL)-2 generated cells that could non-specifically kill a variety of autologous or allogeneic tumour cells (Lotze, Grimm et al. 1981, Grimm, Mazumder et al. 1982, Rosenstein, Yron et al. 1984). These cells, termed lymphokine activated killer (LAK) cells, were the first cells to be used for ACT in humans and achieved modest tumour regression in a minor proportion of patients (Rosenberg, Lotze et al. 1987). Studies then found that human TILs from surgically-resected tumours were able to recognize and kill autologous tumour cells *in vitro* (Muul, Spiess et al. 1987). The first report of ACT using activated TILs in humans showed that autologous TILs induced a higher (60%), albeit transient, tumour response rate compared to LAK cells in patients with metastatic melanoma (Rosenberg, Packard et al. 1988). Efforts to extend these findings to other tumour types were hindered by the fact that TIL cultures from other cancers did not consistently produce cells capable of specific anti-tumour recognition (Rosenberg and Restifo 2015). This fueled studies to explore genetic engineering of T cells to express anti-tumour receptors.

Methods were developed to redirect the specificity of T cells by integrating genes for a regular T cell receptor or, more often, a CAR. CARs are constructed using antibody variable chains linked to intracellular signaling chains with costimulatory domains to activate T cells (Maher, Brentjens et al. 2002). CAR-T cells have been highly successful in treating B cell malignancies. The CD19 antigen, which is expressed on malignant and normal B cells, but no other cell of the body, proved a promising target antigen since B cell loss can be compensated for by regular infusions of immunoglobulin (Hill, Giralt et al. 2019). Landmark trials using CD19-CAR T cells showed potent anti-tumour effects, achieving sustained remissions in patients with lymphomas and lymphocytic leukemias (Kalos, Levine et al. 2011, Brentjens, Davila et al. 2013, Grupp, Kalos et al. 2013, Kochenderfer, Dudley et al. 2015). These led to US Food and Drug Administration (FDA) approval of two CD19-CAR T cells for the treatment of relapsed/refractory B cell lymphomas (Neelapu, Locke et al. 2017, Schuster, Bishop et al. 2019). However, the potency of CD19-CAR T cell responses leads to severe and at times lethal toxicities including cytokine release syndrome, neurotoxicity, infections, and impaired hematopoietic recovery in 30% of patients (Juluri, Wu et al. 2022).

Unfortunately, the success of CAR T cells has so far been limited to a subset of hematologic malignancies. In addition to responding to targets overexpressed on malignant tissue, T cells respond strongly to target antigens expressed even minimally on normal tissue. This has led to severe off-tumour toxicities in patients with other solid tumours, including melanoma and renal cell carcinoma (Johnson, Morgan et al. 2009, Lamers, Sleijfer et al. 2013). Even unforeseen cross-reactivities have occurred with antigens of similar homology to the target antigen and caused death in patients (Morgan, Chinnasamy et al. 2013). To date, the identification of target antigens on solid tumours that are absent on normal tissue has yielded few results.

Indeed, together the heterogeneous nature of tumour antigen expression, difficulty in identifying antigens uniquely expressed by tumour cells but not healthy cells, and propensity for antigenic drift as tumour cells rapidly proliferate and mutate has limited antigen-specific immunotherapies. Other immunotherapeutic approaches that may have broader success include 1) harnessing antigen-unrestricted anti-tumour immunity and 2) identifying and targeting alterations within immune cells that are fundamental to tumour-induced immune cell suppression.

1.3 Natural Killer cells

Natural Killer (NK) cells are innate lymphocytes that exert antigen-unrestricted anti-tumour immunity and as a result have gained tremendous attention as a promising cancer immunotherapeutic. NK cells were first discovered in the 1970s based on their ability to recognize and eliminate malignant cells without requiring prior sensitization nor antigen specificity (Herberman, Nunn et al. 1975, Kiessling, Klein et al. 1975, Kiessling, Klein et al. 1975, Pavie-Fischer, Kourilsky et al. 1975). NK cells make up roughly 5-20% of peripheral blood lymphocytes in humans (Angelo, Banerjee et al. 2015). NK cell activation is regulated by the integration of signals through numerous germline-encoded activation and inhibitory receptors expressed on their cell surface. NK cell inhibitory receptors recognize ligands constitutively expressed by healthy cells whereas activation receptors recognize ligands upregulated on stressed cells, such as cells that have undergone malignant transformation. NK cells are activated when the balance of activation signals outweighs that of inhibitory signals. Upon activation, NK cells can exert numerous effector functions to attack the target cell. These include direct cell cytotoxicity through the release of perforin and granzymes, the production of anti-tumour cytokines (in particular IFN-

γ), receptor-mediated target cell death, and antibody-dependent cell cytotoxicity (ADCC) via the CD16 receptor (Vivier, Tomasello et al. 2008, Bodduluru, Kasala et al. 2015, Freud, Mundy-Bosse et al. 2017). In this way, NK cells discriminate malignant cells from healthy cells without requiring any one specific signal. They are therefore capable of killing a broad array of malignant cells without harming healthy cells or requiring genetic modification.

1.3.1 NK cell immunophenotype and subsets

Classically, NK cell subsets have been primarily identified and studied based on phenotypic markers. Human NK cells are identified as lymphocytes that are positive for the neural cell adhesion molecule-1 CD56 and negative for the T cell marker CD3 ($CD56^{+}CD3^{-}$). NK cells are then broadly dichotomized based on the intensity of CD56 expression and presence of the CD16 ADCC receptor (Lanier, Le et al. 1986). $CD56^{bright}CD16^{-}$ NK cells are considered regulatory with greater cytokine-producing capabilities. $CD56^{dim}CD16^{+}$ NK cells are considered the antiviral/antitumour subset with greater cytotoxic functions (Fehniger, Shah et al. 1999, Cooper, Fehniger et al. 2001).

Additional receptor families function to tune NK cell activation and effector responses. Natural Cytotoxicity Receptors (NCRs) are a family of three transmembrane receptors: NKp30, NKp44, and NKp46. These transmit activation signals through interactions with the immunoreceptor tyrosine-based activation motifs (ITAMs) CD3ζ, FcR, or DAP12. NCRs recognize a diverse set of ligands that can be expressed or secreted by virally infected cells, tumour cells, or other immune cell subsets (Barrow, Martin et al. 2019). There are two main classes of receptors that bind major histocompatibility complex (MHC) I. C-type lectin receptors are nonpolymorphic, heterodimeric receptors that recognize non-classical MHC molecules such as

human leukocyte antigen (HLA)-E. These form by the combination of CD94 with either the inhibitory receptor NKG2A or the activation receptors NKG2D or NKG2C (Le Dréan, Vély et al. 1998, Bauer, Groh et al. 1999). Killer immunoglobulin receptors (KIRs) are highly polygenic and polymorphic reflecting the diversity of the classical MHC I molecules (HLA-A, -B, and -C) that they recognize (Freud, Mundy-Bosse et al. 2017). Inhibitory KIRs have long cytoplasmic domains that transmit inhibitory signals through an immune tyrosine-based inhibitory motif (ITIM) whereas activating KIRs have a short cytoplasmic domain and transduce activating signals through a TYRO protein tyrosine kinase binding protein (Campbell and Purdy 2011). The differential expression of these receptors and others is used to further specify NK cell developmental stages, effector subsets, and memory populations.

NK cells develop in various tissues in the body and as a result are a highly diverse class of immune cell. NK cells originate from the same $CD34^{+}CD45RA^{+}$ hematopoietic bone marrow progenitor cell as B cells and T cells. These progenitors then migrate to other sites in the body where they mature into $CD56^{+}CD3^{-}$ NK cells via an IL-15-dependent mechanism (Scoville, Freud et al. 2017). Peripheral blood NK cells (pbNK) are predominantly $CD56^{dim}CD16^{+}$, with $CD56^{bright}CD16^{-}$ NK cells making up less than 15% of NK cells in the peripheral blood of healthy donors (Caligiuri 2008). $CD56^{dim}$ pbNK cells have low expression of NKp46 and NKG2A, but greater levels of granzyme, perforin, KIRs, and NKG2C (Cooper, Fehniger et al. 2001). $CD56^{dim}$ NK cells are commonly considered to produce less IFNγ than $CD56^{bright}$ pbNK in response to cytokines but produce high amounts in response to receptor-mediated stimulation (Fehniger, Shah et al. 1999, Bjorkstrom, Riese et al. 2010). In contrast, $CD56^{bright}$ pbNK cells constitutively express NKG2A and NKp46 but lack expression of KIRs and NKG2C (Freud, Mundy-Bosse et al. 2017).

They are highly responsive to stimulation with cytokines, including IL-2, IL-12, IL-15, and IL-18, produced by myeloid or T cells (Fehniger, Shah et al. 1999).

In other tissues in the body, the relative proportion of $CD56^{dim}$ and $CD56^{bright}$ NK cells varies substantially from that of the peripheral blood. Whereas $CD56^{dim}$ NK cells make up the greater proportion of NK cells in the bone marrow, spleen, lung, and breast tissue, $CD56^{bright}$ NK cells predominate in secondary lymphoid tissue, liver, visceral adipose tissue, and uterus in healthy individuals (Hanna, Goldman-Wohl et al. 2006, Carrega, Morandi et al. 2008, Dogra, Rancan et al. 2020). Tissue-resident NK cells are capable of a diverse array of functions that can differ markedly from those of pbNK cells. For instance, uterine NK (uNK) cells have a regulatory functional profile and play a critical role in the establishment and progression of pregnancy (Hanna, Goldman-Wohl et al. 2006). uNK cells make up the majority (~70%) of immune cells in the uterus during the first half of human pregnancy (Bulmer, Morrison et al. 1991). Compared to even $CD56^{bright}$ pbNK cells, uNK cells are superbright for CD56 expression ($CD56^{superbright}$) yet express high levels of KIRs and CD9 (Verma, King et al. 1997). They also express distinct isoforms of NKp44 and NKp30 which reduce cytotoxicity and contribute to their unique secretome (Siewiera, Gouilly et al. 2015). Early in pregnancy, uNK cells regulate trophoblast invasion through the secretion of IL-8 and interferon-inducible protein-10 (IP-10). In addition, they are potent producers of pro-angiogenic factors such as VEGF and placental growth factor (PLGF) that are essential for spiral artery growth and remodeling in the decidua (Hanna, Goldman-Wohl et al. 2006). KIRs play a major role in regulating uNK cell function. For example, cross-linking of the activating KIR2DS4 receptor with its ligand on trophoblast cells augmented uNK cell growth factor production, whereas cross-linking of the inhibitory KIR2DL1 receptor suppressed cytokine secretion (Hanna, Goldman-Wohl et al. 2006).

1.4 NK cell cancer immunotherapy

The role of NK cells in tumour immunosurveillance became apparent by studies showing that both mice and humans deficient in NK cells or with defects in NK cell function had an increased occurrence of cancer. For instance, one study demonstrated that mice became unable to reject B cell lymphoma when depleted of NK cells and that this mechanism was perforin-dependent (Street, Hayakawa et al. 2004). In models of spontaneous prostate and lymphoid cancers, mice lacking the NK cell activation receptor NKG2D were found to have increased cancer occurrence and more aggressive tumour growth (Guerra, Tan et al. 2008). Another study found that mice with blockade of tumour necrosis factor-related apoptosis-inducing ligand (TRAIL) on NK cells lost the ability to prevent liver metastases (Takeda, Hayakawa et al. 2001). Similarly, humans with primary NK cell immunodeficiency are highly susceptible to developing cancer (Orange 2013). Furthermore, an 11-year prospective study demonstrated that low NK cell cytotoxic activity was associated with increased cancer risk in an initially healthy population compared to medium and high cytotoxic activity (Imai, Matsuyama et al. 2000). The presence of cytotoxic NK cells in human tumours has also been associated with improved prognosis in many cancer types, including lung, breast, colorectal, and gastric cancers (Coca, Perez-Piqueras et al. 1997, Ishigami, Natsugoe et al. 2000, Villegas, Coca et al. 2002, Bouzidi, Triki et al. 2021). Such studies lay the foundation that potentiating NK cell anti-tumour functions could prove beneficial for cancer treatment.

The first human trials to harness NK cell antitumour functions used IL-2 to activate autologous NK cells *in vitro* and *in vivo*. In these trials, lymphocytes from patients with advanced metastatic cancer were harvested, activated with IL-2, and subsequently infused back into the

patient along with IL-2. These studies demonstrated that NK cells were capable of persisting *in vivo*, however the clinical responses were disappointing and significant toxicities were associated with IL-2 infusion (Rosenberg, Lotze et al. 1987, Rosenberg, Lotze et al. 1993, Hawkins, Atkins et al. 1994, Sparano, Fisher et al. 1994, deMagalhaes-Silverman, Donnenberg et al. 2000). A subsequent trial in patients with metastatic melanoma and renal cell carcinoma treated lymphodepleted patients with purified NK cells that had been pre-activated with irradiated PBMC feeder cells, IL-2, and OKT3. While these NK cells demonstrated high cytotoxic activity *in vitro* following pre-activation, they failed to induce a clinical response and were unable to kill tumour cells *in vitro* following re-isolation unless re-activated with IL-2 (Parkhurst, Riley et al. 2011).

With a growing understanding of inhibitory KIRs and their ligands, studies then focused on using allogeneic NK cells. In the hematopoietic transplant setting, it was shown that NK cell alloreactivity from KIR-mismatched donors could prevent leukemia relapse, graft rejection, and graft-versus-host disease. Indeed, patients receiving NK cells from KIR-mismatched donors had a 55% increase in 5-year event-free survival compared to NK cells from donors without KIR incompatibility (Ruggeri, Capanni et al. 2002). Building on these findings, another trial in patients with poor-prognosis acute myeloid leukemia (AML) found that the adoptive transfer of IL-2-activated NK cells from haploidentical donors induced remission in 26% of patients (Miller, Soignier et al. 2005). However, remission was not durable and patients eventually relapsed.

Despite the therapeutic potential, the development of NK cell therapies has faced two principal limitations. The first was that it was difficult and inefficient to obtain sufficient numbers of NK cells for a clinical effect and wide-scale repeated therapeutic use. The second and outstanding challenge is that, while NK cells have achieved therapeutic effects against hematologic

cancers, they have to date failed to achieve a therapeutic effect against solid tumours. These limitations will be discussed in sections 1.5 and 1.6.

1.5 Generation of large numbers of NK cells through expansion

The reasons underlying the difficulties in generating sufficient numbers of NK cells were twofold. Deficiency in NK cell numbers was due to in part to the fact that NK cells form only a small percent of peripheral blood mononuclear cells (PBMCs) in the blood and it is therefore difficult to obtain large numbers of NK cells by directly isolating them from blood (Denman, Senyukov et al. 2012). The second is that NK cells proved difficult to grow in culture, particularly compared to T cells. However, with increasing knowledge of NK cell survival, activation, and proliferation, methods to expand NK cells *ex vivo* have been developed over the past two decades.

Initial attempts to expand NK cells from either PBMCs or a purified population used cytokine combinations, such as IL-2 and IL-15, that are known to promote NK cell proliferation and antitumour functions. Although cytokine-based expansion effectively increased NK cell antitumour functions *in vitro*, expansion was relatively limited (Klingemann and Martinson 2004). Application of this approach is expensive and was only capable of yielding a single infusion of a limited cell dose – typically less than 2×10^7 NK cells/kg body weight. However, it did produce some clinical responses in patients with hematologic cancers without adverse toxicities (Miller, Soignier et al. 2005, Shi, Tricot et al. 2008, Meyer-Monard, Passweg et al. 2009, Bachanova, Burns et al. 2010, Rubnitz, Inaba et al. 2010).

The use of feeder cells, which naturally or via genetic engineering express NK cell activation ligands, further improved NK cell expansion. Initial studies expanded isolated healthy donor pbNK cells using irradiated autologous PBMCs as feeder cells along with cytokines (IL-2

and/or IL-15) for 19 days. Under these conditions, NK cells expanded ~120-fold but exerted only moderate antitumour functions (Siegler, Meyer-Monard et al. 2010). One of the first studies to investigate expanding NK cells from cancer patients utilized a similar method and found that cancer patient NK cells cultured with allogeneic feeder cells from healthy donors expanded 300-fold over 14 days compared to 160-fold using autologous feeder cells (Kim, Ahn et al. 2013).

In parallel, methods using feeder cell lines as opposed to isolated PBMCs to stimulate NK cell expansion were developed. An early study to this end showed that NK cells isolated from healthy donor PBMCs and expanded using an irradiated Epstein-Barr virus (EBV)-transformed lymphoblastoid cell line and IL-2 achieved 490-fold expansion over 21 days. These NK cells had increased expression of death receptor ligands and activation receptors and enhanced antitumour functions compared to unexpanded NK cells (Berg, Lundqvist et al. 2009). Another feeder cell line developed was a modified K562 cell line. K562 cells are a cell line of AML and highly susceptible to NK cell killing. These K562 cells were genetically engineered to express membrane-bound IL-15 and the activating ligand 4-1BBL (K562-mb15-41BBL). Co-culture of healthy donor PBMCs with irradiated K562-mb15-41BBL cells and IL-2 expanded NK cells 277- to 550-fold over 21 days (Fujisaki, Kakuda et al. 2009, Gong, Xiao et al. 2010). These expanded NK cells displayed enhanced *in vitro* cytotoxicity against AML cells and abrogated disease progression in a xenograft mouse model of AML. AML patient NK cells also expanded comparably to healthy donor NK cells using this method and had similar *in vitro* antitumour functions (Fujisaki, Kakuda et al. 2009). While these studies marked significant progress towards generating large numbers of NK cells, expansion was limited to 21 days due to telomere shortening and cellular senescence in the expanded NK cell product (Fujisaki, Kakuda et al. 2009).

A seminal study by Denman *et al.* further modified the K562 feeder cell line and presented a major advance in NK cell expansion (Denman, Senyukov et al. 2012). K562 cells were engineered to express the stimulatory ligands FcγRI, B7-2, truncated CD19, 4-1BBL as well as either mbIL-15 or mbIL-21. IL-21 is a member of the common γ chain cytokines, alongside IL-2 and IL-15. It was discovered in the year 2000 based on its ability to promote the proliferation and maturation of NK cells from bone marrow (Parrish-Novak, Dillon et al. 2000). IL-21 was later found to signal through signal transducer and activator of transcription (STAT)1 and STAT3 and activate the mitogen-activated protein kinase (MAPK) and phosphatidylinositol-3-kinase (PI3K) pathways to promote NK cell proliferation (Zeng, Spolski et al. 2007). As with other common γ chain cytokines, IL-21 augments NK cell cytotoxicity via the upregulation of perforin and granzymes (Skak, Frederiksen et al. 2008). Denman *et al.* found that K562s expressing membrane-bound IL-21 (K562mbIL21) produced robust log phase expansion of NK cells from the PBMCs of healthy donors without senescence for up to 6 weeks. By day 21, NK cells expanded with K562mbIL21 expanded 48,000-fold as compared to 825-fold with K562mbIL15. Paradoxically, the telomeres of K562mbIL21-expanded NK cells lengthened, rather than shortened, with proliferation. Furthermore, K562mbIL21-expanded NK cells had increased cytotoxicity and antitumour cytokine production against a number of tumour cell lines compared to freshly isolated pbNK cells (Denman, Senyukov et al. 2012). A subsequent clinical trial used K562mbIL21-expanded NK cells to treat patients with high-risk myeloid malignancies. By 15 months post-NK cell treatment, 92% of NK-treated patients were still alive compared to 55% of untreated patients in a retrospective cohort. Furthermore, only 8% of patients in the NK-treated group relapsed in that time compared to 22% of patients in the control group. Importantly, treatment with K562mbIL21-expanded NK cells was found to be safe, with no toxicities observed (Ciurea,

Schafer et al. 2017). These findings underscore the feasibility and therapeutic benefits of using expanded NK cells to treat hematologic malignancies and instigated a myriad of other clinical trials to this end.

1.6 Current limitation for NK cell therapies: the immunosuppressive tumour microenvironment

While promising for the treatment of hematological malignancies, NK cells have yet to demonstrate clinical effects in patients with solid tumours. Solid tumours pose an added challenge for immunotherapies, including NK cells, due to the immunosuppressive TME which impairs immune cell function. NK cells in tumours have an immunoregulatory phenotype with down-regulated expression of activation receptors and impaired cytotoxic functions (Berek, Bast et al. 1984, Lai, Rabinowich et al. 1996, Belisle, Gubbels et al. 2007). Indeed, studies have reported significant differences in the NK cell subsets in malignant versus adjacent non-malignant human tissues. In human breast, colon, and melanoma tumour tissues, there was a selective enrichment in $CD56^{bright}$CD16- NK cells (Levi, Amsalem et al. 2015). Similar enrichment in $CD56^{bright}CD16^{-}$ NK cells was found in NSCLC tissue and the ascites TME of ovarian cancer and these NK cells had broadly reduced expression of activation receptors and an impaired ability to kill tumours cells and produce IFN-γ (Belisle, Gubbels et al. 2007, Carrega, Morandi et al. 2008, Platonova, Cherfils-Vicini et al. 2011). In neoplastic lung and breast tissue, an increase in a $CD56^{bright}CD16^{-}$ NK cell population coincided with reduced expression of $CD56^{dim}$-recruiting chemokines and increased expression of $CD56^{bright}$-recruiting chemokines (Carrega, Bonaccorsi et al. 2014). NK cells in tumours also show an altered maturation profile. In NSCLC, an enrichment in CD11b-CD27- NK cells was reported, which is a highly immature and inactive phenotype (Jin, Fu et al. 2013). These

findings suggest that altered trafficking and maturation may both contribute to the skewing of NK cell subsets in neoplastic tissue.

Further work has shown that tumour-associated NK (taNK) cells not only lose their antitumour phenotype and function, they also adopt a tumour-promoting profile. In multiple tumour types including melanoma, breast, colon, and ovarian tumours, NK cells express surface markers similar to regulatory uNK cells including CD9 and chemokine receptor 3 (CXCR3) and secrete the pro-angiogenic factor VEGF (Levi, Amsalem et al. 2015, Gonzalez, Huang et al. 2021). In NSCLC and colorectal cancer, taNK cells were found to produce multiple proangiogenic factors, including VEGF, PLGF, IL-8, and angiogenin, and directly induce endothelial cell migration and capillary formation (Bruno, Focaccetti et al. 2013, Bruno, Bassani et al. 2018). NK cells in malignant pleural effusions were also shown to express the uNK-like markers CD49a and CD69, secrete VEGF, and promote capillary formation (Bosi, Zanellato et al. 2018). The consequences of regulatory taNK cells in the TME remain unexplored, but are suggested by studies that found that in some cases the presence of NK cells in the tumour can be an indicator of worse prognosis, advanced stage, and increased tumour size in a number of cancers including ovarian, NSCLC, and breast cancer (Vgenopoulou, Lazaris et al. 2003, Dong, Elstrand et al. 2006, Jin, Fu et al. 2013). However, a phenotypic and functional analysis of NK cells in such cases has not been reported.

The TME directly suppresses cytotoxic NK cell phenotype and function. Co-culture of healthy donor pbNK cells with NSCLC cells for 5 days caused a down-regulation of NK cell activating receptors, degranulation, and IFN-γ production via both contact-dependent and-independent mechanisms (Platonova, Cherfils-Vicini et al. 2011). *Ex vivo* culture of healthy donor pbNK cells in ascites fluid from ovarian cancer patients for 3 days similarly caused an increase in

$CD56^{bright}CD16^{-}$ NK cells with reduced activation receptor expression and antitumour function (Belisle, Gubbels et al. 2007). This strong immunosuppression in the TME has so far limited the effectiveness of NK cell therapy using even activated cytotoxic NK cells against solid tumours. Following adoptive transfer to patients with melanoma, renal cell, breast, or ovarian cancers, cytokine-activated pbNK cells were found to have impaired function and failed to achieve clinical effects in tumour reduction (Geller and Miller 2011, Parkhurst, Riley et al. 2011). If the impairment of NK cells by solid tumours can be overcome, NK cell therapy may achieve similar success for solid tumours as it has for the treatment of hematologic malignancies. However, how the TME fundamentally alters NK cells to cause suppression remains poorly understood.

1.7 Immunometabolism: a fundamental regulator of immune cell function

Cellular metabolism plays a critical role in the regulation of immune cell function. Cellular metabolism encompasses the catabolic pathways that generate ATP for energy and the anabolic pathways which use ATP for biosynthesis (Figure 1). As reviewed elsewhere (O'Neill, Kishton et al. 2016), glucose is a major metabolic fuel used by immune cells and is catabolized via glycolysis to pyruvate. Anaerobically, pyruvate is then converted to lactate and secreted by the cell as lactic acid. Glycolysis rapidly generates ATP and is therefore often highly active in immune cells that require rapid energy. Aerobically, pyruvate can also be converted to acetyl-CoA and further oxidized in the mitochondria by the tricarboxylic acid (TCA) cycle to fuel oxidative phosphorylation (OxPhos). The catabolism of other biomolecules, such as glutamine via glutaminolysis and fatty acids via fatty acid oxidation can also be used to fuel the TCA cycle and OxPhos. The TCA cycle contains oxidation steps which generate redox reagents that provide electrons to fuel ATP synthesis via OxPhos. OxPhos is a series of redox reactions that generates a

proton gradient across the inner mitochondrial membrane; the resulting membrane potential is then used to drive ATP production. OxPhos is a slower, but efficient method of ATP production and is therefore predominant in the metabolic profile of resting immune cells or cells in nutrient-low conditions. Depending on the metabolic needs of the cell, intermediates in the TCA cycle can also be diverted to anabolic pathways such as fatty acid synthesis and amino acid synthesis (O'Neill, Kishton et al. 2016).

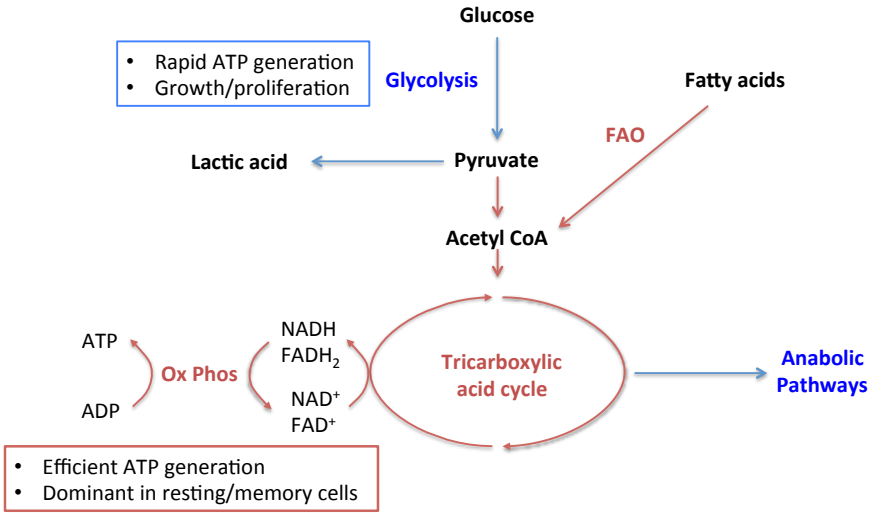

Figure 1. Summary of major intracellular metabolic pathways. Glycolysis is the process by which glucose it catabolized to pyruvate and in the process generates ATP. Pyruvate can be converted to lactate anaerobically and secreted by the cell as lactic acid. In the presence of oxygen, pyruvate can also be converted to acetyl-CoA which is oxidized in the mitochondria by the tricarboxylic acid cycle. The catabolism of other biomolecules, such as glutamine via glutaminolysis and fatty acids via fatty acid oxidation (FAO) can also be used to fuel the TCA cycle. The TCA cycle generates substrates for anabolic pathways and nicotinamide adenine dinucleotide (NADH) and reduced flavin adenine dinucleotide ($FADH_2$) which provide electrons to fuel ATP synthesis via OxPhos. OxPhos is a series of redox reactions that generates a proton gradient and resulting membrane potential across the inner mitochondrial membrane which is used to drive ATP production. Red denotes pathways relatively dominant in resting immune cells; blue denotes relatively dominant pathways in activated immune cells.

It has been demonstrated with numerous immune cell types that differential activity of metabolic pathways dictates different functional states. For instance, in macrophages, high levels of glycolysis and low oxidative metabolic activity supports pro-inflammatory phenotype and functions, whereas a highly oxidative, low glycolytic profile supports anti-inflammatory functions (Jha, Huang et al. , Vats, Mukundan et al. 2006, Rodriguez-Prados, Traves et al. 2010). Similarly, the activity of metabolic pathways regulates T cell polarization and function. Effector T cells up-regulate fatty acid synthesis and glycolysis, both of which are required for effector T cell polarization and cytotoxic functions (Chang, Curtis et al. 2013, Berod, Friedrich et al. 2014). Regulatory T cells are primarily oxidative and require OxPhos for regulatory functions (Michalek, Gerriets et al. 2011). The generation of memory T cells requires a metabolic shift towards fatty acid oxidation and increased oxidative capacity (Pearce, Walsh et al. 2009, van der Windt, Everts et al. 2012, O'Sullivan, van der Windt et al. 2014). The fundamental role for metabolism in T cell function is highlighted by the fact that inducing these different metabolic pathways in T cells determines T cell polarization fate (Pearce, Walsh et al. 2009, Michalek, Gerriets et al. 2011, Buck, O'Sullivan et al. 2016). Importantly, the metabolic signature of T cells has been shown to underpin T cell anti-cancer potential (Kawalekar, O'Connor et al. 2016).

As with other immune cell types, NK cell metabolism critically regulates NK cell effector functions (Marçais, Viel et al. 2013, Donnelly, Loftus et al. 2014, Keppel, Saucier et al. 2015, Mao, van Hoef et al. 2016). Upon activation, NK cells up-regulate glycolysis and OxPhos, both of which have been shown to be critical for NK cell IFN-γ production and cytotoxicity (Donnelly, Loftus et al. 2014, Keppel, Saucier et al. 2015). For instance, cytokine stimulation increases NK cell glycolysis and OxPhos; correspondingly, inhibition of a key regulator of glycolysis, the mechanistic target of rapamycin (mTOR), impaired activation-induced NK cell IFN-γ production,

granzyme B expression, and glucose uptake both *in vitro* and *in vivo* (Marçais, Viel et al. 2013, Donnelly, Loftus et al. 2014). As with glycolysis inhibition, limiting the rate of NK cell OxPhos has also been shown to inhibit NK cell IFN-γ production and degranulation following cytokine stimulation (Keating, Zaiatz-Bittencourt et al. 2016).

Recent evidence indicates that immunosuppressive signals may also mediate NK cell inhibition through metabolic alteration. For instance, Viel and colleagues demonstrated that transforming growth factor beta (TGFβ) inhibits NK cell anti-tumour functions by inhibiting the mTOR pathway and downstream glycolysis (Viel, Marçais et al. 2016). Given that the TME inhibits NK cell function and that glycolysis and OxPhos are critical for NK cell activation and cytotoxic functions, elucidating the effects of the TME on NK cell metabolic state may reveal central nodes in the mechanism of tumour-induced NK cell inhibition.

1.8 The metabolically hostile tumour microenvironment

Altered cellular metabolism is a hallmark of tumour initiation and progression. In the 1920s, Otto Warburg began to characterize this altered metabolism by observing that tumour cells consume enormous amounts of glucose which they convert to lactate via glycolysis, even in the presence of oxygen (Warburg 1924, Warburg 1925, Warburg, Wind et al. 1927). Such a metabolic profile, termed "the Warburg effect," contributes to malignant transformation and tumour progression as it enables numerous cellular growth and proliferative advantages. Increased glycolytic flux functions to funnel more glycolytic intermediates into anabolic pathways for amino acid, lipid, and nucleotide synthesis, which are required for proliferation. For instance, the serine synthesis and one-carbon metabolism pathway is a major offshoot fed by the glycolytic intermediate 3-phosphoglycerate (Locasale and Cantley 2011, Yang and Vousden 2016). In

addition to feeding nucleotide- and amino acid-synthesizing pathways, it also drives glutathione antioxidant production, which conferred tumour cells protection from hypoxia-induced oxidative stress (Ye, Fan et al. 2014). Conversion of glucose to lactate also produces high levels of nicotinamide adenine dinucleotide phosphate (NADPH) all the while limiting ATP production by TCA cycle activity which negatively regulates glucose metabolism. In addition to glucose, tumours also consume large amounts of other nutrients, including amino acids such as glutamine. Such high levels of nutrient consumption and secretion of lactic acid together with aberrant vascularization creates a metabolically hostile environment.

As tumours grow, they must adapt to the changes in the TME that are a consequence of their growth, including increasing levels of nutrient deprivation, hypoxia, and acidification. Tumour cells adapt to this hostile environment via a number of mechanisms, including increased oncogene-driven expression of nutrient transporters, metabolic flexibility, and cellular redox control. For a non-transformed cell, nutrient uptake is regulated by external environment factors. Indeed even in a nutrient-replete environment, mammalian cells require growth factors to take up nutrients in a constitutive manner (Palm and Thompson 2017). However, oncogenes upregulate nutrient receptors on tumour cells enabling them to constitutively take up nutrients independent of growth factors. For instance, the oncogene KRAS endows cancer cells with a survival and growth advantage in low-glucose conditions. Tumour cells bearing the KRAS mutation had increased glucose transporter (GLUT)1 expression which enabled them to outcompete their wild-type (WT) counterparts when glucose was scarce (Yun, Rago et al. 2009). Glutamine is also rapidly consumed by tumour cells and used to synthesize nucleotides and amino acids to support rapid proliferation. Overexpression of the transcription factor c-myc by tumour cells increases expression of glutamine transporters and glutamine-utilising enzymes to facilitate constitutive glutamine uptake

(Eberhardy and Farnham 2001, Mannava, Grachtchouk et al. 2008, Gao, Tchernyshyov et al. 2009). In addition to increased uptake of classic nutrients like glucose and glutamine, tumour cells utilize alternative methods to scavenge nutrients. Expression of mutant Ras enables tumour cells to source free amino acids from extracellular proteins (which are not typically used as a source of amino acids) via macropinocytosis (Commisso, Davidson et al. 2013, Palm, Park et al. 2015). Although lactate is typically considered a waste product, tumour cells have been found to take up lactate via the monocarboxylate transporter 1 (MCT1) and use it to fuel oxidative metabolism (Sonveaux, Végran et al. 2008). Some cancer cells also extract nutrients from neighbouring cells. Ovarian cancer cells were found to directly take up lipids from omental adipocytes via expression of fatty acid-binding protein 4 (FABP4) which promoted tumour growth (Nieman, Kenny et al. 2011). While most mammalian cells require a source of exogenous glutamine to grow and proliferate, some tumour cells are capable of synthesizing glutamine *de novo* (Yuneva, Fan et al. 2012). Cancer cells can also withstand extended periods of nutrient deprivation even without alternative extracellular nutrients by consuming their own macromolecules or organelles via autophagy (Strohecker, Guo et al. 2013). Further evidence of tumour metabolic flexibility is that under acidotic conditions, tumour cells have been shown to rapidly switch from using glycolysis to fatty acid oxidation as the principal method of generating acetyl-CoA which supported continued respiration and growth while restraining ROS production (Corbet, Pinto et al. 2016). The ability to switch to increased fatty acid oxidation by tumour cells has also been reported to confer a survival advantage in response to hypoxia and low-glucose conditions (Zaugg, Yao et al. 2011).

Although tumour cells are well-adapted to deal with the metabolic stressors of the TME, this hostility has consequences for immune cell function. One study found that tumour cells

outcompeted T cells for glucose and the resulting glucose-deficient microenvironment inhibited T cell IFN-γ production by suppressing T cell glycolysis (Chang, Curtis et al. 2013). Furthermore, high levels of lactic acid secreted by tumour cells caused lactic acid accumulation in T cells, disrupting T cell glycolysis and consequent effector function (Fischer, Hoffmann et al. 2007). Elevated levels of lactic acid have been shown to also impair NK cell function and activation-induced increase in intracellular ATP levels, suggesting a disruption in NK cell metabolism (Brand, Singer et al. 2016). However, the effects of the TME on NK cell metabolism have not been defined. Given the metabolic requirements for NK cell activation and effector function, together with the metabolic hostility of the TME, metabolic stress may be a critical regulator of NK cell inhibition in the TME. Thus, modulating NK cell metabolism may be a promising target for improving NK cell function against tumours.

1.9 Central aim and thesis objectives

Harnessing the anti-cancer abilities of immune cells holds promise to treat poor prognosis cancers. In particular, NK cells are an attractive cell therapy candidate due to their ability to broadly discern healthy from malignant cells without requiring prior sensitization nor antigen specificity. Indeed, NK cells have already demonstrated strong therapeutic efficacy in patients with hematologic malignancies. However, the development of broadly effective immunotherapies to treat solid tumours has been hindered for decades due to the highly immunosuppressive TME. Immune suppression by the TME has yet to be overcome largely due to the fact that the mechanisms that cause immune cell inhibition by the TME remained poorly understood.

The central aim *of this thesis is to understand and overcome NK cell inhibition by the TME in order to develop effective NK cell therapies for poor prognosis solid tumours.*

The major findings in this thesis are organized into three chapters, each of which contributes to the overall aim of the thesis. The specific objectives of the thesis that are addressed in **Chapters 2-5** are described below:

Objective 1: *To investigate whether ex vivo expanded NK cells from ovarian cancer patients or healthy donors could reduce ovarian cancer tumour burden.* Results pertaining to this objective have been published in the following manuscript:

Chapter 2: Poznanski SM, Nham T, Chew MV, Lee AJ, Hammill JA, Fan IY, Butcher M, Bramson JL, Lee DA, Hirte H, Ashkar AA. (2018). Expanded $CD56^{superbright}CD16^{+}$ NK cells from ovarian cancer patients are cytotoxic against autologous tumor in a patient-derived xenograft murine model. *Cancer Immunology Research 6*, 1174-1185.

Objective 2: *To investigate whether ex vivo expanded NK cells could kill lung cancer patient tumours and sensitize patients' non-responding tumours to PD1-blockade therapy.* Results pertaining to this objective have been published in the following manuscript:

Chapter 3: Poznanski, S.M., Ritchie, T.R., Fan, I.Y., El-Sayes, A., Portillo, A.L., Ben-Avi, R.A., Chew, M.V., Shargall, Y., and Ashkar, A.A. (2020). Expanded human NK cells from lung cancer patients sensitize patients' PDL1-negative tumours to PD1-blockade therapy. *Journal for Immunotherapy of Cancer 9*, e001933.

Objective 3: *To elucidate and manipulate metabolic mechanisms of NK cell suppression in the TME to overcome NK cell inhibition.* Results pertaining to this objective have been published in the following manuscript:

Chapter 4: Poznanski SM, Singh K, Ritchie TM, Aguiar JA, Fan IY, Portillo AL, Rojas EA, Vahedi F, El-Sayes A, Xing S, Butcher M, Lu Y, Doxey AC, Schertzer JD, Hirte HW, Ashkar AA. (2021) Metabolic flexibility determines human NK cell functional fate in the tumor microenvironment. *Cell Metabolism* 33(6), 1205-1220.e5.

Objective 4: *To elucidate the metabolic programs of regulatory NK cells.* Results pertaining to this objective are in preparation in the following manuscript:

Chapter 5: Poznanski SM, Ritchie TM, Mazen MA, Portillo A, Vahedi F, Chan L, Singh K, Zhang J, Lye S, Ashkar AA. Distinct metabolic programs underpin regulatory and cytotoxic NK cells. [Manuscript in preparation]

The data included in each manuscript required a collaborative effort among numerous institutions, colleagues, and laboratory members. The specific details regarding authorship and contributions can be found in the **Preface** of each chapter.

– CHAPTER 2 –

EXPANDED CD56^{SUPERBRIGHT}CD16^{+} NK CELLS FROM OVARIAN CANCER PATIENTS ARE CYTOTOXIC AGAINST AUTOLOGOUS TUMOUR IN A PATIENT-DERIVED XENOGRAFT MODEL

Expanded CD56^{superbright}CD16^{+} NK cells from ovarian cancer patients are cytotoxic against autologous tumour in a patient-derived xenograft murine model

Sophie M. Poznanski[1], Tina Nham[1], Marianne V. Chew[1], Amanda J. Lee[1], Joanne A. Hammill[1], Isabella Y. Fan[1], Martin Butcher[2], Jonathan L. Bramson[1], Dean A. Lee[3], Hal Hirte[4], Ali A. Ashkar[1]

[1] Department of Pathology and Molecular Medicine, McMaster Immunology Research Centre, McMaster University, Hamilton, ON, Canada.

[2] Juravinski Cancer Centre & McMaster University, Hamilton, ON, Canada.

[3] The Research Institute at Nationwide Children's Hospital, Ohio State University, Columbus, Ohio, USA.

[4] Department of Oncology, Division of Medical Oncology, Juravinski Cancer Centre, Hamilton, ON, Canada

© Poznanski SM *et al. Cancer Immunol Res*, 2018; 6 (10): 1174-1185. https://doi.org/10.1158/2326-6066.CIR-18-0144.

Preface: *The research presented in this manuscript was conducted from 2015-2018. SM Poznanski conceived and designed the project, performed experiments, analyzed the data, and wrote the manuscript. T Nham performed experiments in Figure 5. MV Chew, AJ Lee, JA Hammill and IY Fan provided technical help and expertise for experiments. M Butcher provided assistance in project coordination and patient sample acquisition. JL Bramson provided expertise for experiments. Lee DA assisted with the development of methodology. Hirte HW provided intellectual input and clinical expertise, contributed to experimental design, guided clinical sample*

acquisition, obtained funding support, and edited the manuscript. Ashkar AA conceived and designed the project, performed experiments, obtained funding support, and supervised the project.

Title: Expanded CD56^{superbright}CD16^{+} NK cells from ovarian cancer patients are cytotoxic against autologous tumor in a patient-derived xenograft murine model

Authors: Sophie M. Poznanski[1], Tina Nham[1], Marianne V. Chew[1], Amanda J. Lee[1], Joanne A. Hammill[1], Isabella Y. Fan[1], Martin Butcher[2], Jonathan L. Bramson[1], Dean A. Lee[3], Hal Hirte[4], Ali A. Ashkar[1]

1 Department of Pathology and Molecular Medicine, McMaster Immunology Research Centre, McMaster University, Hamilton, ON, Canada. **2** Juravinski Cancer Centre & McMaster University, Hamilton, ON, Canada. **3** The Research Institute at Nationwide Children's Hospital, Ohio State University, Columbus, Ohio, USA. **4** Department of Oncology, Division of Medical Oncology, Juravinski Cancer Centre, Hamilton, ON, Canada

Running Title: Autologous cytotoxic NK cells for ovarian cancer treatment

Abbreviations List: Natural Killer cell = NK cell; OCP = ovarian cancer patient; HD = healthy donor; PB = peripheral blood; NRG = NOD-*Rag1*^{null} *IL2rg*^{null}; K562-mb-IL21 = K562 cells genetically modified to express membrane-bound IL21; MFI = mean fluorescence intensity

Corresponding author: Ali A. Ashkar; McMaster Immunology Research Centre, Room 4015 Michael DeGroote Centre for Learning & Discovery, 1280 Main Street West, Hamilton, ON L8S 4K1; Phone: (905) 525-9140 ext. 22311; E-mail: ashkara@mcmaster.ca

Keywords: Ovarian cancer, expanded CD56^{superbright} NK cells, autologous cell therapy, immunotherapy, patient-derived xenograft

Conflict of Interest Disclosure: J.A. Hammill has ownership interest in Triumvira Immunologics, Inc. D.A. Lee is Chair of the Medical and Scientific Advisory Board for CytoSen Therapeutics, has received honoraria from speakers bureau honoraria from Miltenyi Biotec, has ownership interest in CytoSen Therapeutics and Ziopharm Oncology, Inc., and is a consultant/advisory board member for Courier Therapeutics. H.W. Hirte is a consultant/advisory board member for AstraZeneca and Roche. No potential conflicts of interest were disclosed by the other authors.

2.1 ABSTRACT

Natural Killer (NK) cells are useful for cancer immunotherapy and have proven clinically effective against hematological malignancies. However, immunotherapies for poor prognosis solid malignancies, including ovarian cancer, have not been as successful due to immunosuppression by solid tumors. Although re-arming patients' own NK cells to treat cancer is an attractive option, success of that strategy is limited by the impaired function of NK cells from cancer patients and by inhibition by self-MHC. In this study, we show that expansion converts healthy donor and immunosuppressed ovarian cancer patient NK cells to a cytotoxic $CD56^{superbright}CD16^{+}$ subset with activation state and antitumor functions that increase with CD56 brightness. We investigated whether these expanded NK cells may overcome the limitations of autologous NK cell therapy against solid tumors. Peripheral blood- and ascites-derived NK cells from ovarian cancer patients were expanded then adoptively transferred into cell-line and autologous patient-derived xenograft models of human ovarian cancer. Expanded ovarian cancer patient NK cells reduced the burden of established tumors and prolonged survival. These results suggest that $CD56^{bright}$ NK cells harbour superior antitumor function compared to $CD56^{dim}$ cells. Thus, NK cell expansion may overcome limitations on autologous NK cell therapy by converting the patient's NK cells to a cytotoxic subset that exerts a therapeutic effect against autologous tumor. These findings suggest that the value of expanded autologous NK cell therapy for ovarian cancer and other solid malignancies should be clinically assessed.

2.2 INTRODUCTION

Ovarian cancer is a deadly gynecological cancer with a 5 year survival rate of less than 50% (1). Each year in the United States, approximately 22,440 women are diagnosed with ovarian cancer and 14,080 die of the disease (2). High grade serous ovarian carcinoma is the most common ovarian cancer subtype and accounts for the majority of these deaths (3). The poor survival rate of ovarian cancer can often be ascribed to a late diagnosis due to the cancer's asymptomatic nature in early stages, a high rate of relapse following first-line treatments, and lack of effective therapies for recurrent, often chemoresistant, cancer (4-6). Second-line therapies that reduce and treat cancer recurrence are needed.

Natural Killer (NK) immune cells have garnered attention as a cancer immunotherapeutic due to their ability to kill malignant cells and spare healthy cells (7). NK cell cytotoxicity is regulated through a balance of activating and inhibitory receptors: through the integration of activation and inhibitory signals, NK cells hone their cytotoxic activity against malignant cells without harming healthy cells (7). This attribute prevents off-tumor toxicity. The safety of adoptive NK cell transfer has been demonstrated in the clinical setting (8). Furthermore, the adoptive transfer of NK cells has demonstrated clinical effectiveness in treating hematological malignancies, underscoring the value of NK cell cancer immunotherapy (8,9).

Despite the therapeutic potential, NK cell therapies have been of limited value against solid tumors due to an inability to maintain NK cell cytotoxicity in the immunosuppressive tumor environment. Although NK cells are cytotoxic against ovarian cancer cells *in vitro* through engagement of activating receptors with respective ligands on ovarian cancer cells (10), the tumor microenvironment *in vivo*, including ascites in the case of ovarian cancer, inhibits NK cell antitumor functions (11-16). In fact, tumor-associated ascites-NK cells are hypo-responsive to

tumor targets due to reduced expression of activation receptors, including NKp30 and DNAM-1, driven by chronic engagement with activating receptor ligands expressed or shed by tumor cells (17,18). In addition, ascites-NK cells over-express certain inhibitory receptors, including the immune checkpoint receptor PD-1 that hampers the NK cell antitumor response (19). In the clinical setting, IL2-activated allogeneic NK cells had limited effects in patients with breast and ovarian cancer (20). Furthermore, the adoptive transfer of *in vitro*-activated autologous NK cells to patients with melanoma or renal cell carcinoma failed to achieve a clinical response as the cytotoxic function of NK cells was impaired (21). If the impairment in function of adoptively transferred NK cells by solid tumors could be overcome, NK cell therapy might be as successful for solid tumors as it already is for hematological malignancies.

NK cells fall into two major subsets: $CD56^{dim}CD16^{+}$ cytotoxic NK cells and $CD56^{bright}CD16^{-}$ immunoregulatory and poorly cytotoxic NK cells (22). However, pre-activation of peripheral blood (PB)-NK cells with IL15 causes $CD56^{bright}$ NK cell anti-tumor functions to exceed those of $CD56^{dim}$ NK cells. Thus modulation of $CD56^{bright}$ NK cells can improve their antitumor functions and merits further exploration as a cancer immunotherapy (23).

A feeder cell-based NK cell expansion protocol has been developed that generates NK cells that are clinically effective against leukemia (8). Expanded NK cells may be promising for the treatment of solid malignancies: one study demonstrated that expanded PB-NK cells from healthy donors reduced tumor burden in a cell-line xenograft ovarian cancer model, suggesting expansion may improve NK cell function against solid tumors (24). Our group has expanded NK cells from the PB of breast and ovarian cancer patients and ascites of ovarian cancer patients (25,26). We found that not only did expansion convert cancer patient PB-NK cells to an activated subset with *in vitro* cytotoxicity comparable to that of expanded healthy donor NK cells, but that expansion

converted immunoregulatory ascites-NK cells to a subset with *in vitro* cytotoxicity against ovarian cancer cells. Together, these previous findings indicate the potential for adoptively transferring patients' own expanded NK cells as an autologous cell therapy for ovarian cancer and other solid malignancies.

In the present study, we show that expansion induces a $CD56^{superbright}CD16^{+}$ NK cell population that possesses better *in vitro* antitumor functions against ovarian cancer cells than IL2-activated unexpanded NK cells, supporting the notion that $CD56^{bright}$ NK cells have untapped cytotoxic potential. Given this enhanced *in vitro* function, we evaluated the ability of expanded ovarian cancer patient PB- and ascites-NK cells to reduce tumor burden *in vivo* using both representative cell-line and autologous patient-derived xenograft models of aggressive human ovarian cancer. We report that expanded ovarian cancer patient PB- and ascites-NK cells reduce burden of well-established tumors, enhance survival, and are effective against patients' own (autologous) aggressive and resistant primary ovarian cancer.

2.3 MATERIALS & METHODS

Ethics Statement

Research using human samples was approved by the Hamilton Integrated Research Ethics Board. PB and ascites from high grade serous ovarian cancer patients with recurrent cancer and PB from healthy donors were obtained with written informed consent. NOD-*Rag1*^{null} *IL2rg*^{null} (NRG) mice were purchased from Jackson Laboratory and bred in pathogen-free conditions in the Central Animal Facility at McMaster University. All breeding and experiments involving mice were approved by the Animal Research Ethics Board at McMaster University.

Cell culture and *in vitro* assays

NK cells were expanded from PBMCs or ascites cells using IL2 and irradiated K562-feeder cells engineered to express membrane-bound IL21 (K562-mb-IL21), as previously described (25,27,28). K562-mb-IL21 cells were kindly provided by Dr. Dean A. Lee (Department of Pediatrics, Nationwide Children's Hospital, Ohio State University Comprehensive Cancer Center, USA) in 2012. K562-mb-IL21 cells were kept in culture for a maximum of 2 months and were not authenticated in the past year. Expanding NK cell cultures were replenished with 100 U/mL IL2 three times per week and irradiated K562-mb-IL21 cells once per week at a 2:1 ratio to NK cells. NK cells were expanded for 3 weeks prior to use in experiments. Unexpanded NK cells were isolated from PBMCs using an NK Cell Enrichment Kit (StemCell Technologies #19055). For *in vitro* assays, expanded and unexpanded NK cells (10^6 cells/mL) were incubated overnight with 100 U/mL IL2 (Peprotech # 200-02). NK cell phenotype and IFNγ were assessed via flow cytometry. Cytotoxicity and degranulation assays against ovarian cancer cells were conducted as previously described (25,26). OVCAR8 ovarian cancer cells were obtained in 2015 as a kind gift from Dr. Karen Mossman (McMaster University) and used for experiments at 10^{th} passage. Mycoplasma testing was performed on K562-mb-IL21 and OVCAR8 cells in 2015 using PlasmoTest™ mycoplasma detection kit (Invivogen #rep-pt1) according to manufacturer's instructions and cells were used from these tested batches. OVCAR8 cells were authenticated by the American Type Culture Collection® Cell Line Authentication Service in 2017.

Generation of OVCAR8-Luciferase Cells

OVCAR8 cells were transduced with a lentiviral vector containing a luciferase reporter gene. For the production of a third-generation lentivirus, a pCCL-based transfer plasmid was used which encodes puromycin resistance and enhanced firefly luciferase in a bi-directional promoter

system (under control of the minimal cytomegalovirus and human EF-1α promoters, respectively) (29). Self-inactivating, non-replicative lentivirus was produced using a third-generation system that has been previously described (30,31). Transduced OVCAR8-Luciferase cells were selected for via puromycin selection.

Establishment of Patient-Derived Xenograft Ovarian Cancer Model

Ovarian cancer patient ascites cells from 5 patients were injected intraperitoneally into female NRG mice in PBS or the indicated volume of ascites fluid. Mice were followed for ascites development and survival. Ascites cells were collected at endpoint, defined by body weight plateau or increase with poor body condition (including decrease or cessation of food or water intake due to abdominal distension) compared to control NRG mice. These passaged ascites cells were injected in PBS intraperitoneally into NRG mice at a range of doses ($0.25 – 3x10^6$ cells/mouse) to determine optimal dose for consistent engraftment and mice were followed for ascites development and survival. At endpoint, ascites was collected and solid peritoneal tumors were harvested, fixed in 2% paraformaldehyde for 48 hours, embedded in paraffin, cross-sectioned, and stained with H&E. Tumor sections were imaged with a Leica Microscope. CA-125 was quantified using a CA-125 ELISA (Abnova #KA0205) according to manufacturer's instructions.

Adoptive Transfer of Expanded NK cells

OVCAR8-Luciferase or primary ovarian cancer cells (passaged once) were injected intraperitoneally into female NRG mice ($2.5x10^5$ cells/mouse) at Day 0. At indicated time points after tumor-cell injection, $20x10^6$ expanded NK cells were injected intraperitoneally. $2x10^4$ U of IL2 (Promega), a dose that was previously determined to support expanded NK cell survival *in*

vivo (25), was injected intraperitoneally 3x/week to support NK cell survival in the absence of a complete host immune system. Control mice received tumor cells and IL2. For experiments with OVCAR8-Luciferase xenografts, tumor burden was quantified 14 minutes after intraperitoneal injection of Luciferin (Perkin Elmer #30356214) via bioluminescence (radiance units: photons/sec/cm^2/sr) using an IVIS Spectrum Imaging System and analyzed using Living Image software (Perkin Elmer). Tumor engraftment was confirmed and bioluminescence was averaged across groups prior to the first NK cell injection. For tumor burden assessment in patient-derived xenografts, abdominal distension was assessed by measuring mouse abdominal circumference as previously described (32). Circumference was measured in line with the iliac crest to ensure consistent measurement across mice. Peritoneal tumors were compared across groups when the first mice reached endpoint. Endpoint across experiments was defined by body weight plateau or increase with poor body condition (including decrease or cessation of food or water intake due to abdominal distension) compared to control NRG mice.

Flow Cytometric Staining

Cells were stained with viability dye (eBioscience #65-0865-14) for 30 minutes. Cells extracted from mice were Fc-blocked for 20 minutes. Extracellular and intracellular staining were conducted at previously described (28). NK cells were gated as live human CD45$^+$CD56$^+$CD3$^-$ cells. The following antibodies were used. From BD Biosciences: anti-human NKp46(#563329), CD3(#560176), CD45(#304017), CD56(#564849), IFNγ(#564791), CD107a(#560664), CD69(#562617), NKG2D(#562364), CD158a(#564319). From BioLegend: CD56(#318328), CD16(#302026), and NKp30(#325210), NKp44(#325108), HLA A,B,C (#311406), CD158b(#312606), CD158e1(#312712), CD112(#337410), CD155(#337610),

MICA/MICB(#320906). From Miltenyi Biotec: NKG2A(#130-105-647). From R&D Systems: ULBP1(#FAB1380A), ULBP3(#FAB1517a), ULBP2/5/6(#FAB1298P), B7H6(#FAB7144A). Data acquisition was conducted on a BD LSRFortessa.

Statistical Analysis

Statistical analysis was conducted using GraphPad Prism software (San Diego, CA, USA). Graphs comparing two conditions were analyzed via unpaired t-test. Graphs comparing more than two conditions were analyzed via one-way ANOVA followed by Tukey correction for multiple comparisons. Graphs with two independent variables were analyzed via two-way ANOVA followed by Tukey correction. Survival was analyzed using the log-rank (Mantel-Cox) test followed by Bonferroni correction for multiple comparisons.

2.4 RESULTS

Expanded $CD56^{superbright}CD16^{+}$ NK cells showed enhanced *in vitro* antitumor function.

IL2-activated NK cells have previously failed to induce clinical responses in patients with solid malignancies (20). With the development of NK cell expansion protocols, clinically-relevant numbers of K562-mb-IL21-expanded NK cells can be generated and have shown therapeutic antitumor capabilities in patients with hematological malignancies (8). We sought to determine whether expanded NK cells may have improved function against a solid malignancy. We first compared the *in vitro* antitumor function of K562-mb-IL21-expanded and unexpanded IL2-activated healthy donor PB-NK cells. Expanded NK cells had enhanced IFNγ expression compared to unexpanded IL2-activated NK cells (Fig. 1A) and superior cytotoxicity against OVCAR8 cells

(Fig. 1B). These improved antitumor functions compared to IL2-activated NK cells suggest that expanded NK cells comprise a more functional subset.

$CD56^{bright}CD16^{-}$ IL15-activated NK cells harbour greater antitumor capacity than $CD56^{dim}CD16^{+}$ NK cells (23). We have previously reported that expanded NK cells are primarily comprised of a $CD56^{bright}CD16^{+}$ population (26). Although the phenotype of unexpanded ovarian cancer patient PB- and ascites-NK cells and healthy donor NK cells differed prior to expansion, after expansion these cell populations exhibited similar phenotype and *in vitro* antitumor functions (26). As we found enhanced *in vitro* function of expanded NK cells compared to unexpanded NK cells, we further characterized expanded NK cell phenotype and function with respect to intensity of CD56 expression. We found that expanded NK cells are comprised primarily of a $CD56^{superbright}$ population: CD56 brightness in expanded NK cells was greater than that of the $CD56^{bright}$ population in unexpanded IL2-activated NK cells (Fig. 1C). Correspondingly, expanded NK cell CD56 mean fluorescence intensity (MFI) was significantly greater than IL2-activated NK cells due to an increase in both percent $CD56^{bright}$ cells and CD56 expression intensity on a per cell basis (Fig. 1C-D). Although $CD56^{bright}$ PB-NK cells do not express CD16, the majority of the expanded $CD56^{bright}$ NK cell population expressed CD16 (Fig. 1E), in accordance with previous findings (26). Indicative that CD56 expression intensity corresponds with activation state, expanded NK cells had increased CD16 expression with increasing CD56 brightness (Figs. 1F and Supplementary Fig. S1A). The expression of other activation receptors, including CD69, NKG2D, NKp30, NKp44, and NKp46, also increased with CD56 brightness (Fig. 1G-K and Supplementary Fig. S1B-F). In contrast, expression of NKG2A and KIR (CD158a, CD158b, CD158e1) inhibitory receptors did not significantly change with CD56 brightness (Figs. 1L-O and Supplementary Fig. S1G-J).

We then assessed the antitumor functions of expanded NK cells with respect to CD56 expression intensity in order to determine whether CD56 brightness corresponds with enhanced function. Expanded NK cells were stratified into $CD56^{dim}$, $CD56^{bright}$, and $CD56^{superbright}$ populations, as gated in Fig. 1C. Indeed, both the percent of cells expressing IFNγ and the IFNγ MFI increased with CD56 brightness (Fig. 2A-C). MFI was assessed on $CD56^{dim}$, $CD56^{bright}$, $CD56^{superbright}$ NK cell populations in order to assess both numbers of $IFN\gamma^{+}$ cells and IFNγ expression intensity on a per cell basis. Furthermore, NK cell degranulation in response to OVCAR8 tumor targets increased with increasing CD56 brightness (Fig. 2D-E). Thus, K562-mb-IL21-expansion produces a $CD56^{superbright}CD16^{+}$ activated NK cell population with enhanced antitumor functions compared to unexpanded IL2-activated NK cells. Activation state and antitumor functions of these cells increased with increasing CD56 expression.

Expanded ovarian cancer patient NK cells effective in a xenograft ovarian cancer model.

Our group has reported that K562-mb-IL21-expansion converts initially impaired cancer patient PB- and tumor-associated NK cells to cytotoxic NK cells with *in vitro* antitumor functions comparable to those of expanded healthy donor NK cells (25,26). Here we asked whether expanded cancer patient NK cells could reduce tumor burden *in vivo* against an established solid tumor.

We compared the therapeutic capacity of expanded ovarian cancer patient PB-NK cells (OCP PB-NK), ascites-NK cells (OCP ascites-NK), and healthy donor PB-NK cells (HD PB-NK) to reduce tumor burden in a murine ovarian cancer xenograft model generated using OVCAR8-Luciferase cells. Expanded OCP PB-NK, OCP ascites-NK, and HD PB-NK cells were adoptively transferred intraperitoneally to mice at indicated time points, for a total of 5 NK cell injections (Fig. 3A). NK cell treatments began 2 days following injection of OVCAR8-Luciferase cells as

this was determined to be the time point by which tumor cells had consistently engrafted and bioluminescence was similar across mice. Five NK cell injections were administered in order to determine whether multiple injections of expanded NK cells (1) could be well-tolerated and (2) could exert a therapeutic effect in this aggressive model. Tumor burden was quantified at regular intervals until bioluminescence became saturated in the tumor only group. The adoptive transfer of expanded NK cells reduced detectable tumor burden to levels equivalent to control mice with no tumor (Fig. 3B and C). Expanded NK cell groups from all sources demonstrated comparable reduction in tumor burden.

In addition to eliminating macroscopic tumor burden, the five NK cell treatments enhanced median survival time 3.4–5.2 times over survival time of tumor-only controls (Fig. 3D). NK-treated mice experienced tumor regrowth at variable time points after cessation of NK cell treatment (a range of 45-135 days following last NK cell treatment), and were sacrificed when they reached the same disease endpoint criteria as untreated tumor-only control mice. No significant difference in survival was observed between HD PB-NK vs. OCP ascites-NK. There was a non-significant trend for improved survival of HD PB-NK vs. OCP PB-NK. However, OCP ascites-NK cells significantly improved survival as compared to OCP PB-NK cells. These results indicate that not only are expanded NK cells effective in reducing tumor burden against solid tumors, but expanded OCP ascites-NK cells are as effective as expanded HD PB-NK cells, indicating the potential for autologous NK cell therapy.

Expanded OCP NK cells reduce burden of established ovarian cancer in xenograft mice

The immunosuppressive environment produced by established solid tumors reduces effectiveness of NK cell therapy. We therefore asked whether expanded OCP-NK cells could

maintain the therapeutic effect observed in Fig. 3 if treatment began at a later time point. This allowed a tumor environment to more fully establish following engraftment. We injected expanded OCP PB-NK cells at Days 8 and 10 following OVCAR8-Luciferase injection, at approximately one-third of the median survival time for untreated mice (Fig. 4A). Mice were monitored until the bioluminescent signal became saturated in the control group. We found that only two injections of expanded OCP-NK cells reduced macroscopic tumour burden to undetectable levels (comparable to mice with no tumour) (Fig. 4B and C). Thus, expanded OCP-NK cells show antitumor activity against established ovarian cancer.

Translational patient-derived xenograft model of primary human ovarian cancer

Our findings that expanded OCP PB-NK and ascites-NK cells are effective at reducing tumor burden in an ovarian cancer cell-line xenograft model indicates potential for autologous NK cell therapy. We therefore asked whether expanded OCP-NK cells can exert a therapeutic effect against the patient's own primary ovarian cancer. To address this question, we first established a translational patient-derived xenograft ovarian cancer murine model. We injected un-passaged ovarian cancer patient ascites cells in PBS or ascites fluid intraperitoneally into NRG mice and monitored ascites development and tumor burden (Fig. 5A). Injection with ascites fluid supported the development and progression of ovarian cancer and reduced the number of cells needed for engraftment (Fig. 5B). However, the volume of ascites fluid was critical: we found that 1–2 mL ascites fluid supported engraftment without inducing lethal toxicities (Fig. 5C). Upon subsequent passage, as few as $2.5x10^5$ passaged cells per mouse were needed for consistent engraftment. Ascites fluid was not required for consistent engraftment in second passage. The progression of ovarian cancer in these patient-derived xenograft murine models paralleled clinical progression:

mice expressed the clinical ovarian cancer biomarker CA-125 (Fig. 5D), and developed ascites and solid tumors in the peritoneal cavity that retained epithelial characteristics (Fig. 5E-G).

Expanded OCP NK cells retain a cytotoxic phenotype in autologous tumor

Establishment of the patient-derived xenograft mice enabled us to assess the adoptive transfer of expanded OCP-NK cells in an autologous model of patients' own cancer. We asked whether the cytotoxic phenotype of expanded NK cells was affected by established ovarian cancer, and whether expanded NK cells from different sources (autologous OCP or allogeneic HD, PB- or ascites-derived) were differentially affected. We adoptively transferred expanded autologous OCP PB-NK, OCP ascites-NK, or allogeneic HD PB-NK cells intraperitoneally into mice with either no tumor (controls) or patient-derived xenograft mice with visible ascites. Peritoneal fluid was collected from the mice 48 hours following adoptive NK cell transfer. NK cells were identified as live human $CD45^{+}CD56^{+}CD3^{-}$ cells (Fig. 6A). Expanded NK cells in all groups demonstrated an enriched $CD56^{superbright}$ population in ascites, compared to in mice without tumors (Fig. 6B). However, in contrast to the ascites-induced $CD56^{bright}CD16^{-}$ immunoregulatory phenotype of unexpanded NK cells (12), expanded NK cells maintained high expression of CD16 (Fig. 6C) and predominantly consisted of a $CD56^{superbright}CD16^{+}$ activated population. In addition, expanded NK cells increased or maintained expression of activation receptors NKp46 and NKp30 in ascites (Fig. 6D and E). These results indicate that expanded NK cells from all sources maintain an activated $CD56^{superbright}CD16^{+}$ cytotoxic phenotype with enhanced or sustained expression of activation receptors at the tumor site. In contrast, with a lack of activation signals in nontumor-bearing mice, expanded NK cells revert to a less activated $CD56^{dim}$ subset.

Expanded ovarian cancer patient NK cells reduce burden of autologous ovarian cancer

Given the maintenance of a cytotoxic phenotype in an autologous tumor model, we next investigated the therapeutic capacity of expanded OCP PB-NK and ascites-NK cells to reduce tumor burden against autologous ovarian cancer. We asked whether expanded OCP NK cells could exert a therapeutic effect against autologous ovarian cancer in even a resistant and aggressive cancer model that constitutively expressed MHCI. We have previously reported that ovarian cancer cells from different patients have variable susceptibility to NK cell killing *in vitro* (26). For assessing the adoptive transfer of expanded NK cells in an autologous model, we used primary ovarian cancer cells that we had identified as resistant to NK cell killing *in vitro* (26). These ovarian cancer cells remained resistant to NK cell killing following passaging in mice and more susceptible cells retained susceptibility (Fig. 7A). Since inhibition by self-MHC is an impediment to autologous NK cell therapy, we verified that the ovarian cancer cells used expressed MHCI (Fig. 7B). Furthermore, primary ovarian cancer cells have variable *in vivo* aggressiveness, with mice reaching endpoint in a range of 20-150 days following tumor cell injection. Cells used in the current experiment were aggressive, with untreated mice reaching endpoint within 24 days (Fig. 7C).

Expanded OCP PB-NK, OCP ascites-NK, or HD PB-NK cells were adoptively transferred intraperitoneally at indicated time points after injection of primary ovarian cancer cells (Fig. 7C). Since survival time of untreated xenografts in this model is similar to that of OVCAR8-Luciferase xenografts in Fig. 3, expanded NK cell treatment began at day 2 following tumor cell injection to allow similar time for tumor cell engraftment. Adoptive transfer of expanded NK cells delayed the onset and progression of ascites compared to control mice, as measured by abdominal circumference (Fig. 7D). Furthermore, no significant difference in abdominal circumference was

observed among any of the NK cell groups. Treatment with expanded NK cells precluded development of large peritoneal tumors, which did develop in control mice (Fig. 7E). To better understand how expanded OCP-NK cells mediate this therapeutic effect despite constitutive autologous-MHCI expression by the tumor, we assessed expression of other activation and inhibitory ligands by ovarian cancer cells. The ovarian cancer cells had a resistant phenotype: they lacked expression of numerous NK cell activation ligands, with the exception of NKG2D ligands ULBP2/5/6. However, these ovarian cancer cells also had low expression of the NKG2A inhibitory ligand HLA E (Supplementary Fig. S2). This indicates a role for NKG2D-mediated activation in the absence of NKG2A-mediated inhibition in the control of resistant tumor by expanded NK cells.

Our results demonstrate not only that expanded NK cells are effective against primary ovarian cancer, but also that expanded OCP PB-NK and ascites-NK cells have a therapeutic effect against aggressive and resistant autologous ovarian cancer.

2.5 DISCUSSION

To date, the adoptive transfer of NK cells has been ineffective at treating solid malignancies because NK cell activation and effector function are not maintained in the solid tumor environment. However, we report that cytotoxic expanded $CD56^{superbright}CD16^{+}$ NK cells may bypass this limitation. We demonstrate that expanded cancer patient NK cells can be therapeutically beneficial against an established solid malignancy. We report that expanded OCP PB- and ascites-NK cells reduce tumor burden and improve survival in allogeneic and autologous tumor settings using translational human ovarian cancer models.

$CD56^{dim}$ NK cells are usually cytotoxic, whereas $CD56^{bright}$ NK cells are immunoregulatory and poorly cytotoxic (22). However, pre-activation of PB-NK cells with IL15

augments $CD56^{bright}$ NK cell antitumor functions, surpassing those of $CD56^{dim}$ NK cells (23). Although such results indicate potential for $CD56^{bright}$ PB-NK cells as a cancer immunotherapeutic, $CD56^{bright}$ NK cells form only a minor portion of PB-NK cells and are thus not available in numbers relevant for clinical therapies.

Here we identified an expansion-induced $CD56^{superbright}CD16^{+}$ NK cell population that produces more IFNγ and shows greater *in vitro* cytotoxicity against ovarian cancer cells than IL2-activated NK cells. The antitumor functions of these expanded NK cells increase with CD56 expression intensity which further contributes to the shifting paradigm that certain populations of $CD56^{bright}$ NK cells harbour greater anti-tumour potential compared to $CD56^{dim}$ NK cells (23). Expansion is a feasible method for obtaining clinically-relevant numbers of cytotoxic $CD56^{bright}$ NK cells since K562-mb-IL21-expansion produces robust numbers of NK cells, the majority of which are $CD56^{superbright}CD16^{+}$. The function of these $CD56^{superbright}CD16^{+}$ NK cells exceeds the antitumor functions of unexpanded IL2-activated NK cells; these $CD56^{superbright}CD16^{+}$ NK cells will likely be more effective than unexpanded NK cells against solid malignancies.

Although NK cells from different sources (HD PB-NK, OCP PB-NK, OCP ascites-NK) have different functionality prior to expansion (16), we found that after expansion they all reduce ovarian cancer tumor burden and improve survival following intraperitoneal delivery in a cell-line xenograft ovarian cancer murine model. Expanded OCP-NK cells maintain their therapeutic ability to reduce tumor burden against well-established tumor. The effectiveness of expanded OCP-NK cells demonstrates that K562-mb-IL21-expansion converts even previously impaired cancer patient NK cells to a cytotoxic subset capable of exerting a therapeutic effect *in vivo* against an established solid malignancy.

Although unexpanded ascites-NK cells have immunoregulatory properties and are poorly cytotoxic, our group has previously demonstrated that expanded ascites-NK cells demonstrate *in vitro* cytotoxicity against ovarian cancer cells similar to that of expanded PB-NK cells (26). The current study extends these findings to an *in vivo* setting by demonstrating that after expansion, ascites-NK cells are as able as PB-NK cells to reduce ovarian cancer tumor burden *in vivo* and in fact induced a 5.2-times increase in median survival compared to untreated mice. Thus immunosuppressed tumor-associated NK cells can be modulated through expansion to induce a therapeutic effect in tumor reduction and survival. These results identify tumor-associated NK cells as a potential NK cell source for therapy. Since large volumes of ascites are collected during standard-care paracentesis, ascites offers an efficient source of NK cells without imposing additional procedures on patients.

We established a clinically-relevant patient-derived xenograft model of ovarian cancer to study autologous NK cell therapy. Using this model, we demonstrate that expanded OCP PB- and ascites-NK cells are capable of reducing autologous tumor. This therapeutic effect was observed despite the fact that these primary ovarian cancer cells were resistant to NK cell killing *in vitro,* constitutively expressed autologous MHCI, and were aggressive *in vivo.* Autologous NK cells have been clinically unsuccessful in reducing tumor burden in the context of solid malignancies and were found to have impaired functionality following adoptive transfer (21). Our findings indicate that the cytotoxic NK cell subset induced by K562-mb-IL21-expansion may be more effective for autologous NK cell therapy. These clinically-relevant findings support future clinical assessment of patients' own expanded NK cells as a therapy for ovarian cancer.

Our assessment of expanded NK cell phenotype following adoptive transfer revealed that expanded NK cells maintain a cytotoxic phenotype after 2 days at the tumor site. Previous reports

have shown that solid tumors induce an immunoregulatory, poorly cytotoxic phenotype in NK cells, which aligns with the lack of therapeutic effect and impaired functionality of NK cells against solid malignancies in previous studies (12,18,21,33). Conversely, we report that expanded NK cells maintain a $CD56^{superbright}CD16^{+}$ phenotype with activation receptor expression at the tumor site but lose this activated phenotype when injected into mice with no tumor, where there is a lack activation signals. This finding indicates that although expanded NK cells can lose their activated state, they remain activated upon interaction with established tumor. NKp30 expression, which recognizes B7-H6 on tumor cells, may be necessary for maintaining expanded NK cell activation, as a previous study demonstrated that NKp30 was down-regulated in ascites NK cells, which impaired NK cell cytotoxicity and IFNγ production (18). Maintenance of CD16 expression by expanded NK cells indicates potential for combining expanded NK cell therapy with a monoclonal antibody targeting a tumor antigen. Monoclonal antibody therapies have had little success against ovarian cancer, largely due to the impaired function and down-regulation of CD16 on NK cells at the tumor site (12,14,16,34). Thus, combining antibody therapy with the adoptive transfer of expanded NK cells that maintain CD16 expression may provide an additional stimulatory signal for expanded NK cells, producing a reciprocally supportive therapeutic combination.

Overall, this study suggests that expanded autologous NK cells are a viable therapy for ovarian cancer that warrants clinical assessment. Overcoming the immunosuppressive challenges posed by solid tumors has been a hurdle for cancer immunotherapies. The present study demonstrates that K562-mbIL21-expanded NK cells may address these hurdles as they show the ability to reduce tumor burden of established tumors in translational models. These results support future clinical investigation to determine whether autologous NK cell therapy can address the

longstanding need for an effective second-line therapy to improve the prognosis of ovarian cancer and other solid malignancies.

2.6 ACKNOWLEDGEMENTS

The authors would like to thank all ovarian cancer patients and healthy donors. This work was supported by a grant to AA Ashkar and H Hirte from the Juravinski Hospital and Cancer Center Foundation. AA Ashkar holds a Tier 1 Canada Research Chair. SM Poznanski holds an Ontario Women's Health Scholars Award funded by the Ontario Ministry of Health and Long-Term Care.

2.7 FIGURES

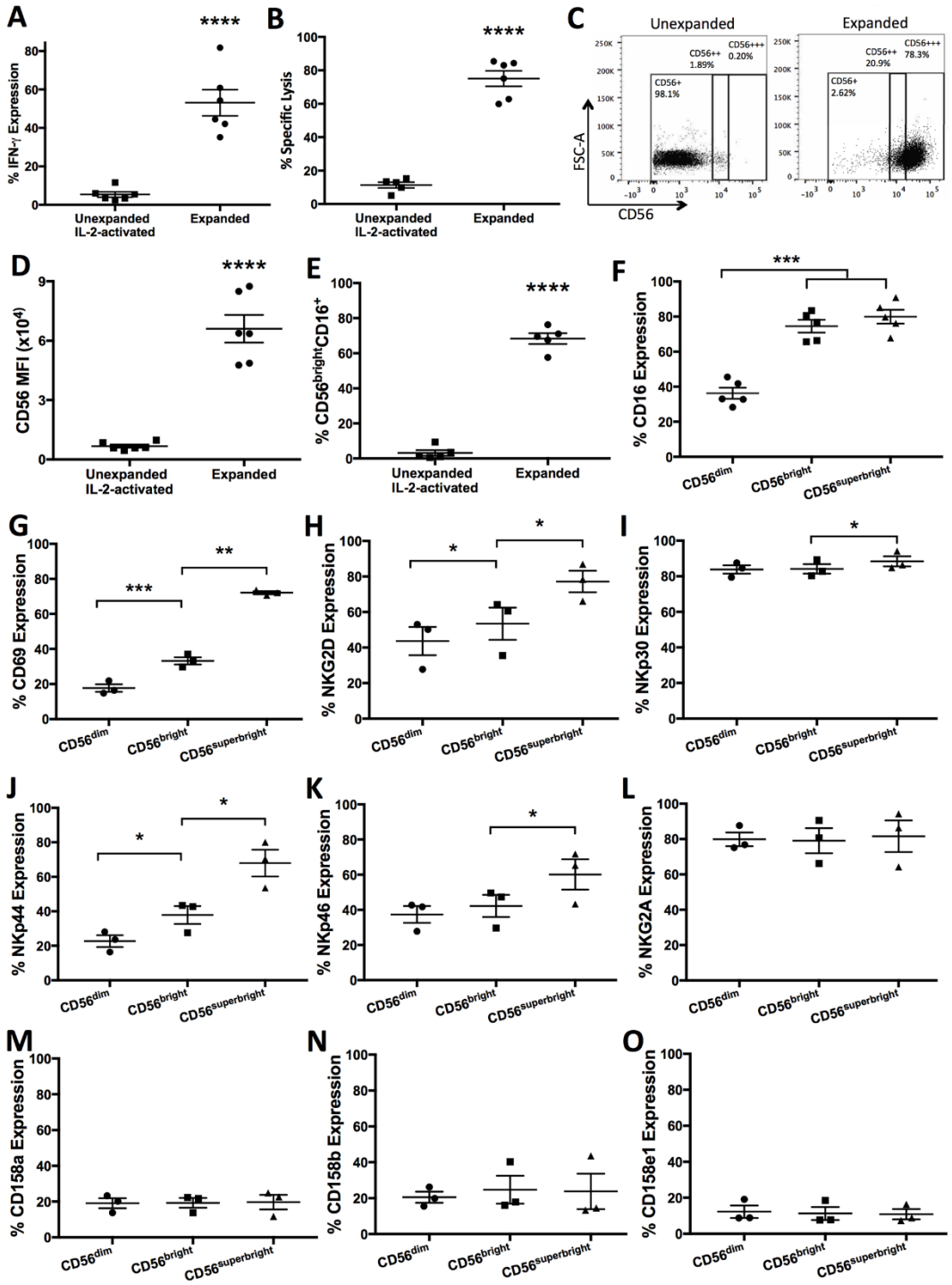

Figure 1. *Ex vivo* K562-mb-IL21-expanded NK cells are a CD56^{superbright}CD16^{+} activated subset with greater antitumor functions compared to IL2-activated NK cells. Expanded and unexpanded NK cells were activated overnight with IL2 (100 U/mL). (A) Percent of IFNγ

expression was compared (n=6 donors per group). (B) NK cell percent specific lysis of OVCAR8 target cells following 5-hour incubation at a 5:1 effector-to-target ratio (unexpanded group n=5; expanded group n=6). (C) Representative flow plots and (D) mean fluorescence intensity (MFI) of CD56 expression (n=6 donors per group). (E) Proportion of $CD56^{bright}CD16^{+}$ cells of total NK cell populations (n=5 donors per group). (F-O) Expanded NK cell population was stratified by flow cytometry analysis based on CD56 expression. Percent expression of activation receptors (F) CD16 (n=5 donors), (G) CD69, (H) NKG2D, (I) NKp30, (J) NKp44, (K) NKp46, and inhibitory receptors (L) NKG2A, (M) CD158a, (N) CD158b, and (O) CD158e1 were compared (G-O: n=3 donors). A-F show results from two independent experiments. G-O show results from one experiment. A-E were analyzed via unpaired t-test. F-O were analyzed via matched one-way ANOVA. *$p<0.05$, **$p<0.01$, ***$p<0.001$, ****$p<0.0001$.

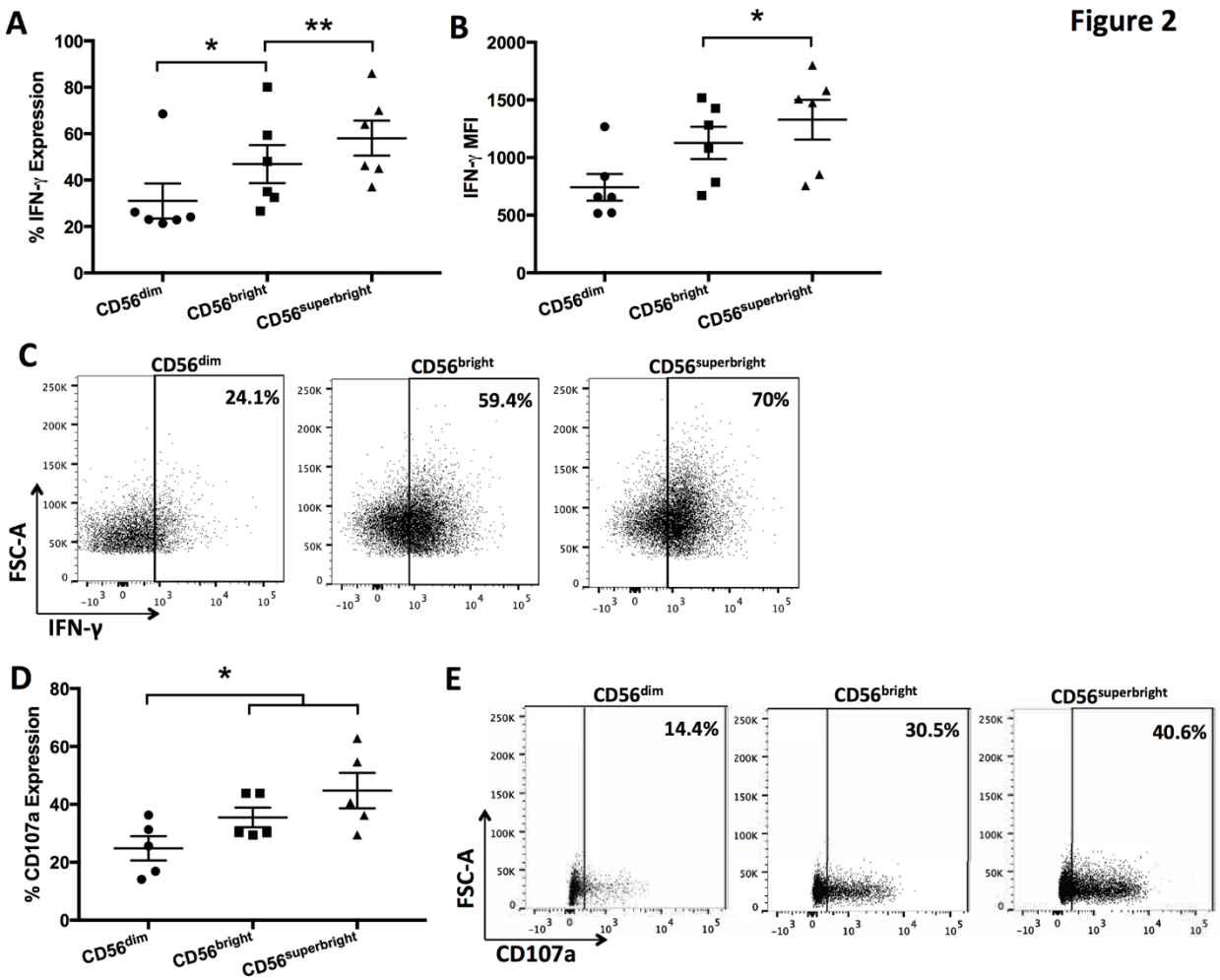

Figure 2. Antitumor functions of expanded NK cells increase with increasing CD56 brightness. Expanded NK cell population was stratified by flow cytometry analysis based on CD56 expression intensity. (A) Percent (n=6 donors), (B) MFI (n=6 donors), and (C) representative flow plots of IFNγ expression. (D) Expanded NK cell percent CD107a expression following 5-hour incubation with OVCAR8 target cells (n=5 donors). (E) Representative flow plots of CD107a expression. Results are from two independent experiments and were analyzed via matched one-way ANOVA, *p<0.05, **p<0.01.

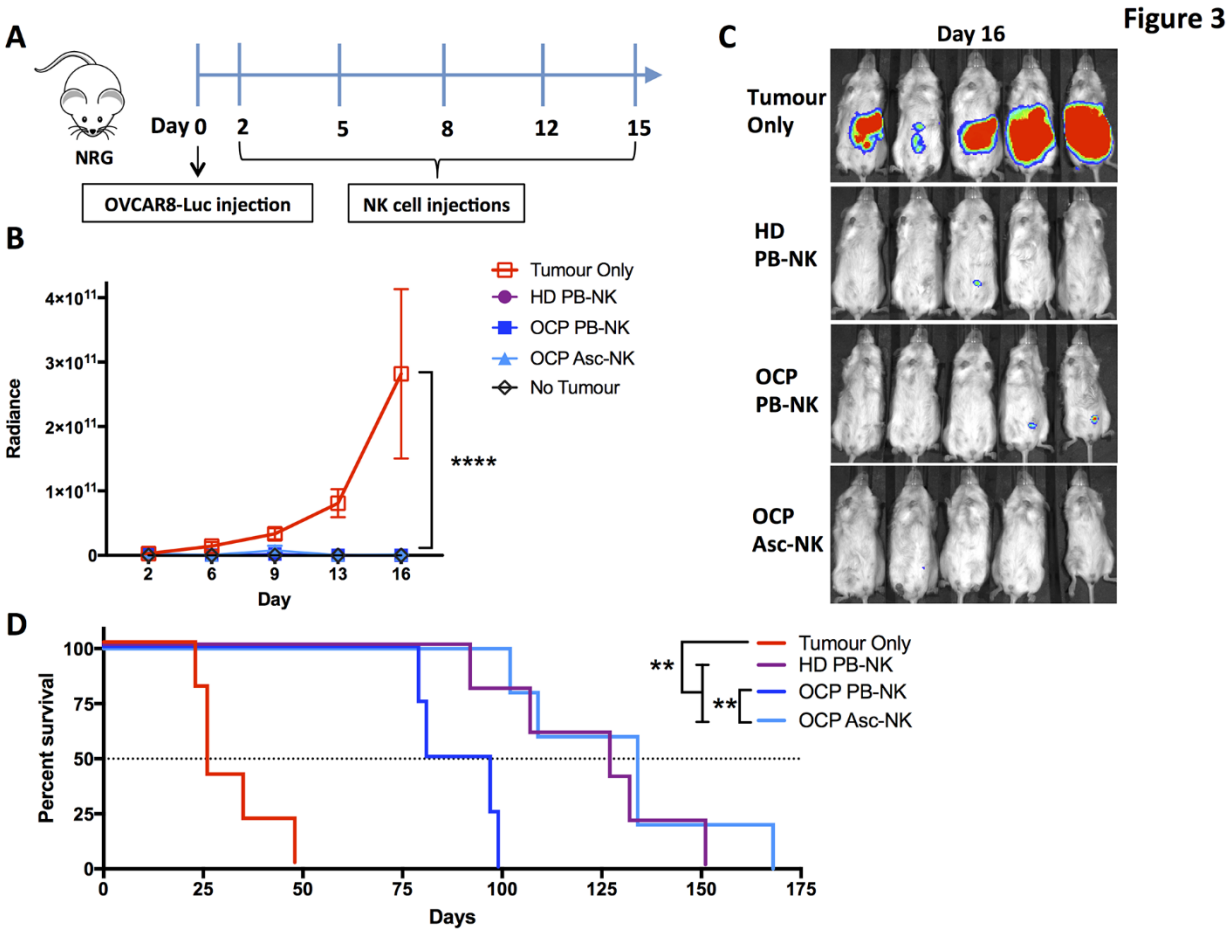

Figure 3. Expanded OCP PB- and ascites-NK cells reduce tumor burden and improve survival in a cell-line xenograft model of human OC. Expanded OCP PB-NK, OCP ascites (Asc)-NK, or HD PB-NK cells were adoptively transferred intra-peritoneally to xenograft mice beginning 2 days following injection of OVCAR8-Luciferase (Luc) ovarian cancer cells. (A) Schematic timeline of NK cell treatments. (B) Mice were imaged at indicated days and tumor burden was quantified via bioluminescence (radiance). Results were analyzed via two-way ANOVA, ****$p<0.0001$ (n=5 mice per group from one experiment). (C) Images of mice at Day 16 with colour scale standardized across images. (D) Survival of mice compared across groups and analyzed using the log-rank (Mantel-Cox) test followed by Bonferroni correction for multiple comparisons, **$p<0.0083$ (n=4-5 mice per group from one experiment).

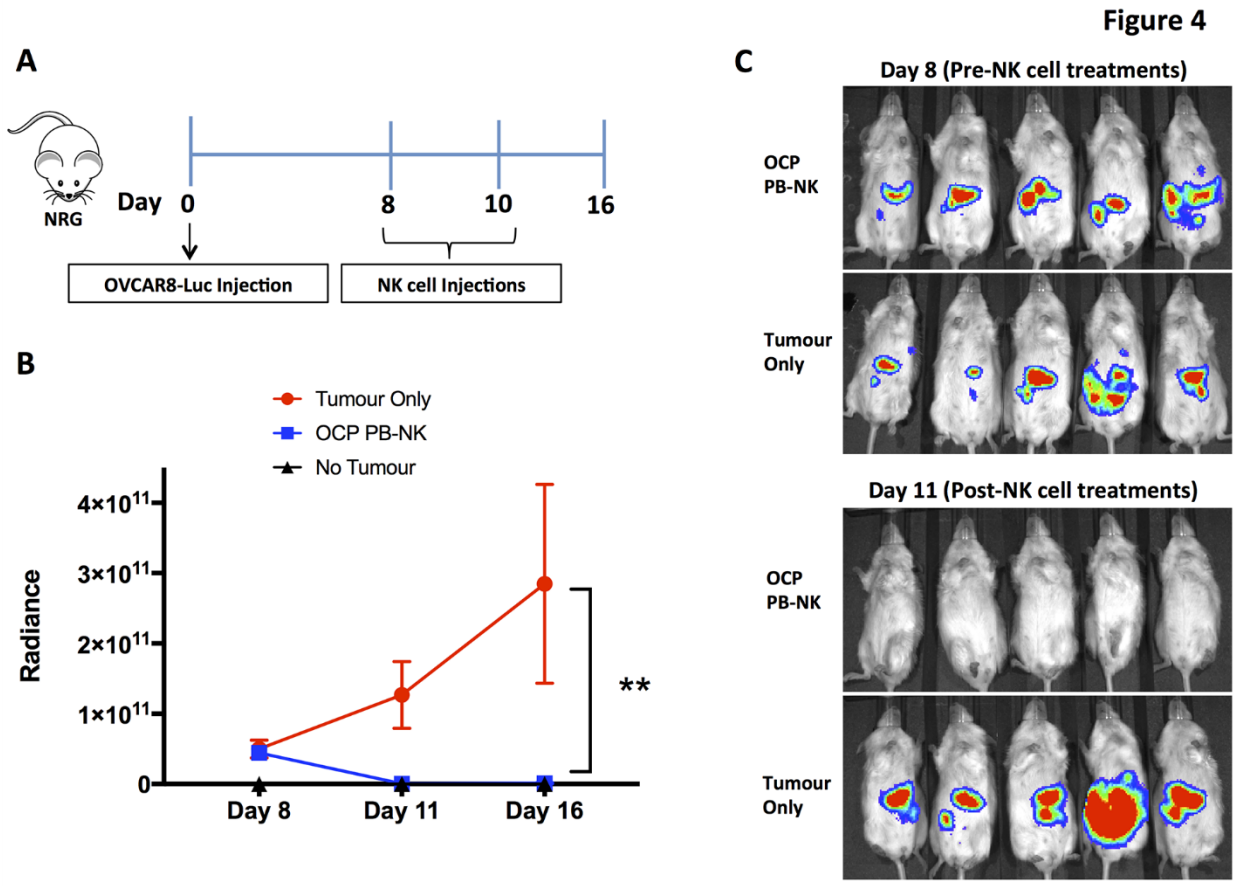

Figure 4. Expanded OCP NK cells reduce burden of established ovarian cancer tumor. Expanded OCP PB-NK cells were adoptively transferred intra-peritoneally to NRG mice beginning 8 days following injection of OVCAR8-Luc ovarian cancer cells. (A) Schematic timeline of NK cell treatments. (B) Mice were imaged at indicated days and tumor burden was quantified via bioluminescence (radiance). Results were analyzed via two-way ANOVA, **$p<0.01$ (n=5 mice per group from one experiment). (C) Images of mice at Days 8 and 11 with colour scale standardized across images.

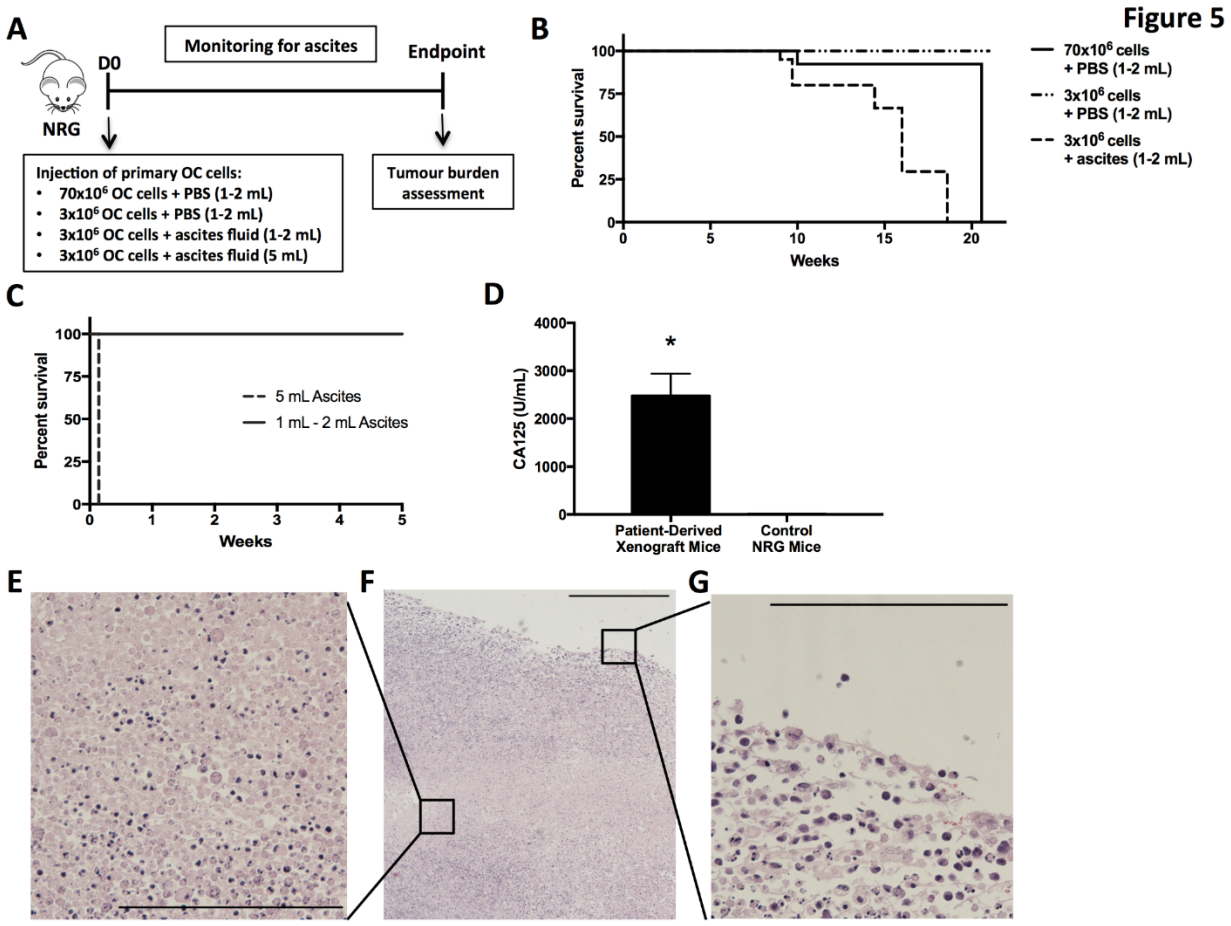

Figure 5. Establishment of patient-derived xenograft (PDX) model of human ovarian cancer. (A) Schematic of model establishment: Primary ovarian cancer cells in indicated volume of either PBS or ascites fluid were injected intra-peritoneally into NRG mice. Tumor burden was assessed at endpoint. (B) Survival of mice following injection of indicated doses of ovarian cancer cells in PBS or ascites fluid. (C) Short-term survival of mice based on volume of ascites fluid injected to assess volume-based toxicity. (D) CA-125 levels quantified in ascites of PDX mice compared to peritoneal fluid of control NRG mice. Results were analyzed via unpaired t-test, *$p<0.05$ (control NRG mice n=3; PDX mice n=5 from 2 experiments). (E-G) Representative histological tumor cross-sections stained with H&E. (E) Image of tumor core taken at 20x objective magnification; scale bar represents 200 µm. (F) Image encompassing tumor edge and core taken at 4x objective

magnification; scale bar represents 500 μm. (G) Image of tumor edge taken at 20x objective magnification; scale bar represents 200 μm.

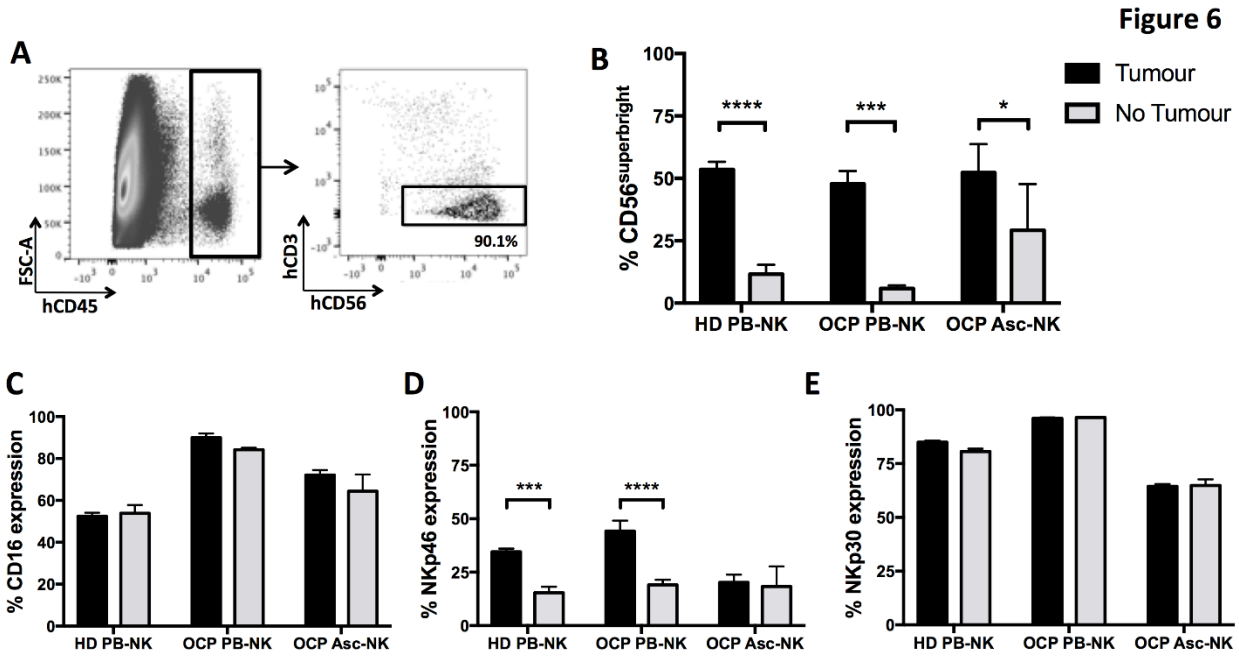

Figure 6. Expanded NK cells maintain a cytotoxic phenotype in an autologous ovarian cancer microenvironment. Expanded OCP PB-NK, OCP ascites (Asc)-NK, or HD PB-NK cells were adoptively transferred intraperitoneally to PDX mice with visible signs of ascites or control NRG mice with no tumor. 48 hours following adoptive NK cell transfer, ascites or peritoneal fluid was collected from mice and cells were stained with NK cell markers for flow cytometric analysis of NK cell phenotype. (A) Representative flow plot of gating strategy. NK cells were identified as human (h)CD45^{+}hCD56^{+}hCD3^{-}. Proportion of (B) CD56^{superbright} NK cells, (C) CD16 expression, (D) NKp46 expression, and (E) NKp30 expression on NK cells. Results were analyzed via two-way ANOVA, *p<0.05, ***p<0.001, ****p<0.0001 (tumor group n=5; no tumor control group n=3 from one experiment).

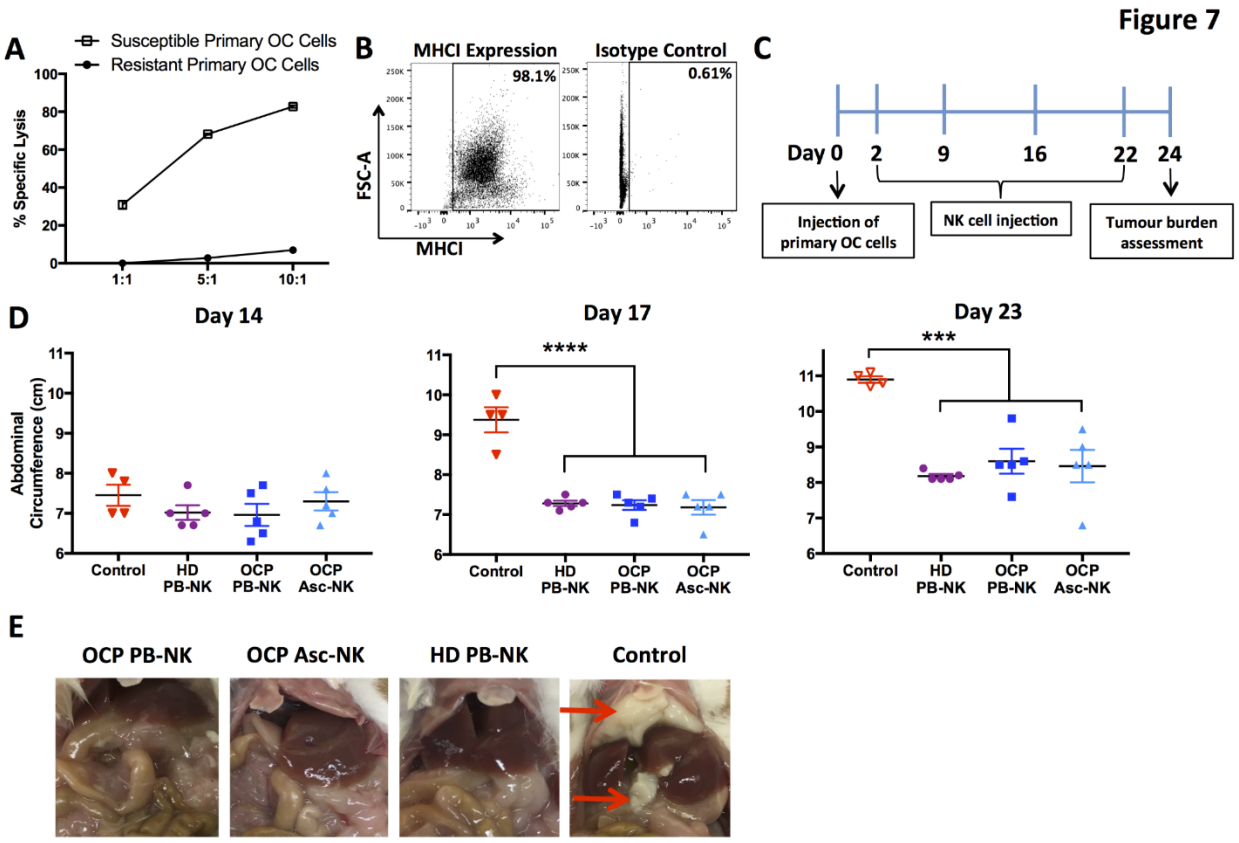

Figure 7. Expanded OCP PB- and ascites-NK cells reduce tumor burden against autologous ovarian cancer. (A) *In vitro* cytotoxicity assay of expanded NK cells against primary ovarian cancer cells passaged once in NRG mice. (B) Representative flow plot of percent expression of MHC I on primary ovarian cancer cells in comparison to cells stained with the corresponding isotype control. (C-E) Expanded OCP PB-NK cells, OCP ascites (Asc)-NK cells, or HD PB-NK cells were adoptively transferred i.p. to PDX mice beginning 2 days following injections of primary ovarian cancer cells. (C) Schematic timeline of NK cell treatments. (D) Abdominal circumference was measured at indicated days. Results were analyzed via one-way ANOVA, ***$p<0.001$, ****$p<0.0001$ (control group n=4; NK cell groups n=5 mice per group from one experiment). (E) Representative images of peritoneal tumor burden at Day 24. Red arrows indicate solid epithelial tumors.

2.8 SUPPLEMENTARY MATERIALS

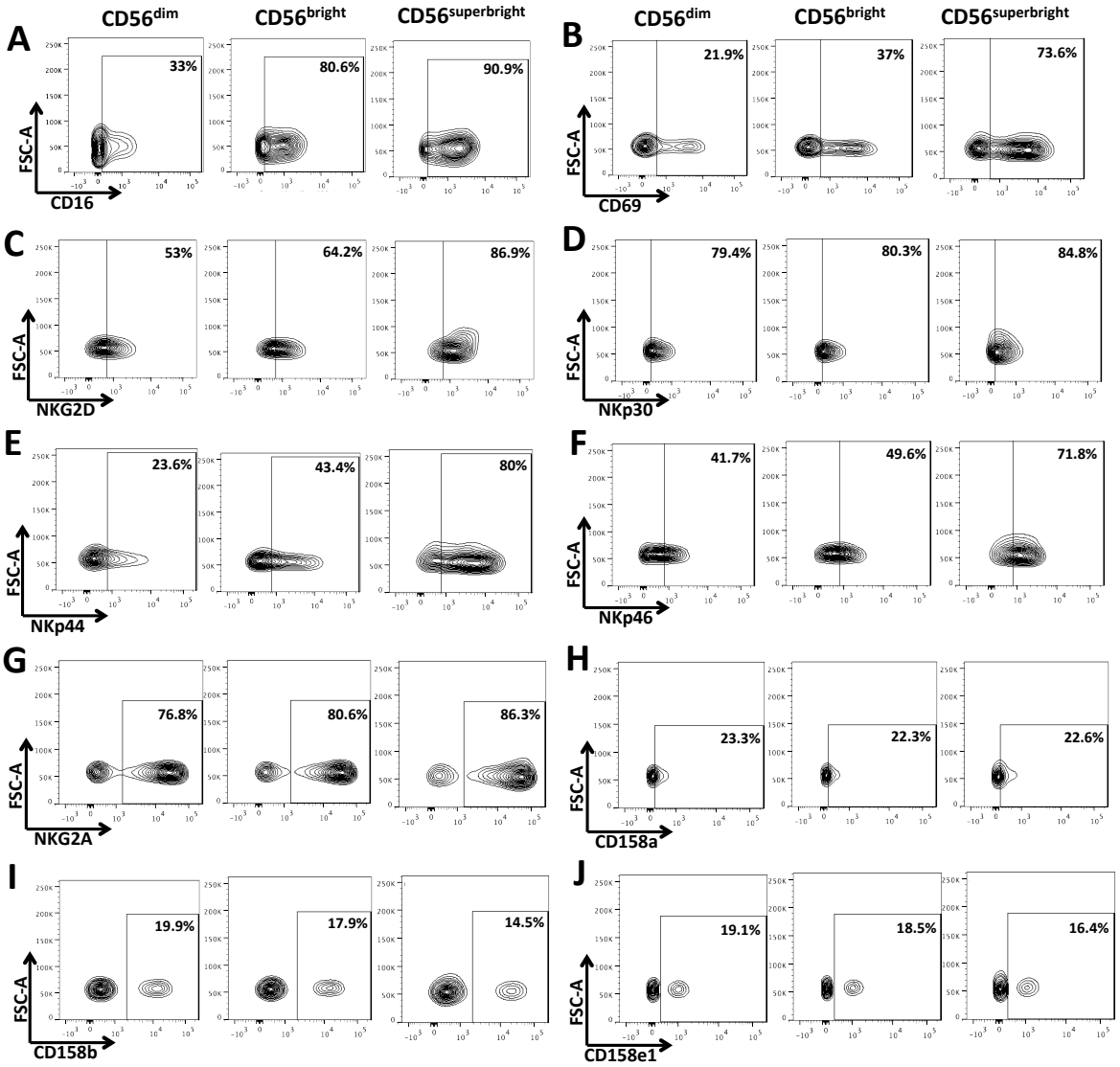

Supplementary Figure S1. Expanded NK cell activation and inhibitory receptor expression with increasing CD56 brightness. Expanded NK cell population was stratified by flow cytometry analysis based on CD56 expression. Representative flow plots of expression of activation receptors CD16 (A), CD69 (B), NKG2D (C), NKp30 (D), NKp44 (E), and NKp46 (F) and inhibitory receptors NKG2A (G), CD158a (H), CD158b (I), and CD158e1 (J) across $CD56^{dim}$, $CD56^{bright}$, and $CD56^{superbright}$ populations.

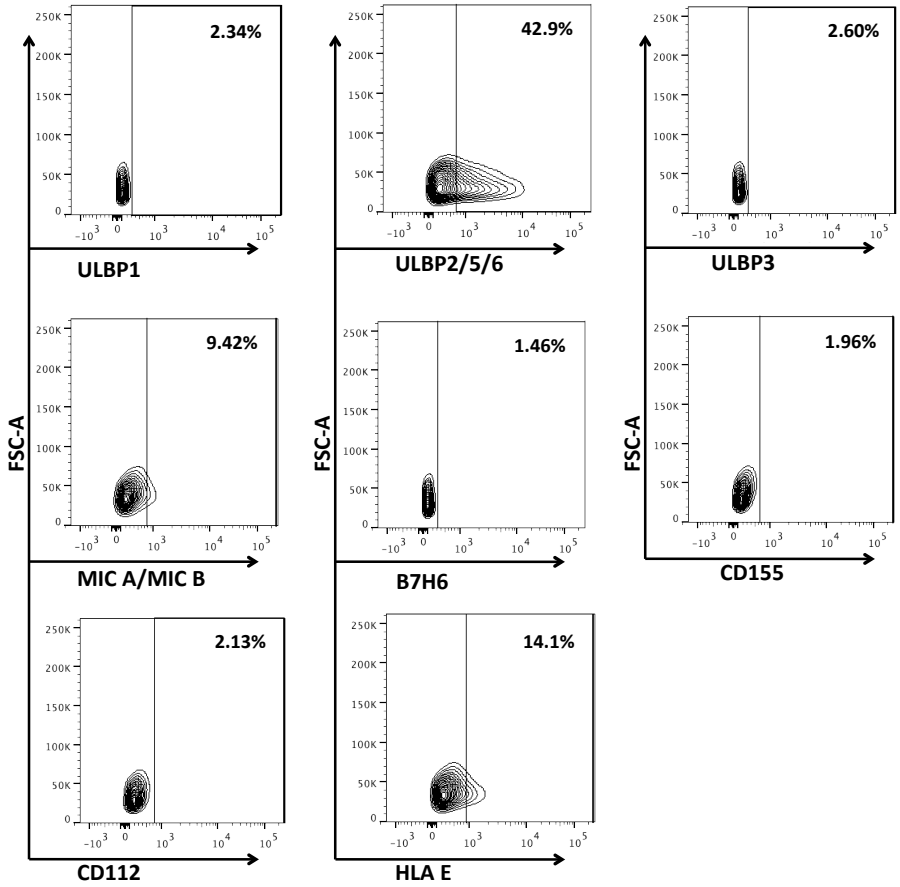

Supplementary Figure S2. Expression of NK cell activation and inhibitory ligands on resistant primary ovarian cancer cells. Primary ovarian cancer cells (passaged once in NRG mice) were assessed for expression of NK cell activation and inhibitory receptor ligands via flow cytometry. Representative flow plots of expression of the activation ligands ULBP1, ULBP2/5/6, ULBP3, MIC A/MIC B, B7H6, CD155, CD112 and inhibitory ligand HLA E.

2.9 REFERENCES

1. Lowe KA, Chia VM, Taylor A, O'Malley C, Kelsh M, Mohamed M*, et al.* An international assessment of ovarian cancer incidence and mortality. Gynecol Oncol **2013**;130:107-14
2. Siegel RL, Miller KD, Jemal A. Cancer statistics, 2017. CA Cancer J Clin **2017**;67:7-30
3. Bowtell DD, Bohm S, Ahmed AA, Aspuria PJ, Bast RCJ, Beral V*, et al.* Rethinking ovarian cancer II: reducing mortality from high-grade serous ovarian cancer. Nat Rev Cancer **2015**;15:668-79
4. Markman M, Webster K, Zanotti K, Peterson G, Kulp B, Belinson J. Survival following the documentation of platinum and taxane resistance in ovarian cancer: a single institution experience involving multiple phase 2 clinical trials. Gynecol Oncol **2004**;93:699-701

5. Markman M, Markman J, Webster K, Zanotti K, Kulp B, Peterson G*, et al.* Duration of response to second-line, platinum-based chemotherapy for ovarian cancer: implications for patient management and clinical trial design. J Clin Oncol **2004**;22:3120-5
6. Maringe C, Walters S, Butler J, Coleman MP, Hacker N, Hanna L*, et al.* Stage at diagnosis and ovarian cancer survival: evidence from the International Cancer Benchmarking Partnership. Gynecol Oncol **2012**;127:75-82
7. Bodduluru LN, Kasala ER, Madhana RM, Sriram CS. Natural killer cells: The journey from puzzles in biology to treatment of cancer. Cancer Lett **2015**;357:454-67
8. Ciurea SO, Schafer JR, Bassett R, Denman CJ, Cao K, Willis D*, et al.* Phase 1 clinical trial using mbIL21 ex-vivo expanded donor-derived NK cells after haploidentical transplantation. Blood **2017**:pii: blood-2017-05-785659
9. Romee R, Rosario M, Berrien-Elliott MM, Wagner JA, Jewell BA, Schappe T*, et al.* Cytokine-induced memory-like natural killer cells exhibit enhanced responses against myeloid leukemia. Sci Transl Med **2016**;8:357ra123
10. Carlsten M, Bjorkstrom NK, Norell H, Bryceson Y, van Hall T, Baumann BC*, et al.* DNAX accessory molecule-1 mediated recognition of freshly isolated ovarian carcinoma by resting natural killer cells. Cancer Res **2007**;67:1317-25
11. Platonova S, Cherfils-Vicini J, Damotte D, Crozet L, Vieillard V, Validire P*, et al.* Profound coordinated alterations of intratumoral NK cell phenotype and function in lung carcinoma. Cancer Res **2011**;71:5412-22
12. Belisle JA, Gubbels JA, Raphael CA, Migneault M, Rancourt C, Connor JP*, et al.* Peritoneal natural killer cells from epithelial ovarian cancer patients show an altered phenotype and bind to the tumour marker MUC16 (CA125). Immunology **2007**;122:418-29
13. Bauernhofer T, Kuss I, Henderson B, Baum AS, Whiteside TL. Preferential apoptosis of CD56dim natural killer cell subset in patients with cancer. Eur J Immunol **2003**;33:119-24
14. Lai P, Rabinowich H, Crowley-Nowick PA, Bell MC, Mantovani G, Whiteside TL. Alterations in expression and function of signal-transducing proteins in tumor-associated T and natural killer cells in patients with ovarian carcinoma. Clin Cancer Res **1996**;2:161-73
15. Carrega P, Morandi B, Costa R, Frumento G, Forte G, Altavilla G*, et al.* Natural killer cells infiltrating human nonsmall-cell lung cancer are enriched in CD56 bright CD16(-) cells and display an impaired capability to kill tumor cells. Cancer **2008**;112:863-75
16. Berek JS, Bast RC, Lichtenstein A, Hacker NF, Spina CA, Lagasse LD*, et al.* Lymphocyte cytotoxicity in the peritoneal cavity and blood of patients with ovarian cancer. Obstet Gynecol **1984**;64:704-14
17. Carlsten M, Norell H, Bryceson YT, Poschke I, Schedvins K, Ljunggren HG*, et al.* Primary human tumor cells expressing CD155 impair tumor targeting by down-regulating DNAM-1 on NK cells. J Immunol **2009**;183:4921-30
18. Pesce S, Tabellini G, Cantoni C, Patrizi O, Coltrini D, Rampinelli F*, et al.* B7-H6-mediated downregulation of NKp30 in NK cells contributes to ovarian carcinoma immune escape. Oncoimmunology **2015**;4:e1001224
19. Pesce S, Greppi M, Tabellini G, Rampinelli F, Parolini S, Olive D*, et al.* Identification of a subset of human natural killer cells expressing high levels of programmed death 1: A

phenotypic and functional characterization. The Journal of allergy and clinical immunology **2017**;139:335-46.e3
20. Geller MA, Knorr DA, Hermanson DA, Pribyl L, Bendzick L, McCullar V*, et al.* Intraperitoneal delivery of human natural killer cells for treatment of ovarian cancer in a mouse xenograft model. Cytotherapy **2013**;15:1297-306
21. Parkhurst MR, Riley JP, Dudley ME, Rosenberg SA. Adoptive transfer of autologous natural killer cells leads to high levels of circulating natural killer cells but does not mediate tumor regression. Clin Cancer Res **2011**;17:6287-97
22. Caligiuri MA. Human natural killer cells. Blood **2008**;112:461-9
23. Wagner JA, Rosario M, Romee R, Berrien-Elliott MM, Schneider SE, Leong JW*, et al.* CD56bright NK cells exhibit potent antitumor responses following IL-15 priming. J Clin Invest **2017**;127:4042-58
24. Hermanson DL, Bendzick L, Pribyl L, McCullar V, Vogel RI, Miller JS*, et al.* Induced pluripotent stem cell-derived natural killer cells for treatment of ovarian cancer. Stem Cells **2016**;34:93-101
25. Shenouda MM, Gillgrass A, Nham T, Hogg R, Lee AJ, Chew MV*, et al.* Ex vivo expanded natural killer cells from breast cancer patients and healthy donors are highly cytotoxic against breast cancer cell lines and patient-derived tumours. Breast Cancer Res **2017**;19:76
26. Nham T, Poznanski SM, Fan IY, Shenouda MM, Chew MV, Lee AJ*, et al.* Ex vivo-expanded NK cells from blood and ascites of ovarian cancer patients are cytotoxic against autologous primary ovarian cancer cells. Cancer Immunol Immunother **2018**:doi.org/10.1007/s00262-017-2112-x
27. Denman CJ, Senyukov VV, Somanchi SS, Phatarpekar PV, Kopp LM, Johnson JL*, et al.* Membrane-bound IL-21 promotes sustained ex vivo proliferation of human natural killer cells. PLoS One **2012**;7:e30264
28. Poznanski SM, Lee AJ, Nham T, Lusty E, Larché MJ, Lee DA*, et al.* Combined stimulation with interleukin-18 and interleukin-12 potently induces interleukin-8 production by Natural Killer cells. J Innate Immun **2017**;9:511-25
29. Rabinovich BA, Ye Y, Etto T, Chen JQ, Levitsky HI, Overwijk WW*, et al.* Visualizing fewer than 10 mouse T cells with an enhanced firefly luciferase in immunocompetent mouse models of cancer. Proc Natl Acad Sci U S A **2008**;105:14342–6
30. Dull T, Zufferey R, Kelly M, Mandel RJ, Nguyen M, Trono D*, et al.* A third-generation lentivirus vector with a conditional packaging system. J Virol **1998**;72:8463-71
31. Hammill JA, Afsahi A, Bramson JL, Helsen CW. Viral engineering of chimeric antigen receptor expression on murine and human T lymphocytes. In: Ursini-Siegel J, Beauchemin N, editors. The Tumour Microenvironment Methods in Molecular Biology. New York, NY: Humana Press; 2016. p 137-57.
32. Vassileva V, Moriyama EH, De Souza R, Grant J, Allen CJ, Wilson BC*, et al.* Efficacy assessment of sustained intraperitoneal paclitaxel therapy in a murine model of ovarian cancer using bioluminescent imaging. British journal of cancer **2008**;99:2037-43
33. Krneta T, Gillgrass A, Chew M, Ashkar AA. The breast tumor microenvironment alters the phenotype and function of natural killer cells. Cell Mol Immunol **2016**;13:628-39
34. Vergote I, Armstrong D, Scambia G, Teneriello M, Sehouli J, Schweizer C*, et al.* A randomized, double-blind, placebo-controlled, phase III study to assess efficacy and

safety of weekly Farletuzumab in combination with carboplatin and taxane in patients with ovarian cancer in first platinum-sensitive relapse. J Clin Oncol **2016**;34:2271-8

– CHAPTER 3 –

EXPANDED HUMAN NK CELLS FROM LUNG CANCER PATIENTS SENSITIZE PATIENTS' PDL1-NEGATIVE TUMOURS TO PD1-BLOCKADE THERAPY

Expanded human NK cells from lung cancer patients sensitize patients' PDL1-negative tumours to PD1-blockade therapy

Sophie M. Poznanski[1], Tyrah M. Ritchie[1], Isabella Y. Fan[1], Abdullah El-Sayes[1], Ana L. Portillo[1], Ronny A. Ben-Avi[2], Eduardo A. Rojas[1], Marianne V. Chew[1], Yaron Shargall[2], Ali A. Ashkar[1*]

[1]Department of Pathology and Molecular Medicine, McMaster University, Hamilton, Ontario

[2]Department of Surgery, Faculty of Health Sciences, McMaster University, Hamilton, Ontario

Preface: *The research presented in this manuscript was conducted from 2017-2021. SMP and AAA conceived the project and designed the experiments. YS provided intellectual input, contributed to experimental design, and guided clinical sample acquisition. SMP, TR and IYF performed experiments. AE-S, ALP, RB-A, ER and MC contributed to performing experiments. YS and RB-A obtained the clinical samples. SMP curated and formally analyzed the data. SMP and AAA wrote the manuscript. TR and YS edited the manuscript. AAA secured funding and supervised the project.*

Title: Expanded human NK cells from lung cancer patients sensitize patients' PDL1-negative tumours to PD1-blockade therapy

Authors: Sophie M. Poznanski[1], Tyrah M. Ritchie[1], Isabella Y. Fan[1], Abdullah El-Sayes[1], Ana L. Portillo[1], Ronny A. Ben-Avi[2], Eduardo A. Rojas[1], Marianne V. Chew[1], Yaron Shargall[2], Ali A. Ashkar[1*]

Feature: Immune cell therapies and immune cell engineering, Short Report

Running Title: Cytotoxic expanded NK cells overcome PD1-blockade therapy non-response

Affiliations:

[1]Department of Pathology and Molecular Medicine, McMaster University, Hamilton, Ontario

[2]Department of Surgery, Faculty of Health Sciences, McMaster University, Hamilton, Ontario

[*]Corresponding author: Ali A. Ashkar, Room 4015 Michael DeGroote Centre for Learning & Discovery, 1280 Main Street West, Hamilton, ON, L8S 4K1;

Phone: (905) 525-9140 ext. 22311; E-mail: ashkara@mcmaster.ca

Author emails: SMP, poznans@mcmaster.ca; TMR, ty.ritchie7@gmail.com; IYF, isabella.fany@gmail.com; AE, elsayesa@mcmaster.ca; ALP, portilal@mcmaster.ca; RAB, ronnybenavi@icloud.com; EAR, jaimesea@mcmaster.ca; MVC, Marianne.Chew@turnstonebio.com; YS, shargal@mcmaster.ca; AAA, ashkara@mcmaster.ca

Keywords: NK cells, immune cell therapy, PD1, immune checkpoint blockade, lung cancer, cancer immunotherapy, solid tumours, tumour microenvironment, interferon-gamma

ABBREVIATIONS

exNK: expanded Natural Killer cells

FBS: fetal bovine serum

IFNγ: interferon gamma

HD: healthy donor

K562-mb-IL21: K562 feeder cells genetically engineered to express membrane-bound IL-21

LCP: lung cancer patient

MFI: mean fluorescence intensity

NK: Natural Killer

NRG: *NOD-Rag1*^{null} *IL2rg*^{null}

NSCLC: non-small-cell lung carcinoma

pbNK: peripheral blood NK cells

PD1: programmed death receptor-1

PDL1: programmed death receptor ligand-1

peNK: pleural effusion NK cells

rh: recombinant human

SCLC: small-cell lung carcinoma

taNK: tumour-associated NK cells

TILs: tumour-infiltrating lymphocytes

TPS: tumour proportion score

3.1 ABSTRACT

Lung cancer remains the leading cause of cancer death worldwide despite the significant progress made by immune checkpoint inhibitors, including PD1/PDL1-blockade therapy. PD1/PDL1-blockade has achieved unprecedented tumour regression in some patients with advanced lung cancer. However, the majority of patients fail to respond to PD1/PDL1 inhibitors. The high rate of therapy non-response results from insufficient PDL1 expression on most patients' tumours and the presence of further immunosuppressive mechanisms in the tumour microenvironment. Here, we sensitize non-responding tumours from lung cancer patients to PD1-blockade therapy using highly cytotoxic expanded NK cells. We uncover that NK cells expanded from lung cancer patients dismantle the immunosuppressive tumour microenvironment by maintaining strong anti-tumour activity against both PDL1+ and PDL1- patient tumours. In the process, through a contact-independent mechanism involving IFNγ, expanded NK cells rescued tumour killing by exhausted endogenous TILs and upregulated the tumour proportion score of PDL1 across patient tumours. In contrast, unexpanded NK cells, which are susceptible to tumour-induced immunosuppression, had no effect on tumour PDL1. As a result, combined treatment of expanded NK cells and PD1-blockade resulted in robust synergistic tumour destruction of initially non-responding patient tumours. Thus, expanded NK cells may overcome the critical roadblocks to extending the prodigious benefits of PD1-blockade therapy to more patients with lung cancer and other tumour types.

3.2 BACKGROUND

Lung cancer is the leading cause of cancer death worldwide. In 2018 alone, there were over 1.7 million lung cancer-related deaths, reflecting a dismal 5-year survival rate of less than 18%. At the time of diagnosis, the majority (80%) of lung cancer patients already have locally advanced or metastatic disease, which continues to progress despite chemotherapy (1). As a result, the progress made by immune checkpoint inhibitors over the past decade has been revolutionary, with antibody blockade of programmed death receptor-1 (PD1) achieving unprecedented durable tumour regression in some patients with advanced lung tumours, melanoma, and a growing list of other cancers. However, only ~10% of patients benefit from the therapy (2). Non-response to PD1-blockade therapy is associated with insufficient PDL1 expression (tumour proportion score) on patient tumours and additional mechanisms of immunosuppression in the tumour microenvironment (3-5). Indeed, a number of landmark trials have shown that an important component for sustained immunotherapeutic efficacy is the ability to shift the immunosuppressive tumour microenvironment to a proinflammatory milieu and restore the anti-tumour functions of exhausted endogenous immune cells (2, 3, 6-9). Thus, new immunotherapies that can both sustain strong inflammatory anti-tumour activity in the tumour microenvironment and increase PDL1 tumour proportion score would hold promise to extend the remarkable therapeutic benefits of PD1-blockade therapy to more patients.

The anti-tumour cytokine interferon-gamma (IFNγ), released by cytotoxic Natural Killer (NK) cells and T cells, is a critical driver of PDL1 expression on tumours and a positive predictor of clinical response to immunotherapies (8, 10-12). However, the anti-tumour functions of NK cells and T cells are significantly hindered by the tumour microenvironment (13, 14). Our previous work uncovered that NK cells from the peripheral blood and tumours of breast and ovarian cancer

patients could be expanded *ex vivo* for cell therapy. Upon adoptive transfer to mice, these expanded NK cells (exNK) were capable of sustaining anti-tumour activity against tumours and eliminated macroscopic ovarian tumours (15-17). Another study has also demonstrated that NK cells expanded using membrane particles were capable of upregulating PDL1 on tumour cell lines (18). In the current study we sought to assess 1) the therapeutic potential of exNK cells against tumours from advanced-stage lung cancer patients and 2) whether exNK cells can additionally sensitize patients' non-responding tumours to PD1-blockade therapy.

3.3 METHODS

Ethics Statement

All research involving human samples was approved by the Hamilton Integrated Research Ethics Board at McMaster University. Peripheral blood, pleural effusions, and tumour pieces were obtained with written informed consent from lung cancer patients at St. Joseph's Healthcare in Hamilton, Ontario. Pleural effusions were collected from patients via thoracentesis and tumour pieces were collected via surgical resection, both of which were conducted as part of the patients' standard care. Peripheral blood was collected from healthy donors with written informed consent at McMaster University. All research involving animals was approved by the Animal Research Ethics Board at McMaster university. *NOD-Rag1*^{null} *IL2rg*^{null} (NRG) mice were originally obtained from Jackson Laboratory and bred and housed in specific pathogen-free conditions at McMaster's Central Animal Facility.

Processing of lung tumours, pleural effusions, and peripheral blood

Lung tumours were minced into ~1mm^3 pieces in αMEM medium containing collagenase IV and DNase I. Tumour pieces were then incubated in the media on a plate shaker at 37°C for 2x, 1-hour intervals and pipetted vigorously in between incubations to break up the pieces. Cells were filtered through a 70 μm filter, pelleted via centrifugation, then washed with PBS. Cells from pleural effusions and peripheral blood were isolated via density-gradient centrifugation with Lymphoprep™ (Stemcell Technologies, Vancouver, BC), then washed with PBS.

NK cell expansion and isolation

NK cells were cultured in RPMI medium supplemented with 10% FBS, 1% hepes, 1% penicillin-streptomycin, and 1% L-glutamine. NK cells were expanded from the peripheral blood mononuclear cells (PBMCs) of healthy donors, or PBMCs, pleural effusion cells, or tumours of lung cancer patients. NK cells were expanded by co-culture with irradiated K562-mb-IL-21 feeder cells and rhIL-2 as described previously (19). Expansion was conducted for at least 3 weeks prior to functional assays. For experiments using freshly isolated NK cells, NK cells were isolated via positive selection from PBMCs using a CD56+ selection kit from Stemcell, according to the manufacturer's instructions.

Flow cytometric staining

To discriminate live/dead cells, cells were first stained for 30 minutes with fixable viability stain (eBioscience). Cells were then washed with FACS buffer (0.2% BSA in PBS) and stained with extracellular antibodies for 30 minutes. Cells not undergoing intracellular staining were then fixed in 1% paraformaldehyde. For intracellular staining, cells were fixed with Cytofix/Cytoperm from BD Biosciences for 20 minutes and then stained with intracellular antibodies in a 1X

Perm/Wash solution (BD Bioscience) for 30 minutes. Sample acquisition was carried out on a BD LSRFortessa and analyzed on FlowJo software. See supplementary methods for a complete list of the antibodies used.

Functional assays and PD1/PDL1 expression

Flow cytometry-based killing and degranulation assays were conducted in complete RPMI medium as described previously (15, 19). Specifically, for killing assays against A549 cells, NK cells were co-incubated with CFSE-labeled A549s at 1:1, 5:1, and 10:1 effector-to-target ratios for 5 hours, following which cells were stained with fixable viability stain. For killing assays against PDL1+ A549 cells, A549s were pre-treated with rhIFNγ (20 ng/mL) for 48 hours to induce PDL1 expression and washed 3 times prior to seeding for the assay.

Killing assays against patient tumours were conducted using a transwell model *ex vivo*. Patient tumours were seeded on both apical and basolateral surfaces of the transwell. NK cells were added to the apical chamber at a 10:1 effector-to-target ratio and co-incubated for 48 hours unless indicated otherwise. Tumours from the same patients were used across NK cell groups (healthy donor [HD] pbNK, and lung cancer patient [LCP] pbNK and taNK). Nivolumab, a PD1 blocking antibody used clinically for the treatment of PDL1+ cancer (11), was added to wells at 1μg/mL where indicated. Low dose IL-15 (1 ng/mL) was added as an NK cell survival factor for this extended incubation. Following incubation, cells in the apical chamber were stained to assess direct NK cell killing and cells in the basolateral chamber were stained to assess killing by endogenous tumour-infiltrating lymphocytes (TILs).

For degranulation assays and IFNγ expression against patient tumours, NK cells were co-incubated with target cells at a 1:1 ratio for 5 hours. Golgi Stop (BD Biosciences) was added following the first hour of incubation.

PD1 expression on NK cells and PDL1 expression on tumour cells were assessed by co-incubating NK cells with tumour cells for 48 hours using the transwell model described above. PD1 expression was assessed by staining cells in the apical chamber for NK cells markers and PD1. PDL1 expression was assessed on live tumour cells in the basolateral chamber.

Statistics

Statistical analysis was conducted using GraphPad Prism software. Graphs with two groups were analyzed using a two-tailed unpaired t-test. Graphs with three or more conditions with one independent variable were analyzed by one-way ANOVA with Tukey correction for multiple comparisons. Graphs with two independent variables were analyzed by two-way ANOVA with Tukey correction. D'Agostino & Pearson normality test was used to determine distribution of the data. Correlation data were analyzed using Pearson correlation.

3.4 RESULTS

We first assessed the therapeutic potential of using NK cells expanded from the pleural effusions, surgically-resected tumours, and peripheral blood of lung cancer patients to treat PDL1+ and PDL1- lung tumours. Table 1 shows the study population and tumour classification. We expanded NK cells from the above sources using irradiated K562 feeder cells genetically engineered to express membrane-bound IL-21. A recent trial demonstrated that NK cells expanded via this method had a high safety profile and remarkably reduced relapse rates in patients with high-risk myeloid malignancies (20). We found that NK cells from all sources reached clinically

applicable fold expansion rates and purity (Figure S1A-C). Notably, NK cells from PDL1- lung tumours expanded comparably to those from PDL1+ tumours and had comparable and high viability (Figures 1A and S1D). exNK cells exhibited a $CD56^{superbright}$ phenotype with high activation receptor expression, which we previously found to be a phenotype associated with the greatest anti-tumour activity (Figures 1B-C and S1E-G)(19).

Consistent with their highly activated phenotype, lung cancer patient exNK cells showed strong killing against human A549 lung cancer cells and significantly reduced tumour burden and controlled tumour growth upon adoptive transfer to NRG mice engrafted with a measurable burden of A549 tumours (Figures 1D-E and S2A-B). We next assessed the antitumour functions of exNK cells against patients' own advanced tumours *ex vivo,* which also contain further immunosuppressive effects from regulatory immune cells. Against patient tumours, exNK cells showed strong killing and activation-induced degranulation and IFNγ production (Figure 1F-I, and S2C). Furthermore, NK cells expanded from lung cancer patient peripheral blood and tumours showed comparable antitumour activity as healthy donor exNK cells. These findings uncover promising therapeutic potential for lung cancer patient exNK cells to treat both PDL1+ and PDL1- tumours.

We next assessed the impact of exNK cells on endogenous immune cells in tumours. Using a transwell model in which lung cancer patient tumours were seeded on both apical and basolateral surfaces, we found that administration of exNK cells to the apical chamber activated endogenous TILs in the basolateral chamber to kill patient tumours (Figure 1J). The contact-independent mechanism through which exNK cells rescued TILs from exhaustion likely involved IFNγ, as treatment of tumours with recombinant human (rh)IFNγ alone partly rescued TIL activity. Together, these results demonstrate that expanded lung cancer patient NK cells are capable of

strong anti-tumour activity upon engagement with patient tumours, through both direct tumour killing and release of proinflammatory mediators that revive exhausted endogenous TILs (Figure 1K).

Degree of tumour PDL1 expression (tumour proportion score; TPS) is associated with PD1-blockade efficacy and used to determine treatment (3, 7, 11, 21). PD1-blockade is routinely used as first-line therapy for lung cancer patients with PDL1^{hi} tumours (TPS ≥50%) and as second-line therapy for patients with PDL1^{lo} tumours (TPS ≥1% and ≤49%)(22, 23). However, only 22% of lung cancer patients have PDL1^{hi} tumours and only ~50% of patients have a TPS ≥1% (24). Given that IFNγ signaling upregulates PDL1 on tumour cells and that exNK cells upregulated IFNγ upon engagement with tumours, we assessed whether exNK cells could induce PDL1 expression on lung tumours. Using the transwell model as in Figure 1H, we seeded A549s on apical and basolateral surfaces, incubated exNK cells in the apical chamber, and assessed PDL1 expression on basolateral A549s after 48 hours (Figure S3A). Compared to untreated A549s which were PDL1-, exNK-treated A549s highly expressed PDL1, with a mean TPS of 90.1% (Figure S3B). Similar to previous reports (18), the increase in PDL1 TPS by exNK cells was consistent across other poor prognosis cancer types and independent of baseline PDL1 TPS, as exNK cells also strikingly increased PDL1 TPS and mean fluorescence intensity (MFI) in OVCAR8 ovarian cancer and MDA-MB-231 triple-negative breast cancer cells, which respectively had low and high PDL1 TPS at baseline (Figure S3C-D).

We next assessed the ability of exNK cells to increase PDL1 expression on tumours from lung cancer patients via flow cytometry (see Table S1 for baseline TPS assessment via flow cytometry and diagnostic immunohistochemistry). Treatment with exNK cells from healthy donors or lung cancer patient peripheral blood or tumours remarkably increased PDL1 expression

on tumours from all patients and comparably to treatment with rhIFNγ alone (Figs. 2A-C, S3E). As a result, while 43% of patient tumours were PDL1- at baseline, following exNK treatment, all patient tumours were PDL1+ (Figure 2D). Further, the majority of tumours became PDL1^{hi}, surpassing the threshold for first-line PD1-blockade therapy. Notably, upregulation of PDL1 on tumour cells required NK cells capable of potent activation in response to tumours, as treatment of tumours with freshly isolated pbNK cells, known to be suppressed by tumours, had no effect on tumour PDL1 (Figure 2E)(14). These findings identify that exNK cells could be harnessed to increase the proportion of patients who are likely to benefit from PD1-blockade therapy.

We thus evaluated the potential for therapeutic synergy between exNK cells and PD1-blockade. It was previously reported that in addition to T cells, endogenous NK cells also respond to anti-PD1 and contribute to its immunotherapeutic efficacy (25). Although exNK cells expressed minimal PD1 at baseline, they significantly upregulated PD1 expression after exposure to patient tumours (Figure 3A). Thus, although exNK cells maintain strong anti-tumour functions against established tumours, PD1-blockade may even further enhance their maximal anti-tumour capacity. To test this, we pre-treated A549s with rhIFNγ for 48 hours to induce PDL1 expression, then assessed exNK cell killing of PDL1+ A549s over 5 hours with or without the clinical anti-PD1 antibody nivolumab. Treatment with nivolumab significantly increased killing by PD1+ exNK cells against PDL1+ A459 cells (Figure 3B). To verify that the effect was specific to PD1-PDL1 blockade, we confirmed that nivolumab did not increase exNK cell killing against non-pretreated (PDL1-) A549s over 5 hours, a timepoint prior to which PDL1 expression is altered by exNK cells (Figure 3C).

Given our findings that exNK cells convert PDL1- patient tumours to PDL1+/hi, we assessed whether exNK cells could induce a response to PD1-blockade therapy in even initially

PDL1- patient tumours. As anticipated, treatment of PDL1- tumours with nivolumab alone for 48 hours had no significant effect on tumour killing (Figure 3D). However, addition of exNK cells with nivolumab synergistically increased tumour cell death compared to treatment with either nivolumab or exNK cells alone. In addition to increasing exNK cytotoxicity, combination therapy of exNK cells with nivolumab significantly enhanced the reactivation of tumour killing by endogenous TILs compared to either treatment in isolation, and to a similar degree as rhIFNγ (Figure 3E). Notably, the ability of exNK cells to kill patient tumours with and without nivolumab correlated significantly with their ability to upregulate tumour PDL1 expression (Figure 3F), indicating that change in PDL1 expression may serve as a predictor for tumours that will be most responsive to exNK cell therapy.

3.5 DISCUSSION

Patients with advanced tumours that do not respond to checkpoint blockade immunotherapy face a dearth of effective treatment options. Although studies have predominantly focused on the role of T cells to mediate the anti-tumour effects of immune checkpoint blockade therapy, there is a growing understanding for the important role of other immune cell types, including NK cells and B cells, in mediating this response (25, 26). Notably, NK cell depletion was shown to reduce response to PD1/L1-blockade therapy in a syngeneic murine model of colon carcinoma (25). A previous study also showed that NK cells expanded from induced-pluripotent stem cells increased PDL1 TPS on tumour cell lines (18). Our study identifies highly cytotoxic expanded NK cells as a promising therapy for lung cancer that may also further extend the benefits of PD1-blockade therapy to patients with non-responding tumours (Figure 3G). A significant barrier to developing broadly effective immunotherapies against solid tumours has been the

inability to sustain cytotoxic and proinflammatory immune cell functions in the tumour microenvironment (3-5). Our findings that NK cells expanded from lung cancer patients maintain strong tumour killing and IFNγ production, both in xenograft models *in vivo* and over prolonged exposure to patient tumours *ex vivo,* suggest that exNK cells overcome the critical hurdle of tumour-induced suppression. Further, our results that exNK cells restore the anti-tumour activity of endogenous TILs indicates a striking ability to not only resist, but dismantle, the immunosuppressive tumour microenvironment and unleash the patient's own antitumour immunity.

Previous work by our group showed that NK cells expanded from breast and ovarian cancer patients have comparable anti-tumour activity against the patients' own autologous tumours as NK cells expanded from healthy donors (15-17). The present study extends these findings to NK cells from lung cancer patients, identifying expanded NK cells as a promising autologous cell therapy for lung cancer.

A seminal study recently found that anti-PDL1-mAbs can directly activate the cytotoxic effector functions of PDL1+ NK cells, irrespective of tumour PDL1 status (27). These findings together with the results in the present study, identify NK cells as critical effectors for inducing responses to PD1/L1-blockade therapy in initially PDL1- tumours.

A recent randomized control trial in patients with PDL1+ non-small-cell lung carcinoma found that combination treatment of NK cells with the PD1 inhibitor pembrolizumab was well-tolerated and improved overall and progression-free survival in patients compared to pembrolizumab treatment alone (28). Importantly, the trial found that there were no adverse events associated with the addition of NK cell therapy. A limitation of our current study is the relatively small study population. Nevertheless, the proven safety profile shown in this previous trial,

together with the robust synergistic tumour killing we observed upon combination treatment of exNK cells and nivolumab against initially PDL1- tumours, suggests that such combination treatment should be investigated in patients with advanced PDL1- tumours.

3.6 DECLARATIONS

Ethics Approval and consent to participate: All research involving human samples was approved by the Hamilton Integrated Research Ethics Board at McMaster University. All human samples were obtained with written informed consent from the participant. All research involving animals was approved by the Animal Research Ethics Board at McMaster university.

Consent for publication: All authors have consented to the publication of this work. Consent from patients not required.

Author Contributions: SMP and AAA conceived the project and designed the experiments; YS provided intellectual input, contributed to experimental design, and guided clinical sample acquisition; SMP, TMR, and IYF performed experiments. AE, ALP, RAB, EAR, and MVC contributed to performing experiments. YS and RAB obtained the clinical samples. SMP curated and formally analyzed the data. SMP and AAA wrote the manuscript; TMR and YS edited the manuscript; AAA secured funding and supervised the project.

Competing interests: The authors declare no competing interests.

Data availability statement: All relevant data are included in the manuscript.

Funding: This work was supported by the Canadian Institutes for Health Research (CIHR) (20009360 to AAA). AAA holds a tier 1 Canada Research Chair in Natural Immunity and NK Cell Function. SMP is supported by a CIHR Vanier Canada Graduate Scholarship.

Acknowledgments: We thank Rebecca Long for administrative assistance and all lung cancer patient and healthy donors who donated samples.

3.7 FIGURES

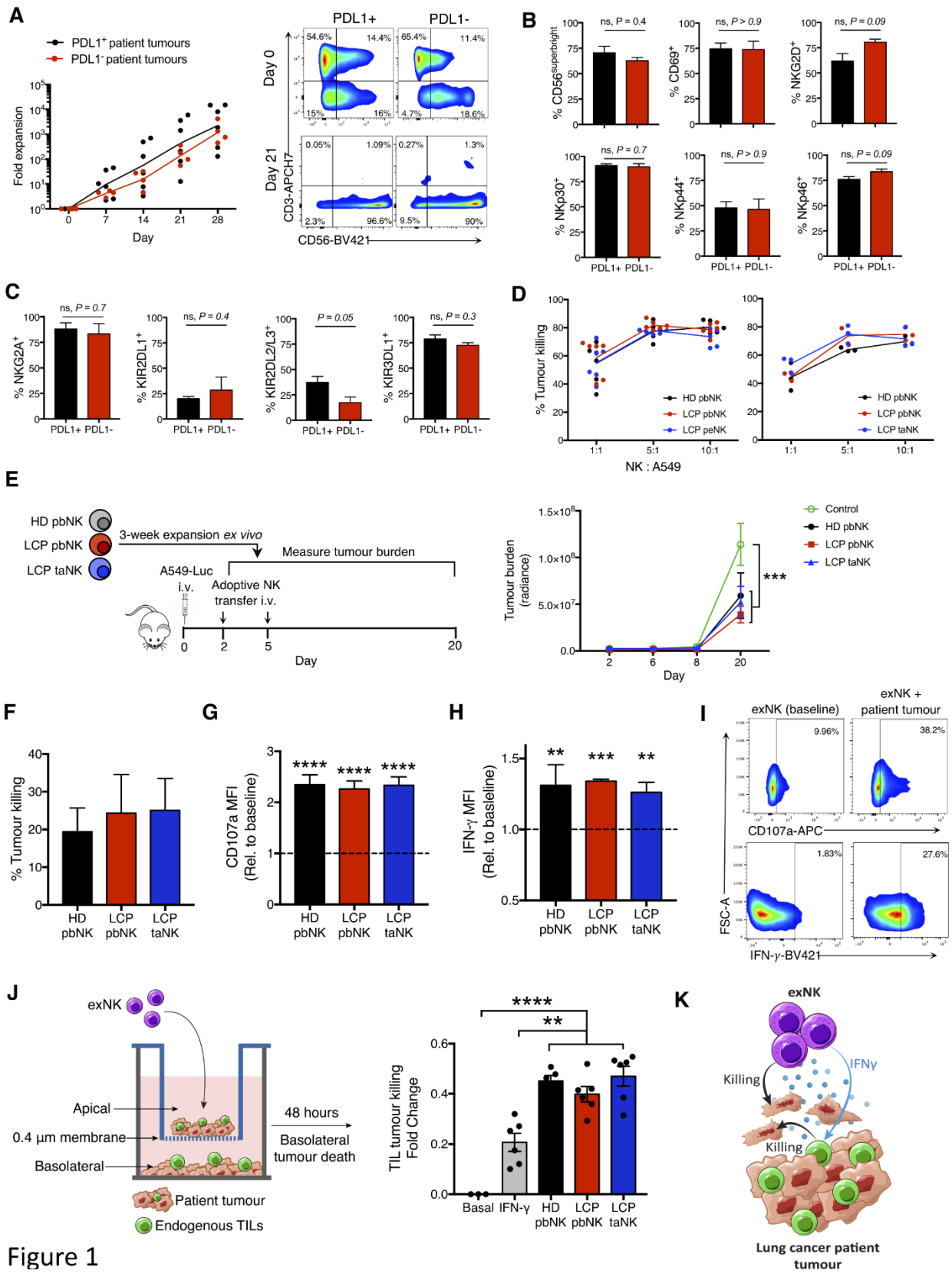

Figure 1

Figure 1. NK cells expanded from lung cancer patients exert strong anti-tumour activity against patient tumours and rescue tumour killing by endogenous TILs. NK cells were expanded from the peripheral blood (pbNK), pleural effusions (peNK), or tumours (taNK) of lung cancer patients (LCP) or peripheral blood of healthy donors (HD). **(A)** Fold expansion of NK cells from PDL1+ vs. PDL1- tumours and representative flow plots showing NK cell (CD56+CD3-) purity pre- and post-expansion. Expression of activation **(B)** and inhibitory **(C)** receptors on exNK cells from PDL1+ and PDL1- tumours at 28-day expansion. **(D)** 5-hour killing of human A549 lung cancer cells by exNK cells. **(E)** Schematic: exNK cells were adoptively transferred to male NRG mice 2 and 5 days after intravenous (i.v.) infusion of Luciferase-expressing A549s (A549-Luc). Graph: quantification of tumour burden via bioluminescence at the indicated days. **(F-I)** Expanded LCP taNK and pbNK cells were co-incubated with lung cancer patient tumours. Five-hour **(F)** killing and relative increase in **(G)** degranulation (CD107a) and **(H)** IFNγ expression against patient tumours compared to expanded HD pbNK cells against these same patient tumours. **(I)** Representative flow plots of NK cell CD107a and IFNγ expression. **(J)** Schematic: patient tumours were seeded in transwell on apical and basolateral surfaces. exNK cells or rhIFNγ (20 ng/mL) or neither (basal) were added to the apical chamber. Graph shows killing of tumours in the basolateral chamber by endogenous TILs after 48 hours. **(K)** Schematic summarizing results. Data show means ±SEM of three to eight replicates per condition. Results analyzed by two-way ANOVA (A,D,E,G,H), unpaired t-test (B,C), or one-way ANOVA (D,F,J). ****$p<0.0001$, ***$p<0.001$, **$p<0.01$.

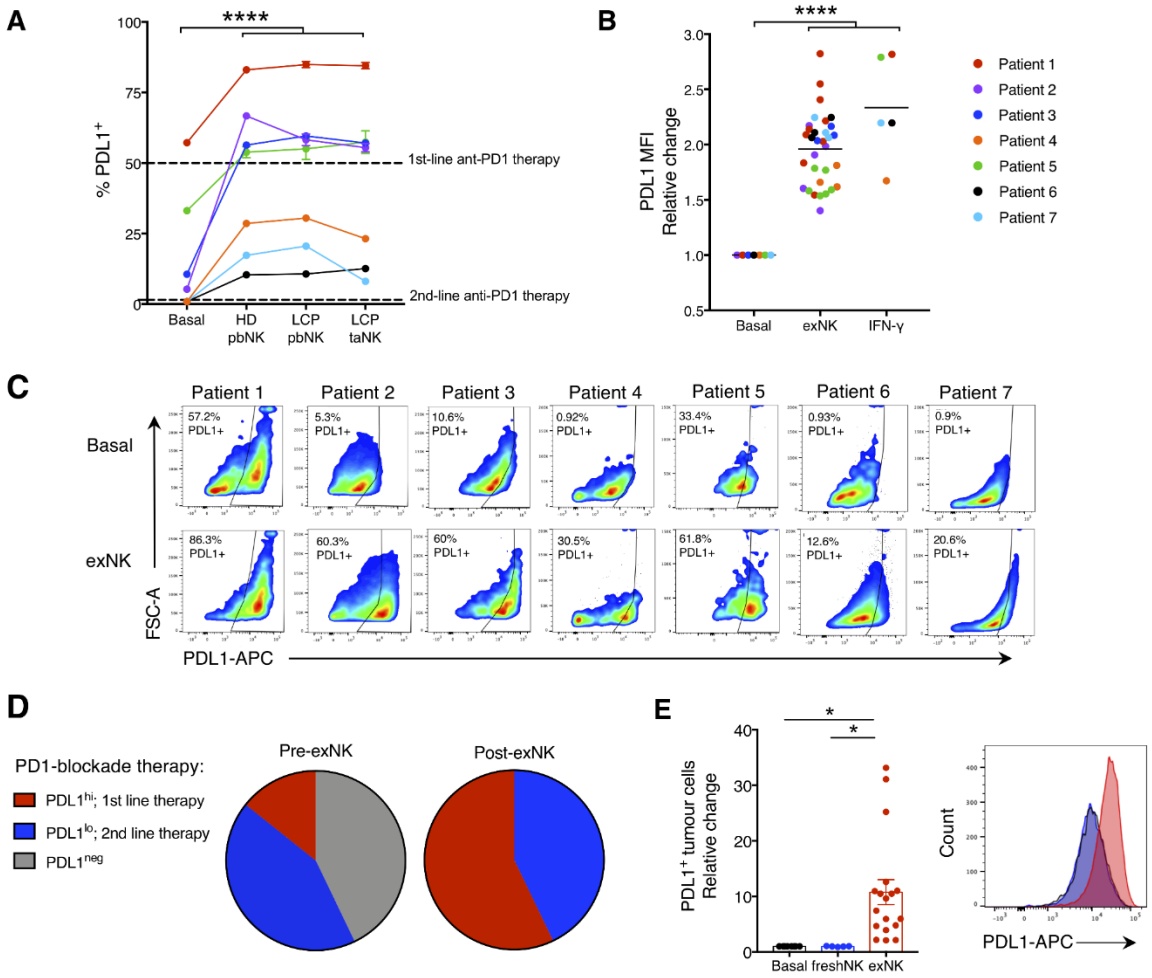

Figure 2. exNK cells convert lung cancer patient PDL1- tumours to PDL1+/hi. Lung cancer patient tumours were seeded in transwell on apical and basolateral surfaces. exNK cells or rhIFNγ (20 ng/mL) or neither (basal) were added to the apical chamber and incubated for 48 hours. **(A)** PDL1 TPS and **(B)** PDL1 mean fluorescence intensity (MFI) on basolateral tumour cells. **(C)** Representative flow plots of PDL1 on exNK-treated vs. untreated patient tumours. **(D)** Proportion of patient tumours that were $PDL1^{neg}$, $PDL1^{lo}$, or $PDL1^{hi}$ pre- and post-exNK treatment. **(E)** Quantification and representative histogram of PDL1 expression on lung cancer patient tumours treated with expanded or unexpanded freshly isolated (fresh) pbNK cells. Data show means ±SEM

of five to thirty-two replicates per condition. A,B,E, analyzed via one-way ANOVA. ****$p<0.0001$, *$p<0.05$.

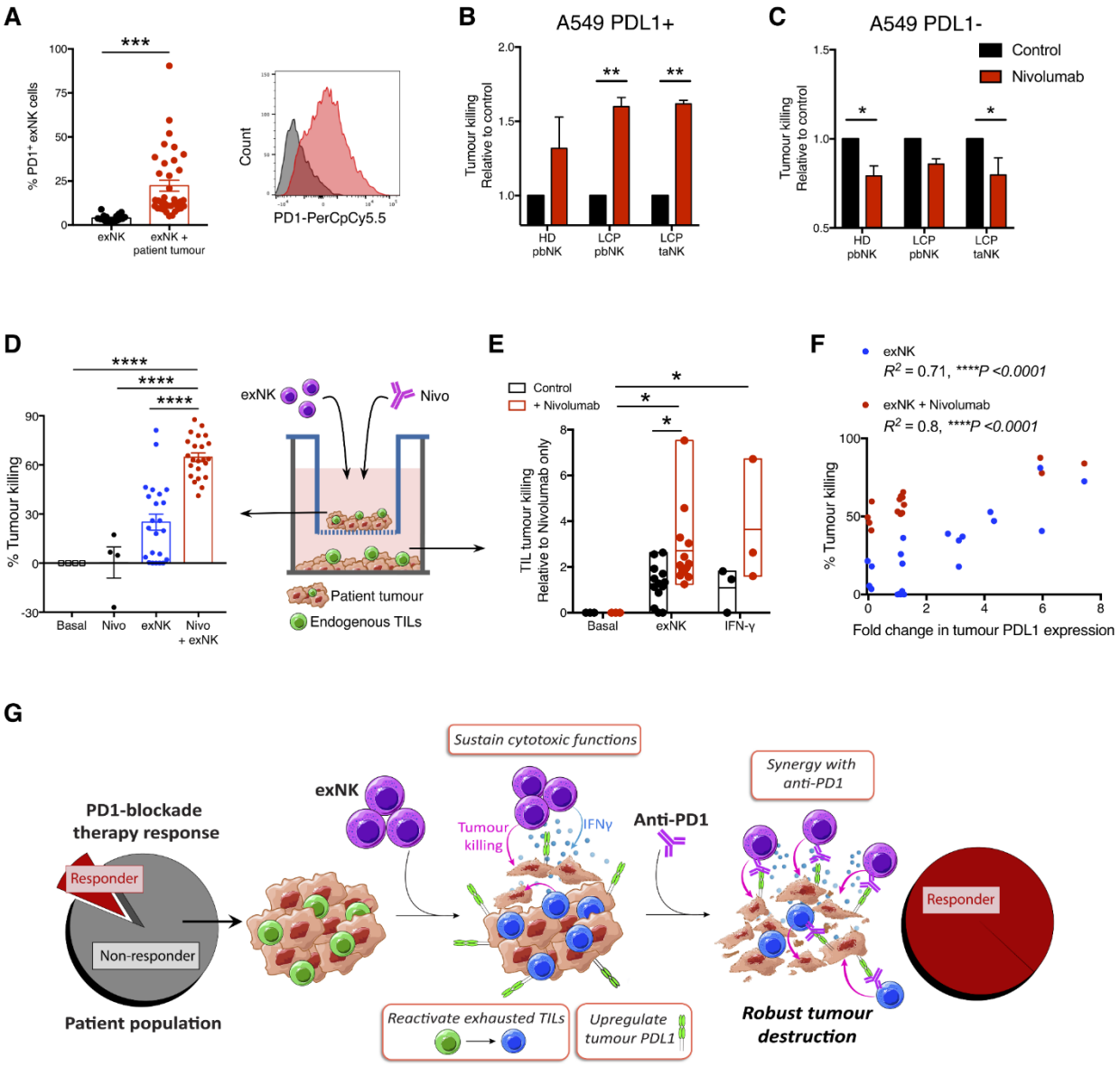

Figure 3. exNK cells sensitize patients' non-responding tumours to PD1-blockade therapy. **(A)** exNK cells were incubated with or without lung cancer patient tumours. Percent PD1+ exNK cells and representative histogram of PD1 expression after 48-hour incubation. (B-C) A549s were left untreated or treated with rhIFNγ (20 ng/mL) for 48 hours to induce PDL1 expression, then washed three times and incubated with exNK cells with or without nivolumab (1 μg/mL) for 5 hours. Relative exNK cell killing of **(B)** IFNγ-treated (PDL1+) A549s or **(C)** untreated (PDL1-) A549s. (D-F) Schematic shows experimental design: patient tumours were seeded on apical and

basolateral transwell surfaces. exNK cells and/or nivolumab (Nivo; 1 μg/mL) were added to the apical chamber for 48 hours. **(D)** Tumour killing in the apical chamber. **(E)** Tumour killing by endogenous TILs in the basolateral chamber. **(F)** Correlation between change in tumour PDL1 expression induced by exNK cells and apical tumour killing. **(G)** Graphical summary of the study's main findings. Data show means ±SEM of four to thirty-six replicates per condition. Results analyzed via unpaired t-test (A), two-way ANOVA (B,C,E), one-way ANOVA (D), or pearson correlation (F). ****p<0.0001, ***p<0.001, **p<0.01, *p<0.05.

3.8 TABLES

Patient #	Age	Sex	Tumour classification	PDL1 Status	ALK	EGFR
1	87	F	NSCLC-adeno	P (HI, >50%)	N	N
2	74	F	NSCLC-squamous	P (LOW, 1-49%)	N	N
3	62	F	NSCLC-squamous	P (LOW, 1-49%)	NA	NA
4	65	M	NSCLC-adeno	N (<1%)	NA	N
5	53	M	NSCLC-adeno	P (LOW, 1-49%)	N	N
6	68	M	Mixed SCLC/NSCLC	NA	NA	NA
7	60	M	NSCLC-squamous	N (<1%)	N	N
8	81	F	NSCLC-adeno	P (HI, >50%)	N	N
9	73	F	NSCLC-squamous	P (HI, >50%)	N	N
10	63	F	NSCLC-adeno	P (LOW, 1-49%)	N	P
11	78	M	NSCLC-adeno	P (HI, >50%)	N	N
12	79	F	NSCLC-adeno	N (<1%)	N	N
13	76	F	NSCLC-large cell neuroendocrine	NA	NA	NA
14	64	M	SCLC	NA	NA	NA
15	76	F	NSCLC-adeno	P (HI, >50%)	N	N
16	63	M	NSCLC-squamous	P (LOW, 1-49%)	NA	NA

Table 1. Study population and tumour characteristics. NSCLC; non-small cell lung cancer. SCLC; small-cell lung cancer. Adeno; adenocarcinoma. P, positive status; N, negative status; NA,

information not available. Tumour proportion score (TPS). High-positive (HI); TPS ≥50%. Low-positive (LOW); TPS ≥1% and ≤49%. Negative; TPS <1%.

3.9 SUPPLEMENTARY MATERIALS

Supplemental Information for:

Expanded human NK cells from lung cancer patients sensitize patients' PDL1-negative tumours to PD1-blockade therapy

Sophie M. Poznanski, Tyrah M. Ritchie, Isabella Y. Fan, Abdullah El-Sayes, Ana L. Portillo, Ronny A. Ben-Avi, Eduardo A. Rojas, Marianne V. Chew, Yaron Shargall, Ali A. Ashkar

This file contains the following:

Supplementary Methods

Supplementary Figures (Figures S1-S3)

Supplementary Table (Table S1)

SUPPLEMENTARY METHODS

Cell lines and reagents

K562 myelogenous leukemia cells that express membrane-bound IL-21 (K562-mb-IL21; Clone 9) described previously (18) were a kind gift in 2012 from Dr. Dean A. Lee at Nationwide Children's Hospital (Ohio State University Comprehensive Cancer Center, USA). K562-mb-

IL21 cells were cultured in RPMI medium supplemented with 10% fetal bovine serum (FBS), 1% hepes, 1% penicillin-streptomycin, and 1% L-glutamine. Cells from the A549 human lung carcinoma cell line, MDA-MB-231 triple-negative breast cancer cell line and OVCAR8 high-grade ovarian serous adenocarcinoma cell line were obtained from the National Cancer Institute. A549 cells were cultured in αMEM supplemented with 10% FBS, 1% hepes, 1% penicillin-streptomycin, and 1% L-glutamine. OVCAR8 and MDA-MB-231 cells were cultured in DMEM supplemented with 10% FBS, 1% hepes, 1% penicillin-streptomycin, and 1% L-glutamine.

Recombinant human IFNγ, IL-15, and IL-2 cytokines were purchased from Peprotech (Rocky Hill, NJ, USA). Collagenase Type IV and DNase I were purchased from ThermoFisher (Waltham, MA, USA).

Cell Staining for flow cytometry

All cell staining was conducted in light-sensitive conditions and incubations carried out at 4°C. For viability staining, fixable viability stain was diluted 1000x in PBS. For extracellular and intracellular antibody stains, fluorescent minus one wells that contained corresponding isotype controls were used as controls to determine population gating.

Antibodies

The following fluorescently conjugated anti-human antibodies were used for cell staining. From BD Biosciences (San Jose, CA, USA): CD45-APCR700 clone HI30, CD56-BV421 clone NCAM16.2, CD56-PECF594 clone NCAM16.2, CD3-APC-H7 clone SK7, CD14-PE-Cy7 clone M5E2, CD107a-APC clone H4A3, IFNγ-BV421 clone 4S.B3, PDL1-APC clone MIH1, CD69-PECF594 clone FN50, NKp46-BV786 clone 9E2, KIR2DL1-APC clone HP-3E4, KIR3DL1-Alexa700 clone NKB1. From BioLegend (San Jose, CA, USA): CD45-Alexa488 clone HI30,

CD3-PerCp/Cy5.5 clone UCHT1, NKG2D-PerCp/Cy5.5 clone 1D11, NKp30-APC clone P30-15, NKp44-PE clone P44-8, KIR2DL2/L3-PE clone NKAT2, PD1-PerCp/Cy5.5 clone EH12.2H7. From Miltenyi Biotec (Bergisch Gladbach, Germany): NKG2A-PE-Vio770 clone REA110.

Killing Assays

For all killing assays, NK cell killing was calculated by percent specific lysis of tumour cells. In assays using CFSE-labeled A549 cells, tumour cells were gated on CFSE+ events. For killing assays against patient tumours, tumour cells were gated as CD45- events. Viability was then assessed on the tumour cell gate. Control wells with tumour cells alone were used to enumerate basal death.

$$\% \text{ specific lysis} = (\% \text{ dead} - \% \text{ basal death})/(100 - \% \text{ basal death}) \times 100.$$

Degranulation Assay

For degranulation assays and IFNγ expression against patient tumours, anti-human CD107a was added at the start of incubation and golgi stop (BD Biosciences) was added following the first hour of incubation. At 5 hours, cells were stained with fixable viability stain and fluorescently conjugated anti-human CD45, CD56, CD3 (extracellular) and IFNγ (intracellular). NK cells were gated on as CD45+CD56+CD3- cells. CD107a and IFNγ expression were assessed on the NK cell gate.

SUPPLEMENTARY FIGURES

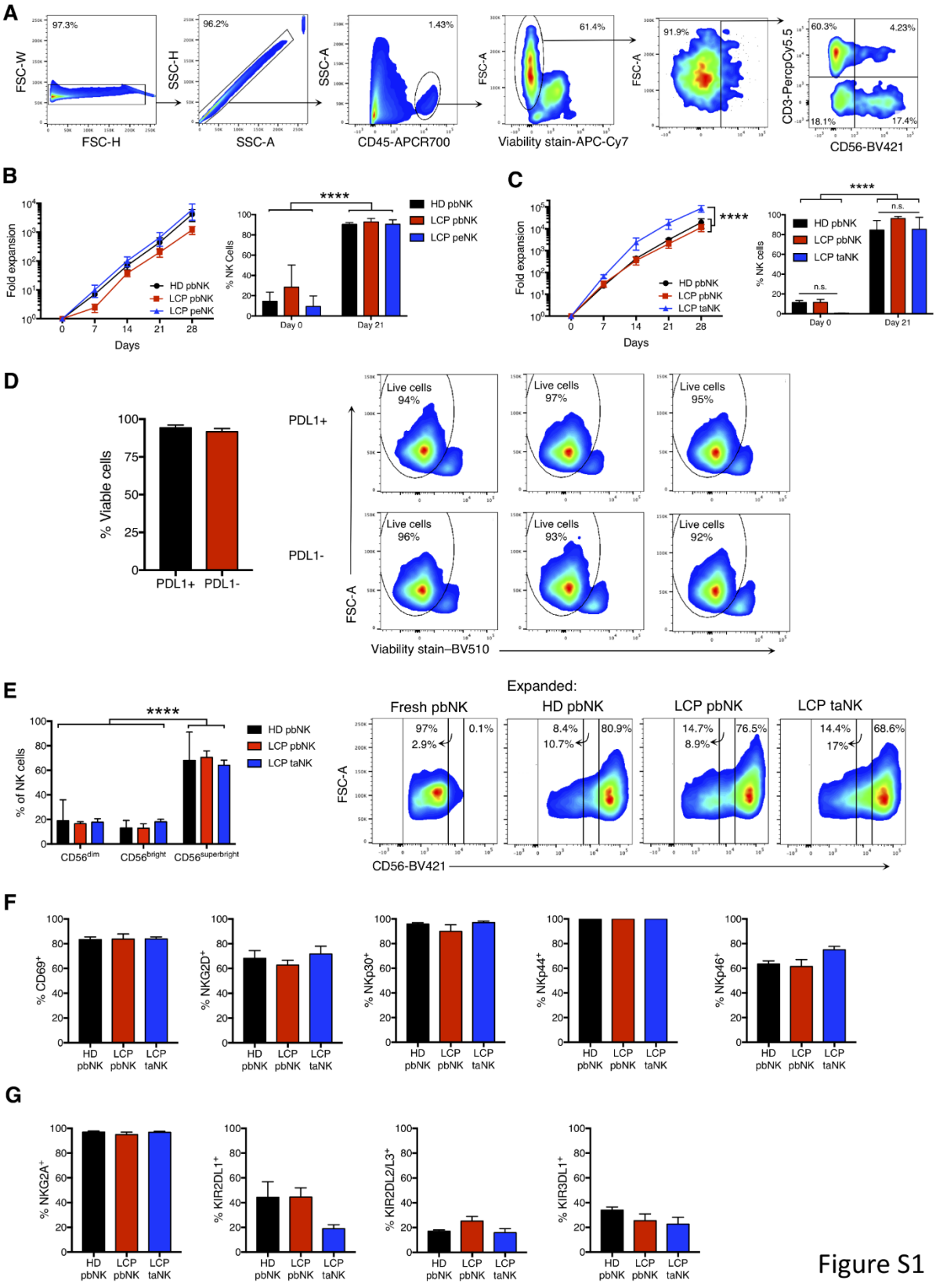
A
97.3%
FSC-W
FSC-H
96.2%
SSC-H
SSC-A
1.43%
SSC-A
CD45-APCR700
61.4%
FSC-A
Viability stain-APC-Cy7
91.9%
FSC-A
60.3%
4.23%
18.1%
17.4%
CD3-PercpCy5.5
CD56-BV421
B
Fold expansion
Days
HD pbNK
LCP pbNK
LCP peNK
% NK Cells
****
Day 0
Day 21
C
Fold expansion
****
Days
HD pbNK
LCP pbNK
LCP taNK
% NK cells
****
n.s.
n.s.
Day 0
Day 21
D
% Viable cells
PDL1+
PDL1-
Live cells 94%
Live cells 97%
Live cells 95%
Live cells 96%
Live cells 93%
Live cells 92%
FSC-A
Viability stain–BV510
E
% of NK cells
****
HD pbNK
LCP pbNK
LCP taNK
CD56dim
CD56bright
CD56superbright
Expanded:
Fresh pbNK
HD pbNK
LCP pbNK
LCP taNK
97%
2.9%
0.1%
8.4%
10.7%
80.9%
14.7%
8.9%
76.5%
14.4%
17%
68.6%
FSC-A
CD56-BV421
F
% CD69+
% NKG2D+
% NKp30+
% NKp44+
% NKp46+
HD pbNK
LCP pbNK
LCP taNK
G
% NKG2A+
% KIR2DL1+
% KIR2DL2/L3+
% KIR3DL1+
HD pbNK
LCP pbNK
LCP taNK

Figure S1

Figure S1. NK cells can be expanded from lung cancer patient blood, pleural effusions, and tumours and show a highly activated phenotype post-expansion. NK cells were expanded *ex vivo* from the peripheral blood (pbNK), pleural effusions (peNK), or tumours (taNK) of lung cancer patients (LCP) or peripheral blood of healthy donors (HD). **(A)** Representative NK cell gating strategy. Sample shown is the pre-expansion NK cell population in a patient tumour. Fold expansion and purity of NK cells from **(B)** donor-matched blood and pleural effusions, or **(C)** matched blood and tumours of lung cancer patients compared to the peripheral blood of healthy donors. **(D)** Quantification and representative flow plots of viability of NK cells from PDL1+ and PDL1- lung cancer patient tumours following 28 days of expansion. **(E)** Quantification and representative flow plots showing the proportion of $CD56^{dim}$, $CD56^{bright}$, and $CD56^{superbright}$ NK cells post-expansion. exNK cell expression of the **(F)** activation receptors CD69, NKG2D, NKp30, NKp44, and NKp46, and **(G)** inhibitory receptors NKG2A and KIR2DL1, KIR2DL2/L3, and KIR3DL1 assessed via flow cytometry. Data show means ±SEM of three to six replicates per condition. B,C, and E, analyzed via two-way ANOVA; D analyzed via unpaired t-test; F and G, analyzed via one-way ANOVA. ****$p<0.0001$.

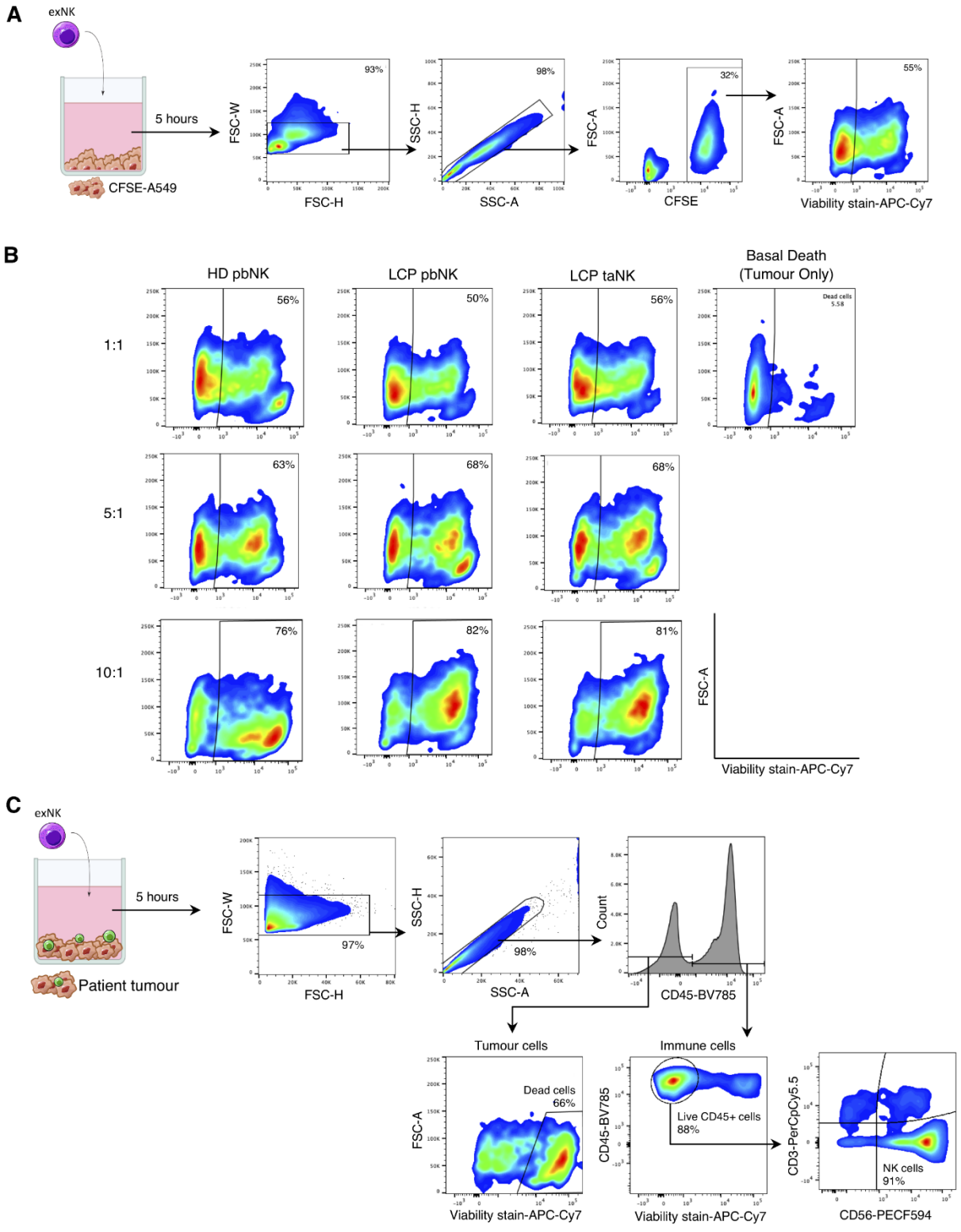

Figure S2. Representative gating strategies for NK cell killing and degranulation assays. (A-B) exNK cells were incubated with CFSE-labelled A549 cells for 5 hours at 1:1, 5:1, or 10:1

effector-to-target ratios (E:T). After 5 hours, cells were stained with fixable viability stain. **(A)** Schematic shows experimental design. Flow plots show representative gating strategy to identify dead tumour cells. Doublets were discriminated via FSC and SSC height (H) and width (W) and live/dead cells were enumerated on the CFSE+ tumour cell population. **(B)** Representative flow plots of tumour cells death following incubation with expanded HD pbNK, LCP pbNK, and LCP taNK cells at the 1:1, 5:1, and 10:1 E:T ratios. Basal tumour cell death is also shown. **(C)** exNK cells were incubated with patient tumours for 5 hours. Flow plots show representative gating for NK cell killing and degranulation. For NK cell tumour killing, tumour cell death was assessed via viability stain on the CD45- cell population. For assessment of NK cell degranulation and IFNγ expression, NK cells were identified as live CD45+CD56+CD3- cells.

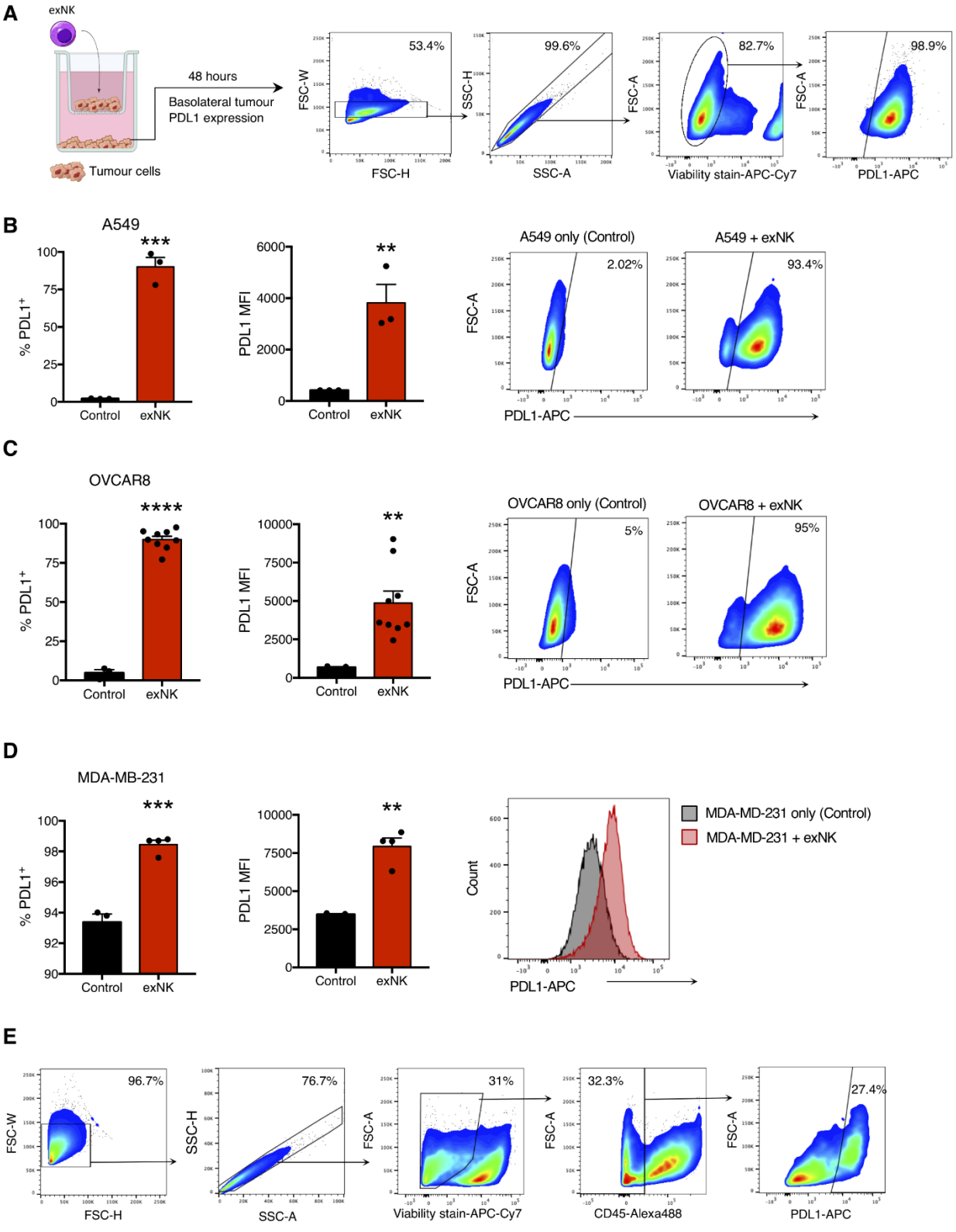
A
exNK
48 hours
Basolateral tumour PDL1 expression
Tumour cells
53.4%
FSC-W
FSC-H
99.6%
SSC-H
SSC-A
82.7%
FSC-A
Viability stain-APC-Cy7
98.9%
PDL1-APC
B
A549
% PDL1+
Control
exNK
PDL1 MFI
A549 only (Control)
A549 + exNK
2.02%
93.4%
C
OVCAR8
OVCAR8 only (Control)
OVCAR8 + exNK
5%
95%
D
MDA-MB-231
MDA-MD-231 only (Control)
MDA-MD-231 + exNK
Count
E
96.7%
76.7%
31%
32.3%
CD45-Alexa488
27.4%

Figure S3. exNK cells increase lung tumour PDL1 expression. A549 cells, OVCAR8 cells, MDA-MB-231 cells, or patient tumours were seeded on apical and basolateral surfaces of a transwell and treated with exNK cells in the apical chamber or left untreated (control). PDL1 expression on live basolateral tumour cells was assessed following 48 hours. **(A)** Schematic shows experimental design and flow plots show representation of gating strategy on A549 cells. Quantification and representative flow plots or histogram of percent PDL1+ cells and PDL1 MFI on **(B)** A549, **(C)** OVCAR8, or **(D)** MDA-MB-231 cells. **(E)** Representative gating strategy of PDL1 expression on patient tumours. Data show means ±SEM of three replicates per condition. Results analyzed via unpaired t-test. ****p<0.0001, ***p<0.001, **p<0.01.

SUPPLEMENTARY TABLE LEGEND

Patient	**Baseline tumour PDL1 status**	
	Diagnostic IHC	**Flow Cytometry**
1	P (HI, >50%)	P (HI, >50%)
2	P (LOW, 1-49%)	P (LOW, 1-49%)
3	P (LOW, 1-49%)	P (LOW, 1-49%)
4	N (<1%)	N (<1%)
5	P (LOW, 1-49%)	P (LOW, 1-49%)
6	NA	N (<1%)
7	N (<1%)	N (<1%)

Table S1. Patient baseline PDL1 status assessment via diagnostic IHC and flow cytometry. Diagnostic IHC; determined clinically via immunohistochemistry. High-positive; TPS ≥50%. Low-positive; TPS ≥1% and ≤49%. Negative; TPS <1%.

3.10 REFERENCES

1. Howlader N, Noone AM, Krapcho M, Miller D, Brest A, Yu M, et al. *SEER Cancer Statistic Review.* Bethesda, MD: National Cancer Institute; 2019.
2. Herbst RS, Soria JC, Kowanetz M, Fine GD, Hamid O, Gordon MS, et al. Predictive correlates of response to the anti-PD-L1 antibody MPDL3280A in cancer patients. *Nature.* 2014;515(7528):563-7.
3. Yu Y, Zeng D, Ou Q, Liu S, Li A, Chen Y, et al. Association of Survival and Immune-Related Biomarkers With Immunotherapy in Patients With Non-Small Cell Lung Cancer: A Meta-analysis and Individual Patient-Level Analysis. *JAMA Netw Open.* 2019;2(7):e196879.
4. Topalian SL, Hodi FS, Brahmer JR, Gettinger SN, Smith DC, McDermott DF, et al. Safety, activity, and immune correlates of anti-PD-1 antibody in cancer. *The New England journal of medicine.* 2012;366(26):2443-54.
5. Benci JL, Xu B, Qiu Y, Wu TJ, Dada H, Twyman-Saint Victor C, et al. Tumor Interferon Signaling Regulates a Multigenic Resistance Program to Immune Checkpoint Blockade. *Cell.* 2016;167(6):1540-54.e12.
6. Amaria RN, Reddy SM, Tawbi HA, Davies MA, Ross MI, Glitza IC, et al. Neoadjuvant immune checkpoint blockade in high-risk resectable melanoma. *Nat Med.* 2018;24(11):1649-54.
7. Fehrenbacher L, Spira A, Ballinger M, Kowanetz M, Vansteenkiste J, Mazieres J, et al. Atezolizumab versus docetaxel for patients with previously treated non-small-cell lung cancer (POPLAR): a multicentre, open-label, phase 2 randomised controlled trial. *Lancet.* 2016;387(10030):1837-46.
8. Ayers M, Lunceford J, Nebozhyn M, Murphy E, Loboda A, Kaufman DR, et al. IFN-γ-related mRNA profile predicts clinical response to PD-1 blockade. *J Clin Invest.* 2017;127(8):2930-40.
9. McDermott DF, Huseni MA, Atkins MB, Motzer RJ, Rini BI, Escudier B, et al. Clinical activity and molecular correlates of response to atezolizumab alone or in combination with bevacizumab versus sunitinib in renal cell carcinoma. *Nat Med.* 2018;24(6):749-57.
10. Taube JM, Anders RA, Young GD, Xu H, Sharma R, McMiller TL, et al. Colocalization of inflammatory response with B7-h1 expression in human melanocytic lesions supports an adaptive resistance mechanism of immune escape. *Sci Transl Med.* 2012;4(127):127ra37.
11. Borghaei H, Paz-Ares L, Horn L, Spigel DR, Steins M, Ready NE, et al. Nivolumab versus Docetaxel in Advanced Nonsquamous Non-Small-Cell Lung Cancer. *The New England journal of medicine.* 2015;373(17):1627-39.
12. Chen S, Crabill GA, Pritchard TS, McMiller TL, Wei P, Pardoll DM, et al. Mechanisms regulating PD-L1 expression on tumor and immune cells. *Journal for immunotherapy of cancer.* 2019;7(1):305.
13. Chang CH, Qiu J, O'Sullivan D, Buck MD, Noguchi T, Curtis JD, et al. Metabolic competition in the tumour microenvironment is a driver of cancer progression. *Cell.* 2015;162(6):1229-41.
14. Uchida A, Colot M, and Micksche M. Suppression of natural killer cell activity by adherent effusion cells of cancer patients. Suppression of motility, binding capacity and lethal hit of NK cells. *British journal of cancer.* 1984;49(1):17-23.

15. Nham T, Poznanski SM, Fan IY, Shenouda MM, Chew MV, Lee AJ, et al. Ex vivo-expanded NK cells from blood and ascites of ovarian cancer patients are cytotoxic against autologous primary ovarian cancer cells. *Cancer Immunol Immunother.* 2018;67(4):575-87.
16. Poznanski SM, Nham T, Chew MV, Lee AJ, Hammill JA, Fan IY, et al. Expanded CD56superbrightCD16+ NK cells from ovarian cancer patients are cytotoxic against autologous tumor in a patient-derived xenograft murine model. *Cancer Immunol Res.* 2018;6(10):1174-85.
17. Shenouda MM, Gillgrass A, Nham T, Hogg R, Lee AJ, Chew MV, et al. Ex vivo expanded natural killer cells from breast cancer patients and healthy donors are highly cytotoxic against breast cancer cell lines and patient-derived tumours. *Breast Cancer Res.* 2017;19(1):76.
18. Oyer JL, Gitto SB, Altomare DA, and Copik AJ. PD-L1 blockade enhances anti-tumor efficacy of NK cells. *Oncoimmunology.* 2018;7(11):e1509819.
19. Poznanski SM, Nham T, Chew MV, Lee AJ, Hammill JA, Fan IY, et al. Expanded CD56(superbright)CD16(+) NK Cells from Ovarian Cancer Patients Are Cytotoxic against Autologous Tumor in a Patient-Derived Xenograft Murine Model. *Cancer Immunol Res.* 2018;6(10):1174-85.
20. Ciurea SO, Schafer JR, Bassett R, Denman CJ, Cao K, Willis D, et al. Phase 1 clinical trial using mbIL21 ex-vivo expanded donor-derived NK cells after haploidentical transplantation. *Blood.* 2017:pii: blood-2017-05-785659.
21. Garon EB, Rizvi NA, Hui R, Leighl N, Balmanoukian AS, Eder JP, et al. Pembrolizumab for the treatment of non-small-cell lung cancer. *The New England journal of medicine.* 2015;372(21):2018-28.
22. Pai-Scherf L, Blumenthal GM, Li H, Subramaniam S, Mishra-Kalyani PS, He K, et al. FDA Approval Summary: Pembrolizumab for Treatment of Metastatic Non-Small Cell Lung Cancer: First-Line Therapy and Beyond. *Oncologist.* 2017;22(11):1392-9.
23. Kazandjian D, Suzman DL, Blumenthal G, Mushti S, He K, Libeg M, et al. FDA Approval Summary: Nivolumab for the Treatment of Metastatic Non-Small Cell Lung Cancer With Progression On or After Platinum-Based Chemotherapy. *Oncologist.* 2016;21(5):634-42.
24. Dietel M, Savelov N, Salanova R, Micke P, Bigras G, Hida T, et al. Real-world prevalence of programmed death ligand 1 expression in locally advanced or metastatic non-small-cell lung cancer: The global, multicenter EXPRESS study. *Lung cancer (Amsterdam, Netherlands).* 2019;134:174-9.
25. Hsu J, Hodgins JJ, Marathe M, Nicolai CJ, Bourgeois-Daigneault MC, Trevino TN, et al. Contribution of NK cells to immunotherapy mediated by PD-1/PD-L1 blockade. *J Clin Invest.* 2018;128(10):4654-68.
26. Cabrita R, Lauss M, Sanna A, Donia M, Skaarup Larsen M, Mitra S, et al. Tertiary lymphoid structures improve immunotherapy and survival in melanoma. *Nature.* 2020;577(7791):561-5.
27. Dong W, Wu X, Ma S, Wang Y, Nalin AP, Zhu Z, et al. The Mechanism of Anti-PD-L1 Antibody Efficacy against PD-L1-Negative Tumors Identifies NK Cells Expressing PD-L1 as a Cytolytic Effector. *Cancer Discov.* 2019;9(10):1422-37.
28. Lin M, Luo H, Liang S, Chen J, Liu A, Niu L, et al. Pembrolizumab plus allogeneic NK cells in advanced non-small cell lung cancer patients. *J Clin Invest.* 2020;130(5):2560-9.

– CHAPTER 4 –

METABOLIC FLEXIBILITY DETERMINES HUMAN NK CELL FUNCTIONAL FATE IN THE TUMOUR MICROENVIRONMENT

Metabolic flexibility determines human NK cell functional fate in the tumour microenvironment

Sophie M. Poznanski[1], Kanwaldeep Singh[2,8], Tyrah M. Ritchie[1,8], Jennifer A. Aguiar[3], Isabella Y. Fan[1], Ana L. Portillo[1], Eduardo A. Rojas[1], Fatemeh Vahedi[1], Abdullah El-Sayes[1], Sansi Xing[4], Martin Butcher[5], Yu Lu[4], Andrew C. Doxey[3], Jonathan D. Schertzer[4,6], Hal W. Hirte[2,7], Ali A. Ashkar[1]

[1]Department of Medicine, McMaster Immunology Research Centre, McMaster University, Hamilton, ON, L8N 3Z5, Canada

[2]Department of Oncology, McMaster University, Hamilton, ON, L8V 5C2, Canada

[3]Department of Biology, University of Waterloo, Waterloo, ON, N2L 3G1, Canada

[4]Department of Biochemistry and Biomedical Sciences, McMaster University, Hamilton, ON, L8S 4K1, Canada

[5]Juravinski Cancer Centre & McMaster University, Hamilton, ON, L8V 5C2, Canada

[6]Farncombe Family Digestive Health Research Institute, McMaster University, Hamilton, ON, L8S 4K1, Canada

[7]Division of Medical Oncology, Juravinski Cancer Centre, Hamilton, ON, L8V 5C2, Canada

[8]KS and TMR contributed equally

Preface: *The research presented in this manuscript was conducted between 2016-2021. S.M.P. and A.A.A. conceived the project and designed the experiments; S.M.P., K.S., T.M.R., and S.X. performed experiments; I.Y.F., A.L.P., E.A.R., F.V., and A.E.-S. contributed to performing experiments; S.M.P., J.A.A., Y.L., and A.C.D. curated and formally analyzed the data; M.B. contributed to project administration; K.S., J.D.S., and H.W.H. provided intellectual and experimental input; S.M.P. and A.A.A. wrote the manuscript; T.M.R., J.A.A., Y.L., J.D.S., and H.W.H. edited the manuscript; H.W.H. and A.A.A. secured funding; and A.A.A. supervised the project.*

Title: Metabolic flexibility determines human NK cell functional fate in the tumour microenvironment

Authors: Sophie M. Poznanski[1], Kanwaldeep Singh[2,8], Tyrah M. Ritchie[1,8], Jennifer A. Aguiar[3], Isabella Y. Fan[1], Ana L. Portillo[1], Eduardo A. Rojas[1], Fatemeh Vahedi[1], Abdullah El-Sayes[1], Sansi Xing[4], Martin Butcher[5], Yu Lu[4], Andrew C. Doxey[3], Jonathan D. Schertzer[4,6], Hal W. Hirte[2,7], Ali A. Ashkar[1]*

Affiliations:

[1]Department of Medicine, McMaster Immunology Research Centre, McMaster University, Hamilton, ON, L8N 3Z5, Canada

[2]Department of Oncology, McMaster University, Hamilton, ON, L8V 5C2, Canada

[3]Department of Biology, University of Waterloo, Waterloo, ON, N2L 3G1, Canada

[4]Department of Biochemistry and Biomedical Sciences, McMaster University, Hamilton, ON, L8S 4K1, Canada

[5]Juravinski Cancer Centre & McMaster University, Hamilton, ON, L8V 5C2, Canada

[6]Farncombe Family Digestive Health Research Institute, McMaster University, Hamilton, ON, L8S 4K1, Canada

[7]Division of Medical Oncology, Juravinski Cancer Centre, Hamilton, ON, L8V 5C2, Canada

[8]KS and TMR contributed equally

*Corresponding author and Lead Contact. Further information and requests for resources and reagents should be directed to and will be fulfilled by the Lead Contact, Ali A. Ashkar: ashkara@mcmaster.ca

4.1 SUMMARY

NK cells are central to anti-tumour immunity and recently showed efficacy for treating hematologic malignancies. However, their dysfunction in the hostile tumour microenvironment remains a pivotal barrier for cancer immunotherapies against solid tumours. Using cancer patient samples and proteomics, we found that human NK cell dysfunction in the tumour microenvironment is due to suppression of glucose metabolism via lipid peroxidation-associated oxidative stress. Activation of the Nrf2 antioxidant pathway restored NK cell metabolism and function and resulted in greater antitumour activity *in vivo*. Strikingly, expanded NK cells reprogrammed with complete metabolic substrate flexibility not only sustained metabolic fitness, but paradoxically augmented their tumour killing in the tumour microenvironment and in response to nutrient deprivation. Our results uncover that metabolic flexibility enables a cytotoxic immune cell to exploit the metabolic hostility of tumours for their advantage, addressing a critical hurdle for cancer immunotherapy.

Keywords: NK cells, tumour microenvironment, cancer immunotherapy, adoptive cell therapy, immunometabolism, metabolic flexibility, metabolic fitness, Warburg effect, oxidative stress, glycolysis, oxidative phosphorylation

4.2 INTRODUCTION

Immune escape has long been recognized as a hallmark necessary for tumour establishment and progression. Solid tumours produce a potent immunosuppressive tumour microenvironment (TME) that causes severe dysfunction in cytotoxic immune cells (Schreiber et al., 2011). Suppression of Natural Killer (NK) cell anti-tumour activity by the TME plays a critical role in tumour development. Defects in NK cell function lead to higher rates of tumour establishment and growth (Liu et al., 2017). Furthermore, NK cells in the TME of cancer patients have impaired cytotoxicity and the extent of their impairment correlates inextricably with prognosis in a number of cancers (Belisle et al., 2007; Coca et al., 1997; Donskov and von der Maase, 2006; Ishigami et al., 2000). However, the fundamental mechanisms inherent to NK cell dysfunction in the TME remain poorly understood.

The hostility of the TME is shaped by the growth requirements of tumours. Tumour cells exert profound metabolic demands to support their rapid proliferation. As a consequence, the TME is deprived of metabolic nutrients including glucose and glutamine, rich in metabolic waste products including lactic acid, and hypoxic (Mockler et al., 2014; Reina-Campos et al., 2017). Tumour cells are adapted to thrive in this metabolically hostile environment due to their increased metabolic substrate flexibility, resistance to oxidative stress and damage, and distinct STAT3-mediated metabolic program known as the Warburg effect (Poli and Camporeale, 2015; Warburg, 1925; Warburg et al., 1927). Warburg metabolism is characterized by an increase in glycolytic and anabolic metabolism combined with reduced reliance on mitochondrial oxidative metabolism (Poli and Camporeale, 2015; Warburg, 1925; Warburg et al., 1927). It is becoming increasingly clear that the effector functions of lymphocytes require substantial bioenergetics, and that these could be limited by the TME. NK cells use glucose as their principal metabolic fuel and require elevated

glucose-driven glycolysis and mitochondrial oxidative phosphorylation (OxPhos) for their anti-tumour response (Assmann et al., 2017; Donnelly et al., 2014; Keating et al., 2016; Keppel et al., 2015). Studies have shown that nutrient-deprivation in the TME critically inhibits T cells by suppressing glycolysis and mitochondrial function (Chang et al., 2015; Scharping et al., 2016). That the TME can at once be favourable for tumour cell metabolism yet detrimental to lymphocyte metabolism suggests that metabolic adaptations determine whether a cell prospers or is hindered in the TME. This unearths tremendous potential for metabolically adapting immune cells to overcome suppression and immune escape in the TME.

NK cells have recently garnered intense focus as an emerging frontier of cell therapies for cancer. Given their antigen-unrestricted mechanism of tumour cell killing, NK cells are 1) inherently resistant to tumour escape by antigenic drift that limits antigen-specific adaptive immunity, and 2) have the potential to be broadly effective against heterogeneous tumour types (Cerwenka and Lanier, 2018). Importantly, due to their ability to discriminate malignant from healthy cells, NK cell therapies have proven effective and safe in patients with hematologic malignancies (Ciurea et al., 2017; Liu et al., 2020; Romee et al., 2016). However, the suppression of NK cell anti-tumour activity by the TME remains a significant hurdle to extending their therapeutic potential to solid tumours (Geller et al., 2011; Parkhurst et al., 2011).

In this study, we investigated the mechanisms for human NK cell dysfunction in the human TME. Using models of human ovarian cancer, we found that the TME directly paralyzes NK cell glucose metabolism via lipid-peroxidation-associated oxidative stress as a central mechanism to inhibition. We identify harnessing the Nrf2 antioxidant pathway as a novel mechanism to restore NK cell metabolism and function in the TME. Most intriguingly, we uncover metabolic flexibility as a key determinant of NK cell fate in the TME. We found that NK cells armed with complete

substrate flexibility not only remained metabolically fit, but paradoxically augmented their tumour killing in response to the hostile TME and nutrient deprivation. These findings show that metabolic insufficiency drives NK cell dysfunction in the TME and identify improving the metabolic resourcefulness of cytotoxic immune cells via substrate flexibility as a promising therapeutic strategy for cancer immunotherapies against solid tumours.

4.3 RESULTS

Dysfunctional tumour-associated NK cells from cancer patients have impaired glucose metabolism

It has been known for decades that NK cells are critical for anti-tumour immunity, but that their anti-tumour functions, including tumour killing and IFNγ production, are impaired by the TME (Berek et al., 1984; Parkhurst et al., 2011). Yet, the direct impact of human NK cell dysfunction on tumour development remains correlative (Belisle et al., 2007; Krneta et al., 2016). We isolated tumour-associated (ta)NK cells from the TME of ovarian cancer patients and confirmed their impaired ability to kill OVCAR8 human ovarian cancer cells *in vitro* compared to peripheral blood (pb)NK cells (Figures 1A and S1A). Viability of NK cells from both sources was comparable and >90% following isolation (Figure S1B). We next assessed the impact of taNK cell dysfunction on tumour development *in vivo*. We co-administered Luciferase-expressing OVCAR8 cells with human pbNK or taNK cells to immunodeficient mice. Compared to pbNK cells, taNK cells had a significantly impaired ability to prevent tumour engraftment and control tumour growth in mice (Figure 1B). Thus, the impaired cytotoxic functions of cancer patient taNK cells directly enable immune escape by tumours.

Given that glucose metabolism is required for NK cell anti-tumour activity, but that tumour cells create a nutrient deprived TME, we investigated whether taNK cells from the ascites fluid of ovarian cancer patients had altered metabolism. We found that taNK cells had significantly lower basal glycolysis, measured by their extracellular acidification rate (ECAR), compared to pbNK cells as well as significantly reduced glycolytic capacity, indicating an impaired ability to up-regulate glycolysis to meet stress-induced energetic demands (Figure 1C). Cell-surface staining revealed lower expression of the Glut1 glucose transporter on taNK cells relative to pbNK cells (Figures 1D and S1C). In pbNK cells, glucose has been shown to be the primary fuel used to drive OxPhos (Assmann et al., 2017). Thus, we next assessed rates of OxPhos by measuring cellular oxygen consumption rate (OCR). As with glycolysis, taNK cells had significantly lower basal and maximal OxPhos compared to pbNK cells (Figure 1E). Consequently, the rate of ATP production linked to mitochondrial respiration was also significantly lower in taNK cells (Figure 1E). It has been shown in T cells that increased mitochondrial mass and fused mitochondrial networks support enhanced OxPhos efficiency (Buck et al., 2016). Staining of NK cells with a MitoTracker mitochondrial-specific dye showed that compared to pbNK cells, taNK cells had a significantly reduced mass and fusion of activated mitochondria (Figures 1F and S1C). We found similar reductions in Glut1 expression and mitochondrial mass in NK cells from the tumours of lung cancer patients compared to peripheral blood, suggesting that these metabolic defects also extend to NK cells from other tumour types (Figure S1D-F). These results uncover that the dysfunction of cancer patient taNK cells corresponds with a broad impairment in glucose metabolic requirements for NK cell anti-tumour responses.

The TME of cancer patients directly arrests glucose metabolism in pbNK cells to impair anti-tumour activity

To investigate whether the TME directly causes the metabolic impairments seen in taNK cells, we assessed the effects of the human TME on pbNK cell glucose metabolism. We generated an *ex vivo* model of the human TME using malignant ascites fluid from ovarian cancer patients. Malignant ascites has been extensively characterized as a highly immunosuppressive TME, containing a number of factors hallmark to the human TME across cancers and which distinguish it from non-malignant ascites and blood plasma (Albillos et al., 1990; Alexandrakis et al., 2001; Jüngst et al., 1986). Malignant ascites contains a high concentration of tumour cells and regulatory immune cells and as a result is rich in tumour-derived factors, waste products including lactate, and immunosuppressive cytokines (Coosemans et al., 2019; Shender et al., 2014; Wei et al., 2017). Furthermore, malignant ascites is acidic and low in metabolic nutrients such as glucose and glutamine, which altogether provide a translational model of the human TME (Bala et al., 2008; Polak and Torres da Costa, 1973; Shender et al., 2014). We confirmed the acidity of the malignant ascites samples used in this study (Figure S2A). In T cells, it is known that the TME significantly impairs glucose metabolism and mitochondrial mass and function. To verify the representativeness of our model, we confirmed that T cells in the ovarian cancer patient ascites TME (taT) displayed similar glucose and mitochondrial metabolic deficits compared to previous reports in other tumour models (Figure S2B-C) (Chang et al., 2015; Scharping et al., 2016).

We incubated pbNK cells *ex vivo* in the ascites-TME (ascTME) or normal media (control) for 3 days (Figure 2A). High pbNK cell viability (>90%) was sustained in both control and ascTME conditions (Figure S2D). The ascTME significantly reduced pbNK cell basal glycolysis, glycolytic capacity, and glycolytic reserve (Figure 2, B and C). ascTME-exposed pbNK cells

showed broad impairments in glucose metabolism and mitochondrial function, as basal and maximal OxPhos, respiration-linked ATP, and mitochondrial mass were significantly reduced relative to control pbNK cells (Figure 2, D and E).

The exchange of glutamine to uptake other amino acids via CD98 is required for NK cell glycolysis as it drives expression of transcription factors that mediate cell growth and expression of glycolytic machinery, including Glut1 and the CD71 transferrin receptor (Loftus et al., 2018). Following exposure to the ascTME, pbNK cells lost over half of their cell-surface expression of CD98 (Figures 2F and S2E). Consistent with impaired amino acid uptake, pbNK cells in the ascTME had significantly lower expression of Glut1 and CD71 and reduced cell size (Figures 2G-H and S2F-H).

In line with defects in metabolism, exposure to the ascTME abrogated the anti-tumour functions of pbNK cells. The ascTME significantly impaired pbNK cell killing of OVCAR8 cells *in vitro* as well as expression of the anti-tumour cytokine IFN-γ (Figures 2I-J and S2I-J). Additionally, the ascTME significantly reduced pbNK cell granularity quantified by side-scatter (SSC-A) and confirmed by transmission electron microscopy (TEM; Figure 2K). Lower granularity was associated with an impairment in degranulation measured by CD107a expression in response to tumour targets (Figure S2K). Similar to taNK cells, pbNK cells in the ascTME lost the ability to prevent tumour cell engraftment and control tumour growth in xenograft mice (Figure 2L). Inhibition of pbNK cell cytotoxicity, glycolysis, and OxPhos, all occurred within the first 12 hours (Figure S2L-N), indicating that both functional and metabolic inhibition occurred rapidly and were sustained over 3 days.

We next assessed the extent to which metabolic inhibition contributes to the impairment of NK cell cytotoxic functions in the TME. We compared the suppression of NK cell cytotoxicity by

the ascTME to that of directly inhibiting OxPhos with the ATP synthase inhibitor Oligomycin. Oligomycin abrogated both pbNK cell killing and degranulation to a similar extent as the ascTME (Figures 2M-N and S2O), demonstrating that direct metabolic inhibition phenocopies the effects of the TME on NK cell function. These results show that the human TME directly impairs metabolic pathways required for NK cell anti-tumour activity.

NK cells can be reprogrammed to mimic tumour cell Warburg metabolism

NK cell inhibition in the TME remains a major hindrance to NK cell therapies for solid tumours (Geller et al., 2011; Parkhurst et al., 2011). However, we recently reported that NK cells expanded using IL-21-expressing feeder cells were capable of eliminating large established tumours in mice bearing human ovarian cancer and were also effective in lung cancer models (Poznanski et al., 2018; Poznanski et al., 2020). These findings suggest that these expanded-NK cells (exNK) harbour features to better sustain function in the TME. STAT3 signaling is a major driver of Warburg metabolic reprogramming in tumour cells, which thrive in the TME (Poli and Camporeale, 2015). Notably, IL-21 signaling through STAT3 was shown to be necessary to drive this NK cell expansion (Wang et al., 2013). Intriguingly, STAT3-exNK cells have a number of adaptations reminiscent of tumour cells: in addition to rapid proliferation, a previous study showed that they resist proliferative senescence and develop longer telomeres as they proliferate (Figure 3A) (Denman et al., 2012). Therefore, we asked whether STAT3-exNK cells have metabolic adaptations similar to those of tumour cells that would enable them to better resist inhibition in the TME.

To address this question, we first compared the metabolic profiles of exNK cells to pbNK cells. exNK cells had significantly elevated basal and maximal glycolysis (Figure 3B). Of note,

while pbNK cells had significant glycolytic reserves, measured by their ability to up-regulate glycolysis in a stressed state relative to basal, exNK cells showed no significant glycolytic reserve, indicating that at their basal rate exNK cells functioned at their maximal glycolytic capacity (Figure 3C). Upregulation of glucose-driven OxPhos is a feature of activated pbNK cells, as OxPhos is required for pbNK cell cytotoxic functions (Assmann et al., 2017; Keppel et al., 2015; Marcais et al., 2014). Surprisingly, exNK cells had comparable basal OxPhos as resting pbNK cells and significantly lower maximal OxPhos and spare respiratory capacity (SRC; Figure 3D). Indeed, resting pbNK cells relied substantially more on oxidative metabolism than exNK cells, measured by the ratio of OCR/ECAR (Figure 3E). This difference in OxPhos was even further pronounced upon overnight IL-2 activation of pbNK cells (Figure 3F-G). exNK cells expressed significantly greater levels than pbNK cells of CD98 and CD71, and a trend for higher Glut1, both at rest and following cytokine activation, suggesting an enhanced capacity for nutrient uptake and glutamine export (Figures 3H-K and S3A-D).

To further understand the mechanisms driving exNK cell metabolism and since metabolic changes occur rapidly and are often translationally regulated, we conducted a mass spectrometry-based global proteomic analysis of exNK cells compared to donor-matched pbNK cells. Proteins significantly differentially expressed were primarily involved in metabolism-related pathways (Figure 3L-M). Compared to pbNK cells, exNK cells showed metabolic changes akin to those of tumour cells: pathways upregulated in exNK cells were those classically involved in tumour metabolism and biosynthesis, whereas proteins involved in oxidative metabolism pathways, including fatty acid beta oxidation, were significantly downregulated. These results demonstrate that exNK cells have a distinct metabolic profile relative to even activated pbNK cells (Figure 3N). Remarkably, the specific up-regulation of glycolysis and down-regulation of OxPhos in exNK

cells mimics the classic Warburg metabolic profile of tumour cells. Thus, STAT3-expansion produces Warburg-like NK cells which suggests that these expanded and reprogrammed NK cells may be better metabolically adapted for the TME.

Human NK cells with Warburg metabolism not only resist suppression, their tumour killing is augmented by the hostile TME

Given their tumour-like adaptations, we next investigated the anti-tumour and metabolic responses of exNK cells in the TME. We incubated pbNK cells or exNK cells *ex vivo* in the ascTME from ovarian cancer patients or media as control (as in Figure 2A). While pbNK cell cytotoxicity was abrogated by the ascTME, not only did exNK cells better resist inhibition, their ability to kill OVCAR8 cells was strikingly augmented in the ascTME compared to media (Figures 4A and S4A). Similar augmentation of exNK cell cytotoxicity was also observed against SKBR3 breast cancer cells, confirming the effect was independent of tumour cell type (Figure S4B). Consistent with cytotoxicity, while pbNK cell granularity was reduced by the ascTME, exNK cells became more highly granular in the ascTME (Figures 4B and S4C). exNK cell IFN-γ expression was marginally reduced by the ascTME relative to media, but to a significantly lesser extent than pbNK cells (Figures 4C and S4D). Importantly, exNK cells incubated in human blood plasma showed comparable killing and granularity as media controls, indicating the augmentation in killing was specific to the ascTME (Figure S4E-F). Furthermore, exNK cell viability was high and unaffected across conditions (Figure S4G).

We then assessed whether the enhanced cytotoxicity of exNK cells by the ascTME translated to greater immunotherapeutic efficacy. We allowed a high tumour burden to develop over 14 days in xenograft mice with human OVCAR8 cells, at which time we adoptively

transferred exNK cells that had been exposed to the ascTME or media for 3 days. Assessment of tumour burden 2 days following NK cell treatment showed that although both media- and TME-exposed exNK cells significantly reduced tumour burden relative to untreated mice, TME-exposed exNK cells showed a trend for greater reduction in tumour burden (Figure 4D).

We next evaluated whether the enhanced function of exNK cells was sustained over a longer time-course in the TME. While pbNK cell inhibition in the ascTME occurred rapidly within the first day, the heightened cytotoxicity of exNK cells continually increased over 5 days in the ascTME relative to media (Figure 4E). These results uncover that exNK cells harbour an unprecedented ability for a cytotoxic immune cell: to function better upon extended exposure to a hostile TME.

Given that tumour cells are metabolically adapted to deal with hostile environments, we hypothesized that exNK cells do not undergo the same energy crisis as pbNK cells in the TME (Corbet et al., 2016; Fan et al., 2014; Maddocks et al., 2013; Tedeschi et al., 2013; Ye et al., 2014; Zaugg et al., 2011; Zhou et al., 2018). Unlike pbNK cells, exNK cells sustained their cell size in the ascTME, indicative of sustained bioenergetics (Figures 4F and S4C). Furthermore, exNK cells broadly maintained rates of glycolytic and oxidative metabolism in the ascTME (Figure 4G and H). While pbNK cells had reduced expression of nutrient receptors in the ascTME, exNK cells sustained expression of Glut1, CD71, and CD98, suggesting their capacity to take up metabolic nutrients was not impaired (Figures 4I-K and S4H-J). Finally, whereas mitochondrial mass, activity, and fusion were significantly reduced in ascTME-exposed pbNK cells, exNK cells sustained mitochondrial mass and fusion in the ascTME (Figures 4L and S4K). These findings demonstrate that exNK cells sustain their metabolic fitness in the TME and are thus metabolically adapted to thrive in this hostile environment.

Activation of the Nrf2 antioxidant pathway restores pbNK cell metabolism and anti-tumour activity in the TME

To elucidate the mechanisms that regulate NK cell metabolic suppression versus sustained metabolic fitness in the TME, we again assessed global differences in protein levels via proteomics in pbNK cells and exNK cells exposed to the ascTME or media. Pheatmap analysis of significantly up- and down-regulated proteins revealed largely inversed protein profiles in poorly cytotoxic ascTME-exposed pbNK cells compared to highly cytotoxic exNK cells (Figure 5A). Gene ontology enrichment analysis of differentially expressed proteins showed significant differences in a number of metabolism-related pathways (Figures 5B and S5A). Notably, pbNK cells in the ascTME had significantly increased expression of proteins involved in lipid peroxidation, oxidative damage, ferroptosis, and senescence and autophagy pathways (Figures 5C and S5B). Ferroptosis occurs due to result of accumulated lipid peroxides and failure of glutathione antioxidant defenses, resulting in deregulated lipid peroxidation and consequent oxidative damage (Dixon et al., 2012). taNK cells and ascTME-exposed pbNK cells showed a cellular morphology consistent with ferroptosis, including a rounded-up plasma membrane and small mitochondria (Figures 1F and 2, E and K). Further, TME-exposed pbNK cells had broadly down-regulated expression of proteins involved in DNA repair and damage response pathways, indicative of an impaired capacity to repair DNA damage from oxidative stress (Figure S5C).

Based on these protein profiles, we next assessed whether targeting oxidative stress could restore pbNK cell metabolism and function in the TME. The Nrf2 transcription factor is a central regulator of antioxidant defenses (Venugopal and Jaiswal, 1998). RTA-408 is a potent activator of Nrf2 antioxidant activity, as it inhibits binding of the adaptor protein Keap1 to Nrf2 in the cytosol,

thus facilitating Nrf2 nuclear translocation (Figure 5D) (Probst et al., 2015). Treatment of pbNK cells with RTA-408 in the ascTME *ex vivo* significantly rescued pbNK cell tumour killing, glycolysis, and OxPhos (Figures 5E-G). RTA-408 had no effect on pbNK cell function in control media, confirming the effect was specific to NK cell dysfunction in the TME (Figure S5D). We next assessed the effects of RTA-408 on NK cell function *in vivo* in mice with established OVCAR8 tumour. Since RTA-408 has previously been shown to have direct tumour toxicity in other studies (Alexeev et al., 2014), we used a lower dose (1μg/g body weight) at which there was no significant effect on tumour growth. As anticipated, pbNK cells in isolation had only a marginal effect on controlling growth of established tumour in mice (Figure 5H). In stark contrast, RTA-408 significantly restored pbNK cell anti-tumour activity, as tumour growth was ablated over 14 days in mice treated with the combination of pbNK cells and RTA-408. These results show that oxidative damage is a critical mechanism through which the TME impairs NK cell glucose metabolism, mitochondrial function, and consequent cytotoxicity.

Notably, exNK cells had down-regulated expression of proteins in lipid peroxidation and oxidative damage pathways which was largely sustained in the TME (Figures 5C and S5B) and higher expression of proteins involved in DNA repair (Figure S5C). These results suggest that exNK cells harbour mechanisms to resist oxidative stress in the TME.

Metabolic flexibility enables NK cells to augment their anti-tumour activity in response to nutrient deprivation

Having delineated the mechanism for how NK cells become metabolically suppressed in the TME, we next investigated the mechanism through which exNK cells sustain their metabolic fitness and specifically augment anti-tumour activity in the TME. We first assessed whether a

factor(s) present in the ascTME increased exNK cell tumour killing by extracting the protein (>10 kDa) or lipid components from ascites. Consistent with the inhibitory effects of immunoregulatory proteins or lipids on pbNK cells (Michelet et al., 2018; Zaiatz-Bittencourt et al., 2018), removal of proteins or lipids from the ascTME partially restored pbNK cell tumour killing (Figure S6A-B). However, neither proteins nor lipids in the ascTME affected exNK cell function, as exNK cells maintained heightened tumour killing in protein- or lipid-depleted ascites (Figure S6C-D). Thus, it is unlikely the presence of a specific factor in the ascites-TME that augments exNK cell cytotoxicity.

Tumour cells harbour a tremendous capacity to adapt their metabolism in response to environmental stressors (Corbet et al., 2016; Maddocks et al., 2013; Zaugg et al., 2011). Elevated serine metabolism through one carbon and folate cycle pathways plays a central role in conferring this metabolic flexibility by endogenously generating substrates for anabolic pathways, including nucleotide and amino acid synthesis, and controlling oxidative stress by driving glutathione synthesis (Fan et al., 2014; Maddocks et al., 2013; Tedeschi et al., 2013; Ye et al., 2014). Similarly, exNK cells had increased expression of proteins involved in serine synthesis, one carbon and folate metabolism, and nucleotide synthesis pathways compared to pbNK cells (Figures 6A and S6E). To adapt to oxidative stress conditions, tumour cells reduce nucleotide and amino acid synthesis in order to funnel more serine and glutamate towards glutathione production (Maddocks et al., 2013). Indicative of this dynamic adaptability to environmental stress, upon exposure to the ascTME, exNK cells significantly up-regulated enzymes involved in glutathione antioxidant defenses, including GPX3 and GLS, and down-regulated expression of a number of enzymes (GPT2, ARG2, P4HA2, ASNS, CBS, ALDH18A1, and GOT1) that use serine and glutamate for other biosynthetic pathways (Figure 6A). Thus, upon exposure to environmental stress, exNK cells

adopt a protein profile that channels metabolites towards antioxidant defenses. This indicates that exNK cells mimic the metabolic adaptations used by tumour cells to mitigate deregulated oxidative damage in the TME.

To directly assess the metabolic plasticity of exNK cells compared to pbNK cells, we measured the ability of pbNK and exNK cells to oxidize glucose, glutamine, or fatty acids to meet their energetic capacity. Strikingly, while pbNK cells showed dependency on both glucose and fatty acid oxidation to meet energetic demands, exNK cells were not dependent on any one single fuel to reach their energetic capacity (Figure 6B). In addition, measures of fuel flexibility demonstrated that pbNK cells were unable to use any single fuel, particularly glutamine, to compensate for the inhibition of the other fuel pathways. In contrast, exNK cells demonstrated complete flexibility with all fuels, revealing a remarkable ability to use any single fuel to meet their full energetic requirements (Figure 6, C and D). To further assess this apparent adaptability, we singularly inhibited a number of different metabolic pathways in exNK cells in the *ex vivo* ascTME. None of the metabolic inhibitors tested affected exNK cell cytotoxicity (Figure 6E). Thus, exNK cells demonstrate extensive metabolic flexibility which enables them to adapt and sustain metabolic fitness in a hostile TME.

We next investigated the direct effects of metabolic hostility on exNK cell function. A hallmark of the TME is the low level of nutrients including glucose and glutamine, which tumour cells rapidly consume to fuel their proliferation (Chang et al., 2015; Pan et al., 2016). Such nutrient deprivation has been shown to impair cytotoxic T cell metabolism and function in the TME (Chang et al., 2015). Given their complete metabolic substrate flexibility, we asked how nutrient deprivation affects the anti-tumour capacities of exNK cells. We cultured exNK cells in glucose-free media (with or without galactose) or in glutamine-free media and assessed cytotoxicity

following 24 hours and 5 days. Similar to the time course of cytotoxicity observed in the ascTME in Figure 4E, exNK cell cytotoxicity was not significantly changed within the first 24 hours (Figure S6F) but was significantly augmented after 5 days in nutrient-deprived media relative to control media (Figure 6F). Consistent with their metabolic fitness in the TME, exNK cells sustained comparable levels of glycolysis and OxPhos following 5 days in nutrient-deprived media compared to control media (Figure 6, G and H).

These results demonstrate that complete metabolic flexibility enables NK cells to avoid an energy crisis in the TME, as flexible NK cells mimic tumour cell adaptations to sustain their energetic requirements in hostile environments. In turn, long-term exposure to metabolic stressors, such as nutrient deprivation, specifically augments the cytotoxicity of metabolically flexible NK cells, conferring a more robust anti-tumour response within the TME than in nutrient-rich environments.

4.4 DISCUSSION

Since their discovery decades ago, NK cells have been central to the study of immunosurveillance and anti-tumour immunity due to their unique ability to spontaneously kill tumour cells (Herberman et al., 1975; Kiessling et al., 1975). However to date, NK cell-based cancer immunotherapy has shown limited efficacy against solid tumours (Geller et al., 2011; Parkhurst et al., 2011). It is well established that NK cells become suppressed in the TME, thus facilitating tumour escape and progression (Morvan and Lanier, 2016). Our study uncovers metabolic fitness and flexibility as central to dictating the functional fate of NK cells in the TME. We elucidate a fundamental mechanism to NK cell inhibition, whereby the human TME directly arrests NK cell glucose metabolism through glycolysis and OxPhos, leading to an abrogation of

their cytotoxic functions. These findings shed light on the longstanding question of how NK cells are rendered dysfunctional by the TME. Furthermore, our data strengthen the proposition that metabolic disequilibrium in the TME is a critical junction in tumour immune escape (Chang et al., 2015; Leone et al., 2019; Scharping et al., 2016; Siska et al., 2017; Vodnala et al., 2019).

The paradox that tumour cells thrive while cytotoxic immune cells are impeded by the hostile TME has been an enduring conundrum in cancer immunotherapy. Seminal works, spanning from Otto von Warburg's initial characterization of tumour aerobic glycolysis to recent studies exposing the profound metabolic resourcefulness and plasticity of tumour cells, have established tumour cell metabolism as central to their ability to thrive in hostile environments (Corbet et al., 2016; Maddocks et al., 2013; Pan et al., 2016; Tedeschi et al., 2013; Warburg, 1925; Warburg et al., 1927; Ye et al., 2014; Zaugg et al., 2011). In contrast, the metabolic insufficiency experienced by T cells in the TME, including glucose restriction and mitochondrial dysfunction, has been shown to hinder CAR-T cell immunotherapeutic efficacy (van Bruggen et al., 2019). Our work uncovers that reprogramming tumour metabolic advantages into a cytotoxic immune cell reverses the disequilibrium in the TME to their favour. Our finding that NK cells armed with Warburg metabolism and complete substrate flexibility not only sustain metabolic fitness, but strikingly augment their ability to kill tumour cells in the hostile conditions of the TME, represents to our knowledge the first and unprecedented report of a cytotoxic immune cell that is specifically strengthened, rather than weakened, by the TME. These results expose metabolic flexibility as central in determining whether NK cells reach an immunosuppressed or highly activated fate in the TME. Importantly, our findings identify increasing metabolic flexibility as a novel and powerful mechanism for immune cell therapies to exploit the hostility of the TME and thus not only overcome, but usurp, a critical mechanism of immune escape for their functional advantage.

The success of CAR-T cells has revolutionized the treatment of B cell malignancies and pioneered the ground-breaking field of cell immunotherapies for cancer. However, the severe toxicities associated with low tumour-antigen expression on healthy cells, together with antigen loss or heterogeneity on tumours, has limited the application of CAR-T cell therapies to other tumour types, particularly solid tumours (Morgan et al., 2013; Morgan et al., 2010; Santomasso et al., 2018; Thistlethwaite et al., 2017). NK cells harbour immense potential to be globally applied for the treatment of heterogeneous tumours, due to their safety profile and antigen-unrestricted method of tumour cell killing (Cerwenka and Lanier, 2018). However, the suppression of NK cell anti-tumour activity in the TME of cancer patients has hindered NK cell therapies against solid tumours for the past decade (Geller et al., 2011; Parkhurst et al., 2011). Our work reveals an unforeseen anti-tumour capacity of NK cells against solid tumours and strongly supports future clinical investigation of metabolically flexible NK cells for the treatment of solid tumours.

Lastly, our data contribute to the emerging paradigm that the metabolic profile of immune cells may predict their functional fate, including in the TME (Poznanski and Ashkar, 2019). This presents extraordinary opportunities for profiling immune cells based on their metabolism to identify cellular therapies with the greatest anti-tumour potential.

4.5 Limitations of Study

This study used pbNK cells as controls for assessing function and metabolism of taNK cells, which enabled the comparison of donor-matched NK cells when possible. However, given the inherent differences between blood and tissue NK cells, another important comparison not conducted in this study is that of NK cells from non-malignant versus malignant ascites fluid. Ovarian cancer patient ascites fluid was used as an *ex vivo* model of the human TME. Although ascites contains a

number of tumour-derived and immunosuppressive factors representative of the human TME, we recognize that this model has certain limitations. Notably, ascites is a fluid model rather than a solid tumour mass and the *ex vivo* conditions do not recapitulate all of the characteristics of an *in vivo* TME.

4.6 STAR METHODS

KEY RESOURCES TABLE

REAGENT or RESOURCE	SOURCE	IDENTIFIER
Antibodies		
APC-H7 Mouse Anti-Human CD3	BD Biosciences	Cat#560176; Clone SK7; RRID:AB_1645475
APC Mouse Anti-Human CD107a	BD Biosciences	Cat#560664; Clone H4A3; RRID:AB_1727417
BV421 Mouse Anti-Human CD56	BD Biosciences	Cat#562751; Clone NCAM16.2; RRID:AB_2732054
BV421 Mouse Anti-Human IFN-gamma	BD Biosciences	Cat#564791; Clone 4S.B3; RRID:AB_2738952
BV711 Mouse Anti-Human CD71	BD Biosciences	Cat#563767; Clone M-A712; RRID:AB_2738413
Human Glut1 Fluorescein-conjugated Antibody	R&D Systems	Cat#FAB1418F; Clone 202915; RRID:AB_2191041
PE-CF594 Mouse Anti-Human CD56	BD Biosciences	Cat#564849; Clone NCAM16.2; RRID:AB_2738983
PE Mouse Anti-Human CD98	BD Biosciences	Cat#556077; Clone UM7F8; RRID:AB_396344
PerCP/Cyanine5.5 anti-human CD3	Biolegend	Cat#300430; Clone UCHT1; RRID:AB_893299
Biological Samples		
Cancer patient pbNK cells	Isolated from ovarian and lung cancer patients	N/A
Cancer patient taNK cells	Isolated from the ascites fluid of ovarian cancer patients or tumour pieces of lung cancer patients	N/A
Healthy adult pbNK cells	Isolated from healthy volunteers	N/A

Lung tumour pieces	Collected from lung cancer patient tumours	N/A
Malignant ascites fluid	Collected from ovarian cancer patients	N/A
Chemicals, Peptides, and Recombinant Proteins		
2-Deoxy-D-glucose (2DG)	Sigma-Aldrich	D8375; CAS 154-17-6
5(6)-Carboxyfluorescein diacetate *N*-succinimidyl ester (CFSE)	Sigma-Aldrich	21888; CAS 150347-59-4
(aminooxy)acetic acid hemihydrochloride (AOA)	Sigma-Aldrich	C13408; CAS 2921-14-4
Bis-2-(5-phenylacetamido-1,3,4-thiadiazol-2-yl)ethyl sulfide (BPTES)	Sigma-Aldrich	SML0601; CAS 314045-39-1
XenoLight D-Luciferin	Perkin Elmer	Cat#122799(PE); CAS 115144-35-9
eBioscience™ Fixable Viability Dye eFluor™ 780	ThermoFisher	Cat#65-0865-18
Etomoxir	Sigma-Aldrich	E1905; CAS 828934-41-4
Fixable Viability Stain 510	BD Biosciences	Cat#564406; RRID:AB_2869572
GSK3787	Sigma-Aldrich	G7423; CAS 188591-46-0
GW6471	Sigma-Aldrich	G5045; CAS 880635-03-0
Human IL-12	Peprotech	Cat#200-12; Accession#P29459, P29460
Human IL-15	Peprotech	Cat#200-15; Accession#P40933
Human IL-2	Peprotech	Cat#200-02; Accession# P60568
Iodoacetamide	Sigma-Aldrich	Cat#I1149; CAS 144-48-9
Lymphoprep™	Stemcell Technologies	Cat#07861
MitoTracker Red CMXRos	ThermoFisher	M7512; CAS 167095-09-2
NCT-503	Sigma-Aldrich	SML1659; CAS1916571-90-8
NCT-503 Inactive Control	Sigma-Aldrich	SML1671; CAS 1914971-16-6
Oligomycin	Sigma-Aldrich	75351; CAS 579-13-5
Omaveloxolone (RTA 408)	MedChemexpress	HY-12212; CAS 1474034-05-3
Poly-L-lysine Solution	Sigma-Aldrich	P4707; CAS 25988-63-0
Shikonin	Sigma-Aldrich	S7576; CAS54952-43-1
SHIN1	Aobious	AOB36697; CAS 2146095-85-2
Tandem Mass Tag 10plex isobaric label reagent	Thermo Fisher	Cat#90406
Tandem Mass Tag 131C isobaric labelign reagent	Thermo Fisher	Cat#A34807
Tris(2-carboxyethyl)phosphine hyrochloride	Sigma-Aldrich	Cat#C4706; CAS 51805-45-9
UK5099	Sigma-Aldrich	PZ0160; CAS 56393-35-1

Critical Commercial Assays		
Human CD56+ selection kit II	Stemcell Technologies	Cat#17855
Human EpCAM+ selection kit II	Stemcell Technologies	Cat#17846
Seahorse XF Glycolysis Stress Test	Agilent	Cat#103020-100
Seahorse XF Mito Fuel Flex Test	Agilent	Cat#103260-100
Seahorse XF Mito Stress Test	Agilent	Cat#103015-100
Deposited Data		
Raw and processed proteomic data	ProteomeXchange Consortium via Proteomics Identification (PRIDE)	PXD016996
Experimental Models: Cell Lines		
Human: K562-mb-IL21 (Clone 9) cells	Laboratory of Dean A. Lee	Denman *et al.* 2012
Human: OVCAR-8 cells	Laboratory of Karen Mossman	RRID: CVCL_1629
Human: SKBR-3 cells	Laboratory of Karen Mossman	RRID: CVCL_0033
Experimental Models: Organisms/Strains		
Mouse: NRG: NOD-*Rag1*^{null} *IL2rg*^{null}	The Jackson Laboratory	JAX: 007799
Software and Algorithms		
Enrichr	Chen et al., 2013. Kuleshov et al., 2016.	https://maayanlab.cloud/Enrichr/
FACSDIVA™ Software	BD Biosciences	https://www.bdbiosciences.com/en-us/instruments/research-instruments/research-software/flow-cytometry-acquisition/facsdiva-software#:~:text=BD%20FACSDivaTM%20software%20is,workflows%20for%20today's%20busy%20laboratory.
FlowJo™ Software	BD Biosciences	https://www.flowjo.com/
ggplot2() R packages (version 3.3.2.) downloaded via CRAN in R (version 3.6.1.)	Wickham, 2016.	https://cran.r-project.org/web/packages/ggplot2/ggplot2.pdf
ImageJ	NIH	https://imagej.nih.gov/ij/
Prism Software (version 7.0)	GraphPad	https://www.graphpad.com/scientific-software/prism/
Living Image Software [IVIS Spectrum Series]	PerkinElmer	Cat#128113; https://www.perkinelmer.com/fr/product/li-software-for-spectrum-1-seat-add-on-128113

pheatmap() R package (version 1.0.12.) downloaded via CRAN in R (version 3.6.1.)	Raivo Kolde, 2018.	https://cran.r-project.org/web/packages/pheatmap/pheatmap.pdf
Proteome Discover Software (version 2.2)	Thermo Fisher	https://www.thermofisher.com/order/catalog/product/OPTON-30812?gclid=CjwKCAiAp4KCBhB6EiwAxRxbpCBU4duffAgpE48qj2kbdRyFtdpdL2TGDmgsJmPdGWTJIu4xPHMLphoC1m8QAvD_BwE&ce=E.21CMD.DL107.34553.01&cid=E.21CMD.DL107.34553.01&ef_id=CjwKCAiAp4KCBhB6EiwAxRxbpCBU4duffAgpE48qj2kbdRyFtdpdL2TGDmgsJmPdGWTJIu4xPHMLphoC1m8QAvD_BwE:G:s&s_kwcid=AL!3652!3!249703669124!e!!g!!proteome%20discoverer#/OPTON-30812?gclid=CjwKCAiAp4KCBhB6EiwAxRxbpCBU4duffAgpE48qj2kbdRyFtdpdL2TGDmgsJmPdGWTJIu4xPHMLphoC1m8QAvD_BwE&ce=E.21CMD.DL107.34553.01&cid=E.21CMD.DL107.34553.01&ef_id=CjwKCAiAp4KCBhB6EiwAxRxbpCBU4duffAgpE48qj2kbdRyFtdpdL2TGDmgsJmPdGWTJIu4xPHMLphoC1m8QAvD_BwE:G:s&s_kwcid=AL!3652!3!249703669124!e!!g!!proteome%20discoverer
Seahorse Wave Desktop Software	Agilent Technologies	https://www.agilent.com/en/product/cell-analysis/real-time-cell-metabolic-analysis/xf-software/seahorse-wave-desktop-software-740897
UniProt Retrieve/ID Mapping algorithm	Uniprot Consortium; ELIXIR	https://www.uniprot.org/uploadlists/

Other		
IVIS Spectrum In Vivo Imaging System	PerkinElmer	N/A
LSRFortessa™ Flow Cytometer	BD Biosciences	N/A
LSRII Flow Cytometer	BD Biosciences	N/A
Orbitrap Q Exactive HF Mass Spectrometer	Thermo Fisher	N/A
Ultimate RSLCNano-3000 LC System	Thermo Fisher	N/A

RESOURCE AVAILABILITY

Lead Contact

Further information and requests for resources and reagents should be directed to and will be fulfilled by the Lead Contact, Ali Ashkar (ashkara@mcmaster.ca).

Materials Availability

This study did not generate new unique reagents.

Data and Code Availability

The datasets generated during this study are available in the main text, supplementary materials, or deposited in the ProteomeXchange Consortium via Proteomics Identification (PRIDE) database (accession number PXD016996). This study did not generate new codes.

EXPERIMENTAL MODEL AND SUBJECT DETAILS

Human Samples

All research involving human samples was approved by the Hamilton Integrated Research Ethics Board in Hamilton, Ontario. Ascites fluid and peripheral blood were collected with written informed consent from patients with high-grade serous ovarian cancer at the Juravinski Cancer Centre in Hamilton, Ontario (total number of participants 27 aged between 43-79 years; Gender F). Tumour pieces and peripheral blood were collected with written informed consent from male and female patients with lung cancer at St. Joseph's Healthcare in Hamilton, Ontario (total number

of participants 5 aged between 63-79 years; Gender M 2: F 3). Ascites fluid was collected via paracentesis and tumour pieces were collected via surgical resection, both conducted as part of the patients' standard care. Peripheral blood from healthy donors was obtained with written informed consent at McMaster University in Hamilton, Ontario (total number of participants 42 aged between 20-70 years; Gender M 23: F 19).

Mouse models

All research using mice was approved by and conducted in accordance with guidelines from the McMaster University Animal Research Ethics Board. NOD-*Rag1*^{null} *IL2rg*^{null} (NRG) mice were originally obtained from Jackson Laboratory (stock no. 007799) and were bred and housed at McMaster University's Central Animal Facility in specific pathogen-free conditions, 12h:12h light/dark cycle, *ad libitum* access to food and water, and with a maximum of 5 mice per cage. Female mice between the ages of 6-24 weeks old were used to model ovarian cancer. Mice were age-matched across groups for experiments. In experiments assessing treatments in mice with established tumour, tumour burden was also averaged across groups immediately prior (same day) to the onset of treatment.

Cell lines and reagents

K562 myelogenous leukemia cells (ATCC CCL-243, female) engineered to express membrane-bound IL-21 (K562mb-IL21, Clone 9) were kindly provided by Dr. Dean A. Lee (Nationwide Children's Hospital, Ohio State University Comprehensive Cancer Center, USA) in 2012 and produced as previously described (Denman et al., 2012). K562mb-IL21 cells were cultured at 0.5-1 x 10^6 cells/mL in RPMI medium containing 10% FBS, 1% L-glutamine, 1% HEPES, and 1%

penicillin-streptomycin (complete). OVCAR8 high-grade ovarian serous adenocarcinoma (RRID: CVCL_1629, female) and SKBR3 breast adenocarcinoma cell lines (RRID: CVCL_0033, female) were cultured in complete DMEM media until ~80% confluent and then used for experiments or further passaged. For visualization and quantification of tumour burden in mice via bioluminescence, OVCAR8 cells previously transduced with a lentiviral vector containing a luciferase reporter gene were used (Poznanski et al., 2018). Cells were maintained at 37 °C with 5% CO_2.

METHOD DETAILS

NK cell isolation and culture

Peripheral blood mononuclear cells (PBMCs) were isolated from the blood of healthy donors and ovarian cancer patients via density centrifugation with Lymphoprep (StemCell Technologies). For the isolation of tumour-infiltrating lymphocytes (TILs), whole ascites fluid was filtered through 100-micron and 40-micron nylon mesh, centrifuged, and cells were washed twice with 2% FBS in PBS. TILs were then separated from tumour cells using a 2-layer (75% and 100%) Lymphoprep density gradient. Any remaining tumour cells in the TIL fraction were removed using an EpCAM+ selection kit II. TILs were isolated from the tumours of lung cancer patients as previously described (Poznanski et al., 2020). Briefly, tumours were minced in αMEM medium supplemented with collagenase IV and DNase I. Tumour pieces were then incubated on a shaker at 37°C for 2 hours then filtered. NK cells were isolated from PBMCs (pbNK) and TILs (taNK) using a CD56+ selection kit. To generate exNK cells, NK cells were expanded from PBMCs for at least 3 weeks, using IL-2 and irradiated K562-mbIL-21 cells, as previously described[29]. exNK cells were cultured in RPMI medium containing 10% FBS, 1% L-glutamine, 1% HEPES, and 1%

Penicillin-streptomycin. For *in vitro* experiments in the ascTME, NK cells were incubated for the indicated durations (12 hours, 3 days, or 5 days) in either cell-free 90% malignant ascites fluid, 10 % complete medium (ascTME) or in 100% complete media as control, with low-dose IL-15 (10 ng/mL) and the indicated inhibitors. Inhibitors were used at the following concentrations: oligomycin (200 nM), etomoxir (50 μM), RTA-408 (1 μM), BPTES (1 μM), AOA (100 μM), NCT-503 (30 μM), SHIN1 (10 μM), GSK3787 (10 μM), GW6471 (10 μM), Shikonin (50 nM), UK5099 (10 μM). For assessment of pbNK versus exNK cell nutrient receptor expression upon cytokine stimulation, NK cells were incubated overnight with IL-15 (100 ng/mL) and IL-12 (30 ng/mL) or rested in IL-15 (1 ng/mL). For experiments in nutrient-deprived media, exNK cells were cultured in glucose-free or glutamine-free medium for 24 hours or 5 days. NK cell *in vitro* cytotoxicity, degranulation, and IFN-γ expression were assessed against OVCAR8 and SKBR3 cells, as previously described[29]. Briefly, NK cells were incubated for 5 hours with CFSE-labeled OVCAR8 or SKBR3 cells at a 1.25:1 effector-to-target ratio, or as indicated, following which cells were stained with fixable viability stain.

Protein and lipid extraction from the TME

Proteins were extracted from ovarian cancer patient ascites fluid (ascTME) using a 10 kDa amicon centrifugal filter device (Sigma-Aldrich), according to manufacturer's instructions. Filtrate was collected following centrifugation and used for experiments. Lipids were extracted from the TME via hexane purification. Hexane was added to ascites fluid at a 1:1 ratio in a glass tube which was then vortexed and centrifuged for 5 minutes at 1500 rpm to separate the hexane and lipid layer from the ascites fluid. The resulting lipid-depleted ascites fluid was collected and used for experiments.

Cell Staining

Live/dead cells were discriminated using fixable viability stain or dye according to the manufacturer's instructions. For assessment of mitochondrial mass, cells were then stained with MitoTracker Red CMXRos, according to the manufacturer's instructions. Cells were subsequently stained for extracellular markers with the indicated anti-human fluorescently labeled antibodies. Control fluorescent minus one wells contained corresponding isotype controls. For intracellular staining, Golgi Stop (BD Biosciences) was added after the first hour of incubation. At 5 hours, cells were stained with viability dye, extracellular antibodies, fixed using BD Biosciences Fixation/Permeabilization solution, and then stained with intracellular antibodies. Samples stained with viability dye and extracellular antibodies only were fixed for 1 hour with 1% paraformaldehyde. Sample acquisition was conducted using BD LSRFortessa or LSRII cytometers and analyzed using FlowJo Software.

Extracellular flux assays

NK cell glycolysis and OxPhos were measured via extracellular flux assays using a Seahorse XFe96 Analyzer and Wave Software. NK cells were washed twice in warmed assay medium and then plated for the assay at a density of 250 000 or 500 000 cells per well in a 96-well Seahorse plate coated with Poly-L-Lysine. ECAR was measured using the Glycolytic Stress Test and OCR was measure using the Mito Stress Test or the Mito Fuel Flex Test, according to manufacturer's instructions. NK cells were assayed in Seahorse XF RPMI Medium (without Phenol Red). For Glycolytic Stress Tests, medium was supplemented with 1 mM L-glutamine. Glucose (11.1 mM), oligomycin (2 μM), and 2-DG (50 mM) were injected subsequently during

the assay. For Mito Stress Tests, medium was supplemented with 1 mM sodium pyruvate, 1 mM L-glutamine, and 11.1 mM glucose. Oligomycin (2 μM), FCCP (0.5 μM), and Rotenone/Antimycin (0.5 μM) were injected subsequently during the assay. For Mito Fuel Flex Tests, media was supplemented as for Mito Stress Tests. OCR was assessed in response to BPTES (3 μM), Shikonin (4 μM), and UK5099 (2 μM).

Tandem Mass Tag Mass Spectrophotometry (TMT-MS)

NK cells were washed 3 times in PBS, pelleted, and then 100 μg total protein was extracted from each sample using 8M urea and 100 mM ammonium bicarbonate. The protein samples were reduced, alkylated, and digested by trypsin overnight at 37°C. The resulting peptides were desalted with 10 mg SOLA C18 Plates (Thermo Scientific), dried, labeled with 11-plex Tandem Mass Tag reagents (Thermo Scientific), before being pooled together. 40 μg of the pooled sample was separated into 36 fractions by reverse phase liquid chromatography (RPLC) at pH=10 using a C18 column (Waters BEH130, 5 μm resin; 200 μm ID x 30cm bed volume). Each fraction was then loaded onto a trap column (200 μm ID x 5 cm bed volume) packed with POROS 10R2 10 μm resin (Thermo Fisher), followed by an analytical column (50 μm ID x 50 cm bed volume) packed with Reprosil-Pur 120 C18-AQ 5 μm particles. LC-MS experiments were performed on a Thermo Fisher UltiMate^{TM} 3000 RSLCNano UPLC system that ran a 3-hour gradient at 70 nL/min, coupled to a Thermo QExactive HF quadrupole-Orbitrap mass spectrometer. A parent ion scan was performed using a resolving power of 120,000 and then up to the 20 most intense peaks were selected for MS/MS (minimum ion count of 1000 for activation), using higher energy collision induced dissociation (HCD) fragmentation. Dynamic exclusion was activated such that MS/MS of the same m/z (within a range of 10ppm; exclusion list size=500) detected twice within 5s were

excluded from analysis for 40s.

Proteomic data processing and analysis

LC-MS data generated was analyzed against a UniProt human protein database (42,173 entries) for protein identification and quantification by Thermo Proteome Discoverer (v 2.2.0). From 2,111,477 MS/MS spectra acquired in all 36 fractions, 161,347 unique peptide groups (with Peptide FDR<0.01) and 9,153 proteins (Protein FDR < 0.01) were identified and quantified. The Significant B values were calculated using the PERSEUS (v.1.6.5) software (Cox and Mann, 2008). Significance B value preset with a FDR<0.01 was used to identify proteins that are significantly differentially abundant and used for downstream integrative analysis. All raw proteomic data have been deposited in the ProteomeXchange Consortium via Proteomics Identification (PRIDE; accession number: PXD016996).

Differential Expression and Functional Enrichment Analyses

Peptide signal intensities as determined by mass spectrometry were normalized by number of peptides per protein prior to downstream analyses. Protein names were identified by searching provided accession numbers in the UniProt database. Fold change and significance (*p* value) were calculated for each comparison. For each comparison, proteins were sorted by *p* value and then by fold change. Lists of significantly differentially expressed proteins ($P< 0.05$) were submitted to Enrichr for functional enrichment and pathway analysis (Chen et al., 2013; Kuleshov et al., 2016). Enriched terms were ranked within ontologies by Enrichr's combined score (log(*p* value) * z-score of the deviation from the expected rank). Expected rank (FDR adjusted *p* value) was calculated by Enrichr by running the Fisher exact test for random protein sets in order to compute

a mean rank and standard deviation from the expected rank for each term in the protein set library. WikiPathways 2019 was the ontology focused on in this study. ggplot2() in R was used to display functional enrichment results: gene count (denoted by circle size) refers to the number of significantly differentially expressed genes that contribute to the total number of genes associated with a given ontology (Wickham, 2016). Mean normalized signal intensities for proteins identified as significantly differentially expressed ($p < 0.05$) in any of the samples (n=2351 proteins total) were analyzed via pheatmap in R (Kolde, 2018). Mean normalized signal intensity was scaled by protein (row). Proteins (rows) and samples (columns) underwent hierarchical clustering in pheatmap using an average clustering method and correlation distance measure which resolved 4 main protein clusters. Proteins contained within each cluster were submitted to Enrichr where WikiPathways 2019 were analyzed as described above with only minor adjustments made to methods for the generation of individual ontology pheatmaps (in this case, rows and columns were not clustered).

Adoptive NK Cell Transfer

Luciferase-expressing OVCAR8 cells (OVCAR8-Luc) were injected intra-peritoneally (i.p.) into NRG mice. For engraftment prevention experiments using pbNK and taNK cells, NK cells (400 000 cells/mouse) and OVCAR8-Luc cells (100 000 cells/mouse) were each injected at Day 0. For experiments testing the ability of expanded NK cells to reduce high tumour burden, 200 000 OVCAR8-Luc cells were injected per mouse at Day 0. At Day 14, tumour burden was averaged across groups and 20 million NK cells/mouse were injected i.p. with IL-2 (20 000 IU/mouse) to support NK cell survival. For testing the effects of RTA-408 on NK cell control of tumour growth, mice were treated with RTA-408 and/or pbNK cells starting 3 days following

engraftment of OVCAR8-Luc cells. In NK cell-treated mice, 2 million pbNK cells were injected i.p. per mouse at days 3 and 7. In mice treated with RTA-408, 1 μg of RTA-408 per gram of body weight was administered i.p. daily. All mice received a maintenance dose of 500 ng of IL-15 daily to sustain NK cell survival. Mice were followed for tumour growth for 14 days. In all experiments, control mice received tumour cells only and vehicle (PBS). Tumour burden was quantified at indicated days by measuring bioluminescence (radiance units: photons/sec/cm2/sr) with an IVIS Spectrum Imaging System 14 minutes after i.p. injection of Luciferin. Analysis was conducted using Living Image Software.

QUANTIFICATION AND STATISTICAL ANALYSIS

Data are reported as Mean ± Standard Error of the Mean (SEM). GraphPad Prism Software (version 7.0) was used to generate graphs and perform statistical analysis unless otherwise indicated. Data comparing two groups were analyzed via two-tailed t-test. Data comparing more than two groups with one independent variable were analyzed using one-way ANOVA and Tukey correction for multiple comparisons. Data with two independent variables were analyzed using two-way ANOVA and Tukey correction. Significance was defined as $p < 0.05$.

4.7 DECLARATIONS

Acknowledgments: The authors thank L. Helpman, L. Elit, and N. Gauvin and the gynecology team at the Juravinski Cancer Centre (Hamilton, ON) for providing ovarian cancer patient blood and ascites samples, Y. Shargall from St. Joseph's Healthcare (Hamilton, ON) for providing lung cancer patient blood and tumour samples, all cancer patient and healthy volunteers who donated samples, A. Nazli, K. Graham, and M. Reid (McMaster University) for assistance with confocal and electron microscopy, and R. Truant (McMaster University) for providing insight on oxidative

stress. This work was supported by the Canadian Institutes for Health Research (CIHR) (20009360 to AAA) and the Juravinski Hospital and Cancer Centre Foundation (to HWH and AAA). AAA holds a tier 1 Canada Research Chair in Natural Immunity and NK Cell Function. SMP is the recipient of a CIHR Vanier Canada Graduate Scholarship, an Ontario Women's Health Scholars Doctoral Award from the Ontario Ministry of Health and Long-Term Care, and a Doctoral Ontario Graduate Scholarship funded by the province of Ontario and McMaster University. EAR and TMR are supported by a Master's Ontario Graduate Scholarship.

Author Contributions: SMP and AAA conceived the project and designed the experiments; SMP, KS, TMR, and SX performed experiments; IYF, ALP, EAR, FV, and AE contributed to performing experiments; SMP, JAA, LY, and ACD curated and formally analyzed the data; MB contributed to project administration; KS, JDS, and HWH provided intellectual and experimental input; SMP and AAA wrote the manuscript; TMR, JAA, LY, JDS, and HWH edited the manuscript; HWH and AAA secured funding; and AAA supervised the project.

Declaration of interests: SMP and AAA are inventors on a pending Canadian Provisional Patent application for the use of metabolic profiling and reprogramming for NK cell immunotherapy. The authors declare no other competing interests.

4.8 FIGURES

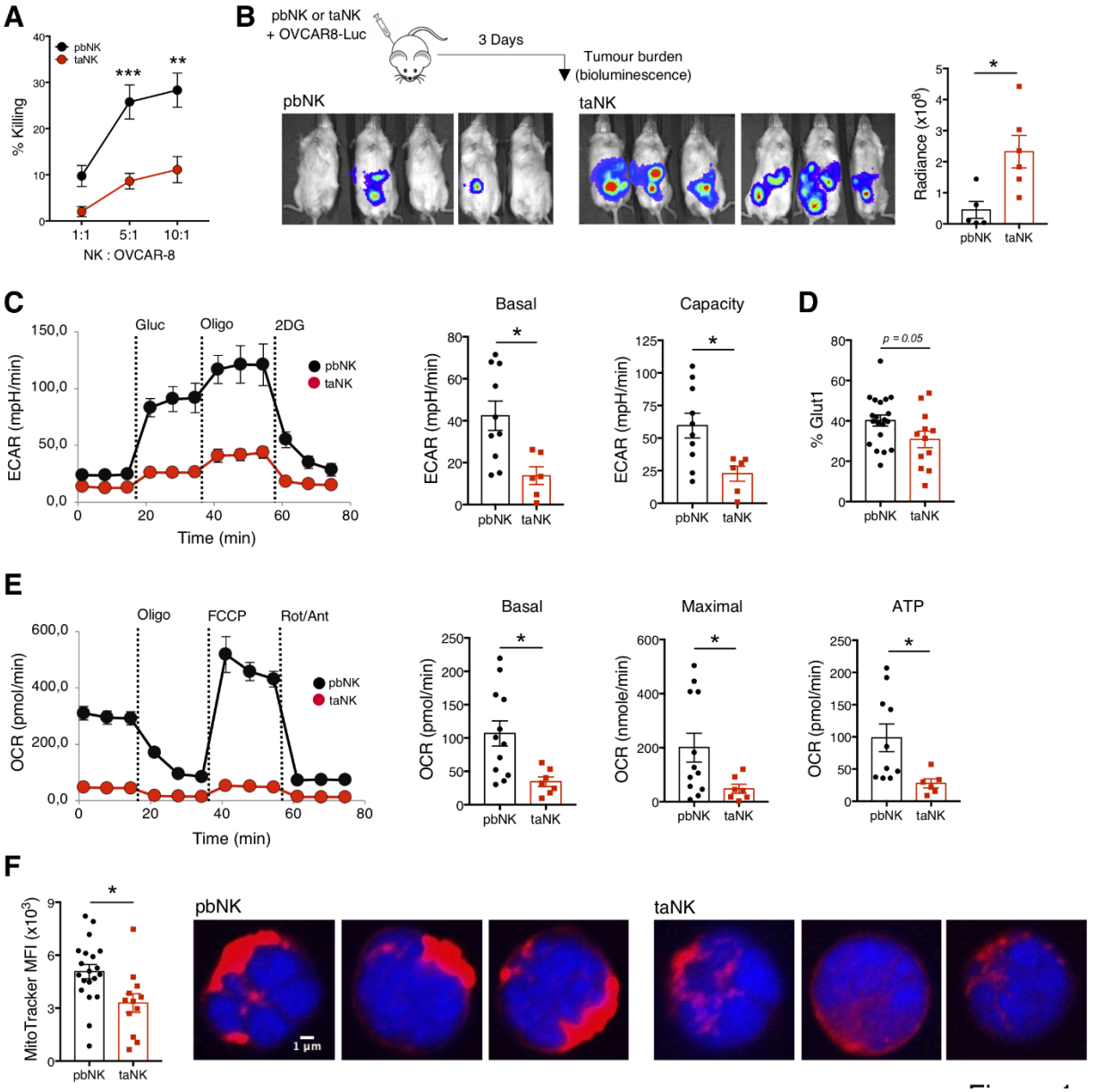

Figure 1. Dysfunctional human taNK cells from ovarian cancer patients have reduced glycolysis and OxPhos. **(A)** Cytotoxicity of purified pbNK or taNK cells against OVCAR8 cells. **(B)** pbNK cells or taNK cells were co-administered with Luciferase-expressing OVCAR8 cells (OVCAR8-Luc) to mice (schematic). Images and quantification of tumor burden at day 3 via bioluminescence (radiance: photons/s/nm/cm^2/str). **(C)** Representative measures of extracellular acidification rate (ECAR) upon addition of glucose (Gluc), oligomycin (Oligo), and 2-Deoxy-D-

glucose (2DG) and quantified basal glycolysis and glycolytic capacity. **(D)** Cell-surface expression of Glut1. **(E)** Representative measures of oxygen consumption rate (OCR) upon addition of Oligo, FCCP, and rotenone and antimycin (Rot/Ant). Quantified basal OxPhos, maximal OxPhos, and respiration-linked ATP. **(F)** Mean fluorescence intensity (MFI) quantified by flow cytometry and representative confocal microscopy images of NK cells stained with MitoTracker (red) and DAPI (blue). Data are means ±SEM of five to twenty biological replicates per condition, $^{***}P<0.001$, $^{**}P<0.01$, $^{*}P<0.05$ (A, two-way ANOVA; B-F, two-tailed *t* tests). See also Figure S1.

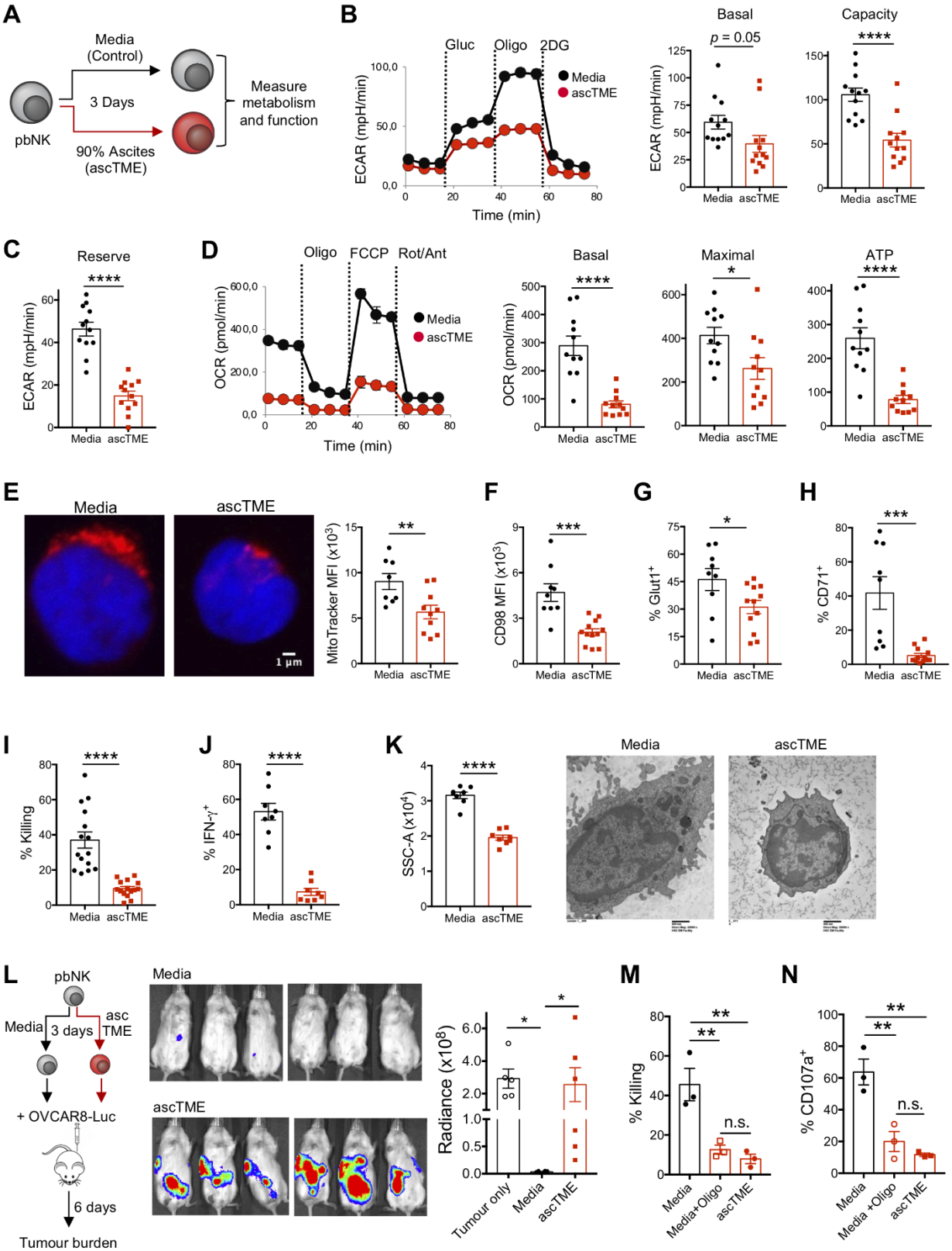
A
Media (Control)
3 Days
pbNK
90% Ascites (ascTME)
Measure metabolism and function
B
Gluc
Oligo
2DG
Media
ascTME
ECAR (mpH/min)
Time (min)
Basal
p = 0.05
Capacity
****
C
Reserve
D
Oligo
FCCP
Rot/Ant
OCR (pmol/min)
Maximal
ATP
E
Media
ascTME
1 µm
MitoTracker MFI (x10³)
F
CD98 MFI (x10³)
G
% Glut1⁺
H
% CD71⁺
I
% Killing
J
% IFN-γ⁺
K
SSC-A (x10⁴)
L
pbNK
Media
3 days
asc TME
+ OVCAR8-Luc
6 days
Tumour burden
Radiance (x10⁸)
Tumour only
M
% Killing
n.s.
Media+Oligo
N
% CD107a⁺

Figure 2

Figure 2. The human ascTME directly inhibits NK cell glycolysis and OxPhos to impair function. (A-K) Purified pbNK cells were incubated *ex vivo* in the ascTME from ovarian cancer patients or in media for 3 days. **(A)** Schematic of experimental design. (**B)** Representative measures of ECAR and quantified basal glycolysis, glycolytic capacity, and **(C)** glycolytic reserve. **(D)** Representative measures of OCR and quantified basal OxPhos, maximal OxPhos, and mitochondrial respiration-linked ATP. **(E)** Representative confocal microscopy images and MFI of MitoTracker(red)- and DAPI(blue)-stained NK cells. Cell-surface expression of **(F)** CD98, **(G)** Glut1, and **(H)** CD71. NK cell **(I)** killing and **(J)** IFN-γ expression against OVCAR8 cells. **(K)** NK cell granularity quantified via side-scatter (SSC-A) and visualized via transmission electron microscopy (TEM). **(L)** Media- or ascTME-incubated pbNK cells were co-administered with OVCAR8-Luc cells to mice (schematic). Day 6 images and quantification of tumor burden. **(M** and **N)** pbNK cells were incubated for 3 days in media with or without Oligomycin, or in the ascTME. Percent NK cell **(M)** killing and **(N)** degranulation measured by CD107a expression against OVCAR8 cells. Data are means ±SEM of three to fifteen biological replicates per condition. $^{****}P<0.0001$, $^{***}P<0.001$, $^{**}P<0.01$, $^{*}P<0.05$ (B-L, two-tailed *t* tests; M and N, one-way ANOVA). See also Figures S2.

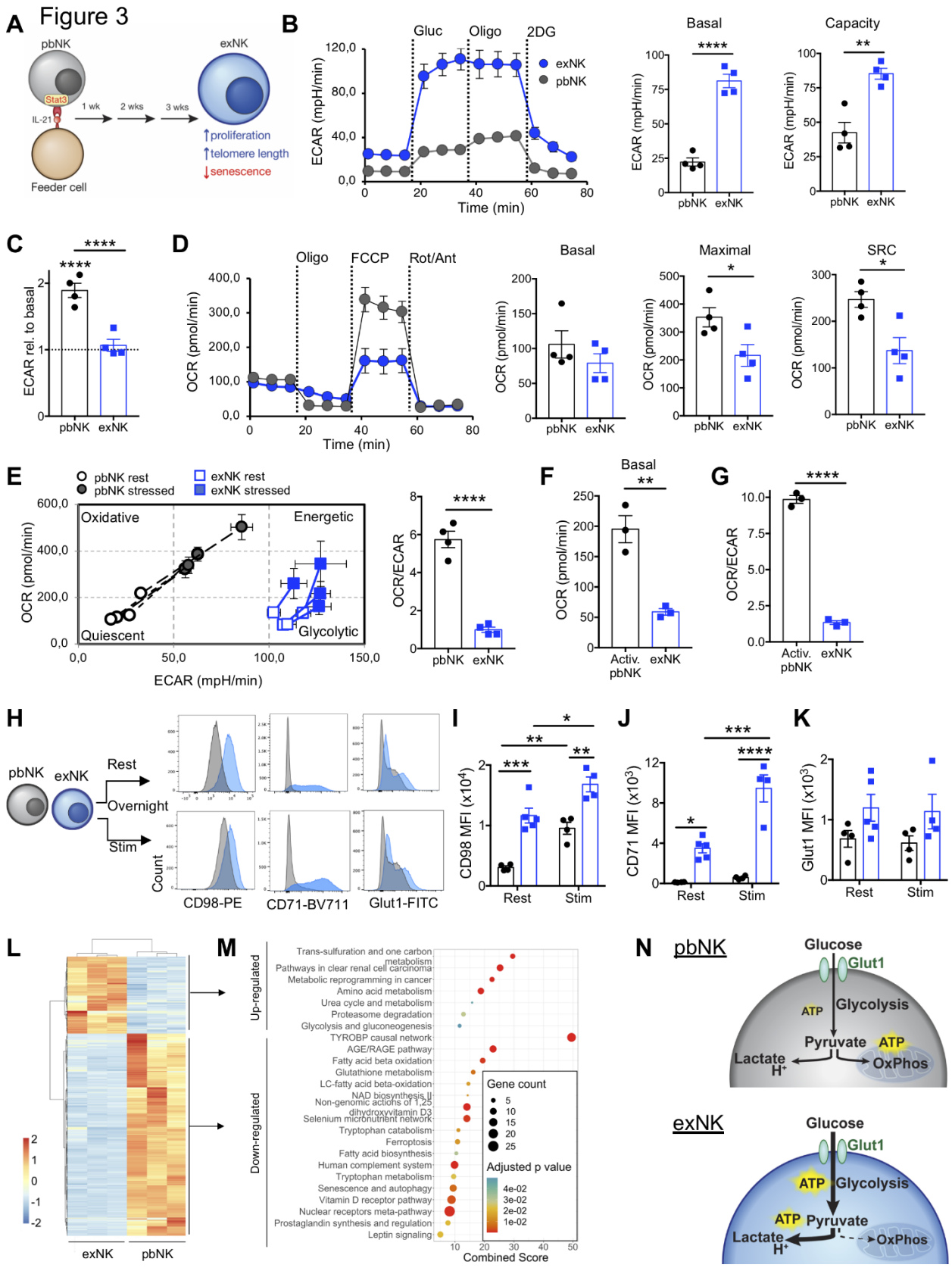
Figure 3
A
pbNK
exNK
Stat3
IL-21
1 wk
2 wks
3 wks
↑proliferation
↑telomere length
↓senescence
Feeder cell
B
Gluc
Oligo
2DG
ECAR (mpH/min)
Time (min)
exNK
pbNK
Basal
Capacity
****
**
C
ECAR rel. to basal
D
Oligo
FCCP
Rot/Ant
OCR (pmol/min)
Basal
Maximal
SRC
*
E
pbNK rest
pbNK stressed
exNK rest
exNK stressed
Oxidative
Energetic
Quiescent
Glycolytic
OCR (pmol/min)
ECAR (mpH/min)
OCR/ECAR
F
Basal
Activ. pbNK
G
H
pbNK
exNK
Rest
Overnight
Stim
Count
CD98-PE
CD71-BV711
Glut1-FITC
I
CD98 MFI (x10⁴)
J
CD71 MFI (x10³)
K
Glut1 MFI (x10³)
L
exNK
pbNK
M
Up-regulated
Down-regulated
Trans-sulfuration and one carbon metabolism
Pathways in clear renal cell carcinoma
Metabolic reprogramming in cancer
Amino acid metabolism
Urea cycle and metabolism
Proteasome degradation
Glycolysis and gluconeogenesis
TYROBP causal network
AGE/RAGE pathway
Fatty acid beta oxidation
Glutathione metabolism
LC-fatty acid beta-oxidation
NAD biosynthesis II
Non-genomic actions of 1,25 dihydroxyvitamin D3
Selenium micronutrient network
Tryptophan catabolism
Ferroptosis
Fatty acid biosynthesis
Human complement system
Tryptophan metabolism
Senescence and autophagy
Vitamin D receptor pathway
Nuclear receptors meta-pathway
Prostaglandin synthesis and regulation
Leptin signaling
Gene count
Adjusted p value
Combined Score
N
pbNK
Glucose
Glut1
ATP
Glycolysis
Pyruvate
Lactate
H⁺
OxPhos
exNK

Figure 3. STAT3-mediated expansion reprograms NK cells to a Warburg metabolism. pbNK cells were purified or expanded for 3 weeks (exNK). **(A)** Schematic for STAT3-mediated expansion with membrane-bound IL21-expressing feeder cells. **(B)** Representative ECAR measures and quantification of basal glycolysis, glycolytic capacity, and **(C)** relative glycolytic reserve. **(D)** Representative OCR measures and quantification of basal OxPhos, maximal OxPhos, and spare respiratory capacity (SRC). **(E)** Representative plots and quantification of the ratio of oxidative (OCR) versus glycolytic (ECAR) metabolism at baseline (open squares) and upon stress (filled squares). **(F)** Basal OxPhos and **(G)** OCR/ECAR following overnight activation in IL-2. **(H-K)** pbNK and exNK cells were activated overnight with IL-15/IL-12 or rested in low-dose IL-15. **(H)** Representative histograms and MFI of **(I)** CD98, **(J)** CD71, and **(K)** Glut1 expression. **(L-M)** Differential protein expression of donor-matched exNK cells compared to pbNK cells. **(L)** Pheatmap analysis of all proteins with significant differential expression. **(M)** Functional enrichment and pathway analysis of significantly up- and down-regulated proteins. Results show pathways that were significantly up- and down-regulated in exNK cells. **(N)** Schematic depicting pbNK cell (grey) oxidative metabolism compared to exNK cell (blue) Warburg metabolism. Data are means ±SEM of three to four biological replicates per condition. $^{****}P<0.0001$, $^{***}P<0.001$, $^{**}P<0.01$, $^{*}P<0.05$ (B-G, two-tailed *t* tests; I-K, two-way ANOVA). See also Figure S3.

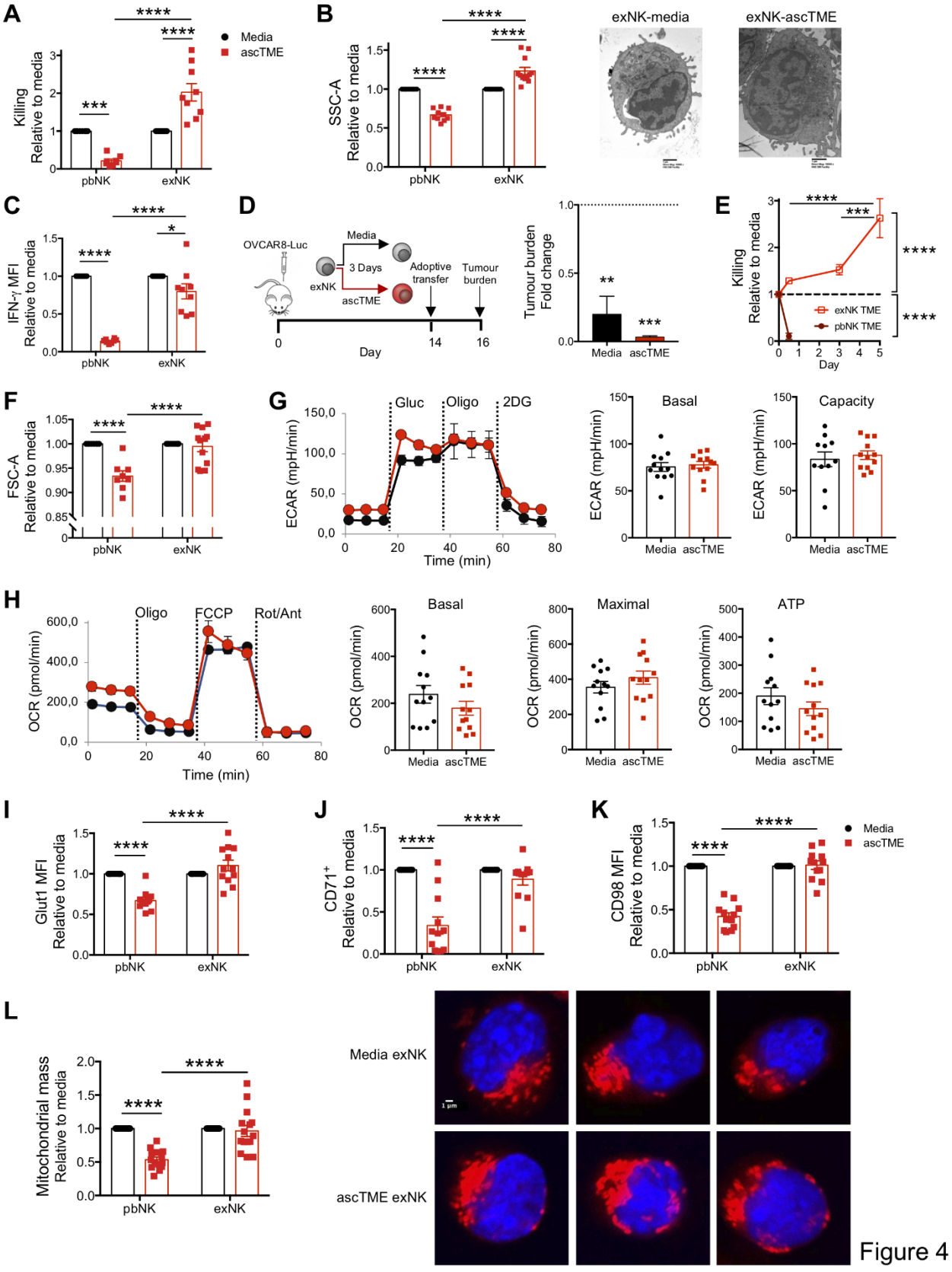
A
Killing
Relative to media
Media
ascTME
pbNK
exNK
B
SSC-A
Relative to media
exNK-media
exNK-ascTME
C
IFN-γ MFI
Relative to media
D
OVCAR8-Luc
Media
3 Days
exNK
ascTME
Adoptive transfer
Tumour burden
Day
Tumour burden
Fold change
E
Killing
Relative to media
exNK TME
pbNK TME
Day
F
FSC-A
Relative to media
G
Gluc
Oligo
2DG
ECAR (mpH/min)
Time (min)
Basal
Capacity
H
Oligo
FCCP
Rot/Ant
OCR (pmol/min)
Time (min)
Basal
Maximal
ATP
I
Glut1 MFI
Relative to media
J
CD71+
Relative to media
K
CD98 MFI
Relative to media
L
Mitochondrial mass
Relative to media
Media exNK
ascTME exNK

Figure 4

Figure 4. Human NK cells with Warburg metabolism become more cytotoxic and remain metabolically fit in the TME. pbNK cells and exNK cells were incubated in media or the ascTME from ovarian cancer patients *ex vivo* for 3 days, unless otherwise indicated, following which anti-tumour functions and metabolism were assessed. **(A)** Relative NK cell killing of OVCAR8 cells. **(B)** NK cell granularity quantified by SSC-A and visualized via TEM. **(C)** Relative change in NK cell IFN-γ expression upon incubation with OVCAR8 cells. **(D)** Media- or ascTME-incubated exNK cells were adoptively transferred to mice 14 days after injection of OVCAR8-Luc cells. Schematic shows experimental design. Graph shows fold change in tumour burden at day 16 relative to tumour only control mice. **(E)** pbNK and exNK cells were incubated in media or the ascTME for the indicated time points. Relative killing of OVCAR8 cells following incubation. **(F)** Relative change in cell size measured by FSC-A. **(G)** Representative ECAR measures, and quantified basal glycolysis and glycolytic capacity of exNK cells. **(H)** Representative OCR measures, and quantified basal OxPhos, maximal OxPhos, and respiration-linked ATP of exNK cells. Cell-surface expression of **(I)** Glut1, **(J)** CD71, and **(K)** CD98. **(L)** Relative change in mitochondrial mass, quantified by MitoTracker MFI, and confocal images from MitoTracker(red)- and DAPI(blue)-stained exNK cells. Data are means ±SEM of eight to fifteen biological replicates per condition. $^{****}P<0.0001$, $^{***}P<0.001$, $^{**}P<0.01$, $^{*}P<0.05$ (A-C, F, I-L, two-way ANOVA; D-E, one-way ANOVA; G-H, two-tailed *t* tests). See also Figure S4.

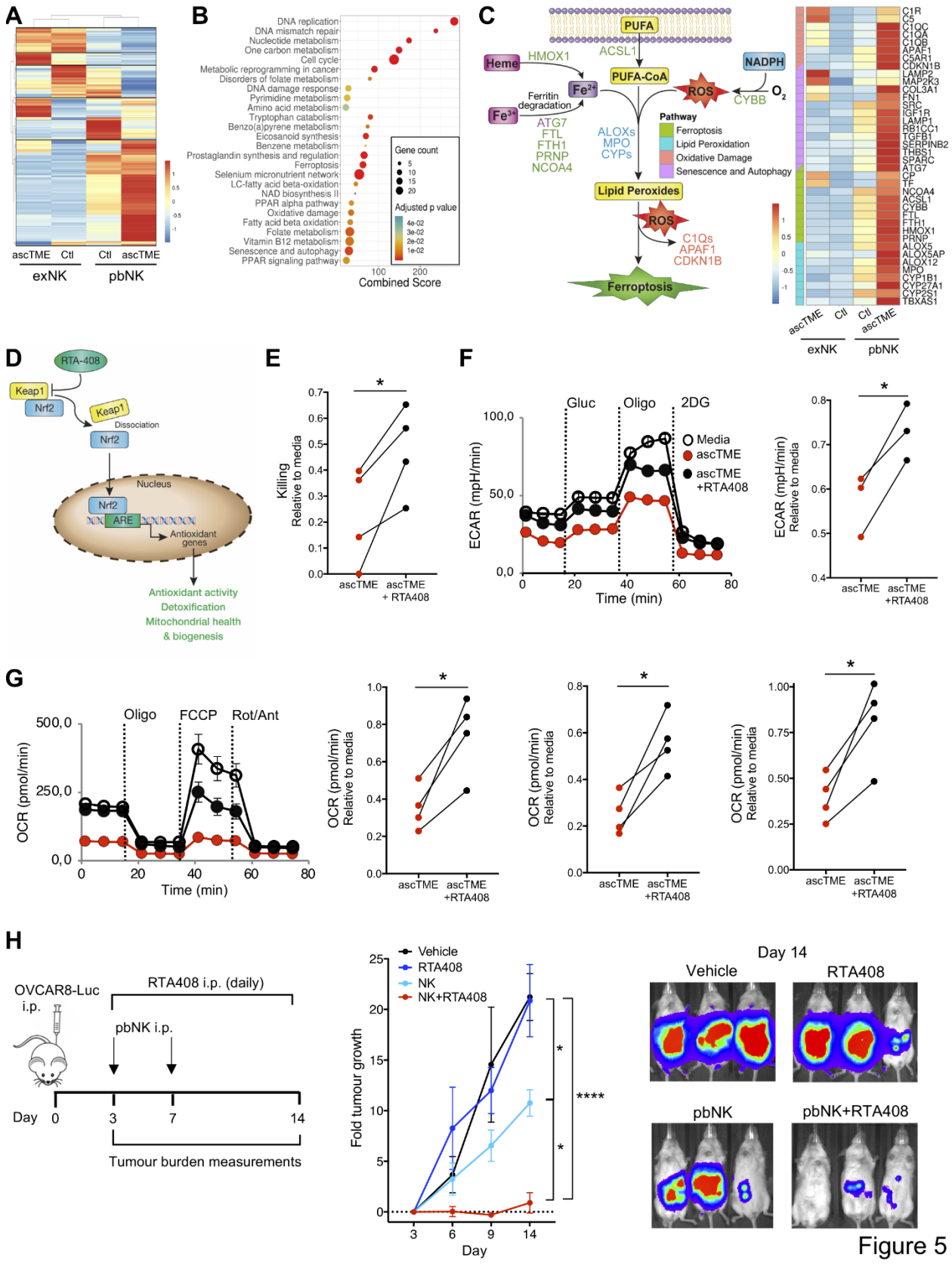
A
ascTME Ctl Ctl ascTME
exNK pbNK
B
DNA replication
DNA mismatch repair
Nucleotide metabolism
One carbon metabolism
Cell cycle
Metabolic reprogramming in cancer
Disorders of folate metabolism
DNA damage response
Pyrimidine metabolism
Amino acid metabolism
Tryptophan catabolism
Benzo(a)pyrene metabolism
Eicosanoid synthesis
Benzene metabolism
Prostaglandin synthesis and regulation
Ferroptosis
Selenium micronutrient network
LC-fatty acid beta-oxidation
NAD biosynthesis II
PPAR alpha pathway
Oxidative damage
Fatty acid beta oxidation
Folate metabolism
Vitamin B12 metabolism
Senescence and autophagy
PPAR signaling pathway
Gene count
Adjusted p value
Combined Score
C
PUFA
ACSL1
Heme
HMOX1
PUFA-CoA
ROS
NADPH
CYBB
Ferritin degradation
ATG7
FTL
FTH1
PRNP
NCOA4
ALOXs
MPO
CYPs
Pathway
Ferroptosis
Lipid Peroxidation
Oxidative Damage
Senescence and Autophagy
Lipid Peroxides
C1Qs
APAF1
CDKN1B
Ferroptosis
exNK
pbNK
D
RTA-408
Keap1
Nrf2
Dissociation
Nucleus
ARE
Antioxidant genes
Antioxidant activity
Detoxification
Mitochondrial health & biogenesis
E
Killing Relative to media
ascTME
ascTME + RTA408
F
Gluc
Oligo
2DG
Media
ascTME
ascTME +RTA408
ECAR (mpH/min)
Time (min)
ECAR (mpH/min) Relative to media
G
Oligo
FCCP
Rot/Ant
OCR (pmol/min)
Time (min)
OCR (pmol/min) Relative to media
H
OVCAR8-Luc i.p.
RTA408 i.p. (daily)
pbNK i.p.
Day 0 3 7 14
Tumour burden measurements
Vehicle
RTA408
NK
NK+RTA408
Fold tumour growth
Day
Day 14
Vehicle
RTA408
pbNK
pbNK+RTA408

Figure 5

Figure 5. exNK cells resist lipid peroxidative damage in the TME that critically impairs pbNK cell cytotoxicity and metabolism. (A-C) Differential protein expression of pbNK cells or exNK cells following 3 days in the ascTME or media (Ctl). **(A)** Pheatmap analysis of all significantly differentially expressed proteins. **(B)** Functional enrichment and pathway analysis of significantly differentially expressed proteins. Results show selection of enriched metabolism-related pathways. **(C)** Schematic shows the pathways of lipid peroxidation-induced oxidative stress and ferroptosis. Pheatmap analyses shows significantly differentially expressed proteins associated with lipid peroxidation, ferroptosis, oxidative damage, and senescence and autophagy pathways. **(D)** Schematic for the mechanism of Nrf2 activation by RTA-408. **(E-G)** pbNK cells were incubated for 3 days in the ascTME in the presence or absence of RTA-408 or in media. **(E)** Relative killing against OVCAR8 cells. **(F)** Representative ECAR measures and quantified glycolytic capacity. **(G)** Representative OCR measures and quantified basal OxPhos, maximal OxPhos, and respiration-linked ATP. **(H)** Mice were treated with pbNK cells and/or RTA408 or vehicle beginning 3 days following engraftment of OVCAR8-Luc cells. Schematic shows experimental design. Graph shows fold change in tumour growth over 14 days. Images show representative tumour burden at day 14 (n = 6-11 mice per group). Results are means ± SEM of three to eleven biological replicates per condition. $^{****}P<0.0001$, $^{**}P<0.01$, $^{*}P<0.05$ (two-tailed *t* tests). See also Figure S5.

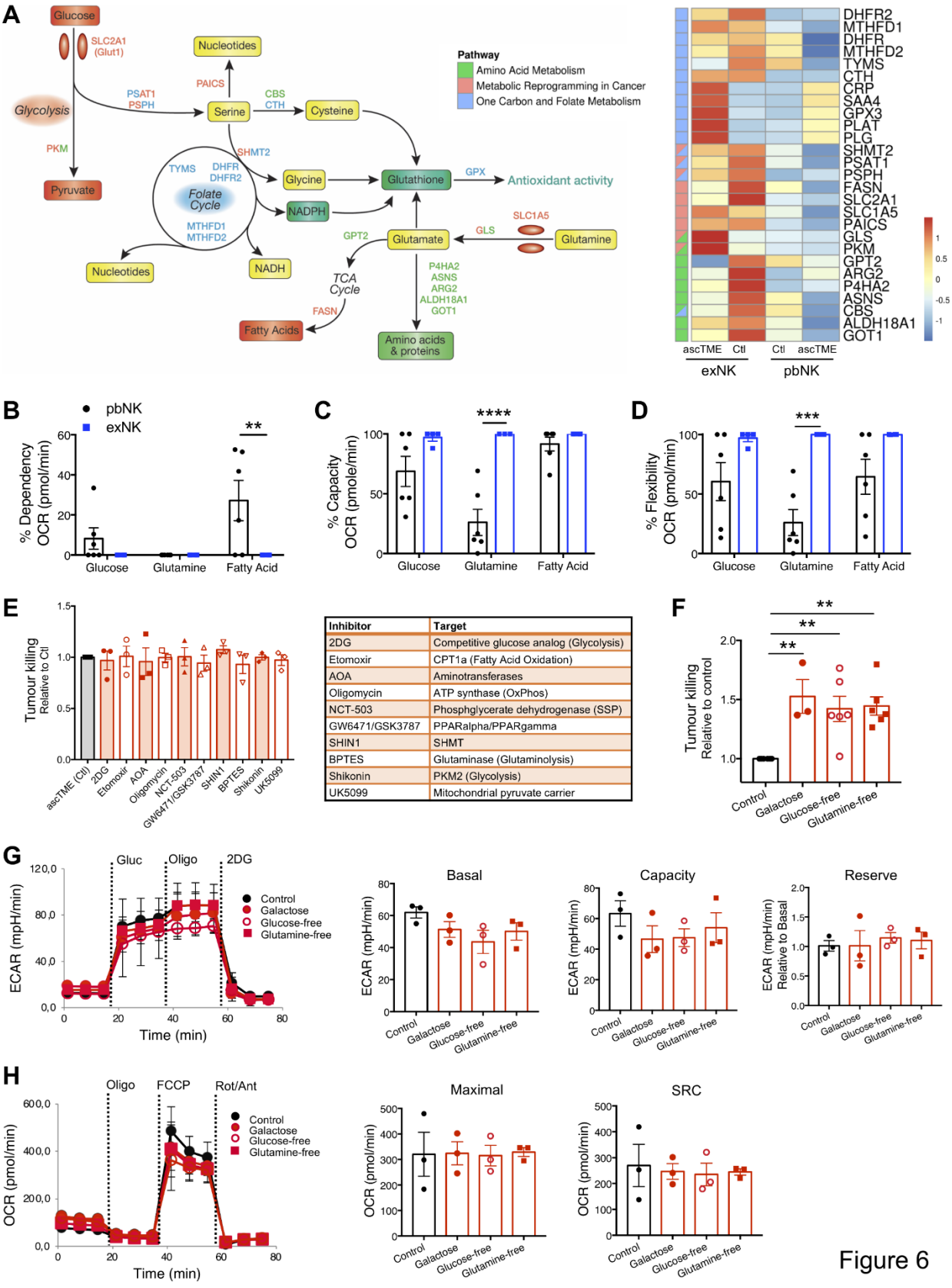

Inhibitor	Target
2DG	Competitive glucose analog (Glycolysis)
Etomoxir	CPT1a (Fatty Acid Oxidation)
AOA	Aminotransferases
Oligomycin	ATP synthase (OxPhos)
NCT-503	Phosphglycerate dehydrogenase (SSP)
GW6471/GSK3787	PPARalpha/PPARgamma
SHIN1	SHMT
BPTES	Glutaminase (Glutaminolysis)
Shikonin	PKM2 (Glycolysis)
UK5099	Mitochondrial pyruvate carrier

Figure 6

Figure 6. Metabolic flexibility enables NK cells to augment their anti-tumour activity in response to nutrient deprivation. (A) pbNK or exNK cells were incubated in ascites fluid (TME) or media (Ctl) for 3 days. Schematic shows Warburg metabolic adaptations in glycolysis, serine and amino acid synthesis, and one carbon and folate metabolism pathways. Pheatmap analyses shows significantly differentially expressed proteins associated with the indicated pathways. **(B-D)** Purified pbNK or exNK cell mitochondrial fuel usage. Percent **(B)** dependency, **(C)** capacity, and **(D)** flexibility of pbNK and exNK cell OCR on glucose, glutamine, and fatty acids. **(E)** exNK cells were incubated in the ascTME for 3 days in the presence or absence of the indicated inhibitors. Results show cytotoxicity relative to the ascTME only control (Ctl). Table indicates targets for each corresponding inhibitor. **(F-H)** exNK cells were cultured in complete media (control), glucose-free media with or without galactose, or glutamine-free media for 5 days at which point cytotoxicity and metabolism were assessed. **(F)** Relative change in cytotoxicity against OVCAR8 cells compared to control media. **(G)** Representative ECAR measures and quantified basal glycolysis, glycolytic capacity, and glycolytic reserve. **(H)** Representative OCR measures and quantification maximal OxPhos and spare respiratory capacity (SRC). Results show means ± SEM of three to six biological replicates per condition. $^{****}P<0.0001$, $^{***}P<0.001$, $^{**}P<0.01$ (B-D, two-way ANOVA; E-H, one-way ANOVA). See also Figure S6.

4.9 SUPPLEMENTAL DATA

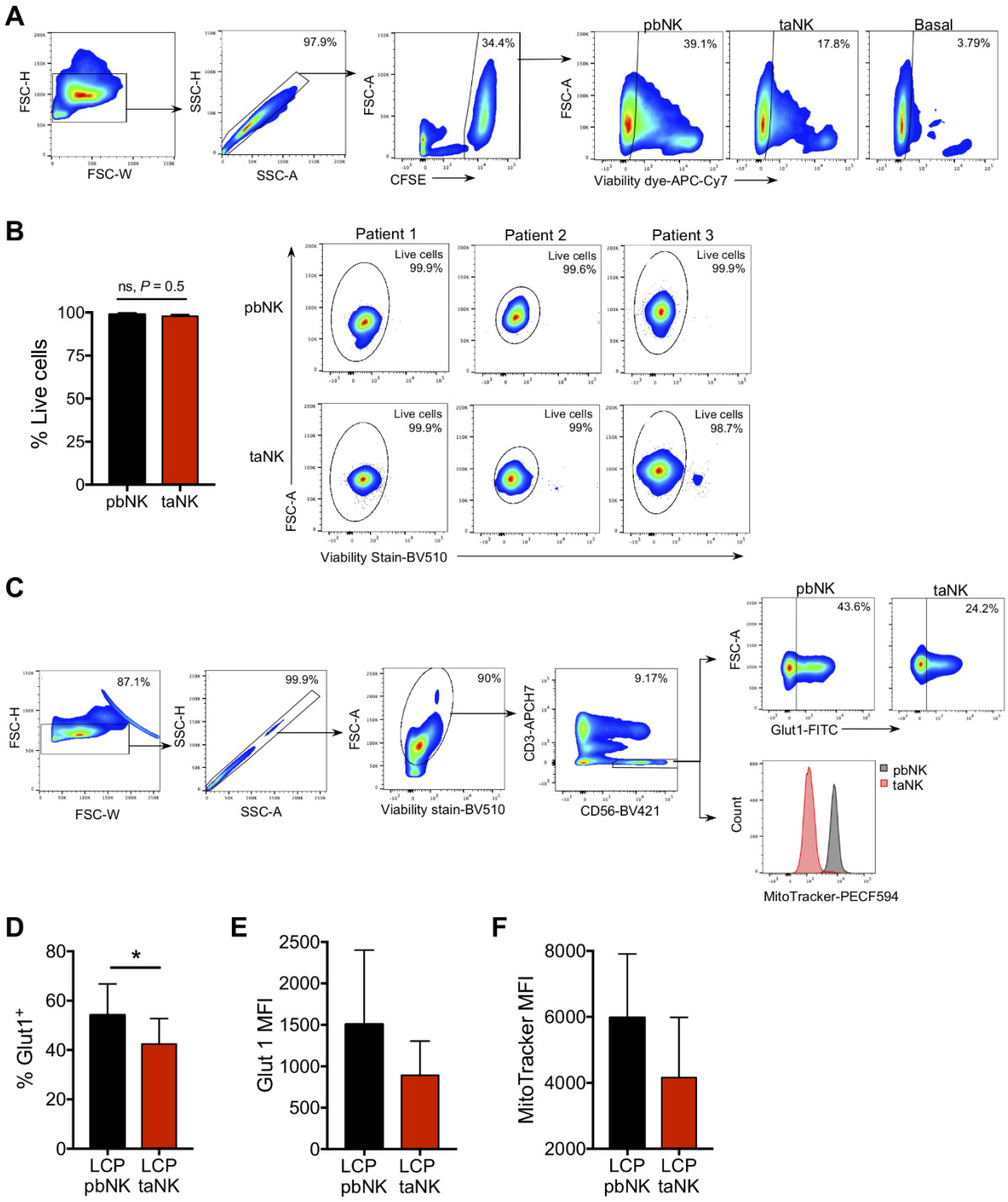

Figure S1. Cancer patient taNK cells have reduced glucose metabolism and anti-tumour functions. Related to Figure 1. (A-C) NK cells were isolated from the blood (pbNK) or ascites fluid (taNK) of ovarian cancer patients. **(A)** pbNK and taNK cell killing of CFSE-labeled OVCAR8 cells. Representative flow plots of gating strategy and OVCAR8 cell death following

incubation with NK cells compared to basal death (no NK cells). **(B)** Quantification and representative flow plots of pbNK and taNK cell viability following isolation. **(C)** Representative flow plots of NK cell gating strategy from PBMCs or TILs, Glut1 expression, and histogram of pbNK and taNK cell mitochondrial staining with MitoTracker. **(D-F)** PBMCs and TILs were respectively isolated from the blood and tumours of lung cancer patients. Glut1 % expression **(D)** and MFI (**E)** and MitoTracker MFI **(F)** of lung cancer patient taNK cells compared to pbNK cells. Data are means ±SEM of 4-10 biological replicates per condition. $^{*}P<0.05$ (two-tailed t-test).

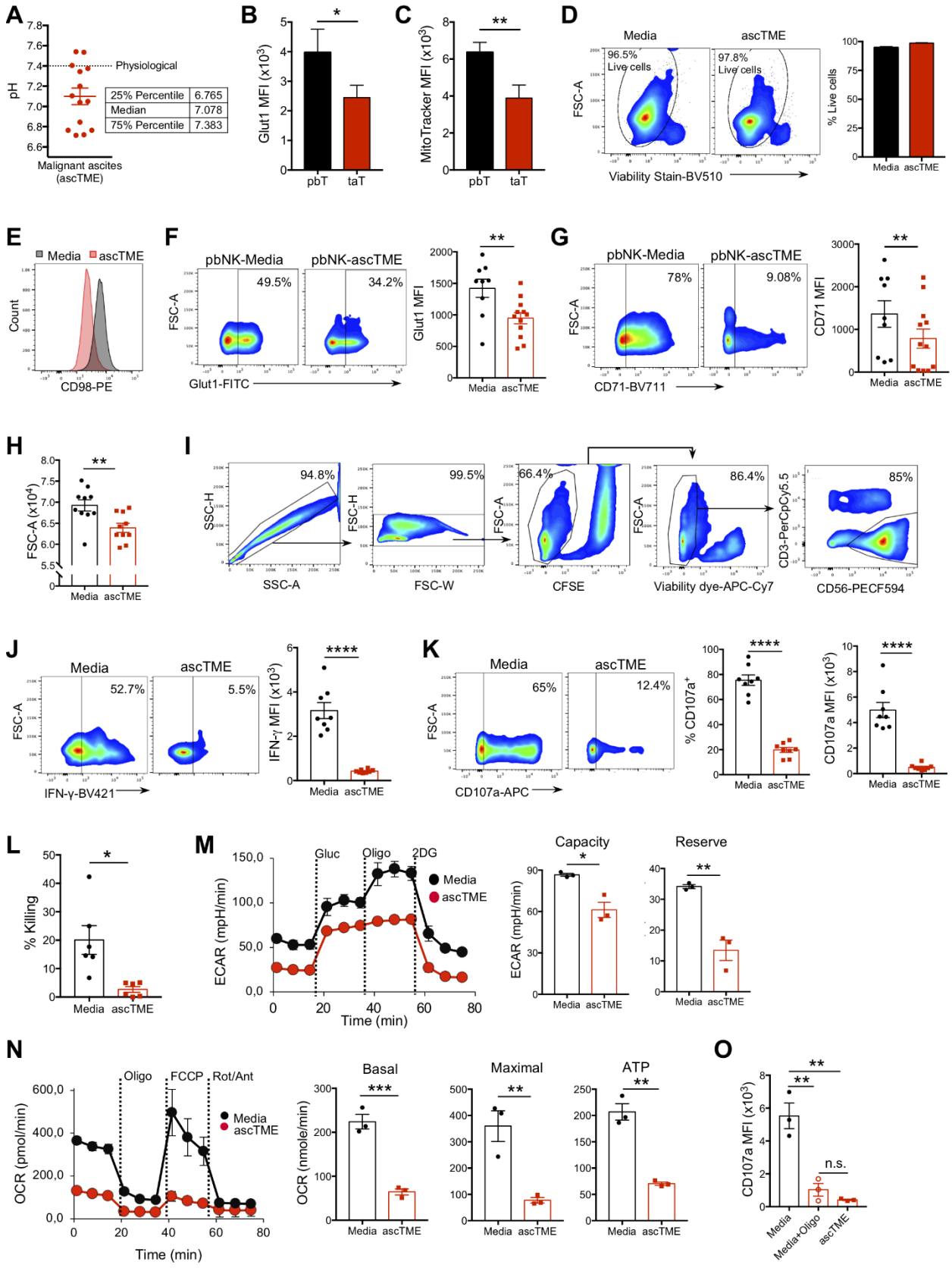
A
pH
Physiological
25% Percentile 6.765
Median 7.078
75% Percentile 7.383
Malignant ascites (ascTME)
B
Glut1 MFI (x10^3)
pbT taT
C
MitoTracker MFI (x10^3)
pbT taT
D
Media ascTME
96.5% Live cells
97.8% Live cells
FSC-A
Viability Stain-BV510
% Live cells
Media ascTME
E
Media ascTME
Count
CD98-PE
F
pbNK-Media pbNK-ascTME
49.5%
34.2%
FSC-A
Glut1-FITC
Glut1 MFI
Media ascTME
G
pbNK-Media pbNK-ascTME
78%
9.08%
FSC-A
CD71-BV711
CD71 MFI
Media ascTME
H
FSC-A (x10^4)
Media ascTME
I
94.8%
99.5%
66.4%
86.4%
85%
SSC-H
SSC-A
FSC-H
FSC-W
FSC-A
CFSE
Viability dye-APC-Cy7
CD3-PerCpCy5.5
CD56-PECF594
J
Media ascTME
52.7%
5.5%
FSC-A
IFN-γ-BV421
IFN-γ MFI (x10^3)
Media ascTME
K
Media ascTME
65%
12.4%
FSC-A
CD107a-APC
% CD107a+
CD107a MFI (x10^3)
Media ascTME
L
% Killing
Media ascTME
M
Gluc Oligo 2DG
Media
ascTME
ECAR (mpH/min)
Time (min)
Capacity
Reserve
ECAR (mpH/min)
Media ascTME
N
Oligo FCCP Rot/Ant
Media
ascTME
OCR (pmol/min)
Time (min)
Basal
Maximal
ATP
OCR (nmole/min)
Media ascTME
O
CD107a MFI (x10^3)
n.s.
Media Media+Oligo ascTME

Figure S2. The human TME directly inhibits pbNK cell metabolism and anti-tumour functions. Related to Figure 2. (A) pH of malignant ascites fluid (ascTME) from fourteen ovarian cancer patients. Glut1 MFI **(B)** and Mitotracker MFI **(C)** of stained CD3+ T cells from the PBMCs (pbT) or ascites (taT) of ovarian cancer patients. **(D-K)** Isolated pbNK cells were incubated in the ascTME from ovarian cancer patients *ex vivo* or in media for 3 days. **(D)** Representative flow plots and quantification of pbNK cell viability at day 3. **(E)** Representative histogram and MFI of NK cell CD98. Representative flow plots and MFI of NK cell **(F)** Glut1 and **(G)** CD71. **(H)** pbNK cell size quantified by forward scatter (FSC-A). **(I-K)** Media- or ascTME-exposed pbNK cells were incubated with CFSE- labeled OVCAR8 cells. **(I)** Representative flow plots of gating strategy on NK cells. Representative flow plots, MFI, and percent expression of pbNK cell **(J)** IFN-γ and **(K)** CD107a expression in response to OVCAR8 cells. **(L-N)** Purified pbNK cells were incubated in normal media or in the *ex vivo* ascTME from ovarian cancer patients for 12 hours. **(L)** NK cell cytotoxicity against OVCAR8 cells. **(M)** Representative measures of ECAR and quantification of glycolytic capacity and glycolytic reserve. **(N)** Representative measures of cellular OCR and quantification of basal OxPhos, maximal OxPhos, and respiration-linked ATP. **(O)** pbNK cells were incubated for 24 hours in media in the presence or absence of Oligomycin (Oligo), or in the ascTME. Following incubation, NK cell degranulation was assessed against OVCAR8 cells. Quantification of NK cell CD107a MFI. Data are means ± SEM of three to twenty biological replicates per condition. $^{****}P<0.0001$, $^{***}P<0.001$, $^{**}P<0.01$, $^{*}P<0.05$ (B-N, two-tailed *t* tests; O, one-way ANOVA).

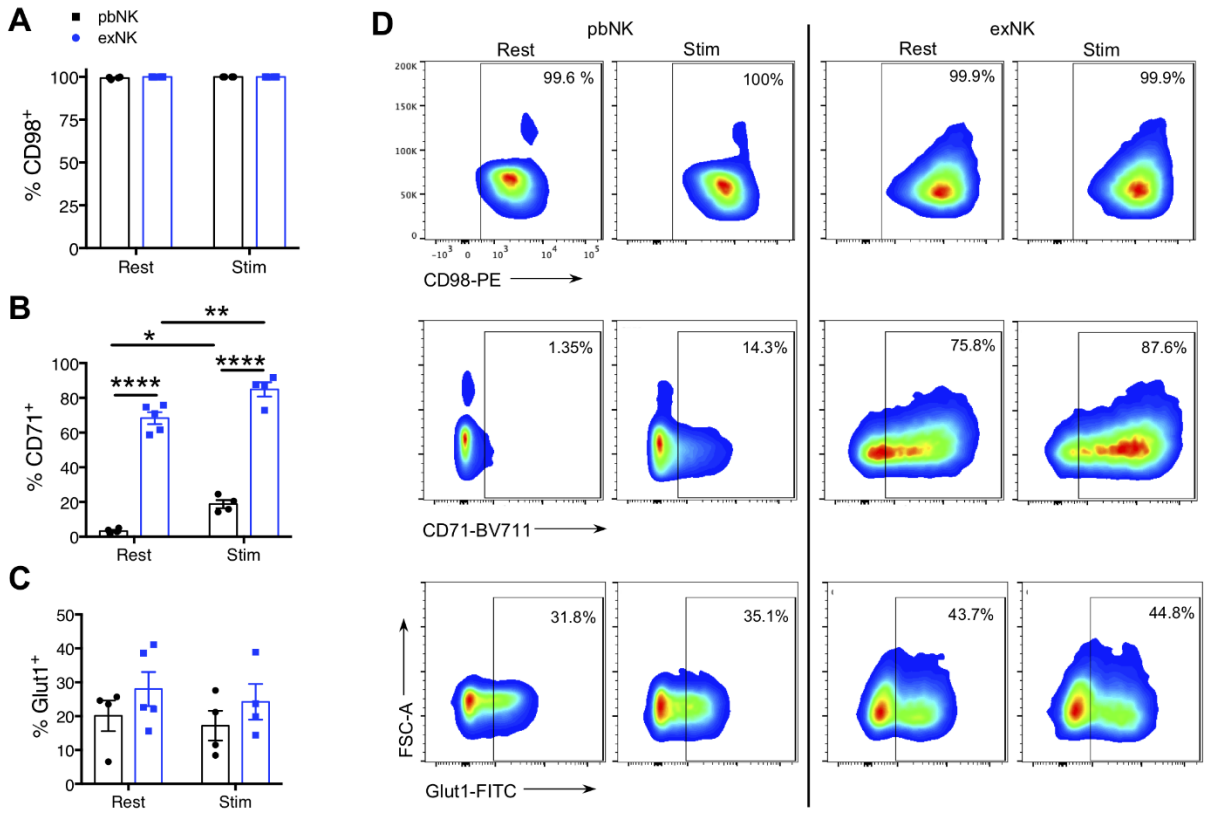

Figure S3. exNK cells have greater expression of nutrient receptors relative to pbNK cells. Related to Figure 3. Purified pbNK cells or exNK cells were stimulated overnight with IL-15 (100 ng/mL) and IL-12 (30 ng/mL) or rested in 1 ng/mL IL-15. Following stimulation, NK cells were stained for cell-surface expression of nutrient receptors. Percent expression of NK cell **(A)** CD98, **(B)** CD71, and **(C)** Glut1. **(D)** Representative flow plots of NK cell nutrient receptor expression. Data are means ± SEM of four to five biological replicates per condition. $^{****}P<0.0001$, $^{**}P<0.01$, $^{*}P<0.05$ (two-way ANOVA).

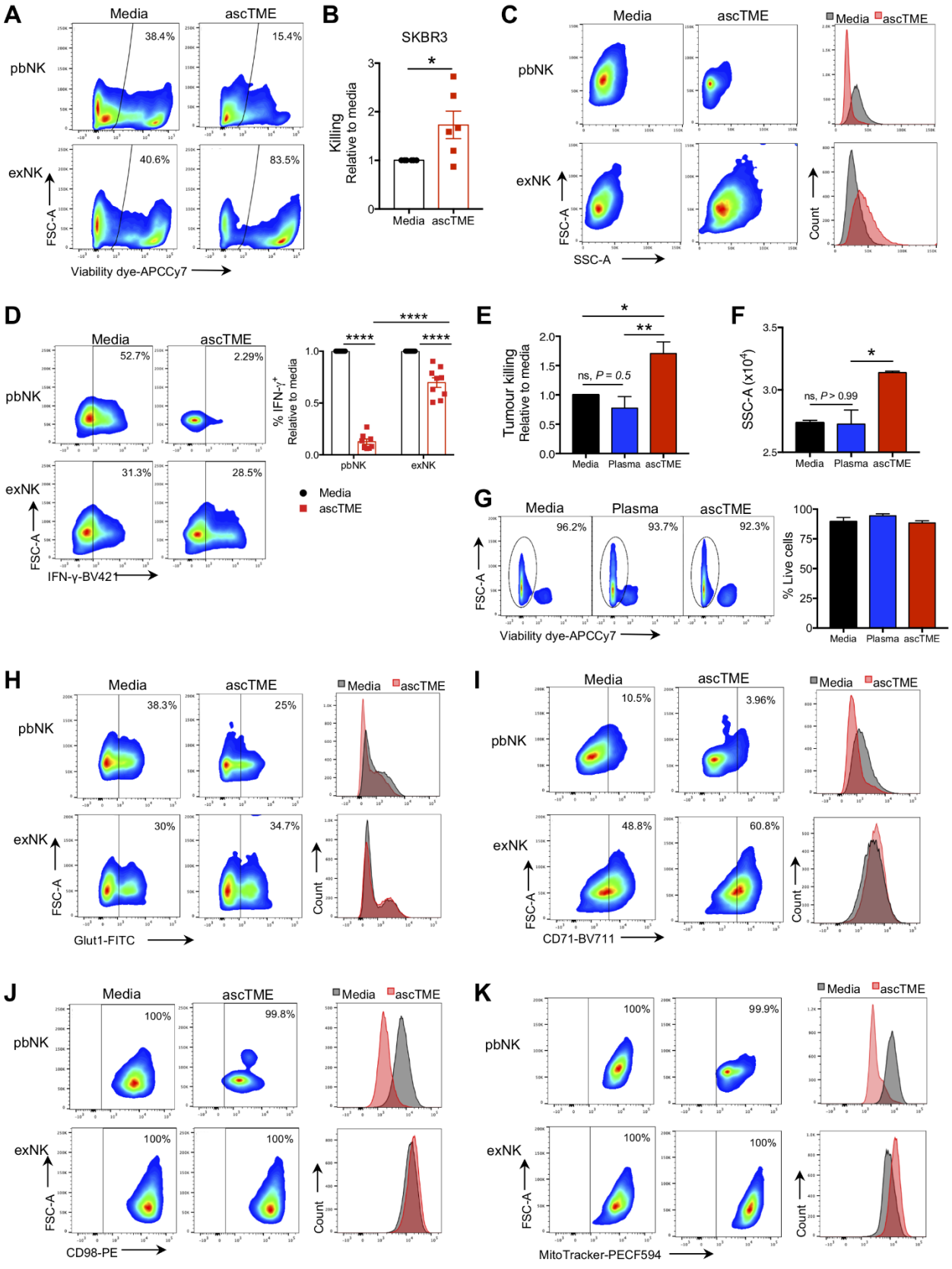
A
Media
ascTME
pbNK
exNK
38.4%
15.4%
40.6%
83.5%
FSC-A
Viability dye-APCCy7
B
SKBR3
Killing
Relative to media
Media
ascTME
C
Media
ascTME
pbNK
exNK
FSC-A
SSC-A
Count
D
52.7%
2.29%
31.3%
28.5%
IFN-γ-BV421
% IFN-γ+
Relative to media
pbNK
exNK
E
Tumour killing
Relative to media
ns, P = 0.5
Plasma
F
SSC-A (x10⁴)
ns, P > 0.99
G
Plasma
96.2%
93.7%
92.3%
% Live cells
H
38.3%
25%
30%
34.7%
Glut1-FITC
I
10.5%
3.96%
48.8%
60.8%
CD71-BV711
J
100%
99.8%
CD98-PE
K
99.9%
MitoTracker-PECF594

Figure S4. exNK cells develop augmented cytotoxicity and sustain nutrient receptor expression in the ascTME. Related to Figure 4. exNK cells or purified pbNK cells were incubated for 3 days in the ascTME of ovarian cancer patients *ex vivo* or in media as control unless otherwise indicated. **(A)** Representative flow plots showing percent OVCAR8 cells killed following 5-hour incubation with media- or ascTME-exposed pbNK and exNK cells. **(B)** Relative killing of SKBR3 breast cancer cells by ascTME-exposed exNK cells compared to media-exposed exNK cells. **(C)** Representative flow plots of pbNK cell and exNK cell size (FSC-A) and granularity measured by SSC-A and representative histogram of SSC-A. **(D)** Representative flow plots and relative change in percent IFN-γ positive cells in media- and ascTME-exposed pbNK and exNK cells in response to OVCAR8 cells. **(E-G)** exNK cells were incubated for 3 days *ex vivo* in media, human plasma, or the ascTME. **(E)** Relative killing of OVCAR8 cells, **(F)** granularity measured by SSC-A, and **(G)** representative flow plots and quantification of cellular viability following incubation. Representative flow plots and histograms of pbNK and exNK cell **(H)** Glut1, **(I)** CD71, and **(J)** CD98 expression and **(K)** activated mitochondria (via MitoTracker) in media compared to the ascTME. Data show means ± SEM of six to twelve biological replicates per condition. $^{****}P<0.0001$, $^{*}P<0.05$ (B**,** two-tailed *t* test; D**,** two-way ANOVA; E-G, one-way ANOVA).

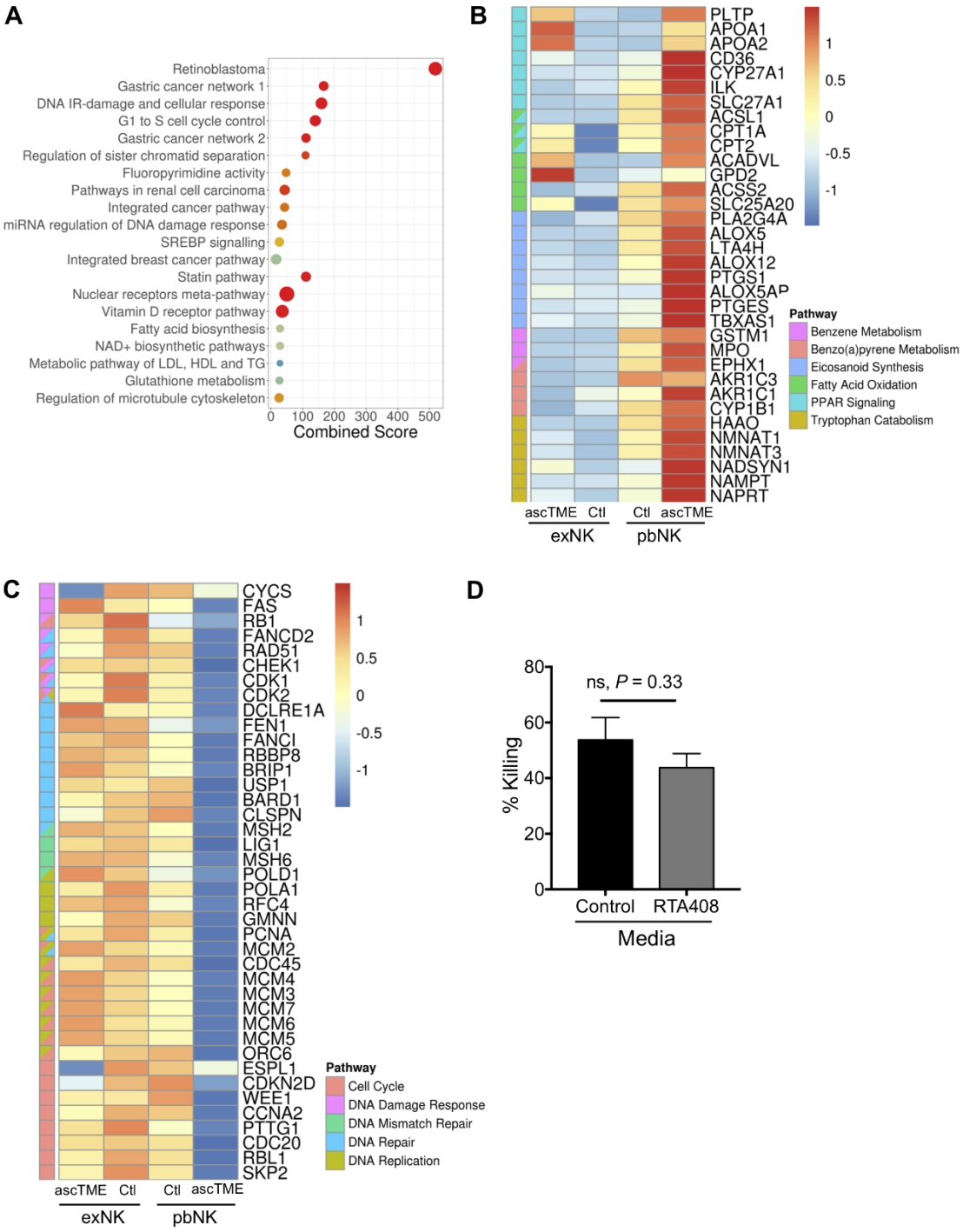

Figure S5. The human ascTME induces a protein profile indicative of oxidative damage in pbNK cells but not in exNK cells. Related to Figure 5. (A-C) Differential protein expression of pbNK cells or exNK cells following 3 days in the human ascTME or media (Ctl). **(A)** Enriched metabolism-related pathways from functional enrichment and pathway analysis of significantly

differentially expressed proteins. **(B** and **C)** Pheatmap analyses of significantly differentially expressed proteins ($P < 0.05$) in the indicated WikiPathways 2019 ontologies. **(B)** Pathways involved in lipid oxidation, lipid peroxidation, and oxidative damage. **(C)** Pathways involved in DNA repair, DNA replication, and cell cycle. Rows clustered using a complete clustering method and euclidean distance measure. Results show mean normalized signal intensities per row (protein). **(D)** pbNK cells were incubated in media with or without RTA-408 for 3 days, then seeded with OVCAR8 tumour targets. Graph shows pbNK cell killing of OVCAR8 cells. Data show means ± SEM of 4 biological replicates per condition. Results analyzed by unpaired t-test; ns denotes not significant.

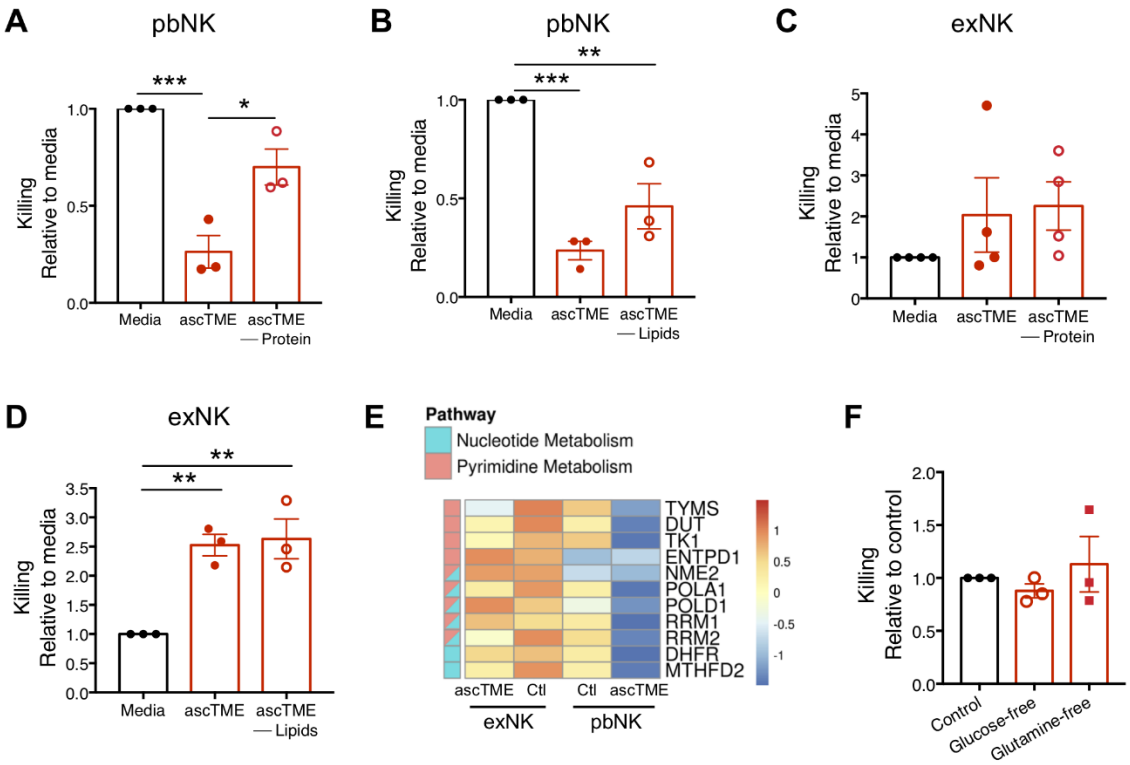

Figure S6. Neither protein nor lipid components of the ascTME nor short-term nutrient deprivation affect exNK cell function. Related to Figure 6. (A-D) Purified pbNK cells or exNK cells were incubated in media, the ascTME, or the ascTME depleted of proteins or lipids for 3 days. Cytotoxicity against OVCAR8 cells was assessed after incubation. Cytotoxicity of pbNK cells exposed to the **(A)** protein-depleted or **(B)** lipid-depleted ascTME relative to control ascTME or media. Relative cytotoxicity of exNK cells exposed to the **(C)** protein-depleted or **(D)** lipid-depleted ascTME relative to control ascTME or media. **(E)** Differential protein expression of pbNK cells or exNK cells following 3 days in the human ascTME or media (Ctl). Significantly differentially expressed proteins in nucleotide metabolism pathways from functional enrichment and pathway analysis. **(F)** exNK cells were incubated in complete media (control), or media free of glucose or glutamine for 24 hours. exNK cell killing of OVCAR8 cells after incubation. Data are means ± SEM of three to four replicates per condition. $^{***}P<0.001$, $^{**}P<0.01$, $^{*}P<0.05$ (one-way ANOVA).

4.10 REFERENCES

Albillos, A., Cuervas-Mons, V., Millán, I., Cantón, T., Montes, J., Barrios, C., Garrido, A., and Escartín, P. (1990). Ascitic fluid polymorphonuclear cell count and serum to ascites albumin gradient in the diagnosis of bacterial peritonitis. Gastroenterology *98*, 134-140.

Alexandrakis, M.G., Moschandrea, J., Kyriakou, D.S., Alexandraki, R., and Kouroumalis, E. (2001). Use of a variety of biological parameters in distinguishing cirrhotic from malignant ascites. Int J Biol Markers *16*, 45-49.

Alexeev, V., Lash, E., Aguillard, A., Corsini, L., Bitterman, A., Ward, K., Dicker, A.P., Linnenbach, A., and Rodeck, U. (2014). Radiation protection of the gastrointestinal tract and growth inhibition of prostate cancer xenografts by a single compound. Mol Cancer Ther *13*, 2968-2977.

Assmann, N., O'Brien, K.L., Donnelly, R.P., Dyck, L., Zaiatz-Bittencourt, V., Loftus, R.M., Heinrich, P., Oefner, P.J., Lynch, L., Gardiner, C.M., et al. (2017). Srebp-controlled glucose metabolism is essential for NK cell functional responses. Nat Immunol *18*, 1197-1206.

Bala, L., Sharma, A., Yellapa, R.K., Roy, R., Choudhuri, G., and Khetrapal, C.L. (2008). (1)H NMR spectroscopy of ascitic fluid: discrimination between malignant and benign ascites and comparison of the results with conventional methods. NMR in biomedicine *21*, 606-614.

Belisle, J.A., Gubbels, J.A., Raphael, C.A., Migneault, M., Rancourt, C., Connor, J.P., and Patankar, M.S. (2007). Peritoneal natural killer cells from epithelial ovarian cancer patients show an altered phenotype and bind to the tumour marker MUC16 (CA125). Immunology *122*, 418-429.

Berek, J.S., Bast, R.C., Lichtenstein, A., Hacker, N.F., Spina, C.A., Lagasse, L.D., Knapp, R.C., and Zighelboim, J. (1984). Lymphocyte cytotoxicity in the peritoneal cavity and blood of patients with ovarian cancer. Obstet Gynecol *64*, 704-714.

Buck, M.D., O'Sullivan, D., Klein Geltink, R.I., Curtis, J.D., Chang, C.H., Sanin, D.E., Qiu, J., Kretz, O., Braas, D., van der Windt, G.J., et al. (2016). Mitochondrial dynamics controls T cell fate through metabolic programming. Cell *166*, 63-76.

Cerwenka, A., and Lanier, L.L. (2018). Natural killers join the fight against cancer. Science *359*, 1460-1461.

Chang, C.H., Qiu, J., O'Sullivan, D., Buck, M.D., Noguchi, T., Curtis, J.D., Chen, Q., Gindin, M., Gubin, M.M., van der Windt, G.J., et al. (2015). Metabolic competition in the tumour microenvironment is a driver of cancer progression. Cell *162*, 1229-1241.

Chen, E.Y., Tan, C.M., Kou, Y., Duan, Q., Wang, Z., Meirelles, G.V., Clark, N.R., and Ma'ayan, A. (2013). Enrichr: interactive and collaborative HTML5 gene list enrichment analysis tool. BMC Bioinformatics *14*, 128.

Ciurea, S.O., Schafer, J.R., Bassett, R., Denman, C.J., Cao, K., Willis, D., Rondon, G., Chen, J., Soebbing, D., Kaur, I., et al. (2017). Phase 1 clinical trial using mbIL21 ex-vivo expanded donor-derived NK cells after haploidentical transplantation. Blood, pii: blood-2017-2005-785659.

Coca, S., Perez-Piqueras, J., Martinez, D., Colmenarejo, A., Saez, M.A., Vallejo, C., Martos, J.A., and Moreno, M. (1997). The prognostic significance of intratumoral natural killer cells in patients with colorectal carcinoma. Cancer *79*, 2320-2328.

Coosemans, A.N., Baert, T., D'Heygere, V., Wouters, R., L, D.E.L., A, V.A.N.H., Thirion, G., Ceusters, J., Laenen, A., Vandecaveye, V., et al. (2019). Increased Immunosuppression Is Related

to Increased Amounts of Ascites and Inferior Prognosis in Ovarian Cancer. Anticancer Res *39*, 5953-5962.

Corbet, C., Pinto, A., Martherus, R., Santiago de Jesus, J.P., Polet, F., and Feron, O. (2016). Acidosis Drives the Reprogramming of Fatty Acid Metabolism in Cancer Cells through Changes in Mitochondrial and Histone Acetylation. Cell Metab *24*, 311-323.

Denman, C.J., Senyukov, V.V., Somanchi, S.S., Phatarpekar, P.V., Kopp, L.M., Johnson, J.L., Singh, H., Hurton, L., Maiti, S.N., Huls, M.H., et al. (2012). Membrane-bound IL-21 promotes sustained ex vivo proliferation of human natural killer cells. PLoS One *7*, e30264.

Dixon, S.J., Lemberg, K.M., Lamprecht, M.R., Skouta, R., Zaitsev, E.M., Gleason, C.E., Patel, D.N., Bauer, A.J., Cantley, A.M., Yang, W.S., et al. (2012). Ferroptosis: an iron-dependent form of nonapoptotic cell death. Cell *149*, 1060-1072.

Donnelly, R.P., Loftus, R.M., Keating, S.E., Liou, K.T., Biron, C.A., Gardiner, C.M., and Finlay, D.K. (2014). mTORC1-dependent metabolic reprogramming is a prerequisite for NK cell effector function. J Immunol *193*, 4477-4484.

Donskov, F., and von der Maase, H. (2006). Impact of immune parameters on long-term survival in metastatic renal cell carcinoma. J Clin Oncol *24*, 1997-2005.

Fan, J., Ye, J., Kamphorst, J.J., Shlomi, T., Thompson, C.B., and Rabinowitz, J.D. (2014). Quantitative flux analysis reveals folate-dependent NADPH production. Nature *510*, 298-302.

Geller, M.A., Cooley, S., Judson, P.L., Ghebre, R., Carson, L.F., Argenta, P.A., Jonson, A.L., Panoskaltsis-Mortari, A., Curtsinger, J., McKenna, D., et al. (2011). A phase II study of allogeneic natural killer cell therapy to treat patients with recurrent ovarian and breast cancer. Cytotherapy *13*, 98-107.

Herberman, R.B., Nunn, M.E., Holden, H.T., and Lavrin, D.H. (1975). Natural cytotoxic reactivity of mouse lymphoid cells against syngeneic and allogeneic tumors. II. Characterization of effector cells. Int J Cancer *16*, 230-239.

Ishigami, S., Natsugoe, S., Tokuda, K., Nakajo, A., Che, X., Iwashige, H., Aridome, K., Hokita, S., and Aikou, T. (2000). Prognostic value of intratumoral natural killer cells in gastric carcinoma. Cancer *88*, 577-583.

Jüngst, D., Gerbes, A.L., Martin, R., and Paumgartner, G. (1986). Value of ascitic lipids in the differentiation between cirrhotic and malignant ascites. Hepatology *6*, 239-243.

Keating, S.E., Zaiatz-Bittencourt, V., Loftus, R.M., Keane, C., Brennan, K., Finlay, D.K., and Gardiner, C.M. (2016). Metabolic Reprogramming Supports IFN-γ Production by CD56bright NK Cells. J Immunol *196*, 2552-2560.

Keppel, M.P., Saucier, N., Mah, A.Y., Vogel, T.P., and Cooper, M.A. (2015). Activation-specific metabolic requirements for NK cell IFN-g production. J Immunol *194*, 1954-1962.

Kiessling, R., Klein, E., Pross, H., and Wigzell, H. (1975). "Natural" killer cells in the mouse. II. Cytotoxic cells with specificity for mouse Moloney leukemia cells. Characteristics of the killer cell. Eur J Immunol *5*, 117-121.

Kolde, R. (2018). pheatmap: Pretty Heatmaps. In R package.

Krneta, T., Gillgrass, A., Chew, M., and Ashkar, A.A. (2016). The breast tumor microenvironment alters the phenotype and function of natural killer cells. Cell Mol Immunol *13*, 628-639.

Kuleshov, M.V., Jones, M.R., Rouillard, A.D., Fernandez, N.F., Duan, Q., Wang, Z., Koplev, S., Jenkins, S.L., Jagodnik, K.M., Lachmann, A., et al. (2016). Enrichr: a comprehensive gene set enrichment analysis web server 2016 update. Nucleic Acids Res *44*, W90-97.

Leone, R.D., Zhao, L., Englert, J.M., Sun, I.M., Oh, M.H., Sun, I.H., Arwood, M.L., Bettencourt, I.A., Patel, C.H., Wen, J., et al. (2019). Glutamine blockade induces divergent metabolic programs to overcome tumor immune evasion. Science *366*, 1013-1021.

Liu, E., Marin, D., Banerjee, P., Macapinlac, H.A., Thompson, P., Basar, R., Nassif Kerbauy, L., Overman, B., Thall, P., Kaplan, M., et al. (2020). Use of CAR-Transduced Natural Killer Cells in CD19-Positive Lymphoid Tumors. The New England journal of medicine *382*, 545-553.

Liu, Y., Cheng, Y., Xu, Y., Wang, Z., Du, X., Li, C., Peng, J., Gao, L., Liang, X., and Ma, C. (2017). Increased expression of programmed cell death protein 1 on NK cells inhibits NK-cell-mediated anti-tumor function and indicates poor prognosis in digestive cancers. Oncogene *36*, 6143-6153.

Loftus, R.M., Assmann, N., Kedia-Mehta, N., O'Brien, K.L., Garcia, A., Gillespie, C., Hukelmann, J.L., Oefner, P.J., Lamond, A.I., Gardiner, C.M., et al. (2018). Amino acid-dependent cMyc expression is essential for NK cell metabolic and functional responses in mice. Nat Commun *9*, 2341.

Maddocks, O.D., Berkers, C.R., Mason, S.M., Zheng, L., Blyth, K., Gottlieb, E., and Vousden, K.H. (2013). Serine starvation induces stress and p53-dependent metabolic remodelling in cancer cells. Nature *493*, 542-546.

Marcais, A., Cherfils-Vicini, J., Viant, C., Degouve, S., Viel, S., Fenis, A., Rabilloud, J., Mayol, K., Tavares, A., Bienvenu, J., et al. (2014). The metabolic checkpoint kinase mTOR is essential for interleukin-15 signaling during NK cell development and activation. Nat Immunol *15*, 749-757.

Michelet, X., Dyck, L., Hogan, A., Loftus, R.M., Duquette, D., Wei, K., Beyaz, S., Tavakkoli, A., Foley, C., Donnelly, R., et al. (2018). Metabolic reprogramming of natural killer cells in obesity limits antitumor responses. Nat Immunol *19*, 1330-1340.

Mockler, M.B., Conroy, M.J., and Lysaght, J. (2014). TargetingT cell immunometabolism for cancer immunotherapy; understanding the impact of the tumor microenvironment. Front Oncol *4*, 107.

Morgan, R.A., Chinnasamy, N., Abate-Daga, D., Gros, A., Robbins, P.F., Zheng, Z., Dudley, M.E., Feldman, S.A., Yang, J.C., Sherry, R.M., et al. (2013). Cancer regression and neurological toxicity following anti-MAGE-A3 TCR gene therapy. Journal of immunotherapy (Hagerstown, Md. : 1997) *36*, 133-151.

Morgan, R.A., Yang, J.C., Kitano, M., Dudley, M.E., Laurencot, C.M., and Rosenberg, S.A. (2010). Case report of a serious adverse event following the administration of T cells transduced with a chimeric antigen receptor recognizing ERBB2. Mol Ther *18*, 843-851.

Morvan, M.G., and Lanier, L.L. (2016). NK cells and cancer: you can teach innate cells new tricks. Nat Rev Cancer *16*, 7-19.

Pan, M., Reid, M.A., Lowman, X.H., Kulkarni, R.P., Tran, T.Q., Liu, X., Yang, Y., Hernandez-Davies, J.E., Rosales, K.K., Li, H., et al. (2016). Regional glutamine deficiency in tumours promotes dedifferentiation through inhibition of histone demethylation. Nature cell biology *18*, 1090-1101.

Parkhurst, M.R., Riley, J.P., Dudley, M.E., and Rosenberg, S.A. (2011). Adoptive transfer of autologous natural killer cells leads to high levels of circulating natural killer cells but does not mediate tumor regression. Clin. Cancer Res. *17*, 6287-6297.

Polak, M., and Torres da Costa, A.C. (1973). Diagnostic value of the estimation of glucose in ascitic fluid. Digestion *8*, 347-352.

Poli, V., and Camporeale, A. (2015). STAT3-Mediated Metabolic Reprograming in Cellular Transformation and Implications for Drug Resistance. Front Oncol *5*, 121.

Poznanski, S.M., and Ashkar, A.A. (2019). What Defines NK Cell Functional Fate: Phenotype or Metabolism? Front Immunol *10*, 1414.

Poznanski, S.M., Nham, T., Chew, M.V., Lee, A.J., Hammill, J.A., Fan, I.Y., Butcher, M., Bramson, J.L., Lee, D.A., Hirte, H., et al. (2018). Expanded CD56superbrightCD16+ NK cells from ovarian cancer patients are cytotoxic against autologous tumor in a patient-derived xenograft murine model. Cancer Immunol Res *6*, 1174-1185.

Poznanski, S.M., Ritchie, T.R., Fan, I.Y., El-Sayes, A., Portillo, A.L., Ben-Avi, R.A., Chew, M.V., Shargall, Y., and Ashkar, A.A. (2020). Expanded human NK cells from lung cancer patients sensitize patients' PDL1-negative tumours to PD1-blockade therapy. Journal for immunotherapy of cancer *9*, e001933.

Probst, B.L., Trevino, I., McCauley, L., Bumeister, R., Dulubova, I., Wigley, W.C., and Ferguson, D.A. (2015). RTA 408, A Novel Synthetic Triterpenoid with Broad Anticancer and Anti-Inflammatory Activity. PLoS One *10*, e0122942.

Reina-Campos, M., Moscat, J., and Diaz-Meco, M. (2017). Metabolism shapes the tumor microenvironment. Current opinion in cell biology *48*, 47-53.

Romee, R., Rosario, M., Berrien-Elliott, M.M., Wagner, J.A., Jewell, B.A., Schappe, T., Leong, J.W., Abdel-Latif, S., Scheider, S.E., Willey, S., et al. (2016). Cytokine-induced memory-like natural killer cells exhibit enhanced responses against myeloid leukemia. Sci Transl Med *8*, 357ra123.

Santomasso, B.D., Park, J.H., Salloum, D., Riviere, I., Flynn, J., Mead, E., Halton, E., Wang, X., Senechal, B., Purdon, T., et al. (2018). Clinical and Biological Correlates of Neurotoxicity Associated with CAR T-cell Therapy in Patients with B-cell Acute Lymphoblastic Leukemia. Cancer discovery *8*, 958-971.

Scharping, N.E., Menk, A.V., Moreci, R.S., Whetstone, R.D., Dadey, R.E., Watkins, S.C., Ferris, R.L., and Delgoffe, G.M. (2016). The Tumor Microenvironment Represses T Cell Mitochondrial Biogenesis to Drive Intratumoral T Cell Metabolic Insufficiency and Dysfunction. Immunity *45*, 374-388.

Schreiber, R.D., Old, L.J., and Smyth, M.J. (2011). Cancer immunoediting: integrating immunity's roles in cancer suppression and promotion. Science *331*, 1565-1570.

Shender, V.O., Pavlyukov, M.S., Ziganshin, R.H., Arapidi, G.P., Kovalchuk, S.I., Anikanov, N.A., Altukhov, I.A., Alexeev, D.G., Butenko, I.O., Shavarda, A.L., et al. (2014). Proteome-metabolome profiling of ovarian cancer ascites reveals novel components involved in intercellular communication. Mol Cell Proteomics *13*, 3558-3571.

Siska, P.J., Beckermann, K.E., Mason, F.M., Andrejeva, G., Greenplate, A.R., Sendor, A.B., Chiang, Y.J., Corona, A.L., Gemta, L.F., Vincent, B.G., et al. (2017). Mitochondrial dysregulation and glycolytic insufficiency functionally impair CD8 T cells infiltrating human renal cell carcinoma. JCI insight *2*.

Tedeschi, P.M., Markert, E.K., Gounder, M., Lin, H., Dvorzhinski, D., Dolfi, S.C., Chan, L.L., Qiu, J., DiPaola, R.S., Hirshfield, K.M., et al. (2013). Contribution of serine, folate and glycine metabolism to the ATP, NADPH and purine requirements of cancer cells. Cell death & disease *4*, e877.

Thistlethwaite, F.C., Gilham, D.E., Guest, R.D., Rothwell, D.G., Pillai, M., Burt, D.J., Byatte, A.J., Kirillova, N., Valle, J.W., Sharma, S.K., et al. (2017). The clinical efficacy of first-generation carcinoembryonic antigen (CEACAM5)-specific CAR T cells is limited by poor persistence and transient pre-conditioning-dependent respiratory toxicity. Cancer Immunol Immunother *66*, 1425-1436.

van Bruggen, J.A.C., Martens, A.W.J., Fraietta, J.A., Hofland, T., Tonino, S.H., Eldering, E., Levin, M.D., Siska, P.J., Endstra, S., Rathmell, J.C., et al. (2019). Chronic lymphocytic leukemia cells impair mitochondrial fitness in CD8(+) T cells and impede CAR T-cell efficacy. Blood *134*, 44-58.

Venugopal, R., and Jaiswal, A.K. (1998). Nrf2 and Nrf1 in association with Jun proteins regulate antioxidant response element-mediated expression and coordinated induction of genes encoding detoxifying enzymes. Oncogene *17*, 3145-3156.

Vodnala, S.K., Eil, R., Kishton, R.J., Sukumar, M., Yamamoto, T.N., Ha, N.H., Lee, P.H., Shin, M., Patel, S.J., Yu, Z., et al. (2019). T cell stemness and dysfunction in tumors are triggered by a common mechanism. Science *363*.

Wang, X., Lee, D.A., Wang, Y., Wang, L., Yao, Y., Lin, Z., Cheng, J., and Zhu, S. (2013). Membrane-bound interleukin-21 and CD137 ligand induce functional human natural killer cells from peripheral blood mononuclear cells through STAT-3 activation. Clinical and experimental immunology *172*, 104-112.

Warburg, O. (1925). The Metabolism of Carcinoma Cells. The Journal of Cancer Research *9*, 148-163.

Warburg, O., Wind, F., and Negelein, E. (1927). THE METABOLISM OF TUMORS IN THE BODY. The Journal of General Physiology *8*, 519-530.

Wei, M., Yang, T., Chen, X., Wu, Y., Deng, X., He, W., Yang, J., and Wang, Z. (2017). Malignant ascites-derived exosomes promote proliferation and induce carcinoma-associated fibroblasts transition in peritoneal mesothelial cells. Oncotarget *8*, 42262-42271.

Wickham, H. (2016). ggplot2: Elegant Graphics for Data Analysis. (Springer-Verlag New York).

Ye, J., Fan, J., Venneti, S., Wan, Y.W., Pawel, B.R., Zhang, J., Finley, L.W., Lu, C., Lindsten, T., Cross, J.R., et al. (2014). Serine catabolism regulates mitochondrial redox control during hypoxia. Cancer discovery *4*, 1406-1417.

Zaiatz-Bittencourt, V., Finlay, D.K., and Gardiner, C.M. (2018). Canonical TGF-beta signaling pathway represses human NK cell metabolism. J Immunol *200*, 3934-3941.

Zaugg, K., Yao, Y., Reilly, P.T., Kannan, K., Kiarash, R., Mason, J., Huang, P., Sawyer, S.K., Fuerth, B., Faubert, B., et al. (2011). Carnitine palmitoyltransferase 1C promotes cell survival and tumor growth under conditions of metabolic stress. Genes & development *25*, 1041-1051.

Zhou, X., Curbo, S., Li, F., Krishnan, S., and Karlsson, A. (2018). Inhibition of glutamate oxaloacetate transaminase 1 in cancer cell lines results in altered metabolism with increased dependency of glucose. BMC cancer *18*, 559.

– CHAPTER 5 –

DISTINCT METABOLIC PROGRAMS UNDERPIN REGULATORY AND CYTOTOXIC NK CELLS

Distinct metabolic programs underpin regulatory and cytotoxic NK cells

Sophie M. Poznanski[1], Tyrah M. Ritchie[1], Nooran Abu Mazen[2], Jianhong Zhang[3], Fatemeh Vahedi[1], Ana L. Portillo[1], Kanwaldeep Singh,[4] Lauren Chan[1], Eduardo A. Rojas, [1] Stephen J. Lye,[4,5] Andrew C. Doxey[2], Ali A. Ashkar[1*]

[1]Department of Medicine, McMaster Immunology Research Centre, McMaster University, Hamilton, ON, L8N 3Z5, Canada

[2]Department of Biology, University of Waterloo, Waterloo, ON, N2L 3G1, Canada

[3]Lunenfeld Tanenbaum Research Institute, Mount Sinai Hospital, Toronto, Canada

[4]Department of Oncology, McMaster University, Hamilton, ON, L8V 5C2, Canada

[5]Departments of Physiology and Obstetrics & Gynecology, University of Toronto, Ontario, Canada

[*]Corresponding author: Ali A. Ashkar, McMaster University, 1280 Main Street West, MDCL 4015, Hamilton, Ontario, Canada. Email address: ashkara@mcmaster.ca

Preface: *The research presented in this manuscript was conducted between 2018-2023. SMP and AAA conceived and designed the project. SMP, TMR, and AAA designed the experiments. SMP, TMR, and JZ performed experiments. ALP, FV, KS, LC, and EAR assisted with experiments. JZ and SJL acquired clinical samples. SMP, TMR, NAM, and ACD curated and formally analyzed the data. SMP wrote the manuscript. AAA edited the manuscript, secured funding, and supervised the project.*

5.1 ABSTRACT

Regulatory NK cells are vital for immune tolerance and tissue remodeling but present a significant barrier to anti-cancer immunity, as the TME induces their polarization and function. A substantial body of work has shown that glucose-driven metabolic programs are fundamental for cytotoxic NK cell anti-tumour functions. The profound metabolic demands of tumours produce a metabolically hostile TME that is low in glucose, hypoxic, and rich in metabolic waste products such as lactic acid. This environment is directly prohibitive to the metabolic requirements for cytotoxic NK cell immunity. However, the metabolic programs that are fundamental to regulatory NK cell polarization and function remain poorly understood. Given that the TME promotes NKreg activity, we hypothesized that regulatory NK cells utilise distinct metabolic programs that are supported by the TME and in direct opposition to those of cytotoxic NK cells. Here, we report that both natural regulatory NK cells and *in vitro*-polarized regulatory NK cells that have tumour-promoting functions have low levels of glucose metabolism. In addition, regulatory NK cells upregulated pathways involved in lactate and serine metabolism. These findings identify that distinct metabolic programs underpin cytotoxic and regulatory NK cell subsets. Further, our results suggest that regulatory NK cells use alternative metabolic fuels that are abundant in the TME and provide a metabolic basis for why regulatory NK cells thrive in the TME and other similar environments. This study suggests that therapeutically tuning NK cell metabolism could, at the same time, unleash NK cell anti-tumour immunity while suppressing NK cell tumour-promoting functions in the TME.

5.2 INTRODUCTION

While NK cells are classically known as critical effectors in anti-tumour immune defenses, in tumours with particularly immunosuppressive environments, such as ovarian, lung, and breast cancers, presence of NK cells can also be associated with advanced disease and poor prognosis (Chang et al., 2021; Dong et al., 2006; Melichar et al., 2001; Vgenopoulou et al., 2003). A number of reports have shown that tumour-associated (ta)NK cells – in addition to having suppressed antitumour functions including cytotoxicity and IFNγ cytokine production – have regulatory, tumour promoting abilities, including the production of pro-angiogenic factors such as VEGF and Treg-recruiting cytokines (Bosi et al., 2018; Bruno et al., 2018; Bruno et al., 2013; Guan et al., 2020; Levi et al., 2015). Notably, these regulatory taNK cells phenotypically and functionally resemble uterine (u)NK cells - perhaps the most studied subset of regulatory NK cells (NKreg) - that secrete of high levels of angiogenic and immunoregulatory factors (Albini and Noonan, 2021). While uNK cells are vital for proper trophoblast invasion and spiral artery remodeling in pregnancy, they also significantly enhance growth of transplanted tumours (Gamliel et al., 2018; Hanna et al., 2006). Increased levels of NKregs in tumours was shown to be associated with worse prognosis in ovarian cancer patients and these NKregs directly inhibited cytotoxic T cell proliferation and function (Crome et al., 2017). NKreg cells likely present a major barrier for anti-cancer immunity as the tumour microenvironment (TME) directly induces the function of these cells while suppressing cytotoxic NK (NKctx) cells. Despite the important role of NKregs in many physiological processes and likely consequences in cancer progression, little is known about what regulates NKreg functions.

A number of reports have recently emerged demonstrating the critical role of metabolism in NKctx functions. Indeed, NK cell direct tumour cytotoxicity and production of the antitumour

cytokine IFNγ require an up-regulation of glucose-driven oxidative phosphorylation (OxPhos) that is facilitated by mitochondrial biogenesis and fusion (Assmann et al., 2017; Donnelly et al., 2014; Loftus et al., 2018). Notably, a hallmark feature of tumour progression is the accumulation of metabolic stress, including hypoxia, nutrient depletion, and acidification in the tumour microenvironment (TME) caused by rapidly proliferating tumour cells (Hanahan and Weinberg, 2011). Metabolic stress and competition with tumour cells plays a key role in tumour immune evasion of cytotoxic T cells and NK cells (Brand et al., 2016; Chang et al., 2015; Poznanski et al., 2021; Zheng et al., 2019). Elevated lactic acid levels like those seen in the TME directly impair NK cell production of ATP and IFNγ (Brand et al., 2016). Hypoxia and consequent mitochondrial fragmentation have also been shown to suppress the functions of NKctx cells (Zheng et al., 2019). Furthermore, selective deletion of HIF1α in murine NK cells reduced tumour growth and increased NK cell degranulation, expression of IFNγ, and granzyme B in the presence of hypoxia (Ni et al., 2020). We recently reported that human taNK cells from ovarian and lung cancer patients have reduced glycolysis, OxPhos, and mitochondrial mass and that the human TME directly suppresses these metabolic pathways by causing lipid peroxidation-mediated oxidative stress (Poznanski et al., 2021). It is well known that in the context of other immune cells, such as T cells and macrophages, the engagement of distinct metabolic pathways regulates polarization to proinflammatory cytotoxic- versus anti-inflammatory regulatory- subsets (Gerriets et al., 2016; Jha et al.; Michalek et al., 2011; Rodriguez-Prados et al., 2010). Notably, the metabolic conditions of the TME, while hostile to NKctx functions are supportive of NKreg functions, suggesting that metabolic requirements for these subsets are in direct opposition. However, while the metabolic pathways that support NKctx functions have been defined, how metabolism influences NKreg functions has not been elucidated.

In this study, we aimed to determine the metabolic fingerprint of NKreg cells. We found that both *in vitro*-polarized NKregs and uNK cells have reduced glycolysis and OxPhos compared to NKctx cells. Further, we found that a metabolic gene signature of increased ketone, serine, and one-carbon metabolism distinguish NKreg from NKctx cells.

5.3 RESULTS

To begin to investigate the metabolic profile of NKreg cells, we utilised regulatory uNK cells isolated from the uterine tissues of terminated pregnancies, since uNK cells are known to have strong regulatory capabilities. We first confirmed the regulatory functions of these uNK cells compared to pbNK cells using an *in vivo* tumour burden model. We co-administered luciferase-expressing OVCAR8 cells (OVCAR-Luc) with isolated pbNK cells, uNK cells, or no NK cells (control) intraperitoneal (i.p.) injection to NRG mice and measured tumour burden 5 days later. While cytotoxic pbNK cells reduced tumour burden compared to control mice, mice treated with uNK cells had exponentially larger tumours than both pbNK-treated and control mice, confirming their strong regulatory tumour-promoting activity (Figure 1A). Since NKctx cells are known to rely on glucose-driven glycolysis and OxPhos for their functions, we next compared rates of glycolysis and OxPhos in pbNK and uNK cells using extracellular flux assays. uNK cells had significantly reduced basal glycolysis and glycolytic capacity, measured by the extracellular acidification rate (ECAR) compared to cytotoxic pbNK cells (Figure 1B). Furthermore, uNK cells had broadly reduced rates of OxPhos measured by cellular oxygen consumption rate (OCR), including lower basal and maximal respiration, spare respiratory capacity (SRC), and respiration-linked ATP, compared to pbNK cells (Figure 1C). Notably, the metabolic profile of reduced

glycolysis and OxPhos in uNK cells is similar to what we previously reported in cancer patient taNK cells and in pbNK cells exposed to the human TME (Poznanski et al., 2021).

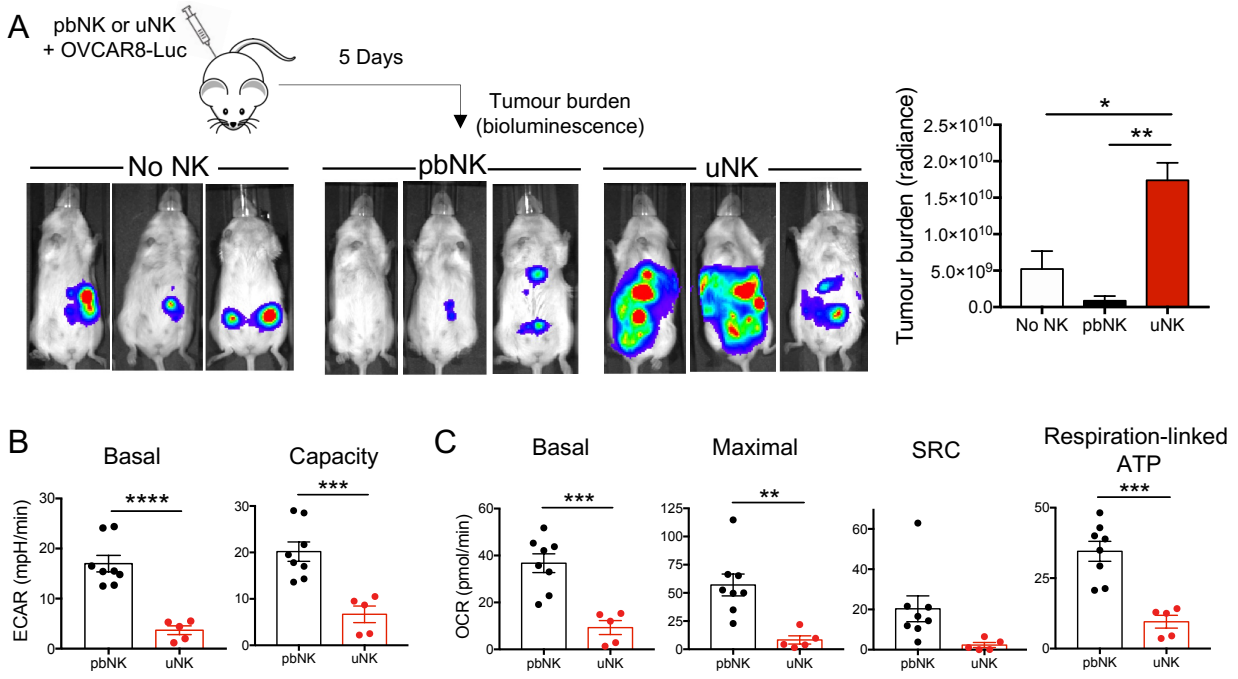

Figure 1. Regulatory uNK cells have reduced glycolysis and OxPhos compared to pbNK cells. (A) Freshly isolated pbNK or uNK cells or vehicle (no NK) were co-administered i.p. to NRG mice with OVCAR8-Luc tumour cells at Day 0. Representative images and quantification of tumour burden via bioluminescence at Day 5. (B) Basal and maximal glycolysis of freshly isolated pbNK and uNK cells. (C) Basal OxPhos, maximal OxPhos, spare respiratory capacity (SRC), and respiration-linked ATP of pbNK and uNK cells. Results show means ± SEM of 3-8 biological replicates. A, analyzed via one-way ANOVA. B and C, analyzed via unpaired t-test; *p<0.05, **p<0.01, ***p<0.001, ****p<0.0001.

Low glucose-driven metabolism broadly distinguishes NKreg from NKctx subsets

To confirm the universality of this metabolic profile for NKregs and omit the confounding factor of different tissue localization, we utilised a model of *in vitro*-polarized human NKctx vs. NKreg cells. We employed a method of polarization previously reported by Cerdeira *et al.*, in which culture of human pbNK cells with IL-15+TGFβ under hypoxic conditions for 7 days induced NK cell VEGF production while suppressing NK cell cytotoxicity.(Cerdeira et al., 2013) We cultured freshly isolated human peripheral blood (pb)NK cells with IL-15 alone (control) or IL-15+TGFβ (TGFβ) under 21% or 1% O_2 (hypoxia) conditions for 3 and 7 days (Figure 2A). By day 3, NK cell cytotoxicity was significantly suppressed in hypoxia+TGFβ, but not hypoxia alone, compared to control (Figure 2B). NK cell IFNγ was significantly reduced by either TGFβ or hypoxia but the greatest suppression was with the combination of both (Figure 2C). In contrast, hypoxia was sufficient to induce VEGF production, irrespective of the presence of TGFβ (Figure 2D). Similar results were observed at day 7 (data not shown). These findings demonstrate that polarization to NKregs occurs by day 3 and requires both hypoxia and TGFβ: hypoxia for the induction of VEGF, and TGFβ for maximal suppression of NK cell cytotoxicity.

We next assessed how this polarization affected NK cell phenotype. Both human and mouse NK cell subsets can be defined by the expression CD11b and CD27. Cytotoxic NK cells are CD11b+CD27- (CD11b single positive), whereas regulatory and tolerant NK cells can be either CD11b+CD27+ (double positive), CD27 single positive, or double negative.(Fu et al., 2014; Fu et al., 2011) NK cells cultured in hypoxia+TGFβ compared to controls had a significantly reduced proportion of the NKctx CD11b single positive subset along with a significantly increased proportion of NKreg CD11b/CD27 subsets, aligning with their functions (Figure 2E). Thus, hypoxia+TGFβ polarizes NK cells to an NKreg subset.

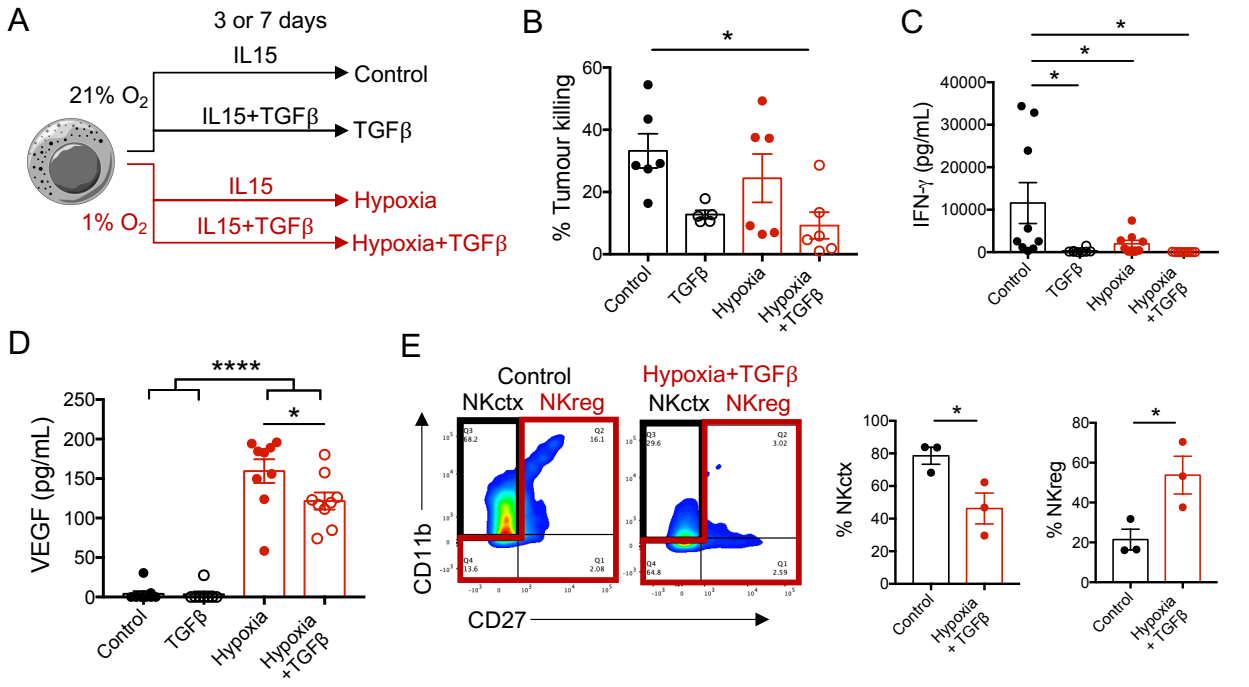

Figure 2. *In vitro*-polarization of NK cells to NKctx and NKreg subsets. Freshly isolated pbNK cells were polarized *in vitro* for 3 or 7 days under 21% O_2 with IL-15 alone (control) or IL-15+TGFβ (TGFβ) or under 1% O_2 with IL-15 alone (hypoxia) or IL-15+TGFβ (hypoxia+TGFβ). (A) Schematic of experimental design and conditions. (B) NK cell cytotoxicity against OVCAR-8 cells at day 3. (C) IFNγ and (D) VEGF cytokine levels in the supernatants of NK cells at day 3 measured via ELISA. (E) Representative flow plots and proportion of NK cells with a cytotoxic (CD11b+CD27-) or regulatory (CD27+ or CD11b-CD27-) phenotype in control vs. hypoxia+TGFβ conditions. Results show means ± SEM of 3-6 biological replicates. B-D analyzed via one-way ANOVA; E analyzed via unpaired t-test; *p<0.05, ****p<0.0001.

Next, we looked to further characterize the functional profile of *in vitro*-polarized NKreg cells (hypoxia+TGFβ) compared to NKctx cells (control) (Figure 3A). We conducted a broad cytokine array of 71 human cytokines/chemokines and found that NKregs produced greater levels of tumour-promoting cytokines including the angiogenic factor VEGF, platelet-derived growth factor (PDGF), RANTES, IL-20, and the Treg-recruiting cytokine TARC, all of which have been shown to be directly involved in tumour promotion and associated with poor prognosis in a variety of cancers (Figure 3B) (Heldin et al., 2018; Huang et al., 2020; Lu et al., 2020; Lv et al., 2013; Maeda et al., 2022; Olkhanud et al., 2009; Shikada et al., 2005; Sulzbacher et al., 2003; Thomas et al., 2019). In contrast, NKregs produced significantly lower levels of a number of proinflammatory anti-tumour cytokines compared to NKctx (Figure 3C). To look at direct effects on tumour cell growth, we cultured OVCAR8 ovarian cancer cells for 24 hours in the 3-day supernatants of NKctx or NKreg cells. The supernatants of NKregs substantially enhanced growth of the tumour cell culture compared to those of NKctx, demonstrating the hallmark capacity of NKreg cells to directly promote tumour progression (Figure 3D).

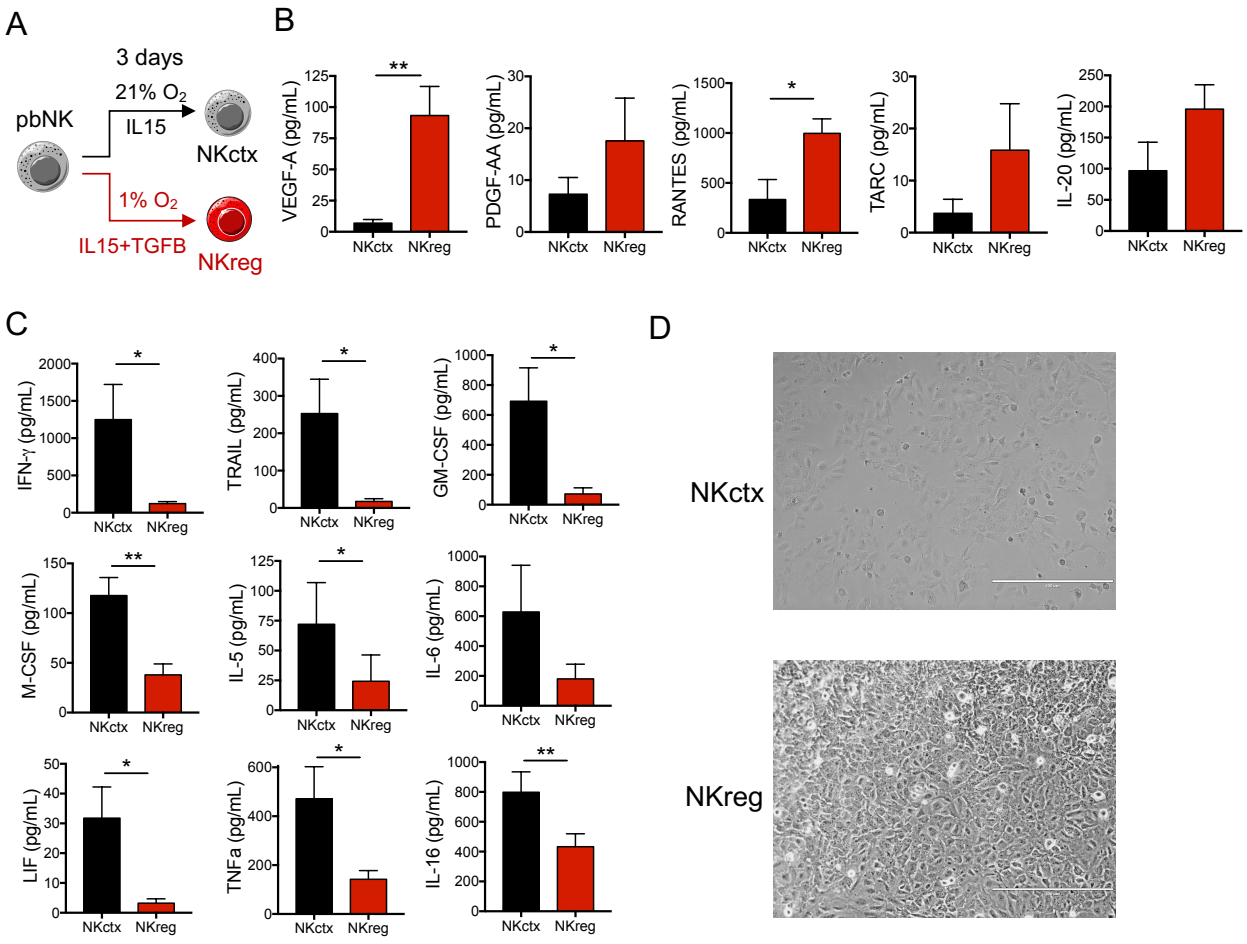

Figure 3. Cytokine profiles and effects on tumour growth of polarized NKctx vs. NKreg. Freshly isolated human pbNK cells were *in vitro*-polarized for 3 days to NKctx with IL-15 in 21% O_2 or to NKreg with IL-15+TGFβ in 1% O_2. (A) Schematic of polarization. Supernatants were collected at day 3 and used to quantify cytokine levels via multiplex cytokine array. (B) Cytokines elevated in NKreg vs. NKctx supernatants. (C) Cytokines elevated in NKctx vs. NKreg supernatants. (D) OVCAR-8 cells were incubated in 3-day supernatants of NKctx or NKreg cultures from 3 NK cell donors. Representative images of tumour cell cultures taken with an EVOS microscope after 24 hours. Results show means ± SEM of 3-6 biological replicates. B, C analyzed via two-tailed t-test; *p<0.05, **p<0.01.

We next assessed whether *in vitro*-polarized NKreg cells had an altered metabolism compared to NKctx cells. NKreg cells had significantly lower glycolytic capacity compared to NKctx (Figure 4A). Cell-surface staining further showed that NKregs expressed lower levels of the glucose transporter Glut1 compared to NKctx, suggesting a reduced capacity to take up glucose (Figure 4B). In addition, NKregs displayed lower rates of OxPhos, including reduced basal and maximal respiration and respiration-linked ATP (Figure 4C). In line with reduced mitochondrial activity, staining of NK cells with the mitochondrial-specific dye MitoTracker showed that NKreg had reduced mitochondrial mass compared to NKctx (Figure 4D). Consistent with this overall reduced bioenergetic capacity, NKregs were smaller in size compared to NKctx as measured by forward-scatter (FSC) via flow cytometry (Figure 4E). Furthermore, NKregs showed significantly lower levels of the cell-surface transferrin receptor CD71 and amino acid transporter CD98, both of which have been shown to play important roles in supporting the bioenergetics and function of NKctx cells (Figure 4, F and G). These results uncover that a metabolic profile of reduced glycolysis and OxPhos is a hallmark of NKregs and distinguished them from NKctx subsets.

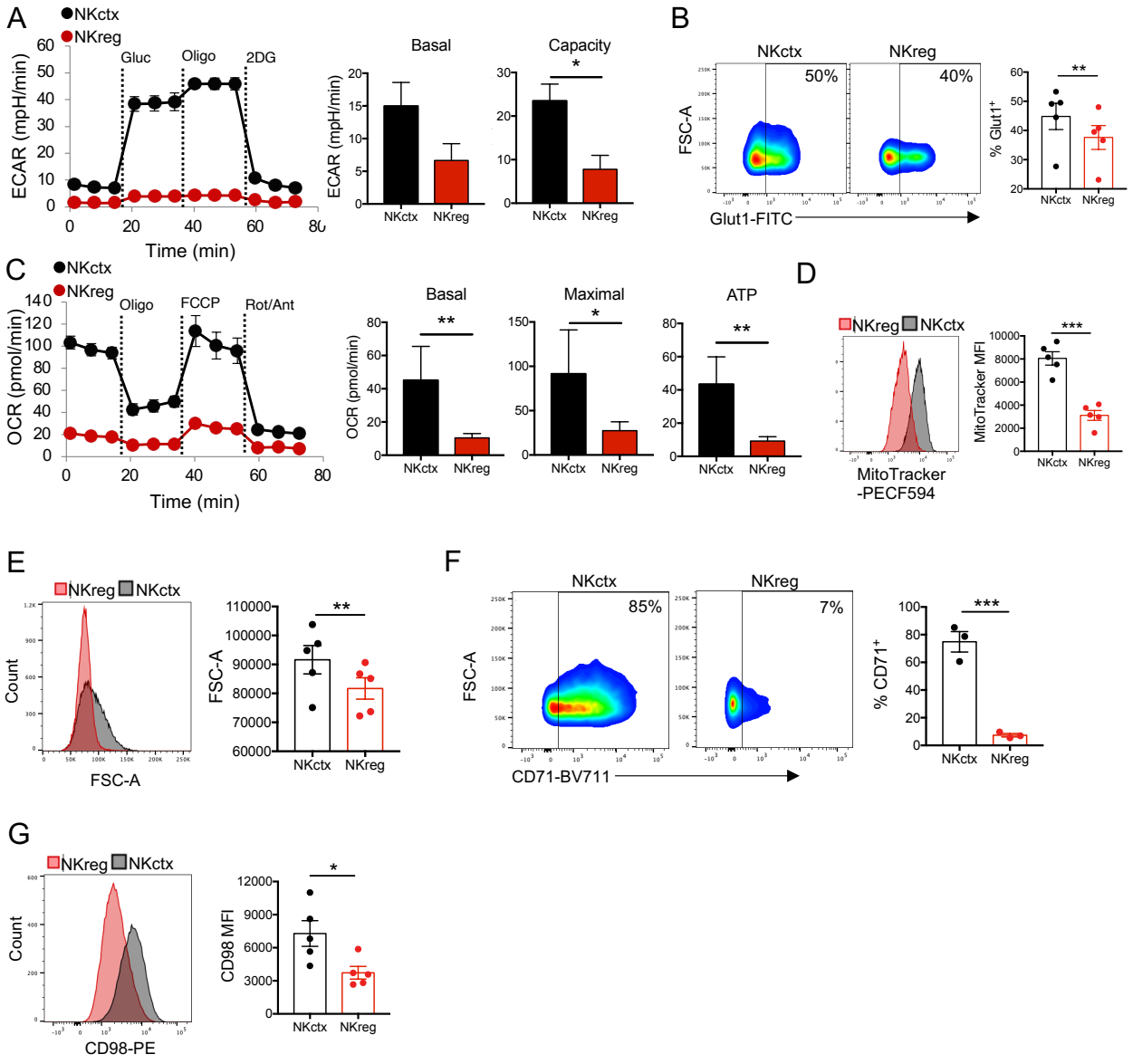

Figure 4. NKregs have reduced glycolysis and OxPhos compared to NKctx. Freshly isolated human pbNK cells were polarized *in vitro* for 3 days to NKctx or NKreg subsets. (A) Representative measures of NK cell extracellular acidification rate (ECAR) at baseline and upon addition of glucose (Gluc), oligomycin (Oligo), and 2-deoxy-D-glucose (2DG) and quantification of glycolytic capacity and reserve. (B) Representative flow plots and percent expression of Glut1 cell-surface staining. (C) Representative measures of NK cell oxygen consumption rate (OCR) at baseline and upon addition of Oligo, FCCP, and Rotenone+Antimycin (Rot/Ant) and

quantification of basal and maximal respiration and respiration-linked ATP. (D) Representative histograms and quantified mean fluorescence intensity (MFI) of NK cells stained with MitoTracker. (E) Representative histograms and quantification NK cell size measured by forward-scatter (FSC-A). (F) Representative flow plots and quantified percent expression of NK cell-surface CD71. (G) Representative histogram and quantified MFI of NK cell CD98 expression. Results show means ± SEM of 5-6 biological replicates. A-G analyzed via t-test; *$p<0.05$, **$p<0.01$, ***$p<0.001$.

NKregs are enriched in genes involved in lactate and serine metabolism

To gain better insight into the differences in metabolism between NKreg and NKctx subsets, we conducted RNAseq on *in vitro*-polarized NKreg vs. NKctx cells. Principal component analysis showed clear distinctions between NKreg (hypoxia+TGFβ) and NKctx (control) subsets (Figure 5A). Pheatmap analysis of NKreg vs. NKctx subsets showed two distinct clusters with a largely inversed gene expression profile (Figure 5B). Pathway analysis of significantly differentially expressed genes revealed that a number of metabolic pathways were altered between the two subsets (Figure 5C). Consistent with our data showing reduced glycolysis in NKreg cells, enzymes involved in the glycolysis pathway were broadly downregulated in NKreg cells compared to NKctx, with the exception of lactate dehydrogenase (LDH) B which was upregulated (Figure 5D). While both LDHA and LDHB can bidirectionally convert pyruvate and lactate, LDHA has a higher affinity for pyruvate and so favours its conversion to lactic acid, while LDHB has a higher affinity for lactate, thus favouring its conversion to pyruvate (Urbańska and Orzechowski, 2019). NKregs also had reduced gene expression of the glucose transporters GLUT1 and GLUT3, indicative of a reduced capacity to take up glucose (Figure 5D). However, NKregs were enriched

in genes involved in ketone metabolism, including the lactate transporter monocarboxylate transporter 1 (MCT1) (Figure 5E). Notably, tumour cells utilize lactate as a fuel by importing it via MCT1 and converting it to pyruvate via LDHB (Sonveaux et al., 2008). The increase in MCT1 and LDHB suggests that NKreg may utilize this mechanism of lactate metabolism in lieu of glucose to fuel energy and biosynthesis pathways. Other genes upregulated in ketone metabolism were OXCT1 and uncoupling protein 2 (UCP2). UCP2 is an anion carrier that limits glucose oxidation but enhances glutaminolysis (Vozza et al., 2014). Genes involved in the serine and one carbon metabolism pathway were also broadly enriched in NKreg cells (Figure 5F). Serine and one carbon metabolism pathways take part in the synthesis of purines and pyrimidines, and also the generation of NADH, ATP, and the antioxidant NADPH (Yang and Vousden, 2016). These results identify that serine metabolism may play an important role in NKreg ATP and NADH production in lieu of OxPhos and support redox balance. Notably, glutamine can provide cells with carbons for serine synthesis under conditions of metabolic stress through glutaminolysis (Yang and Vousden, 2016). Thus, these findings identify that NKreg cells are equipped with higher levels of metabolic machinery to support serine and one-carbon metabolism that may be driven by glutamine. Overall, these findings identify that low glycolysis and OxPhos coupled with increased lactate, serine, and one carbon metabolism pathways distinguish NKreg from NKctx cells.

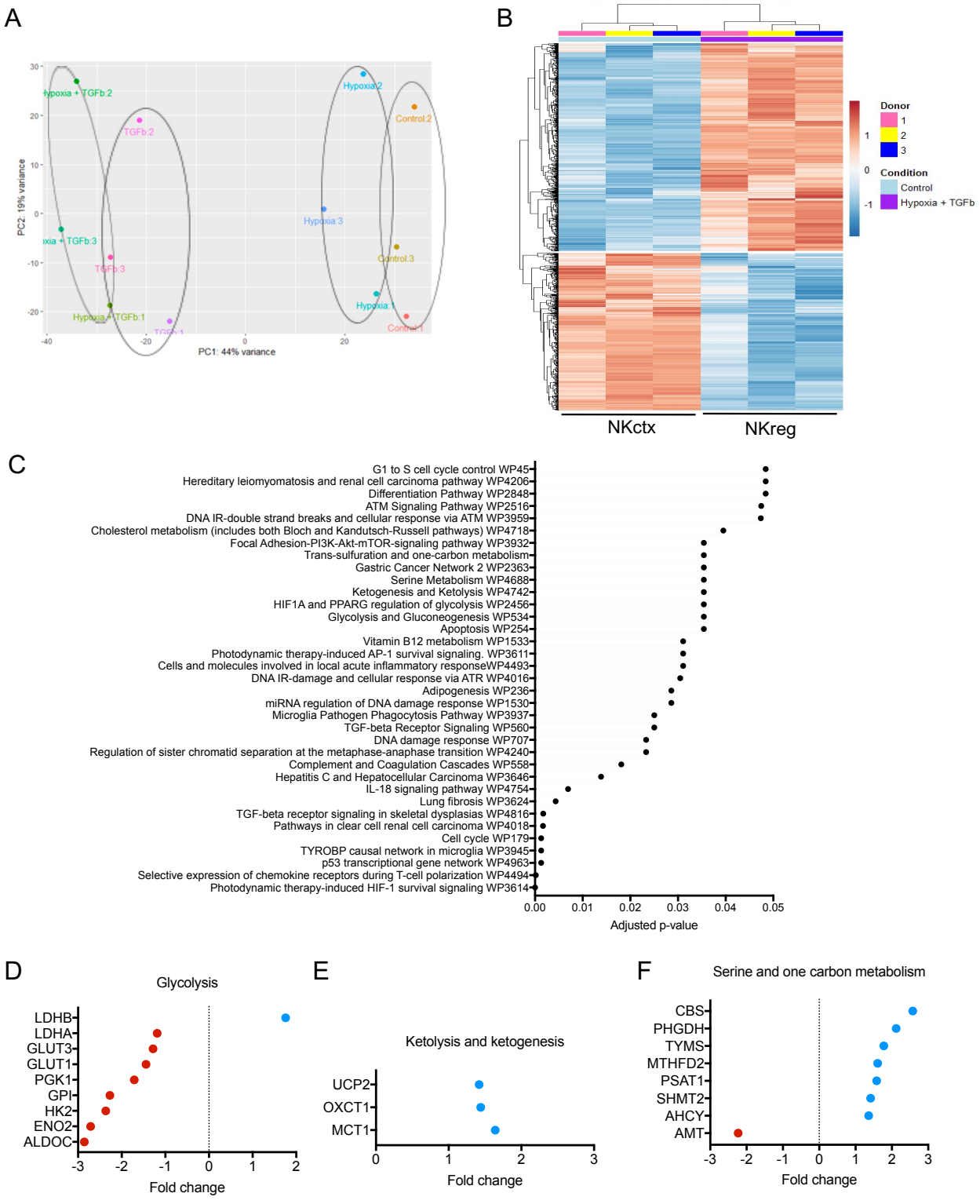

Figure 5. NKreg downregulate glucose metabolism and upregulate genes in ketone and serine metabolism. (A) Principal component analysis of differential gene expression between *in-vitro*-

polarized NKreg (hypoxia+TGFβ) and NKctx cells (control) as well as NK cells treated with hypoxia or TGFβ alone. (B) Pheatmap analysis and (C) pathway analysis via Wikipathways 2021 of significantly differentially expressed genes between NKreg and NKctx cells. Fold change of significantly differentially expressed genes involved in (D) glycolysis-, (E) ketone-, and (E) serine-metabolism pathways; red dots denote downregulated in NKreg; blue dots denote upregulated in NKreg. Results show 3 biological replicates.

5.4 DISCUSSION

It is increasingly evident that metabolic reprogramming plays a central role in NK cell functional fate. Metabolic mechanisms that regulate NKctx cell functions and the important role of these in cancer immunosurveillance and defense against viral infections have been well-documented (Assmann et al., 2017; Donnelly et al., 2014; Mah et al., 2017; Michelet et al., 2018; Poznanski et al., 2021). Despite the important role NKregs play in supporting a number of physiological and pathological contexts, including a healthy pregnancy and promoting tumour growth respectively, the metabolic mechanisms that underpin NKreg polarization remain poorly understood. Here, we define the metabolic programs that distinguish NKreg and NKctx subsets, wherein NKregs downregulate glucose-driven glycolysis and OxPhos and tandemly upregulate ketone, serine, and one carbon metabolism. These findings uncover that fundamental energetic differences underpin NK cell polarization and present metabolism as a promising tool to modulate NK cell polarization fate.

Notably, the metabolic profile of NKregs contains several adaptations that are beneficial for the TME. Unlike NKctx, the metabolic profile of NKregs suggests a reduced reliance on glucose, including low levels of glycolysis and OxPhos and lower expression of glucose

transporters. Glucose competition in the TME between tumour cells and immune cells has been found to be a critical mechanism of immunosuppression by the TME (Chang et al., 2015). The reduced reliance on glucose of NKregs that we report suggests that NKreg evade such competition with tumours by utilising other mechanisms, such as increased serine synthesis and one-carbon metabolism, to generate energy and biosynthetic products. Low levels of OxPhos in NKregs provides additional resilience in the face of a hypoxic TME and limits oxidative stress. Tumour cells also secrete high levels of lactic acid as a waste product of glycolysis, resulting in high levels of lactic acid in the TME (Brizel et al., 2001; Walenta et al., 2000). The increase in expression of proteins involved in taking up and utilising lactic acid as a nutrient rather than a waste product suggest that NKreg may capitalize on a lactic acid-rich environment. Overall, our findings support a model in which the TME is supportive of the metabolic requirements of NKreg cells whilst being prohibitive to those of NKctx.

Notably, many parallels exist between the metabolic conditions of the TME other environments where NKregs dominate. During early pregnancy, when uterine NKreg cells are at their peak function, trophoblast and other fetal cells are dividing rapidly and highly glycolytic, producing a hypoxic, low-glucose, and lactic acid-rich environment (Rodesch et al., 1992). The liver is another site enriched in NKregs involved in tissue remodeling and the suppression of T cell function. Liver tissue is poorly oxygenated due to its portal venous blood supply, with oxygen levels dipping as low as 1.3% in a healthy liver (Carreau et al., 2011; Corpechot et al., 2002; Kessler et al., 1976). Our findings suggest the metabolic programs of NKregs are fostered by these environments, which may explain why NKregs are abundant and highly functional at these sites. This also evokes the notion that perhaps tumours evolved to exploit similar conditions to maintain a tolerogenic environment.

In a recent study, we reported that highly cytotoxic expanded NK cells were metabolically adapted to thrive in the TME and exerted robust antitumour activity (Poznanski et al., 2021). Interestingly, these expanded NK cells shared some metabolic similarities to the NKregs in this study, including upregulated levels of the serine and one carbon metabolism pathway compared to unexpanded pbNK cells. Such adaptations enabled expanded NK cells to paradoxically upregulate their cytotoxicity in the TME compared to in nutrient-rich conditions. However, these expanded NK cells differed from NKregs in that they also upregulated high rates of glucose-driven glycolysis. Together, these studies point to glucose metabolism as a key regulator of NK cell polarization fate.

Certainly, the direct effects of metabolic pathways on NKreg functions remain to be determined. Since NKregs have a metabolic profile indicative of low glucose use, the main fuel(s) that drive their functions need to be identified. Intratumoural Treg cells have been found to take up lactic acid, which stabilized their regulatory functions in part by enhancing TGFβ signaling (Gu et al., 2022; Watson et al., 2021). Tregs were also found to convert lactate to phosphoenolpyruvate (via malate) which can in turn contribute to upstream glycolytic intermediates, decreasing the cellular need for glucose (Watson et al., 2021). Our results suggest that lactate is likely important for NKregs, but how NKregs use lactate will need to be confirmed with metabolic tracer studies. Hypoxia has previously been shown to induce mitochondrial fission and fragmentation in NK cells (Zheng et al., 2019). Our data showing reduced mitochondrial mass and upregulation of mitochondrial fission proteins in NKregs support these prior findings and point to a role for mitochondrial remodeling in NK cell polarization.

Overall, our study supports a paradigm in which the metabolic profile of NK cells defines and drives NK cell functional fates. Our study provides a metabolic basis for why NKreg and

NKctx immunity occur in opposition, as they have discordant metabolic programs. This likely means that NKreg use alternative fuels that are prevalent in tissue microenvironments in which NKctx nutrients, particularly glucose, are limited. In the TME, this presents the opportunity that modulating NK cell metabolism may harbour a double-punch for immunotherapy, wherein it interferes with the tumour-promoting functions of NKreg cells while augmenting the functions of NKctx cells.

5.5 METHODS

Ethics

All research involving human samples was approved by the Hamilton Integrated Research Ethics Board in Hamilton, Ontario. All human samples were collected with written informed consent from donors. All research using mice was approved by the Animal Research Ethics Board at McMaster University in Hamilton, Ontario. NOD-*Rag1*^{null} *IL2rg*^{null} (NRG) mice, which contain the targeted mutations *Rag*^{1tm1Mom} (MGI:1857241) and *Il2rg*^{tm1Wjll} (MGI:1857455), were obtained from Jackson Laboratory (stock no. 007799). Mice were bred and housed at McMaster University's Central Animal Facility in specific pathogen-free conditions.

Cell lines

The OVCAR-8 high grade ovarian serous adenocarcinoma cell line was cultured in DMEM containing 10% FBS, 1% penicillin/streptomycin, 1% HEPES, and 1% L-glutamine. Cultures were grown until ~80% confluent then used for experiments or further passaged. Luciferase-expressing OVCAR-8 cells (OVCAR8-Luc) used for *in vivo* tumour burden experiments were generated previously using a lentiviral vector with a luciferase reporter gene (Poznanski et al., 2018).

In vitro polarization of NK cells

NK cells were isolated from the peripheral blood of healthy donors using the custom whole blood NK cell isolation kit from Miltenyi Biotec, according to the manufacturer's instructions. Purity of NK cells was checked upon each isolation and >90%. NK cells were cultured in RPMI medium supplemented with 10% FBS, 1% penicillin/streptomycin, 1% HEPES, and 1% L-glutamine and 50 nM 2-Mercaptoethanol. NK cells were incubated under 21% O_2 conditions or under 1% O_2 using a hypoxia incubator chamber (StemCell Technologies) and mixed gas tank (1% O_2, 5% CO_2, 94% N_2) from AirLiquide. NK cells were cultured at concentration of 1 million cells/mL for polarization with 10 ng/mL IL-15 (Peprotech) and where indicated, 2 ng/mL TGFβ (R&D Systems). NK cell *in vitro* cytotoxicity was assessed as previously described (Poznanski et al., 2018) by incubating NK cells with CFSE-labeled OVCAR8 target cells at a 1:1 effector-to-target ratio for 5 hours, after which tumour cell viability was assessed by staining cells with fixable viability dye eFluor780 (eBiosciences). NK cell IFNγ and VEGF production were measured in the cell supernatants via DuoSet ELISAs (R&D Systems) conducted according to the manufacturer's instructions. The Human Cytokine/Chemokine 71-Plex Discovery Assay Array was also conducted by Eve Technologies on the supernatants of polarized NK cells.

Cell Staining and flow cytometry

All staining was conducted under light-sensitive conditions. Live/dead cells were discriminated using fixable viability dye according to the manufacturer's instructions. To assess mitochondrial mass, cells were subsequently stained with MitoTracker Red CMXRos (ThermoFisher), according to the manufacturer's instructions. Cells were then stained for

extracellular markers for 30 minutes at 4 degrees Celsius with the indicated anti-human fluorescently labeled antibodies. Control fluorescent minus one wells contained corresponding isotype controls were used to set gates. Samples were fixed for 1 h with 1% paraformaldehyde. Samples were acquired using BD LSRFortessa or LSRII cytometers and analyzed using FlowJo Software.

The following fluorescently-labeled antibodies were used. From BD Biosciences: BV421 mouse anti-human CD56, APC-H7 mouse anti-human CD3, BV711 mouse anti-human CD71, PE mouse anti-human CD98, PE-CF594 mouse anti-human CD11b, PE/Cy7 mouse anti-human CD14. From Biolegend: PerCP/Cy5.5 mouse anti-human CD27. From R&D Systems: Human Glut1 FITC-conjugated antibody.

Extracellular flux assays

NK cell glycolysis and OxPhos were measured using Seahorse extracellular flux assays on a Seahorse XFe96 analyzer and Wave Software as previously described. 200 000 NK cells were plated per well and adhered to a Seahorse plate coated with Poly-L-Lysine. Assays were conducted as previously described (Poznanski et al., 2021).

***In vivo* tumour model**

Female NRG mice were injected i.p. with 250 000 OVCAR8-Luc cells at Day 0, followed immediately by i.p. injection of $1x10^6$ freshly isolated pbNK cells, uNK cells, or vehicle (no NK controls). 500 ng of IL-15/mouse was administered i.p. at Day 0 and Day 2 to support NK cell survival. To measure tumour burden, bioluminescence (radiance units: photons/sec/cm2/sr) was quantified using an IVIS Spectrum Imaging System 14 minutes after i.p. injection of Luciferin.

RNA sequencing and analysis

RNA isolation was conducted using an RNAspin Mini kit from Cytiva according to manufacturer's instructions. RNA sequencing was conducted using an Illumina NextSeq 2000, with 2x50 base pairs per run configuration and a depth of 33.33 million clusters per sample. Human gene transcript counts were produced using Salmon version 1.7.0 and Human Gencode v39 transcripts from the raw sequencing files. Transcript counts were imported to R and differentially expressed genes (DEGs) were detected using DESeq2 in R. R was used to create a PCA plot of the transcript counts after normalization using variance stabilizing transformation. Pairwise DESEQ analysis was done between the four experimental conditions groups (Control, Hypoxia, TGFb, Hypoxia + TGFb) for a total of 6 pairwise comparisons, where the DESeq design variable included the Donor variable to control for differences arising from differences between donors as opposed to the main experimental variable. Differentially expressed genes from each pairwise comparison were filtered such that only genes with adjusted p-value < 0.005 and log fold change value > 0.585 or < -0.585 were reported. Next, DESeq analysis involving all 4 experimental condition groups was done and a heatmap was produced where the genes displayed were the combined DEGs from the previously conducted six pairwise analysis. The list of DEGs which passed the filtering criteria for the DESeq analysis were extracted in R and used as input for the online EnrichR tool with the Wikipathways Human 2021 gene-set database. The EnrichR results were filtered by p-adjusted < 0.05.

Statistical Analysis

Data comparing two groups were analyzed via two-tailed t-tests. Data comparing more than 2 groups with one independent variable were analyzed via one-way ANOVA using Tukey correction for multiple comparisons. Graphs and statistical analysis were generated using GraphPad Prism Software (v7.0). In all analyses, significance was defined as $p<0.05$.

5.6 REFERENCES

(Washington, DC: The National Academies Press).

Albini, A., and Noonan, D.M. (2021). Decidual-Like NK Cell Polarization: From Cancer Killing to Cancer Nurturing. Cancer discovery *11*, 28-33.

Assmann, N., O'Brien, K.L., Donnelly, R.P., Dyck, L., Zaiatz-Bittencourt, V., Loftus, R.M., Heinrich, P., Oefner, P.J., Lynch, L., Gardiner, C.M.*, et al.* (2017). Srebp-controlled glucose metabolism is essential for NK cell functional responses. Nat Immunol *18*, 1197-1206.

Bosi, A., Zanellato, S., Bassani, B., Albini, A., Musco, A., Cattoni, M., Desio, M., Nardecchia, E., D'Urso, D.G., Imperatori, A.*, et al.* (2018). Natural Killer Cells from Malignant Pleural Effusion Are Endowed with a Decidual-Like Proangiogenic Polarization. J Immunol Res *2018*, 2438598.

Brand, A., Singer, K., Koehl, G.E., Kolitzus, M., Schoenhammer, G., Thiel, A., Matos, C., Bruss, C., Klobuch, S., Peter, K.*, et al.* (2016). LDHA-associated lactic acid production blunts tumor immunosurveillance by T and NK cells. Cell Metab *24*, 657-671.

Brizel, D.M., Schroeder, T., Scher, R.L., Walenta, S., Clough, R.W., Dewhirst, M.W., and Mueller-Klieser, W. (2001). Elevated tumor lactate concentrations predict for an increased risk of metastases in head-and-neck cancer. International Journal of Radiation Oncology*Biology*Physics *51*, 349-353.

Bruno, A., Bassani, B., D'Urso, D.G., Pitaku, I., Cassinotti, E., Pelosi, G., Boni, L., Dominioni, L., Noonan, D.M., Mortara, L.*, et al.* (2018). Angiogenin and the MMP9-TIMP2 axis are up-regulated in proangiogenic, decidual NK-like cells from patients with colorectal cancer. Faseb j *32*, 5365-5377.

Bruno, A., Focaccetti, C., Pagani, A., Imperatori, A.S., Spagnoletti, M., Rotolo, N., Cantelmo, A.R., Franzi, F., Capella, C., Ferlazzo, G.*, et al.* (2013). The proangiogenic phenotype of natural killer cells in patients with non-small cell lung cancer. Neoplasia (New York, NY) *15*, 133-142.

Carreau, A., El Hafny-Rahbi, B., Matejuk, A., Grillon, C., and Kieda, C. (2011). Why is the partial oxygen pressure of human tissues a crucial parameter? Small molecules and hypoxia. J Cell Mol Med *15*, 1239-1253.

Cerdeira, A.S., Rajakumar, A., Royle, C.M., Lo, A., Husain, Z., Thadhani, R.I., Sukhatme, V.P., Karumanchi, S.A., and Kopcow, H.D. (2013). Conversion of peripheral blood NK cells to a decidual NK-like phenotype by a cocktail of defined factors. J Immunol *190*, 3939-3948.

Chang, C.H., Qiu, J., O'Sullivan, D., Buck, M.D., Noguchi, T., Curtis, J.D., Chen, Q., Gindin, M., Gubin, M.M., van der Windt, G.J.*, et al.* (2015). Metabolic competition in the tumour microenvironment is a driver of cancer progression. Cell *162*, 1229-1241.

Chang, W.A., Tsai, M.J., Hung, J.Y., Wu, K.L., Tsai, Y.M., Huang, Y.C., Chang, C.Y., Tsai, P.H., and Hsu, Y.L. (2021). miR-150-5p-Containing Extracellular Vesicles Are a New Immunoregulator That Favor the Progression of Lung Cancer in Hypoxic Microenvironments by Altering the Phenotype of NK Cells. Cancers (Basel) *13*.

Corpechot, C., Barbu, V., Wendum, D., Kinnman, N., Rey, C., Poupon, R., Housset, C., and Rosmorduc, O. (2002). Hypoxia-induced VEGF and collagen I expressions are associated with angiogenesis and fibrogenesis in experimental cirrhosis. Hepatology *35*, 1010-1021.

Crome, S.Q., Nguyen, L.T., Lopez-Verges, S., Yang, S.Y., Martin, B., Yam, J.Y., Johnson, D.J., Nie, J., Pniak, M., Yen, P.H.*, et al.* (2017). A distinct innate lymphoid cell population regulates tumor-associated T cells. Nat Med *23*, 368-375.

Dong, H.P., Elstrand, M.B., Holth, A., Silins, I., Berner, A., Trope, C.G., Davidson, B., and Risberg, B. (2006). NK- and B-cell infiltration correlates with worse outcome in metastatic ovarian carcinoma. American journal of clinical pathology *125*, 451-458.

Donnelly, R.P., Loftus, R.M., Keating, S.E., Liou, K.T., Biron, C.A., Gardiner, C.M., and Finlay, D.K. (2014). mTORC1-dependent metabolic reprogramming is a prerequisite for NK cell effector function. J Immunol *193*, 4477-4484.

Fu, B., Tian, Z., and Wei, H. (2014). Subsets of human natural killer cells and their regulatory effects. Immunology *141*, 483-489.

Fu, B., Wang, F., Sun, R., Ling, B., Tian, Z., and Wei, H. (2011). CD11b and CD27 reflect distinct population and functional specialization in human natural killer cells. Immunology *133*, 350-359.

Gamliel, M., Goldman-Wohl, D., Isaacson, B., Gur, C., Stein, N., Yamin, R., Berger, M., Grunewald, M., Keshet, E., Rais, Y.*, et al.* (2018). Trained Memory of Human Uterine NK Cells Enhances Their Function in Subsequent Pregnancies. Immunity *48*, 951-962.e955.

Gerriets, V.A., Kishton, R.J., Johnson, M.O., Cohen, S., Siska, P.J., Nichols, A.G., Warmoes, M.O., de Cubas, A.A., MacIver, N.J., Locasale, J.W.*, et al.* (2016). Foxp3 and Toll-like receptor signaling balance Treg cell anabolic metabolism for suppression. Nat Immunol *17*, 1459-1466.

Gu, J., Zhou, J., Chen, Q., Xu, X., Gao, J., Li, X., Shao, Q., Zhou, B., Zhou, H., Wei, S.*, et al.* (2022). Tumor metabolite lactate promotes tumorigenesis by modulating MOESIN lactylation and enhancing TGF-β signaling in regulatory T cells. Cell reports *39*, 110986.

Guan, Y., Chambers, C.B., Tabatabai, T., Hatley, H., Delfino, K.R., Robinson, K., Alanee, S.R., Ran, S., Torry, D.S., and Wilber, A. (2020). Renal cell tumors convert natural killer cells to a proangiogenic phenotype. Oncotarget *11*, 2571-2585.

Hanahan, D., and Weinberg, R.A. (2011). Hallmarks of cancer: the next generation. Cell *144*, 646-674.

Hanna, J., Goldman-Wohl, D., Hamani, Y., Avraham, I., Greenfield, C., Natanson-Yaron, S., Prus, D., Cohen-Daniel, L., Arnon, T.I., Manaster, I.*, et al.* (2006). Decidual NK cells regulate key developmental processes at the human fetal-maternal interface. Nat Med *12*, 1065-1074.

Heldin, C.H., Lennartsson, J., and Westermark, B. (2018). Involvement of platelet-derived growth factor ligands and receptors in tumorigenesis. J Intern Med *283*, 16-44.

Huang, R., Wang, S., Wang, N., Zheng, Y., Zhou, J., Yang, B., Wang, X., Zhang, J., Guo, L., Wang, S.*, et al.* (2020). CCL5 derived from tumor-associated macrophages promotes prostate cancer stem cells and metastasis via activating β-catenin/STAT3 signaling. Cell death & disease *11*, 234.

Jha, Abhishek K., Huang, Stanley C.-C., Sergushichev, A., Lampropoulou, V., Ivanova, Y., Loginicheva, E., Chmielewski, K., Stewart, Kelly M., Ashall, J., Everts, B.*, et al.* Network integration of parallel metabolic and transcriptional data reveals metabolic modules that regulate macrophage polarization. Immunity *42*, 419-430.

Kessler, M., Hoper, J., and Krumme, B.A. (1976). Monitoring of tissue perfusion and cellular function. Anesthesiology *45*, 184-197.

Levi, I., Amsalem, H., Nissan, A., Darash-Yahana, M., Peretz, T., Mandelboim, O., and Rachmilewitz, J. (2015). Characterization of tumor infiltrating natural killer cell subset. Oncotarget *6*, 13835-13843.

Loftus, R.M., Assmann, N., Kedia-Mehta, N., O'Brien, K.L., Garcia, A., Gillespie, C., Hukelmann, J.L., Oefner, P.J., Lamond, A.I., Gardiner, C.M.*, et al.* (2018). Amino acid-dependent cMyc expression is essential for NK cell metabolic and functional responses in mice. Nat Commun *9*, 2341.

Lu, S.W., Pan, H.C., Hsu, Y.H., Chang, K.C., Wu, L.W., Chen, W.Y., and Chang, M.S. (2020). IL-20 antagonist suppresses PD-L1 expression and prolongs survival in pancreatic cancer models. Nat Commun *11*, 4611.

Lv, D., Zhang, Y., Kim, H.-J., Zhang, L., and Ma, X. (2013). CCL5 as a potential immunotherapeutic target in triple-negative breast cancer. Cellular & molecular immunology *10*, 303-310.

Maeda, S., Motegi, T., Iio, A., Kaji, K., Goto-Koshino, Y., Eto, S., Ikeda, N., Nakagawa, T., Nishimura, R., Yonezawa, T.*, et al.* (2022). Anti-CCR4 treatment depletes regulatory T cells and leads to clinical activity in a canine model of advanced prostate cancer. Journal for immunotherapy of cancer *10*, e003731.

Mah, A.Y., Rashidi, A., Keppel, M.P., Saucier, N., Moore, E.K., Alinger, J.B., Tripathy, S.K., Agarwal, S.K., Jeng, E.K., Wong, H.C.*, et al.* (2017). Glycolytic requirement for NK cell cytotoxicity and cytomegalovirus control. JCI insight *2*, pii: 95128.

Melichar, B., Tousková, M., Tosner, J., and Kopecký, O. (2001). The phenotype of ascitic fluid lymphocytes in patients with ovarian carcinoma and other primaries. Onkologie *24*, 156-160.

Michalek, R.D., Gerriets, V.A., Jacobs, S.R., Macintyre, A.N., N.J., M., Mason, E.F., Sullivan, S.A., G., N.A., and Rathmell, J.C. (2011). Cutting edge: distinct glycolytic and lipid oxidative metabolic programs are essential for effector and regulatory CD4+ T cell subsets. J Immunol *186*, 3299-3303.

Michelet, X., Dyck, L., Hogan, A., Loftus, R.M., Duquette, D., Wei, K., Beyaz, S., Tavakkoli, A., Foley, C., Donnelly, R.*, et al.* (2018). Metabolic reprogramming of natural killer cells in obesity limits antitumor responses. Nat Immunol *19*, 1330-1340.

Ni, J., Wang, X., Stojanovic, A., Zhang, Q., Wincher, M., Bühler, L., Arnold, A., Correia, M.P., Winkler, M., Koch, P.S.*, et al.* (2020). Single-Cell RNA Sequencing of Tumor-Infiltrating NK Cells Reveals that Inhibition of Transcription Factor HIF-1α Unleashes NK Cell Activity. Immunity *52*, 1075-1087.e1078.

Olkhanud, P.B., Baatar, D., Bodogai, M., Hakim, F., Gress, R., Anderson, R.L., Deng, J., Xu, M., Briest, S., and Biragyn, A. (2009). Breast cancer lung metastasis requires expression of chemokine receptor CCR4 and regulatory T cells. Cancer Res *69*, 5996-6004.

Poznanski, S.M., Nham, T., Chew, M.V., Lee, A.J., Hammill, J.A., Fan, I.Y., Butcher, M., Bramson, J.L., Lee, D.A., Hirte, H.*, et al.* (2018). Expanded CD56superbrightCD16+ NK cells from ovarian cancer patients are cytotoxic against autologous tumor in a patient-derived xenograft murine model. Cancer Immunol Res *6*, 1174-1185.

Poznanski, S.M., Singh, K., Ritchie, T.M., Aguiar, J.A., Fan, I.Y., Portillo, A.L., Rojas, E.A., Vahedi, F., El-Sayes, A., Xing, S.*, et al.* (2021). Metabolic flexibility determines human NK cell functional fate in the tumor microenvironment. Cell Metab.

Rodesch, F., Simon, P., Donner, C., and Jauniaux, E. (1992). Oxygen measurements in endometrial and trophoblastic tissues during early pregnancy. Obstet Gynecol *80*, 283-285.

Rodriguez-Prados, J.C., Traves, P.G., Cuenca, J., Rico, D., Aragones, J., Martin-Sanz, P., Cascante, M., and Bosca, L. (2010). Substrate fate in activated macrophages: a comparison between innate, classic, and alternative activation. J Immunol *185*, 605-614.

Shikada, Y., Yonemitsu, Y., Koga, T., Onimaru, M., Nakano, T., Okano, S., Sata, S., Nakagawa, K., Yoshino, I., Maehara, Y.*, et al.* (2005). Platelet-derived growth factor-AA is an essential and autocrine regulator of vascular endothelial growth factor expression in non-small cell lung carcinomas. Cancer Res *65*, 7241-7248.

Sonveaux, P., Végran, F., Schroeder, T., Wergin, M.C., Verrax, J., Rabbani, Z.N., De Saedeleer, C.J., Kennedy, K.M., Diepart, C., Jordan, B.F.*, et al.* (2008). Targeting lactate-fueled respiration selectively kills hypoxic tumor cells in mice. J Clin Invest *118*, 3930-3942.

Sulzbacher, I., Birner, P., Trieb, K., Träxler, M., Lang, S., and Chott, A. (2003). Expression of platelet-derived growth factor-AA is associated with tumor progression in osteosarcoma. Mod Pathol *16*, 66-71.

Thomas, J.K., Mir, H., Kapur, N., Bae, S., and Singh, S. (2019). CC chemokines are differentially expressed in Breast Cancer and are associated with disparity in overall survival. Scientific reports *9*, 4014-4014.

Urbańska, K., and Orzechowski, A. (2019). Unappreciated Role of LDHA and LDHB to Control Apoptosis and Autophagy in Tumor Cells. Int J Mol Sci *20*.

Vgenopoulou, S., Lazaris, A.C., Markopoulos, C., Boltetsou, E., Kyriakou, V., Kavantzas, N., Patsouris, E., and Davaris, P.S. (2003). Immunohistochemical evaluation of immune response in invasive ductal breast cancer of not-otherwise-specified type. Breast *12*, 172-178.

Vozza, A., Parisi, G., De Leonardis, F., Lasorsa, F.M., Castegna, A., Amorese, D., Marmo, R., Calcagnile, V.M., Palmieri, L., Ricquier, D.*, et al.* (2014). UCP2 transports C4 metabolites out of mitochondria, regulating glucose and glutamine oxidation. Proc Natl Acad Sci U S A *111*, 960-965.

Walenta, S., Wetterling, M., Lehrke, M., Schwickert, G., Sundfør, K., Rofstad, E.K., and Mueller-Klieser, W. (2000). High Lactate Levels Predict Likelihood of Metastases, Tumor Recurrence, and Restricted Patient Survival in Human Cervical Cancers1. Cancer Research *60*, 916-921.

Watson, M.J., Vignali, P.D.A., Mullett, S.J., Overacre-Delgoffe, A.E., Peralta, R.M., Grebinoski, S., Menk, A.V., Rittenhouse, N.L., DePeaux, K., Whetstone, R.D.*, et al.* (2021). Metabolic support of tumour-infiltrating regulatory T cells by lactic acid. Nature *591*, 645-651.

Yang, M., and Vousden, K.H. (2016). Serine and one-carbon metabolism in cancer. Nature Reviews Cancer *16*, 650.

Zheng, X., Qian, Y., Fu, B., Jiao, D., Jiang, Y., Chen, P., Shen, Y., Zhang, H., Sun, R., Tian, Z.*, et al.* (2019). Mitochondrial fragmentation limits NK cell-based tumor immunosurveillance. Nat Immunol *20*, 1656-1667.

– CHAPTER 6 –

DISCUSSION

6.1 Summary

An improved understanding of how immune cells are inhibited in the TME is needed to develop effective immunotherapies against solid tumours. *Therefore, the central aim of my PhD studies was to develop effective NK cell therapies against hard-to-treat solid tumours. To do so, I sought to elucidate central mechanisms to NK cell inhibition in the TME.* Collectively, the results in **Chapters 2-5** address this central aim.

The results in **Chapter 2** revealed that NK cells expanded using K562-mbIL21 cells are a unique, highly cytotoxic $CD56^{superbright}CD16^{+}$ subset that reduced ovarian cancer tumour burden in translational mouse models of human ovarian cancer. Specifically, NK cells expanded from either ovarian cancer patient ascites or peripheral blood or healthy donor peripheral blood were equally effective in reducing tumour burden against cell-line and autologous patient-derived xenograft models. The work outlined in **Chapter 3** extended these findings to the context of lung cancer. NK cells expanded from the pleural effusions, tumours, or peripheral blood of lung cancer patients or the peripheral blood of healthy donors demonstrated strong anti-tumour activity *in vitro* and in *in vivo* xenograft lung cancer models. Further, due to their sustained anti-tumour activity, expanded NK cells sensitized patients' non-responding tumours to PD1-blockade therapy. The work in **Chapter 4** uncovered that NK cells undergo a metabolic energy crisis in tumours that causes their dysfunction. Second, the work discovered that reprogramming NK cell metabolism through expansion enables expanded NK cells to not only resist suppression, but paradoxically heighten their tumour killing in the TME. Finally, the results in **Chapter 5** demonstrate that regulatory NK cells, like those in tumours and the uterus, have a distinct metabolic program from cytotoxic NK cells that may underpin the functional polarization of these subsets.

The research presented in this thesis contributes to our understanding of the mechanisms through which NK cells are inhibited by tumours. Through numerous experimental approaches and models, the results demonstrate that metabolic programs play a key role in determining NK cell functional fate in tumours. Furthermore, they present expanded NK cells as a promising therapy to treat poor prognosis tumours such as ovarian and lung cancer.

The key findings of this thesis have been discussed in detail in each manuscript **(Chapters 2-6)**. Hence, this final chapter will discuss how these manuscripts relate, their overall significance and implications, limitations to the work, and future directions that stem from the findings.

6.2 Implications and future directions

The development of broadly effective immunotherapies to treat solid tumours has been hampered for decades due to strong immunosuppression by the TME. A myriad of factors in the TME are known to be immunosuppressive, including immunosuppressive cytokines, regulatory immune cells, factors secreted by tumour cells, inhibitory ligands, metabolic waste, and nutrient deprivation. Much work has focused on targeting one or a few of these external factors. However, such strategies have failed to be broadly effective due to the plethora of both known and unknown factors at play. Conversely, the fundamental changes that occur *within* immune cells in response to the combination of these factors remained poorly understood but may provide a central inhibitory hub to target.

The collective work in this thesis provides new knowledge of how NK cells become suppressed by the TME. Furthermore, it uncovers that expanded NK cells overcome the immunosuppressive TME and show remarkable effectiveness against tumours in translational preclinical models.

The findings in this thesis extend from the TME of advanced ovarian cancer **(Chapters 2 and 4)** to advanced lung cancer **(Chapters 3 and 4)** – two poor prognosis cancers that are among the most immunosuppressive TMEs. Indeed, although TILs are present in a high proportion of ovarian cancer tumours, to date no immunotherapy has proven clinically effective for the treatment of ovarian cancer due to the hostility of the ascites TME (Zhang, Conejo-Garcia et al. 2003, Li, Wang et al. 2017). Indeed, clinical trials investigating monotherapy or multi-agent ICI therapy alone or in combination with chemotherapy have yet to demonstrate meaningful anti-tumour activity in patients with EOC (Porter and Matulonis 2022). However, generally the presence of IFN-g-producing TILs correlates positively with EOC survival time, indicating the important role for cytotoxic immunity in slowing disease progression (Zhang, Conejo-Garcia et al. 2003, Sato, Olson et al. 2005, Li, Wang et al. 2017). As such, clinical trials combining ICI with other immune activating strategies are underway (NCT02335918). Similarly, while ICIs have shown sustained anti-tumour efficacy in a small proportion of lung cancer patients, the majority of lung cancer patients remain unresponsive to ICI and other immunotherapies (Topalian, Hodi et al. 2012, Herbst, Soria et al. 2014, Yu, Zeng et al. 2019).

It is noteworthy that the degree of cytotoxic immunity in the TME is a positive prognostic indicator and positively correlates with immunotherapy response across tumour types (Havel, Chowell et al. 2019). For instance in lung cancer patients, a higher Th1 gene expression score was associated with higher response to PD1-blockade therapy (Herbst, Soria et al. 2014). In melanoma patients, presence of cytotoxic CD8 T cells was associated with greater checkpoint blockade therapy response, whereas presence of exhausted CD8 T cells or a high Treg:CD8 T cell ratio was associated with therapy resistance (Hodi, Butler et al. 2008). The results in **Chapters 2-4** demonstrate that expanded NK cells not only resist suppression, but also dismantle the highly

immunosuppressive TMEs of ovarian and lung cancer and reactivate endogenous exhausted TILs. The restoration of cytotoxic immunity in these hostile TMEs by expanded NK cells suggests that expanded NK cells hold promising therapeutic potential for patients. Further, these findings propose that expanded NK cells could be broadly used to enhance other immunotherapies that are hindered by the immunosuppressive effects of the TME. Proof-of-concept of this notion is demonstrated in the results in **Chapter 3**, whereby expanded NK cells synergized with PD1-blockade therapy to induce strong tumour destruction of patient tumours that were initially non-responsive to PD1-blockade. An important future direction will be to determine whether expanded NK cells can sensitize other non-responsive tumour types, such as ovarian cancer, to PD1-blockade therapy or other ICIs. Further, our results in **Chapter 2** that expanded NK cells maintain CD16 expression in the TME suggest that the efficacy of ADCC-inducing antibody therapies may also be improved by combined treatment with expanded NK cells.

In **Chapters 2 and 3**, NK cells expanded from cancer patient tumours, effusions or peripheral blood showed comparable anti-tumour efficacy as NK cells expanded from the peripheral blood of healthy donors. These results show that expansion overrides the anti-tumour advantage that unexpanded allogeneic NK cells have shown over unexpanded autologous NK cells (Ruggeri, Capanni et al. 2002, Miller, Soignier et al. 2005). This suggests that expanded NK cells are sensitive enough to tumour-derived activation that tumour-induced inhibitory KIR signals are outweighed. Importantly, this overriding of KIR activation is specific to the tumour, as expanded NK cells have been reported to be safe and not attack healthy tissue upon adoptive transfer to patients with hematologic cancer (Ciurea, Schafer et al. 2017). Such findings reinvigorate the potential of autologous NK cell therapy. These results also identify peritoneal and pleural effusions as an attractive source of NK cells for expansion, since large volumes of effusions can be collected

upon routine paracentesis or thoracentesis without added invasive procedures to the patient. Our results that the source of NK cells has no bearing on therapeutic capacity of the expanded product aligns with other studies that have shown comparable antitumour activity of allogeneic NK cells derived from PBMCs versus various other sources, including cord blood and induced pluripotent stem cells (Nham, Poznanski et al. 2018, Cichocki, Bjordahl et al. 2020). However, while autologous NK cell therapy may be appealing, it will have to be weighed against the lower cost and ease of manufacturing of NK cells from allogeneic sources since the latter can be used to produce off-the-shelf products which may be more feasible for wide-spread therapeutic application.

The work in **Chapters 4 and 5** contribute to an emerging understanding that the activity of metabolic pathways regulates NK cell polarization and function. While previous reports had shown that glycolysis, OxPhos, and amino acid metabolism are critical for cytotoxic NK cell functions, the effect of an immunosuppressive environment on cytotoxic NK cell metabolism had not been characterized (Donnelly, Loftus et al. 2014, Keating, Zaiatz-Bittencourt et al. 2016, Assmann, O'Brien et al. 2017, Loftus, Assmann et al. 2018). The findings in **Chapter 4** present metabolism as a key node of NK cell functional fate in tumours. The reversal of NK cell inhibition in the TME by RTA-408 shows proof-of-concept that the metabolism of taNK cells can be manipulated for therapeutic purposes. There are likely many other possible metabolic targets that could be harnessed for therapeutic purposes which will be an important area of future work.

Chapter 5 takes these findings further by uncovering that metabolic pathways not only distinguish the capacity of NK cell cytotoxic functions, they also differentiate cytotoxic from regulatory NK cells that are present in the TME as well as other tissues such as the uterus. This suggests that metabolic targeting could manipulate not only the activity or lack thereof of NK cell

cytotoxic functions but also NK cell polarization from cytotoxic to equally functional, but non-cytotoxic, regulatory NK cells. In terms of cancer therapy, this could mean metabolic targeting of NK cells has potential to provide a double punch, whereby it suppresses tumour-promoting abilities of NK cells all the while harnessing NK cell cytotoxic capacities. This is particularly pertinent as work emerges showing the capacity of regulatory NK cells to also suppress cytotoxic T cells in addition to their direct effects on tumours and angiogenesis (Crome, Nguyen et al. 2017, Neo, Yang et al. 2020). Future work will need to further delineate metabolic targets to suppress regulatory NK cell functions. One consideration that will need to be kept in mind when targeting metabolism *in vivo* for cancer immunotherapy is the effects the metabolic agent has on tumour cells to ensure no tumour growth advantages are inadvertently stimulated along with immune activation. Implications of these findings could also extend to other disease contexts, including those in which regulatory uNK cells play a role such as pregnancy complications (Mahajan, Sharma et al. 2022).

In **Chapter 4,** we found that expanded NK cells mimic tumour cell Warburg metabolism and metabolic flexibility and as a result function better in the TME and nutrient-deprived conditions. This work demonstrates that NK cells can be conditioned in culture for hostile environments and thus raises important considerations for culture conditions of cell therapies. Typical *in vitro* culture conditions to expand and activate cytotoxic immune cells for cell therapy contain higher levels of nutrients, such as glucose and amino acids, than even those present in human blood. While such nutrient-rich conditions may be necessary to initially expand and activate immune cells, our work suggests they leave immune cells unequipped to deal with the metabolic stressors of the TME. In contrast, expanded NK cells are co-cultured with nutrient-consuming, lactate-secreting K562 tumour cells with added activation signals. Thus, these culture

conditions likely reflect more closely the conditions of the TME and may be key to preparing them to thrive in the TME. Future work should continue to investigate the utility of modifying culture conditions, such as lowering oxygen levels, lowering nutrient levels, or culturing in the presence of tumour cells or metabolic waste, to optimize the function of cell therapies in solid tumours.

While the work in **Chapter 4** demonstrates that expanded NK cells have extensive metabolic flexibility and resilience, an interesting area of future research will be to further delineate the mechanisms of nutrient flexibility. Like tumour cells, we found that expanded NK cells have increased nutrient receptor expression compared to unexpanded NK cells, thus perhaps they exhibit similar constitutive nutrient uptake mechanisms as tumour cells. It is equally possible that, like tumour cells, they consume unconventional nutrients for energy, such as lactic acid or extracellular proteins. Furthermore, it is possible that they adopt other tumour-scavenging mechanisms such as nutrient uptake from neighbouring cells, macropinocytosis, or autophagy. Such questions remain to be answered but would provide important insight into the mechanisms through which immune cells can compete with tumour cells.

Finally, the work in **Chapters 2, 4, and 5** demonstrates that both highly cytotoxic and highly regulatory NK cells can be superbright for CD56 expression. These findings, together with other recent publications, call into question whether NK cells can in fact be profiled based on phenotype, with bright CD56 expression as a hallmark indictor of regulatory NK cells and dim CD56 expression classically defining cytotoxic NK cells. Indeed, a recent study demonstrated that following priming with IL-15, $CD56^{bright}$ pbNK cells in fact had greater cytotoxicity against tumour cells compared to $CD56^{dim}$ pbNK cells (Wagner, Rosario et al. 2017). Furthermore, hepatic $CD56^{bright}$ NK cells were found to produce lower levels of cytokine than their $CD56^{dim}$ counterparts (Lunemann, Langeneckert et al. 2019). To this end, in a recent review article we investigated the

relationship between NK cell phenotype, metabolism, and functional fate and proposed a new paradigm that distinct metabolic fingerprints, rather than phenotype, may better distinguish NK cell functional subsets (Poznanski and Ashkar 2019). Our work in **Chapter 5** corroborates that indeed distinct metabolic fingerprints distinguish at least regulatory from cytotoxic NK cells. Further discernment of the metabolic fingerprints that dictate NK cell fates are needed to comprehensively profile NK cells based on metabolism.

6.3 Concluding remarks

The work presented in this thesis provides a novel understanding of the central mechanisms involved in NK cell inhibition in the TME. It demonstrates that metabolic fitness is of paramount importance to determining NK cell fate in the TME. Furthermore, it identifies expanded NK cells as a promising immunotherapy to treat solid tumours that overcomes previous challenges of tumour-induced inhibition faced by immunotherapies. The work adds evidence that choosing the source from which to derive expanded NK cells can be driven by feasibility, since expanded NK cells can be derived from various sources (be it autologous, allogeneic, peripheral blood- or tumour-derived) without compromising therapeutic efficacy. The findings support future clinical investigation of expanded NK cells for patients with poor prognosis solid tumours, including- but not limited to- ovarian and lung cancer.

The collective work in this thesis further defines the metabolic programs of NK cell polarization and functional fates. The findings present a model in which glucose-driven metabolism tips the balance between cytotoxic and regulatory NK cell polarization and elevated serine and one carbon metabolism through the folate cycle defines NK cells that are metabolically adapted to functionally thrive in the TME (Figure 2). These studies indicate that profiling and

modulating metabolism hold promise as powerful therapeutic strategies to predict and control NK cell fate in tumours and beyond.

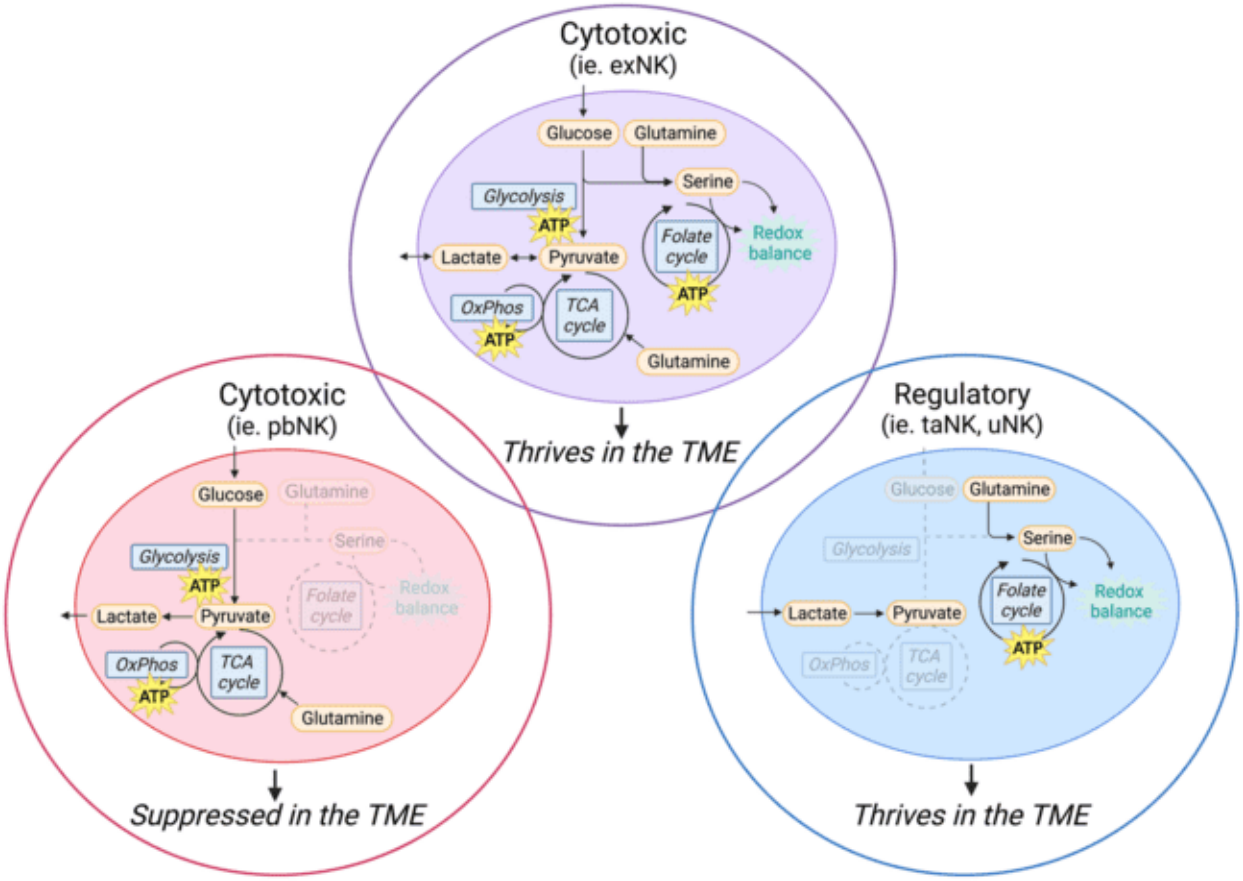

Figure 2. Metabolic profiles that define NK cell polarization and functional fate in the TME. Red circle (left): Classic cytotoxic NK cells, such as pbNK cells, have high levels of glucose-driven glycolysis and OxPhos, which are critical for their functions but in direct competition with tumour glucose utilisation. As a result, these NK cells undergo metabolic paralysis and functional inhibition in the TME. Blue circle (right): Regulatory NK cells, such as taNK cells and uNK cells, are defined by downregulated glucose metabolism and increased lactate and serine and one carbon metabolism through the folate cycle and functionally thrive in the TME. Purple circle (top/centre):

cytotoxic NK cells that combine high levels of glucose metabolism with serine and one carbon metabolism are metabolically flexible and remain highly cytotoxic in the TME.

– APPENDIX I –

PERMISSION TO REPRINT PULBISHED MANUSCRIPTS

1.1 Chapter 2 AACR permissions policy

Article Reuse

Authors of articles published under copyright in AACR journals have generous reuse rights of the article and its component parts as described below. Reuse by others is available upon request. Reuse of articles published under an Open Access license is governed by the terms of the specific Creative Commons license used.

Article Reuse by Authors

Authors of articles published under standard copyright in AACR journals are permitted to use their article or parts of their article in the following ways **without requesting permission from the AACR**. All such uses must include appropriate attribution to the original AACR publication. Authors may do the following as applicable:

1. Reproduce parts of their article, including figures and tables, in books, reviews, or subsequent research articles they write;
2. Use parts of their article in presentations, including figures downloaded into PowerPoint, which can be done directly from the journal's website;
3. Post the accepted version of their article (after revisions resulting from peer review, but before editing and formatting) on their institutional website, if this is required by their institution. The version on the institutional repository must contain a link to the final, published version of the article on the AACR journal website so that any subsequent corrections to the published record will continue to be available to the broadest readership. The posted version may be released publicly (made open to anyone) 12 months after its publication in the journal;
4. Submit a copy of the article to a doctoral candidate's university in support of a doctoral thesis or dissertation.

Article Reuse by Others

Third parties or individuals who are seeking permission to copy, reproduce, or republish content from an AACR journal and who are not the author of that content may use the Copyright Clearance Center's Rightslink® service to request permission to reuse identified content. Please see **Third Party Permission and Reprints** for detailed instructions on how to submit a request.

https://aacrjournals.org/pages/copyright

1.2 Chapter 3 BMJ permissions policy

Author Permissions Policy

	Reproduce and share copies	Right to create derivative works	Right to publish within book essay, position paper or non peer-reviewed article	Right to use in course packs, training, seminars and conferences	Right to post on a website
CC-BY-NC	✓ Only for non-commercial uses. Attribution must be made	✓ Only for non-commercial uses. Attribution must be made	✓ Only for non-commercial uses. Attribution must be made	✓ Only for non-commercial purposes. Attribution must be made	Please see Self-Archiving Policy
CC-BY	✓ Attribution must be made	✓ Attribution must be made	✓ Attribution must be made	✓ Attribution must be made	
Non Open Access	✓ A reasonable number (fewer than 100) copies of the final article may be distributed for non-commercial purposes in print or electronic form **X** this cannot be done on a systematic basis (which includes via mass e-mailings).	**X** Permission for commercial publications must be sought	✓One BMJ article may be reused in a book edited by the author **X** Permission for more than one article must be sought	✓ Course packs, to be distributed free of charge to students at the Author's institution ✓ stored in digitally for access by students for course work ✓in house training programmes of the Contributor(s)'s employer ✓ 100 copies distributed per conference or seminar	

Any permissions not covered by the author licence permission can be acquired through our online service, RightsLink, by clicking on 'Request Permissions' next to the article abstract. Instructions for this service can be found here. If you have any questions please contact RightsLink customer services or email bmj.permissions@bmj.com.
"Commercial Use" includes:

- copying or downloading of documents, or linking to such postings, for further redistribution, sale or licensing, for a fee;
- copying, downloading or posting by a site or service that incorporates advertising with such content;
- the inclusion or incorporation of document content in other works or services (other than for legally permitted quotations with an appropriate citation) that is then available for sale or licensing, for a fee.
- use of documents or document content (other than for legally permitted quotations with appropriate citation) organisations for promotional purposes, whether for a fee or otherwise.
- use for the purposes of monetary reward by means of sale, resale, license, loan, transfer or other form of commercial exploitation.

https://www.bmj.com/company/wp-content/uploads/2019/03/Author-Permissions-Policy.pdf

1.3 Chapter 4 Elsevier permissions policy

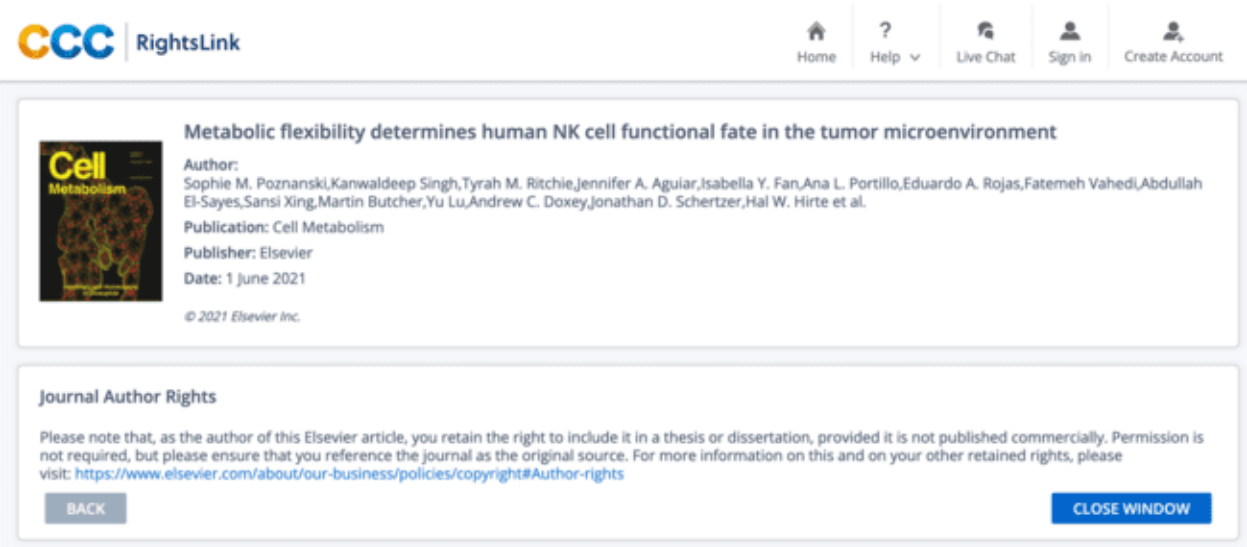
CCC RightsLink
Home
Help
Live Chat
Sign in
Create Account
Metabolic flexibility determines human NK cell functional fate in the tumor microenvironment
Author:
Sophie M. Poznanski,Kanwaldeep Singh,Tyrah M. Ritchie,Jennifer A. Aguiar,Isabella Y. Fan,Ana L. Portillo,Eduardo A. Rojas,Fatemeh Vahedi,Abdullah El-Sayes,Sansi Xing,Martin Butcher,Yu Lu,Andrew C. Doxey,Jonathan D. Schertzer,Hal W. Hirte et al.
Publication: Cell Metabolism
Publisher: Elsevier
Date: 1 June 2021
© 2021 Elsevier Inc.
Journal Author Rights
Please note that, as the author of this Elsevier article, you retain the right to include it in a thesis or dissertation, provided it is not published commercially. Permission is not required, but please ensure that you reference the journal as the original source. For more information on this and on your other retained rights, please visit: https://www.elsevier.com/about/our-business/policies/copyright#Author-rights
BACK
CLOSE WINDOW

- APPENDIX II -

REFERENCES

References

Ahmed, N., and Stenvers, K.L. (2013). Getting to know ovarian cancer ascites: opportunities for targeted therapy-based translational research. Front Oncol *3*, 256.

Al-Shibli, K.I., Donnem, T., Al-Saad, S., Persson, M., Bremnes, R.M., and Busund, L.T. (2008). Prognostic effect of epithelial and stromal lymphocyte infiltration in non-small cell lung cancer. Clin Cancer Res *14*, 5220-5227.

Angelo, L.S., Banerjee, P.P., Monaco-Shawver, L., Rosen, J.B., Makedonas, G., Forbes, L.R., Mace, E.M., and Orange, J.S. (2015). Practical NK cell phenotyping and variability in healthy adults. Immunologic research *62*, 341-356.

Ansell, S.M., Lesokhin, A.M., Borrello, I., Halwani, A., Scott, E.C., Gutierrez, M., Schuster, S.J., Millenson, M.M., Cattry, D., Freeman, G.J.*, et al.* (2015). PD-1 blockade with nivolumab in relapsed or refractory Hodgkin's lymphoma. The New England journal of medicine *372*, 311-319.

Assmann, N., O'Brien, K.L., Donnelly, R.P., Dyck, L., Zaiatz-Bittencourt, V., Loftus, R.M., Heinrich, P., Oefner, P.J., Lynch, L., Gardiner, C.M.*, et al.* (2017). Srebp-controlled glucose metabolism is essential for NK cell functional responses. Nat Immunol *18*, 1197-1206.

Aydin, Y., Turkyilmaz, A., Intepe, Y.S., and Eroglu, A. (2009). Malignant pleural effusions: appropriate treatment approaches. Eurasian J Med *41*, 186-193.

Bachanova, V., Burns, L.J., McKenna, D.H., Curtsinger, J., Panoskaltsis-Mortari, A., Lindgren, B.R., Cooley, S., Weisdorf, D., and Miller, J.S. (2010). Allogeneic natural killer cells for refractory lymphoma. Cancer Immunol Immunother *59*, 1739-1744.

Barrow, A.D., Martin, C.J., and Colonna, M. (2019). The Natural Cytotoxicity Receptors in Health and Disease. Front Immunol *10*, 909.

Bauer, S., Groh, V., Wu, J., Steinle, A., Phillips, J.H., Lanier, L.L., and Spies, T. (1999). Activation of NK cells and T cells by NKG2D, a receptor for stress-inducible MICA. Science *285*, 727-729.

Belisle, J.A., Gubbels, J.A., Raphael, C.A., Migneault, M., Rancourt, C., Connor, J.P., and Patankar, M.S. (2007). Peritoneal natural killer cells from epithelial ovarian cancer patients show an altered phenotype and bind to the tumour marker MUC16 (CA125). Immunology *122*, 418-429.

Bellmunt, J., de Wit, R., Vaughn, D.J., Fradet, Y., Lee, J.L., Fong, L., Vogelzang, N.J., Climent, M.A., Petrylak, D.P., Choueiri, T.K.*, et al.* (2017). Pembrolizumab as Second-Line Therapy for Advanced Urothelial Carcinoma. The New England journal of medicine *376*, 1015-1026.

Berek, J.S., Bast, R.C., Lichtenstein, A., Hacker, N.F., Spina, C.A., Lagasse, L.D., Knapp, R.C., and Zighelboim, J. (1984). Lymphocyte cytotoxicity in the peritoneal cavity and blood of patients with ovarian cancer. Obstet Gynecol *64*, 704-714.

Berendt, M.J., and North, R.J. (1980). T-cell-mediated suppression of anti-tumor immunity. An explanation for progressive growth of an immunogenic tumor. Journal of Experimental Medicine *151*, 69-80.

Berg, M., Lundqvist, A., McCoy, P., Jr., Samsel, L., Fan, Y., Tawab, A., and Childs, R. (2009). Clinical-grade ex vivo-expanded human natural killer cells up-regulate activating receptors and death receptor ligands and have enhanced cytolytic activity against tumor cells. Cytotherapy *11*, 341-355.

Berod, L., Friedrich, C., Nandan, A., Freitag, J., Hagemann, S., Harmrolfs, K., Sandouk, A., Hesse, C., Castro, C.N., Bahre, H.*, et al.* (2014). De novo fatty acid synthesis controls the fate between regulatory T and T helper 17 cells. Nat Med *20*, 1327-1333.

Birkeland, S.A., Storm, H.H., Lamm, L.U., Barlow, L., Blohmé, I., Forsberg, B., Eklund, B., Fjeldborg, O., Friedberg, M., Frödin, L.*, et al.* (1995). Cancer risk after renal transplantation in the Nordic countries, 1964-1986. Int J Cancer *60*, 183-189.

Bjorkstrom, N.K., Riese, P., Heuts, F., Andersson, S., Fauriat, C., Ivarsson, M.A., Bjorklund, A.T., Flodstrom-Tullberg, M., Michaelsson, J., Rottenberg, M.E.*, et al.* (2010). Expression patterns of NKG2A, KIR, and CD57 define a process of CD56dim NK-cell differentiation uncoupled from NK-cell education. Blood *116*, 3853-3864.

Bodduluru, L.N., Kasala, E.R., Madhana, R.M., and Sriram, C.S. (2015). Natural killer cells: The journey from puzzles in biology to treatment of cancer. Cancer Lett *357*, 454-467.

Borghaei, H., Paz-Ares, L., Horn, L., Spigel, D.R., Steins, M., Ready, N.E., Chow, L.Q., Vokes, E.E., Felip, E., Holgado, E.*, et al.* (2015). Nivolumab versus Docetaxel in Advanced Nonsquamous Non-Small-Cell Lung Cancer. The New England journal of medicine *373*, 1627-1639.

Bosi, A., Zanellato, S., Bassani, B., Albini, A., Musco, A., Cattoni, M., Desio, M., Nardecchia, E., D'Urso, D.G., Imperatori, A.*, et al.* (2018). Natural Killer Cells from Malignant Pleural Effusion Are Endowed with a Decidual-Like Proangiogenic Polarization. J Immunol Res *2018*, 2438598.

Bouzidi, L., Triki, H., Charfi, S., Kridis, W.B., Derbel, M., Ayadi, L., Sellami-Boudawara, T., and Cherif, B. (2021). Prognostic Value of Natural Killer Cells Besides Tumor-Infiltrating Lymphocytes in Breast Cancer Tissues. Clin Breast Cancer *21*, e738-e747.

Brand, A., Singer, K., Koehl, G.E., Kolitzus, M., Schoenhammer, G., Thiel, A., Matos, C., Bruss, C., Klobuch, S., Peter, K.*, et al.* (2016). LDHA-associated lactic acid production blunts tumor immunosurveillance by T and NK cells. Cell Metab *24*, 657-671.

Brentjens, R.J., Davila, M.L., Riviere, I., Park, J., Wang, X., Cowell, L.G., Bartido, S., Stefanski, J., Taylor, C., Olszewska, M.*, et al.* (2013). CD19-targeted T cells rapidly induce molecular remissions in adults with chemotherapy-refractory acute lymphoblastic leukemia. Sci Transl Med *5*, 177ra138.

Brunet, J.-F., Denizot, F., Luciani, M.-F., Roux-Dosseto, M., Suzan, M., Mattei, M.-G., and Golstein, P. (1987). A new member of the immunoglobulin superfamily—CTLA-4. Nature *328*, 267-270.

Bruno, A., Bassani, B., D'Urso, D.G., Pitaku, I., Cassinotti, E., Pelosi, G., Boni, L., Dominioni, L., Noonan, D.M., Mortara, L.*, et al.* (2018). Angiogenin and the MMP9-TIMP2 axis are up-regulated in proangiogenic, decidual NK-like cells from patients with colorectal cancer. Faseb j *32*, 5365-5377.

Bruno, A., Focaccetti, C., Pagani, A., Imperatori, A.S., Spagnoletti, M., Rotolo, N., Cantelmo, A.R., Franzi, F., Capella, C., Ferlazzo, G.*, et al.* (2013). The proangiogenic phenotype of natural killer cells in patients with non-small cell lung cancer. Neoplasia (New York, NY) *15*, 133-142.

Buck, M.D., O'Sullivan, D., Klein Geltink, R.I., Curtis, J.D., Chang, C.H., Sanin, D.E., Qiu, J., Kretz, O., Braas, D., van der Windt, G.J.*, et al.* (2016). Mitochondrial dynamics controls T cell fate through metabolic programming. Cell *166*, 63-76.

Bulmer, J.N., Morrison, L., Longfellow, M., Ritson, A., and Pace, D. (1991). Granulated lymphocytes in human endometrium: histochemical and immunohistochemical studies. Hum Reprod *6*, 791-798.

Burnet, F.M. (1970). The concept of immunological surveillance. Prog Exp Tumor Res *13*, 1-27.

Burnet, M. (1964). IMMUNOLOGICAL FACTORS IN THE PROCESS OF CARCINOGENESIS. Br Med Bull *20*, 154-158.

Caligiuri, M.A. (2008). Human natural killer cells. Blood *112*, 461-469.

Campbell, K.S., and Purdy, A.K. (2011). Structure/function of human killer cell immunoglobulin-like receptors: lessons from polymorphisms, evolution, crystal structures and mutations. Immunology *132*, 315-325.

Carlino, M.S., Larkin, J., and Long, G.V. (2021). Immune checkpoint inhibitors in melanoma. The Lancet *398*, 1002-1014.

Carrega, P., Bonaccorsi, I., Di Carlo, E., Morandi, B., Paul, P., Rizzello, V., Cipollone, G., Navarra, G., Mingari, M.C., Moretta, L.*, et al.* (2014). CD56(bright)perforin(low) noncytotoxic human NK cells are abundant in both healthy and neoplastic solid tissues and recirculate to secondary lymphoid organs via afferent lymph. J Immunol *192*, 3805-3815.

Carrega, P., Morandi, B., Costa, R., Frumento, G., Forte, G., Altavilla, G., Ratto, G.B., Mingari, M.C., Moretta, L., and Ferlazzo, G. (2008). Natural killer cells infiltrating human nonsmall-cell lung cancer are enriched in CD56 bright CD16(-) cells and display an impaired capability to kill tumor cells. Cancer *112*, 863-875.

CCSAC (2021). Canadian Cancer Statistics Advisory Committee in collaboration with the Canadian Cancer Society, Statistics Canada and the Public Health Agency of Canada. Canadian Cancer Statistics 2021. Toronto, ON: Canadian Cancer Society; 2021.

Chang, C.H., Curtis, J.D., Maggi, L.B.J., Faubert, B., Villarino, A.V., O'Sullivan, D., Huang, S.C., van der Windt, G.J., Blagih, J., Qiu, J.*, et al.* (2013). Posttranscriptional control of T cell effector function by aerobic glycolysis. Cell *153*, 1239-1251.

Cichocki, F., Bjordahl, R., Gaidarova, S., Mahmood, S., Abujarour, R., Wang, H., Tuininga, K., Felices, M., Davis, Z.B., Bendzick, L.*, et al.* (2020). iPSC-derived NK cells maintain high

cytotoxicity and enhance in vivo tumor control in concert with T cells and anti-PD-1 therapy. Sci Transl Med *12*.

Ciurea, S.O., Schafer, J.R., Bassett, R., Denman, C.J., Cao, K., Willis, D., Rondon, G., Chen, J., Soebbing, D., Kaur, I.*, et al.* (2017). Phase 1 clinical trial using mbIL21 ex-vivo expanded donor-derived NK cells after haploidentical transplantation. Blood, pii: blood-2017-2005-785659.

Coca, S., Perez-Piqueras, J., Martinez, D., Colmenarejo, A., Saez, M.A., Vallejo, C., Martos, J.A., and Moreno, M. (1997). The prognostic significance of intratumoral natural killer cells in patients with colorectal carcinoma. Cancer *79*, 2320-2328.

Commisso, C., Davidson, S.M., Soydaner-Azeloglu, R.G., Parker, S.J., Kamphorst, J.J., Hackett, S., Grabocka, E., Nofal, M., Drebin, J.A., Thompson, C.B.*, et al.* (2013). Macropinocytosis of protein is an amino acid supply route in Ras-transformed cells. Nature *497*, 633-637.

Cooper, M.A., Fehniger, T.A., and Caligiuri, M.A. (2001). The biology of human natural killer-cell subsets. Trends Immunol *22*, 633-640.

Corbet, C., Pinto, A., Martherus, R., Santiago de Jesus, J.P., Polet, F., and Feron, O. (2016). Acidosis Drives the Reprogramming of Fatty Acid Metabolism in Cancer Cells through Changes in Mitochondrial and Histone Acetylation. Cell Metab *24*, 311-323.

Crome, S.Q., Nguyen, L.T., Lopez-Verges, S., Yang, S.Y., Martin, B., Yam, J.Y., Johnson, D.J., Nie, J., Pniak, M., Yen, P.H.*, et al.* (2017). A distinct innate lymphoid cell population regulates tumor-associated T cells. Nat Med *23*, 368-375.

Delorme, E.J., and Alexander, P. (1964). TREATMENT OF PRIMARY FIBROSARCOMA IN THE RAT WITH IMMUNE LYMPHOCYTES. Lancet *2*, 117-120.

deMagalhaes-Silverman, M., Donnenberg, A., Lembersky, B., Elder, E., Lister, J., Rybka, W., Whiteside, T., and Ball, E. (2000). Posttransplant adoptive immunotherapy with activated natural killer cells in patients with metastatic breast cancer. Journal of immunotherapy (Hagerstown, Md : 1997) *23*, 154-160.

Denman, C.J., Senyukov, V.V., Somanchi, S.S., Phatarpekar, P.V., Kopp, L.M., Johnson, J.L., Singh, H., Hurton, L., Maiti, S.N., Huls, M.H.*, et al.* (2012). Membrane-bound IL-21 promotes sustained ex vivo proliferation of human natural killer cells. PLoS One *7*, e30264.

Dietel, M., Savelov, N., Salanova, R., Micke, P., Bigras, G., Hida, T., Antunez, J., Guldhammer Skov, B., Hutarew, G., Sua, L.F.*, et al.* (2019). Real-world prevalence of programmed death ligand 1 expression in locally advanced or metastatic non-small-cell lung cancer: The global, multicenter EXPRESS study. Lung cancer (Amsterdam, Netherlands) *134*, 174-179.

Dogra, P., Rancan, C., Ma, W., Toth, M., Senda, T., Carpenter, D.J., Kubota, M., Matsumoto, R., Thapa, P., Szabo, P.A.*, et al.* (2020). Tissue Determinants of Human NK Cell Development, Function, and Residence. Cell *180*, 749-763.e713.

Dong, H., Strome, S.E., Salomao, D.R., Tamura, H., Hirano, F., Flies, D.B., Roche, P.C., Lu, J., Zhu, G., Tamada, K.*, et al.* (2002). Tumor-associated B7-H1 promotes T-cell apoptosis: a potential mechanism of immune evasion. Nat Med *8*, 793-800.

Dong, H.P., Elstrand, M.B., Holth, A., Silins, I., Berner, A., Trope, C.G., Davidson, B., and Risberg, B. (2006). NK- and B-cell infiltration correlates with worse outcome in metastatic ovarian carcinoma. American journal of clinical pathology *125*, 451-458.

Donnelly, R.P., Loftus, R.M., Keating, S.E., Liou, K.T., Biron, C.A., Gardiner, C.M., and Finlay, D.K. (2014a). mTORC1-dependent metabolic reprogramming Is
a prerequisite for NK cell effector function. J Immunol *193*, 4477-4484.

Donnelly, R.P., Loftus, R.M., Keating, S.E., Liou, K.T., Biron, C.A., Gardiner, C.M., and Finlay, D.K. (2014b). mTORC1-dependent metabolic reprogramming is a prerequisite for NK cell effector function. J Immunol *193*, 4477-4484.

Dunn, G.P., Bruce, A.T., Ikeda, H., Old, L.J., and Schreiber, R.D. (2002). Cancer immunoediting: from immunosurveillance to tumor escape. Nature Immunology *3*, 991-998.

Eberhardy, S.R., and Farnham, P.J. (2001). c-Myc mediates activation of the cad promoter via a post-RNA polymerase II recruitment mechanism. J Biol Chem *276*, 48562-48571.

Ehrlich, P. (1908). Über den jetzigen Stand der Karzinomforschung.

El-Khoueiry, A.B., Sangro, B., Yau, T., Crocenzi, T.S., Kudo, M., Hsu, C., Kim, T.Y., Choo, S.P., Trojan, J., Welling, T.H.R.*, et al.* (2017). Nivolumab in patients with advanced hepatocellular carcinoma (CheckMate 040): an open-label, non-comparative, phase 1/2 dose escalation and expansion trial. Lancet *389*, 2492-2502.

Fefer, A. (1969). Immunotherapy and chemotherapy of Moloney sarcoma virus-induced tumors in mice. Cancer Res *29*, 2177-2183.

Fehniger, T.A., Shah, M.H., Turner, M.J., VanDeusen, J.B., Whitman, S.P., Cooper, M.A., Suzuki, K., Wechser, M., Goodsaid, F., and Caligiuri, M.A. (1999). Differential cytokine and chemokine gene expression by human NK cells following activation with IL-18 or IL-15 in combination with IL-12: implications for the innate immune response. J Immunol *162*, 4511-4520.

Ferlay, J., Colombet, M., Soerjomataram, I., Parkin, D.M., Piñeros, M., Znaor, A., and Bray, F. (2021). Cancer statistics for the year 2020: An overview. Int J Cancer.

Fernandez-Cruz, E., Woda, B.A., and Feldman, J.D. (1980). Elimination of syngeneic sarcomas in rats by a subset of T lymphocytes. Journal of Experimental Medicine *152*, 823-841.

Ferris, R.L., Blumenschein, G., Jr., Fayette, J., Guigay, J., Colevas, A.D., Licitra, L., Harrington, K., Kasper, S., Vokes, E.E., Even, C.*, et al.* (2016). Nivolumab for Recurrent Squamous-Cell Carcinoma of the Head and Neck. The New England journal of medicine *375*, 1856-1867.

Fischer, K., Hoffmann, P., Voelkl, S., Meidenbauer, N., Ammer, J., Edinger, M., Gottfried, E., Schwarz, S., Rothe, G., Hoves, S.*, et al.* (2007). Inhibitory effect of tumor cell-derived lactic acid on human T cells. Blood *109*, 3812-3819.

Freeman, G.J., Long, A.J., Iwai, Y., Bourque, K., Chernova, T., Nishimura, H., Fitz, L.J., Malenkovich, N., Okazaki, T., Byrne, M.C.*, et al.* (2000). Engagement of the PD-1 immunoinhibitory receptor by a novel B7 family member leads to negative regulation of lymphocyte activation. J Exp Med *192*, 1027-1034.

Freud, A.G., Mundy-Bosse, B.L., Yu, J., and Caligiuri, M.A. (2017). The Broad Spectrum of Human Natural Killer Cell Diversity. Immunity *47*, 820-833.

Fujisaki, H., Kakuda, H., Shimasaki, N., Imai, C., Ma, J., Lockey, T., Eldridge, P., Leung, W.H., and Campana, D. (2009). Expansion of highly cytotoxic human natural killer cells for cancer cell therapy. Cancer Res *69*, 4010-4017.

Galon, J., Costes, A., Sanchez-Cabo, F., Kirilovsky, A., Mlecnik, B., Lagorce-Pagès, C., Tosolini, M., Camus, M., Berger, A., Wind, P.*, et al.* (2006). Type, density, and location of immune cells within human colorectal tumors predict clinical outcome. Science *313*, 1960-1964.

Gao, P., Tchernyshyov, I., Chang, T.C., Lee, Y.S., Kita, K., Ochi, T., Zeller, K.I., De Marzo, A.M., Van Eyk, J.E., Mendell, J.T.*, et al.* (2009). c-Myc suppression of miR-23a/b enhances mitochondrial glutaminase expression and glutamine metabolism. Nature *458*, 762-765.

Garon, E.B., Rizvi, N.A., Hui, R., Leighl, N., Balmanoukian, A.S., Eder, J.P., Patnaik, A., Aggarwal, C., Gubens, M., Horn, L.*, et al.* (2015). Pembrolizumab for the treatment of non-small-cell lung cancer. The New England journal of medicine *372*, 2018-2028.

Gatti, R.A., and Good, R.A. (1971). Occurrence of malignancy in immunodeficiency diseases. A literature review. Cancer *28*, 89-98.

Geller, M.A., and Miller, J.S. (2011). Use of allogeneic NK cells for cancer immunotherapy. Immunotherapy *3*, 1445-1459.

Genestreti, G., Grossi, F., Genova, C., Burgio, M.A., Bongiovanni, A., Gavelli, G., Bartolotti, M., Di Battista, M., Cavallo, G., and Brandes, A.A. (2014). Third- and further-line therapy in advanced non-small-cell lung cancer patients: an overview. Future Oncology *10*, 2081+.

Gong, J., Chehrazi-Raffle, A., Reddi, S., and Salgia, R. (2018). Development of PD-1 and PD-L1 inhibitors as a form of cancer immunotherapy: a comprehensive review of registration trials and future considerations. Journal for immunotherapy of cancer *6*, 8.

Gong, W., Xiao, W., Hu, M., Weng, X., Qian, L., Pan, X., and Ji, M. (2010). Ex vivo expansion of natural killer cells with high cytotoxicity by K562 cells modified to co-express major histocompatibility complex class I chain-related protein A, 4-1BB ligand, and interleukin-15. Tissue Antigens *76*, 467-475.

Gonzalez, V.D., Huang, Y.W., Delgado-Gonzalez, A., Chen, S.Y., Donoso, K., Sachs, K., Gentles, A.J., Allard, G.M., Kolahi, K.S., Howitt, B.E.*, et al.* (2021). High-grade serous ovarian tumor cells modulate NK cell function to create an immune-tolerant microenvironment. Cell reports *36*, 109632.

Grimm, E.A., Mazumder, A., Zhang, H.Z., and Rosenberg, S.A. (1982). Lymphokine-activated killer cell phenomenon. Lysis of natural killer-resistant fresh solid tumor cells by interleukin 2-activated autologous human peripheral blood lymphocytes. J Exp Med *155*, 1823-1841.

Grupp, S.A., Kalos, M., Barrett, D., Aplenc, R., Porter, D.L., Rheingold, S.R., Teachey, D.T., Chew, A., Hauck, B., Wright, J.F.*, et al.* (2013). Chimeric antigen receptor-modified T cells for acute lymphoid leukemia. The New England journal of medicine *368*, 1509-1518.

Guerra, N., Tan, Y.X., Joncker, N.T., Choy, A., Gallardo, F., Xiong, N., Knoblaugh, S., Cado, D., Greenberg, N.M., and Raulet, D.H. (2008). NKG2D-deficient mice are defective in tumor surveillance in models of spontaneous malignancy. Immunity *28*, 571-580.

Hanna, J., Goldman-Wohl, D., Hamani, Y., Avraham, I., Greenfield, C., Natanson-Yaron, S., Prus, D., Cohen-Daniel, L., Arnon, T.I., Manaster, I.*, et al.* (2006). Decidual NK cells regulate key developmental processes at the human fetal-maternal interface. Nat Med *12*, 1065-1074.

Hansen, J.M., Coleman, R.L., and Sood, A.K. (2016). Targeting the tumour microenvironment in ovarian cancer. Eur J Cancer *56*, 131-143.

Havel, J.J., Chowell, D., and Chan, T.A. (2019). The evolving landscape of biomarkers for checkpoint inhibitor immunotherapy. Nat Rev Cancer *19*, 133-150.

Hawkins, M.J., Atkins, M.B., Dutcher, J.P., Fisher, R.I., Weiss, G.R., Margolin, K.A., Rayner, A.A., Sznol, M., Parkinson, D.R., Paietta, E.*, et al.* (1994). A phase II clinical trial of interleukin-2 and lymphokine-activated killer cells in advanced colorectal carcinoma. J Immunother Emphasis Tumor Immunol *15*, 74-78.

Herberman, R.B., Nunn, M.E., Holden, H.T., and Lavrin, D.H. (1975). Natural cytotoxic reactivity of mouse lymphoid cells against syngeneic and allogeneic tumors. II. Characterization of effector cells. Int J Cancer *16*, 230-239.

Herbst, R.S., Morgensztern, D., and Boshoff, C. (2018). The biology and management of non-small cell lung cancer. Nature *553*, 446-454.

Herbst, R.S., Soria, J.C., Kowanetz, M., Fine, G.D., Hamid, O., Gordon, M.S., Sosman, J.A., McDermott, D.F., Powderly, J.D., Gettinger, S.N.*, et al.* (2014). Predictive correlates of response to the anti-PD-L1 antibody MPDL3280A in cancer patients. Nature *515*, 563-567.

Heuvers, M.E., Hegmans, J.P., Stricker, B.H., and Aerts, J.G. (2012). Improving lung cancer survival; time to move on. BMC Pulmonary Medicine *12*, 77-77.

Hill, J.A., Giralt, S., Torgerson, T.R., and Lazarus, H.M. (2019). CAR-T - and a side order of IgG, to go? - Immunoglobulin replacement in patients receiving CAR-T cell therapy. Blood Rev *38*, 100596.

Hodi, F.S., Butler, M., Oble, D.A., Seiden, M.V., Haluska, F.G., Kruse, A., Macrae, S., Nelson, M., Canning, C., Lowy, I.*, et al.* (2008). Immunologic and clinical effects of antibody blockade of cytotoxic T lymphocyte-associated antigen 4 in previously vaccinated cancer patients. Proc Natl Acad Sci U S A *105*, 3005-3010.

Hodi, F.S., O'Day, S.J., McDermott, D.F., Weber, R.W., Sosman, J.A., Haanen, J.B., Gonzalez, R., Robert, C., Schadendorf, D., Hassel, J.C.*, et al.* (2010). Improved survival with ipilimumab in patients with metastatic melanoma. The New England journal of medicine *363*, 711-723.

Howlader, N., Noone, A.M., Krapcho, M., Miller, D., Brest, A., Yu, M., Ruhl, J., Tatalovich, Z., Mariotto, A., Lewis, D.R.*, et al.* (2019). SEER Cancer Statistic Review (Bethesda, MD: National Cancer Institute).

Hui, E., Cheung, J., Zhu, J., Su, X., Taylor, M.J., Wallweber, H.A., Sasmal, D.K., Huang, J., Kim, J.M., Mellman, I.*, et al.* (2017). T cell costimulatory receptor CD28 is a primary target for PD-1-mediated inhibition. Science *355*, 1428-1433.

Imai, K., Matsuyama, S., Miyake, S., Suga, K., and Nakachi, K. (2000). Natural cytotoxic activity of peripheral-blood lymphocytes and cancer incidence: an 11-year follow-up study of a general population. Lancet *356*, 1795-1799.

Ishigami, S., Natsugoe, S., Tokuda, K., Nakajo, A., Che, X., Iwashige, H., Aridome, K., Hokita, S., and Aikou, T. (2000). Prognostic value of intratumoral natural killer cells in gastric carcinoma. Cancer *88*, 577-583.

Jha, Abhishek K., Huang, Stanley C.-C., Sergushichev, A., Lampropoulou, V., Ivanova, Y., Loginicheva, E., Chmielewski, K., Stewart, Kelly M., Ashall, J., Everts, B.*, et al.* Network integration of parallel metabolic and transcriptional data reveals metabolic modules that regulate macrophage polarization. Immunity *42*, 419-430.

Jin, J., Fu, B., Mei, X., Yue, T., Sun, R., Tian, Z., and Wei, H. (2013). CD11b(-)CD27(-) NK cells are associated with the progression of lung carcinoma. PLoS One *8*, e61024.

Johnson, L.A., Morgan, R.A., Dudley, M.E., Cassard, L., Yang, J.C., Hughes, M.S., Kammula, U.S., Royal, R.E., Sherry, R.M., Wunderlich, J.R.*, et al.* (2009). Gene therapy with human and mouse T-cell receptors mediates cancer regression and targets normal tissues expressing cognate antigen. Blood *114*, 535-546.

Juluri, K.R., Wu, Q.V., Voutsinas, J., Hou, J., Hirayama, A.V., Mullane, E., Miles, N., Maloney, D.G., Turtle, C.J., Bar, M.*, et al.* (2022). Severe cytokine release syndrome is associated with hematologic toxicity following CD19 CAR T-cell therapy. Blood Adv *6*, 2055-2068.

Kalos, M., Levine, B.L., Porter, D.L., Katz, S., Grupp, S.A., Bagg, A., and June, C.H. (2011). T cells with chimeric antigen receptors have potent antitumor effects and can establish memory in patients with advanced leukemia. Sci Transl Med *3*, 95ra73.

Kamphorst, A.O., Wieland, A., Nasti, T., Yang, S., Zhang, R., Barber, D.L., Konieczny, B.T., Daugherty, C.Z., Koenig, L., Yu, K.*, et al.* (2017). Rescue of exhausted CD8 T cells by PD-1-targeted therapies is CD28-dependent. Science *355*, 1423-1427.

Kawalekar, O.U., O'Connor, R.S., Fraietta, J.A., Guo, L., McGettigan, S.E., Posey, A.D., Patel, P.R., Guedan, S., Scholler, J., Keith, B.*, et al.* (2016). Distinct Signaling of Coreceptors Regulates Specific Metabolism Pathways and Impacts Memory Development in CAR T Cells. Immunity *44*, 380-390.

Kazandjian, D., Suzman, D.L., Blumenthal, G., Mushti, S., He, K., Libeg, M., Keegan, P., and Pazdur, R. (2016). FDA Approval Summary: Nivolumab for the Treatment of Metastatic Non-Small Cell Lung Cancer With Progression On or After Platinum-Based Chemotherapy. Oncologist *21*, 634-642.

Keating, S.E., Zaiatz-Bittencourt, V., Loftus, R.M., Keane, C., Brennan, K., Finlay, D.K., and Gardiner, C.M. (2016). Metabolic Reprogramming Supports IFN-γ Production by CD56bright NK Cells. J Immunol *196*, 2552-2560.

Keppel, M.P., Saucier, N., Mah, A.Y., Vogel, T.P., and Cooper, M.A. (2015). Activation-specific metabolic requirements for NK cell IFN-g production. J Immunol *194*, 1954-1962.

Kiessling, R., Klein, E., Pross, H., and Wigzell, H. (1975a). "Natural" killer cells in the mouse. II. Cytotoxic cells with specificity for mouse Moloney leukemia cells. Characteristics of the killer cell. Eur J Immunol *5*, 117-121.

Kiessling, R., Klein, E., and Wigzell, H. (1975b). "Natural" killer cells in the mouse. I. Cytotoxic cells with specificity for mouse Moloney leukemia cells. Specificity and distribution according to genotype. Eur J Immunol *5*, 112-117.

Kim, E.K., Ahn, Y.O., Kim, S., Kim, T.M., Keam, B., and Heo, D.S. (2013). Ex vivo activation and expansion of natural killer cells from patients with advanced cancer with feeder cells from healthy volunteers. Cytotherapy *15*, 231-241.e231.

Klingemann, H.G., and Martinson, J. (2004). Ex vivo expansion of natural killer cells for clinical applications. Cytotherapy *6*, 15-22.

Kochenderfer, J.N., Dudley, M.E., Kassim, S.H., Somerville, R.P., Carpenter, R.O., Stetler-Stevenson, M., Yang, J.C., Phan, G.Q., Hughes, M.S., Sherry, R.M.*, et al.* (2015). Chemotherapy-refractory diffuse large B-cell lymphoma and indolent B-cell malignancies can be effectively treated with autologous T cells expressing an anti-CD19 chimeric antigen receptor. J Clin Oncol *33*, 540-549.

Kuroki, L., and Guntupalli, S.R. (2020). Treatment of epithelial ovarian cancer. Bmj *371*, m3773.

Lai, P., Rabinowich, H., Crowley-Nowick, P.A., Bell, M.C., Mantovani, G., and Whiteside, T.L. (1996). Alterations in expression and function of signal-transducing proteins in tumor-associated T and natural killer cells in patients with ovarian carcinoma. Clin Cancer Res *2*, 161-173.

Lamers, C.H., Sleijfer, S., van Steenbergen, S., van Elzakker, P., van Krimpen, B., Groot, C., Vulto, A., den Bakker, M., Oosterwijk, E., Debets, R.*, et al.* (2013). Treatment of metastatic renal cell carcinoma with CAIX CAR-engineered T cells: clinical evaluation and management of on-target toxicity. Mol Ther *21*, 904-912.

Lanier, L.L., Le, A.M., Civin, C.I., Loken, M.R., and Phillips, J.H. (1986). The relationship of CD16 (Leu-11) and Leu-19 (NKH-1) antigen expression on human peripheral blood NK cells and cytotoxic T lymphocytes. J Immunol *136*, 4480-4486.

Latchman, Y., Wood, C.R., Chernova, T., Chaudhary, D., Borde, M., Chernova, I., Iwai, Y., Long, A.J., Brown, J.A., Nunes, R.*, et al.* (2001). PD-L2 is a second ligand for PD-1 and inhibits T cell activation. Nat Immunol *2*, 261-268.

Le Dréan, E., Vély, F., Olcese, L., Cambiaggi, A., Guia, S., Krystal, G., Gervois, N., Moretta, A., Jotereau, F., and Vivier, E. (1998). Inhibition of antigen-induced T cell response and antibody-induced NK cell cytotoxicity by NKG2A: association of NKG2A with SHP-1 and SHP-2 protein-tyrosine phosphatases. Eur J Immunol *28*, 264-276.

Leach, D.R., Krummel, M.F., and Allison, J.P. (1996). Enhancement of antitumor immunity by CTLA-4 blockade. Science *271*, 1734-1736.

Levi, I., Amsalem, H., Nissan, A., Darash-Yahana, M., Peretz, T., Mandelboim, O., and Rachmilewitz, J. (2015). Characterization of tumor infiltrating natural killer cell subset. Oncotarget *6*, 13835-13843.

Li, J., Wang, J., Chen, R., Bai, Y., and Lu, X. (2017). The prognostic value of tumor-infiltrating T lymphocytes in ovarian cancer. Oncotarget *8*, 15621-15631.

Linsley, P.S., Brady, W., Urnes, M., Grosmaire, L.S., Damle, N.K., and Ledbetter, J.A. (1991). CTLA-4 is a second receptor for the B cell activation antigen B7. J Exp Med *174*, 561-569.

Linsley, P.S., Greene, J.L., Brady, W., Bajorath, J., Ledbetter, J.A., and Peach, R. (1994). Human B7-1 (CD80) and B7-2 (CD86) bind with similar avidities but distinct kinetics to CD28 and CTLA-4 receptors. Immunity *1*, 793-801.

Locasale, J.W., and Cantley, L.C. (2011). Metabolic flux and the regulation of mammalian cell growth. Cell Metab *14*, 443-451.

Loftus, R.M., Assmann, N., Kedia-Mehta, N., O'Brien, K.L., Garcia, A., Gillespie, C., Hukelmann, J.L., Oefner, P.J., Lamond, A.I., Gardiner, C.M.*, et al.* (2018). Amino acid-

dependent cMyc expression is essential for NK cell metabolic and functional responses in mice. Nat Commun *9*, 2341.

Lotze, M.T., Grimm, E.A., Mazumder, A., Strausser, J.L., and Rosenberg, S.A. (1981). Lysis of fresh and cultured autologous tumor by human lymphocytes cultured in T-cell growth factor. Cancer Res *41*, 4420-4425.

Lowe, K.A., Chia, V.M., Taylor, A., O'Malley, C., Kelsh, M., Mohamed, M., Mowat, F.S., and Goff, B. (2013). An international assessment of ovarian cancer incidence and mortality. Gynecol Oncol *130*, 107-114.

Lunemann, S., Langeneckert, A.E., Martrus, G., Hess, L.U., Salzberger, W., Ziegler, A.E., Lobl, S.M., Poch, T., Ravichandran, G., Sauter, J.*, et al.* (2019). Human liver-derived CXCR6(+) NK cells are predominantly educated through NKG2A and show reduced cytokine production. J Leukoc Biol, [Epub ahead of print].

Mahajan, D., Sharma, N.R., Kancharla, S., Kolli, P., Tripathy, A., Sharma, A.K., Singh, S., Kumar, S., Mohanty, A.K., and Jena, M.K. (2022). Role of Natural Killer Cells during Pregnancy and Related Complications. Biomolecules *12*, 68.

Maher, J., Brentjens, R.J., Gunset, G., Rivière, I., and Sadelain, M. (2002). Human T-lymphocyte cytotoxicity and proliferation directed by a single chimeric TCRzeta /CD28 receptor. Nat Biotechnol *20*, 70-75.

Mannava, S., Grachtchouk, V., Wheeler, L.J., Im, M., Zhuang, D., Slavina, E.G., Mathews, C.K., Shewach, D.S., and Nikiforov, M.A. (2008). Direct role of nucleotide metabolism in C-MYC-dependent proliferation of melanoma cells. Cell Cycle *7*, 2392-2400.

Mao, Y., van Hoef, V., Zhang, X., Wennerberg, E., Lorent, J., Witt, K., Sanz, L.M., Liang, S., Murray, S., LArsson, O.*, et al.* (2016). IL-15 activates mTOR and primes stress-activated gene-expression leading to

prolonged anti-tumor capacity of NK cells. Blood *128*, 1475-1489.

Marçais, A., Viel, S., Grau, M., Henry, T., Marvel, J., and Walzer, T. (2013). Regulation of mouse NK cell development and function by cytokines. Front Immunol *4*, 450.

Maringe, C., Walters, S., Butler, J., Coleman, M.P., Hacker, N., Hanna, L., Mosgaard, B.J., Nordin, A., Rosen, B., Engholm, G.*, et al.* (2012). Stage at diagnosis and ovarian cancer survival: evidence from the International Cancer Benchmarking Partnership. Gynecol Oncol *127*, 75-82.

Markman, M., Markman, J., Webster, K., Zanotti, K., Kulp, B., Peterson, G., and Belinson, J. (2004a). Duration of response to second-line, platinum-based chemotherapy for ovarian cancer: implications for patient management and clinical trial design. J Clin Oncol *22*, 3120-3125.

Markman, M., Webster, K., Zanotti, K., Peterson, G., Kulp, B., and Belinson, J. (2004b). Survival following the documentation of platinum and taxane resistance in ovarian cancer: a single institution experience involving multiple phase 2 clinical trials. Gynecol Oncol *93*, 699-701.

Meyer-Monard, S., Passweg, J., Siegler, U., Kalberer, C., Koehl, U., Rovó, A., Halter, J., Stern, M., Heim, D., Alois Gratwohl, J.R.*, et al.* (2009). Clinical-grade purification of natural killer cells in haploidentical hematopoietic stem cell transplantation. Transfusion *49*, 362-371.

Michalek, R.D., Gerriets, V.A., Jacobs, S.R., Macintyre, A.N., N.J., M., Mason, E.F., Sullivan, S.A., G., N.A., and Rathmell, J.C. (2011). Cutting edge: distinct glycolytic and lipid oxidative

metabolic programs are essential for effector and regulatory CD4+ T cell subsets. J Immunol *186*, 3299-3303.

Miller, J.S., Soignier, Y., Panoskaltsis-Mortari, A., McNearney, S.A., Yun, G.H., Fautsch, S.K., McKenna, D., Le, C., Defor, T.E., Burns, L.J.*, et al.* (2005). Successful adoptive transfer and in vivo expansion of human haploidentical NK cells in patients with cancer. Blood *105*, 3051-3057.

Mithoowani, H., and Febbraro, M. (2022). Non-Small-Cell Lung Cancer in 2022: A Review for General Practitioners in Oncology. Curr Oncol *29*, 1828-1839.

Mizuno, R., Sugiura, D., Shimizu, K., Maruhashi, T., Watada, M., Okazaki, I.M., and Okazaki, T. (2019). PD-1 Primarily Targets TCR Signal in the Inhibition of Functional T Cell Activation. Front Immunol *10*, 630.

Morgan, R.A., Chinnasamy, N., Abate-Daga, D., Gros, A., Robbins, P.F., Zheng, Z., Dudley, M.E., Feldman, S.A., Yang, J.C., Sherry, R.M.*, et al.* (2013). Cancer regression and neurological toxicity following anti-MAGE-A3 TCR gene therapy. Journal of immunotherapy (Hagerstown, Md : 1997) *36*, 133-151.

Motzer, R.J., Escudier, B., McDermott, D.F., George, S., Hammers, H.J., Srinivas, S., Tykodi, S.S., Sosman, J.A., Procopio, G., Plimack, E.R.*, et al.* (2015). Nivolumab versus Everolimus in Advanced Renal-Cell Carcinoma. The New England journal of medicine *373*, 1803-1813.

Muul, L.M., Spiess, P.J., Director, E.P., and Rosenberg, S.A. (1987). Identification of specific cytolytic immune responses against autologous tumor in humans bearing malignant melanoma. J Immunol *138*, 989-995.

Neelapu, S.S., Locke, F.L., Bartlett, N.L., Lekakis, L.J., Miklos, D.B., Jacobson, C.A., Braunschweig, I., Oluwole, O.O., Siddiqi, T., Lin, Y.*, et al.* (2017). Axicabtagene Ciloleucel

CAR T-Cell Therapy in Refractory Large B-Cell Lymphoma. The New England journal of medicine *377*, 2531-2544.

Neo, S.Y., Yang, Y., Record, J., Ma, R., Chen, X., Chen, Z., Tobin, N.P., Blake, E., Seitz, C., Thomas, R.*, et al.* (2020). CD73 immune checkpoint defines regulatory NK cells within the tumor microenvironment. J Clin Invest *130*, 1185-1198.

Nham, T., Poznanski, S.M., Fan, I.Y., Vahedi, F., Shenouda, M.M., Lee, A.J., Chew, M.V., Hogg, R.T., Lee, D.A., and Ashkar, A.A. (2018). Ex Vivo-expanded Natural Killer Cells Derived From Long-term Cryopreserved Cord Blood are Cytotoxic Against Primary Breast Cancer Cells. Journal of immunotherapy (Hagerstown, Md : 1997) *41*, 64-72.

Nieman, K.M., Kenny, H.A., Penicka, C.V., Ladanyi, A., Buell-Gutbrod, R., Zillhardt, M.R., Romero, I.L., Carey, M.S., Mills, G.B., Hotamisligil, G.S.*, et al.* (2011). Adipocytes promote ovarian cancer metastasis and provide energy for rapid tumor growth. Nat Med *17*, 1498-1503.

Nishimura, H., Okazaki, T., Tanaka, Y., Nakatani, K., Hara, M., Matsumori, A., Sasayama, S., Mizoguchi, A., Hiai, H., Minato, N.*, et al.* (2001). Autoimmune dilated cardiomyopathy in PD-1 receptor-deficient mice. Science *291*, 319-322.

O'Neill, L.A., Kishton, R.J., and Rathmell, J. (2016). A guide to immunometabolism for immunologists. Nat Rev Immunol *16*, 553-565.

O'Sullivan, D., van der Windt, G.J., Huang, S.C., Curtis, J.D., Chang, C.H., Buck, M.D., Qiu, J., Smith, A.M., Lam, W.Y., DiPlato, L.M.*, et al.* (2014). Memory CD8(+) T cells use cell-intrinsic lipolysis to support the metabolic programming necessary for development. Immunity *41*, 75-88.

Old, L.J., and Boyse, E.A. (1964). Immunology of experimental tumors. Annu Rev Med *15*, 167-186.

Orange, J.S. (2013). Natural killer cell deficiency. The Journal of allergy and clinical immunology *132*, 515-525.

Ott, P.A., Hodi, F.S., and Robert, C. (2013). CTLA-4 and PD-1/PD-L1 blockade: new immunotherapeutic modalities with durable clinical benefit in melanoma patients. Clin Cancer Res *19*, 5300-5309.

Pai-Scherf, L., Blumenthal, G.M., Li, H., Subramaniam, S., Mishra-Kalyani, P.S., He, K., Zhao, H., Yu, J., Paciga, M., Goldberg, K.B.*, et al.* (2017). FDA Approval Summary: Pembrolizumab for Treatment of Metastatic Non-Small Cell Lung Cancer: First-Line Therapy and Beyond. Oncologist *22*, 1392-1399.

Palm, W., Park, Y., Wright, K., Pavlova, N.N., Tuveson, D.A., and Thompson, C.B. (2015). The Utilization of Extracellular Proteins as Nutrients Is Suppressed by mTORC1. Cell *162*, 259-270.

Palm, W., and Thompson, C.B. (2017). Nutrient acquisition strategies of mammalian cells. Nature *546*, 234-242.

Park, J.H., Riviere, I., Gonen, M., Wang, X., Senechal, B., Curran, K.J., Sauter, C., Wang, Y., Santomasso, B., Mead, E.*, et al.* (2018). Long-Term Follow-up of CD19 CAR Therapy in Acute Lymphoblastic Leukemia. The New England journal of medicine *378*, 449-459.

Parkhurst, M.R., Riley, J.P., Dudley, M.E., and Rosenberg, S.A. (2011). Adoptive transfer of autologous natural killer cells leads to high levels of circulating natural killer cells but does not mediate tumor regression. Clin Cancer Res *17*, 6287-6297.

Parrish-Novak, J., Dillon, S.R., Nelson, A., Hammond, A., Sprecher, C., Gross, J.A., Johnston, J., Madden, K., Xu, W., West, J.*, et al.* (2000). Interleukin 21 and its receptor are involved in NK cell expansion and regulation of lymphocyte function. Nature *408*, 57-63.

Pavie-Fischer, J., Kourilsky, F.M., Picard, F., Banzet, P., and Puissant, A. (1975). Cytotoxicity of lymphocytes from healthy subjects and from melanoma patients against cultured melanoma cells. Clinical and experimental immunology *21*, 430-441.

Pearce, E.L., Walsh, M.C., Cejas, P.J., Harms, G.M., Shen, H., Wang, L.S., Jones, R.G., and Choi, Y. (2009). Enhancing CD8 T-cell memory by modulating fatty acid metabolism. Nature *460*, 103-107.

Penn, I. (1995). Sarcomas in organ allograft recipients. Transplantation *60*, 1485-1491.

Penn, I. (1996). Malignant melanoma in organ allograft recipients. Transplantation *61*, 274-278.

Platonova, S., Cherfils-Vicini, J., Damotte, D., Crozet, L., Vieillard, V., Validire, P., André, P., Dieu-Nosjean, M.C., Alifano, M., Régnard, J.F.*, et al.* (2011). Profound coordinated alterations of intratumoral NK cell phenotype and function in lung carcinoma. Cancer Res *71*, 5412-5422.

Porter, R., and Matulonis, U.A. (2022). Immunotherapy for ovarian cancer. Clin Adv Hematol Oncol *20*, 240-253.

Poznanski, S.M., and Ashkar, A.A. (2019). What Defines NK Cell Functional Fate: Phenotype or Metabolism? Front Immunol *10*, 1414.

Robert, C., Schachter, J., Long, G.V., Arance, A., Grob, J.J., Mortier, L., Daud, A., Carlino, M.S., McNeil, C., Lotem, M.*, et al.* (2015). Pembrolizumab versus Ipilimumab in Advanced Melanoma. The New England journal of medicine *372*, 2521-2532.

Robert, C., Thomas, L., Bondarenko, I., O'Day, S., Weber, J., Garbe, C., Lebbe, C., Baurain, J.-F., Testori, A., Grob, J.-J.*, et al.* (2011). Ipilimumab plus Dacarbazine for Previously Untreated Metastatic Melanoma. New England Journal of Medicine *364*, 2517-2526.

Rodriguez-Prados, J.C., Traves, P.G., Cuenca, J., Rico, D., Aragones, J., Martin-Sanz, P., Cascante, M., and Bosca, L. (2010). Substrate fate in activated macrophages: a comparison between innate, classic, and alternative activation. J Immunol *185*, 605-614.

Rosenberg, S.A., Lotze, M.T., Muul, L.M., Chang, A.E., Avis, F.P., Leitman, S., Linehan, W.M., Robertson, C.N., Lee, R.E., Rubin, J.T.*, et al.* (1987). A progress report on the treatment of 157 patients with advanced cancer using lymphokine-activated killer cells and interleukin-2 or high-dose interleukin-2 alone. The New England journal of medicine *316*, 889-897.

Rosenberg, S.A., Lotze, M.T., Yang, J.C., Topalian, S.L., Chang, A.E., Schwartzentruber, D.J., Aebersold, P., Leitman, S., Linehan, W.M., Seipp, C.A.*, et al.* (1993). Prospective randomized trial of high-dose interleukin-2 alone or in conjunction with lymphokine-activated killer cells for the treatment of patients with advanced cancer. J Natl Cancer Inst *85*, 622-632.

Rosenberg, S.A., Packard, B.S., Aebersold, P.M., Solomon, D., Topalian, S.L., Toy, S.T., Simon, P., Lotze, M.T., Yang, J.C., Seipp, C.A.*, et al.* (1988). Use of tumor-infiltrating lymphocytes and interleukin-2 in the immunotherapy of patients with metastatic melanoma. A preliminary report. The New England journal of medicine *319*, 1676-1680.

Rosenberg, S.A., and Restifo, N.P. (2015). Adoptive cell transfer as personalized immunotherapy for human cancer. Science *348*, 62-68.

Rosenberg, S.A., Yang, J.C., Sherry, R.M., Kammula, U.S., Hughes, M.S., Phan, G.Q., Citrin, D.E., Restifo, N.P., Robbins, P.F., Wunderlich, J.R.*, et al.* (2011). Durable complete responses in heavily pretreated patients with metastatic melanoma using T-cell transfer immunotherapy. Clin Cancer Res *17*, 4550-4557.

Rosenstein, M., Yron, I., Kaufmann, Y., and Rosenberg, S.A. (1984). Lymphokine-activated killer cells: lysis of fresh syngeneic natural killer-resistant murine tumor cells by lymphocytes cultured in interleukin 2. Cancer Res *44*, 1946-1953.

Rubnitz, J.E., Inaba, H., Ribeiro, R.C., Pounds, S., Rooney, B., Bell, T., Pui, C.H., and Leung, W. (2010). NKAML: a pilot study to determine the safety and feasibility of haploidentical natural killer cell transplantation in childhood acute myeloid leukemia. J Clin Oncol *28*, 955-959.

Ruggeri, L., Capanni, M., Urbani, E., Perruccio, K., Shlomchik, W.D., Tosti, A., Posati, S., Rogaia, D., Frassoni, F., Aversa, F.*, et al.* (2002). Effectiveness of donor natural killer cell alloreactivity in mismatched hematopoietic transplants. Science *295*, 2097-2100.

Sato, E., Olson, S.H., Ahn, J., Bundy, B., Nishikawa, H., Qian, F., Jungbluth, A.A., Frosina, D., Gnjatic, S., Ambrosone, C.*, et al.* (2005). Intraepithelial CD8+ tumor-infiltrating lymphocytes and a high CD8+/regulatory T cell ratio are associated with favorable prognosis in ovarian cancer. Proc Natl Acad Sci U S A *102*, 18538-18543.

Schuster, S.J., Bishop, M.R., Tam, C.S., Waller, E.K., Borchmann, P., McGuirk, J.P., Jäger, U., Jaglowski, S., Andreadis, C., Westin, J.R.*, et al.* (2019). Tisagenlecleucel in Adult Relapsed or Refractory Diffuse Large B-Cell Lymphoma. The New England journal of medicine *380*, 45-56.

Scoville, S.D., Freud, A.G., and Caligiuri, M.A. (2017). Modeling Human Natural Killer Cell Development in the Era of Innate Lymphoid Cells. Front Immunol *8*, 360.

Shankaran, V., Ikeda, H., Bruce, A.T., White, J.M., Swanson, P.E., Old, L.J., and Schreiber, R.D. (2001). IFNgamma and lymphocytes prevent primary tumour development and shape tumour immunogenicity. Nature *410*, 1107-1111.

Shi, J., Tricot, G., Szmania, S., Rosen, N., Garg, T.K., Malaviarachchi, P.A., Moreno, A., Dupont, B., Hsu, K.C., Baxter-Lowe, L.A.*, et al.* (2008). Infusion of haplo-identical killer

immunoglobulin-like receptor ligand mismatched NK cells for relapsed myeloma in the setting of autologous stem cell transplantation. Br J Haematol *143*, 641-653.

Siegler, U., Meyer-Monard, S., Jörger, S., Stern, M., Tichelli, A., Gratwohl, A., Wodnar-Filipowicz, A., and Kalberer, C.P. (2010). Good manufacturing practice-compliant cell sorting and large-scale expansion of single KIR-positive alloreactive human natural killer cells for multiple infusions to leukemia patients. Cytotherapy *12*, 750-763.

Siewiera, J., Gouilly, J., Hocine, H.R., Cartron, G., Levy, C., Al-Daccak, R., and Jabrane-Ferrat, N. (2015). Natural cytotoxicity receptor splice variants orchestrate the distinct functions of human natural killer cell subtypes. Nat Commun *6*, 10183.

Skak, K., Frederiksen, K.S., and Lundsgaard, D. (2008). Interleukin-21 activates human natural killer cells and modulates their surface receptor expression. Immunology *123*, 575-583.

Sonveaux, P., Végran, F., Schroeder, T., Wergin, M.C., Verrax, J., Rabbani, Z.N., De Saedeleer, C.J., Kennedy, K.M., Diepart, C., Jordan, B.F.*, et al.* (2008). Targeting lactate-fueled respiration selectively kills hypoxic tumor cells in mice. J Clin Invest *118*, 3930-3942.

Sparano, J.A., Fisher, R.I., Weiss, G.R., Margolin, K., Aronson, F.R., Hawkins, M.J., Atkins, M.B., Dutcher, J.P., Gaynor, E.R., Boldt, D.H.*, et al.* (1994). Phase II trials of high-dose interleukin-2 and lymphokine-activated killer cells in advanced breast carcinoma and carcinoma of the lung, ovary, and pancreas and other tumors. J Immunother Emphasis Tumor Immunol *16*, 216-223.

Street, S.E., Hayakawa, Y., Zhan, Y., Lew, A.M., MacGregor, D., Jamieson, A.M., Diefenbach, A., Yagita, H., Godfrey, D.I., and Smyth, M.J. (2004). Innate immune surveillance of spontaneous B cell lymphomas by natural killer cells and gammadelta T cells. J Exp Med *199*, 879-884.

Strohecker, A.M., Guo, J.Y., Karsli-Uzunbas, G., Price, S.M., Chen, G.J., Mathew, R., McMahon, M., and White, E. (2013). Autophagy sustains mitochondrial glutamine metabolism and growth of BrafV600E-driven lung tumors. Cancer discovery *3*, 1272-1285.

Sznol, M., Powderly, J.D., Smith, D.C., Brahmer, J.R., Drake, C.G., McDermott, D.F., Lawrence, D.P., Wolchok, J.D., Topalian, S.L., and Lowy, I. (2010). Safety and antitumor activity of biweekly MDX-1106 (Anti-PD-1, BMS-936558/ONO-4538) in patients with advanced refractory malignancies. Journal of Clinical Oncology *28*, 2506-2506.

Takeda, K., Hayakawa, Y., Smyth, M.J., Kayagaki, N., Yamaguchi, N., Kakuta, S., Iwakura, Y., Yagita, H., and Okumura, K. (2001). Involvement of tumor necrosis factor-related apoptosis-inducing ligand in surveillance of tumor metastasis by liver natural killer cells. Nat Med *7*, 94-100.

Tanizaki, Y., Kobayashi, A., Toujima, S., Shiro, M., Mizoguchi, M., Mabuchi, Y., Yagi, S., Minami, S., Takikawa, O., and Ino, K. (2014). Idoleamine 2,3-dioxygenase promotes peritoneal metastasis of ovarian cancer by inducing an immunosuppressive environment. Cancer Sci *105*, 966-973.

Topalian, S.L., Hodi, F.S., Brahmer, J.R., Gettinger, S.N., Smith, D.C., McDermott, D.F., Powderly, J.D., Carvajal, R.D., Sosman, J.A., Atkins, M.B.*, et al.* (2012). Safety, activity, and immune correlates of anti-PD-1 antibody in cancer. The New England journal of medicine *366*, 2443-2454.

Uyttenhove, C., Van Snick, J., and Boon, T. (1980). Immunogenic variants obtained by mutagenesis of mouse mastocytoma P815. I. Rejection by syngeneic mice. J Exp Med *152*, 1175-1183.

van der Windt, G.J., Everts, B., Chang, C.H., Curtis, J.D., Freitas, T.C., Amiel, E., Pearce, E.J., and Pearce, E.L. (2012). Mitochondrial respiratory capacity is a critical regulator of CD8+ T cell memory development. Immunity *31*, 68-78.

Vats, D., Mukundan, L., Odegaard, J.I., Zhang, L., Smith, K.L., Morel, C.R., Wagner, R.A., Greaves, D.R., Murray, P.J., and Chawla, A. (2006). Oxidative metabolism and PGC-1beta attenuate macrophage-mediated inflammation. Cell Metab *4*, 13-24.

Verma, S., King, A., and Loke, Y.W. (1997). Expression of killer cell inhibitory receptors on human uterine natural killer cells. Eur J Immunol *27*, 979-983.

Vgenopoulou, S., Lazaris, A.C., Markopoulos, C., Boltetsou, E., Kyriakou, V., Kavantzas, N., Patsouris, E., and Davaris, P.S. (2003). Immunohistochemical evaluation of immune response in invasive ductal breast cancer of not-otherwise-specified type. Breast *12*, 172-178.

Vici, P., Pizzuti, L., Natoli, C., Moscetti, L., Mentuccia, L., Vaccaro, A., Sergi, D., Di Lauro, L., Trenta, P., Seminara, P.*, et al.* (2014). Outcomes of HER2-positive early breast cancer patients in the pre-trastuzumab and trastuzumab eras: a real-world multicenter observational analysis. The RETROHER study. Breast cancer research and treatment *147*, 599-607.

Viel, S., Marçais, A., Guimaraes, F.S., Loftus, R., Rabilloud, J., Grau, M., Degouve, S., Djebali, S., SanIaville, A., Charrier, E.*, et al.* (2016). TGF-β inhibits the activation and functions of NK cells by repressing the mTOR pathway. Sci Signal *9*, ra19.

Villegas, F.R., Coca, S., Villarrubia, V.G., Jiménez, R., Chillón, M.J., Jareño, J., Zuil, M., and Callol, L. (2002). Prognostic significance of tumor infiltrating natural killer cells subset CD57 in patients with squamous cell lung cancer. Lung cancer (Amsterdam, Netherlands) *35*, 23-28.

Vivier, E., Tomasello, E., Baratin, T., Walzer, T., and Ugolini, S. (2008). Functions of natural killer cells. Nat Immunol *9*, 503-510.

Wagner, J.A., Rosario, M., Romee, R., Berrien-Elliott, M.M., Schneider, S.E., Leong, J.W., Sullivan, R.P., Jewell, B.A., Becker-Hapak, M., Schappe, T.*, et al.* (2017). CD56bright NK cells exhibit potent antitumor responses following IL-15 priming. J Clin Invest *127*, 4042-4058.

Warburg, O. (1924). Über den Stoffwechsel der Carcinomzelle. Naturwissenschaften *12*, 1131-1137.

Warburg, O. (1925). The Metabolism of Carcinoma Cells. The Journal of Cancer Research *9*, 148-163.

Warburg, O., Wind, F., and Negelein, E. (1927). THE METABOLISM OF TUMORS IN THE BODY. The Journal of General Physiology *8*, 519-530.

Yang, M., and Vousden, K.H. (2016). Serine and one-carbon metabolism in cancer. Nature Reviews Cancer *16*, 650.

Ye, J., Fan, J., Venneti, S., Wan, Y.W., Pawel, B.R., Zhang, J., Finley, L.W., Lu, C., Lindsten, T., Cross, J.R.*, et al.* (2014). Serine catabolism regulates mitochondrial redox control during hypoxia. Cancer discovery *4*, 1406-1417.

Yeung, T.L., Leung, C.S., Yip, K.P., Yeung, C.L.A., Wong, S.T.C., and Mok, S.C. (2015). Cellular and molecular processes in ovarian cancer metastasis. A review in the theme: cell and molecular processes in cancer metastasis. Am J Physiol Cell Physiol *309*, C444–C456.

Yu, Y., Zeng, D., Ou, Q., Liu, S., Li, A., Chen, Y., Lin, D., Gao, Q., Zhou, H., Liao, W.*, et al.* (2019). Association of Survival and Immune-Related Biomarkers With Immunotherapy in Patients With Non-Small Cell Lung Cancer: A Meta-analysis and Individual Patient-Level Analysis. JAMA Netw Open *2*, e196879.

Yun, J., Rago, C., Cheong, I., Pagliarini, R., Angenendt, P., Rajagopalan, H., Schmidt, K., Willson, J.K., Markowitz, S., Zhou, S.*, et al.* (2009). Glucose deprivation contributes to the development of KRAS pathway mutations in tumor cells. Science *325*, 1555-1559.

Yuneva, M.O., Fan, T.W., Allen, T.D., Higashi, R.M., Ferraris, D.V., Tsukamoto, T., Matés, J.M., Alonso, F.J., Wang, C., Seo, Y.*, et al.* (2012). The metabolic profile of tumors depends on both the responsible genetic lesion and tissue type. Cell Metab *15*, 157-170.

Zaugg, K., Yao, Y., Reilly, P.T., Kannan, K., Kiarash, R., Mason, J., Huang, P., Sawyer, S.K., Fuerth, B., Faubert, B.*, et al.* (2011). Carnitine palmitoyltransferase 1C promotes cell survival and tumor growth under conditions of metabolic stress. Genes & development *25*, 1041-1051.

Zeng, R., Spolski, R., Casas, E., Zhu, W., Levy, D.E., and Leonard, W.J. (2007). The molecular basis of IL-21-mediated proliferation. Blood *109*, 4135-4142.

Zhang, L., Conejo-Garcia, J.R., Katsaros, D., Gimotty, P.A., Massobrio, M., Regnani, G., Makrigiannakis, A., Gray, H., Schlienger, K., Liebman, M.N.*, et al.* (2003). Intratumoral T cells, recurrence, and survival in epithelial ovarian cancer. The New England journal of medicine *348*, 203-213.